ENERGY, EXERGY AND ECONOMIC ANALYSIS OF PHASE CHANGE MATERIAL BASED HYBRID PHOTOVOLTAIC THERMAL SYSTEMS

MD. SHOUQUAT HOSSAIN

INSTITUTE OF GRADUATE STUDIES
UNIVERSITY OF MALAYA
KUALA LUMPUR

2018

University of Malaya

ENERGY, EXERGY AND ECONOMIC ANALYSIS OF PHASE CHANGE MATERIAL BASED HYBRID PHOTOVOLTAIC THERMAL SYSTEMS

MD. SHOUQUAT HOSSAIN

THESIS SUBMITTED IN FULFILMENT OF THE REQUIREMENTS FOR THE DEGREE OF DOCTOR OF PHILOSOPHY

INSTITUTE OF GRADUATE STUDIES
UNIVERSITY OF MALAYA
KUALA LUMPUR

2018

University of Malaya

ORIGINAL LITERARY WORK DECLARATION

Name of the candidate: **Md. Shouquat Hossain**

Registration/Matric No: **HHD130003**

Name of the Degree: **Doctor of Philosophy (Ph. D)**

Title of Project Paper/ Research Report/ Dissertation / Thesis ("this work"): **Energy, exergy and economic analysis of phase change material based hybrid photovoltaic thermal systems**

Field of Study: **Renewable Energy (Electricity and Energy)**

I do solemnly and sincerely declare that:

(1) I am the sole author /writer of this work;
(2) This work is original;
(3) Any use of any work in which copyright exists was done by way of fair dealings and any expert or extract from, or reference to or reproduction of any copyright work has been disclosed expressly and sufficiently and the title of the Work and its authorship has been acknowledged in this Work;
(4) I do not have any actual knowledge nor do I ought reasonably to know that the making of this work constitutes an infringement of any copyright work;
(5) I, hereby assign all and every rights in the copyrights to this Work to the University of Malaya (UM), who henceforth shall be owner of the copyright in this Work and that any reproduction or use in any form or by any means whatsoever is prohibited without the written consent of UM having been first had and obtained actual knowledge;
(6) I am fully aware that if in the course of making this Work I have infringed any copyright whether internationally or otherwise, I may be subject to legal action or any other action as may be determined by UM.

Candidate's Signature Date:

Subscribed and solemnly declared before,

Witness's Signature Date:

Name:

Designation:

University of Malaya

ENERGY, EXERGY AND ECONOMIC ANALYSIS OF PHASE CHANGE MATERIAL BASED HYBRID PHOTOVOLTAIC THERMAL SYSTEMS

ABSTRACT

Efficient extraction and conversion of energy is a burning issue in today's world. Photovoltaic (PV) technology suffers from the major drawback of poor energy conversion efficiency that is further worsen by overheating of the module. Hybrid photovoltaic thermal (PV/T) collectors have bring about a notable change in this technology by enabling the extraction of both electricity and heat from the same module, thereby improving the overall efficiency. However, there are some technical challenges with these devices that obstacles their wide-scale application. The major shortcoming of conventional water based PV/T collectors is that their operation is limited only in daytime. Use of phase change materials (PCM) in PV/T collectors as an intermediate thermal storage media offers a promising solution to this problem by storing large amount of heat. The aim of this research work is to design and develop a PV/T-PCM system with self-cleaning facility (PV/T-PCM-SC) and evaluate its performance through energy, exergy and economic analysis. The thermal collector of the PV/T is a novel parallel serpentine pipe flow channel that extracts maximum heat from the PV module. Lauric acid PCM contained in leak-proof aluminum foil packets are placed around the flow channel allowing extended period of thermal storage. The PV glass cover is equipped with a self-cleaning mechanism to ensure well transmittance of solar irradiation allowing more energy to intercept. In order to make comparative performance study with a reference PV module, three systems, viz., PV/T-only, PV/T-PCM and PV/T-PCM with self-cleaning has been developed. Energy analysis, which is based on the first law of thermodynamics, gives the maximum thermal efficiency of PV/T-only, PV/T-PCM and PV/T-PCM with self-cleaning system as 74.62%, 87.72% and 77.60%, respectively. On the other hand, a second law analysis of all of the systems reveals that maximum exergy

University of Malaya

efficiency of PV/T-only, PV/T-PCM and PV/T-PCM with self-cleaning system are 12.98%, 12.19% and 12.68%, respectively. Electrical performance of all the three systems has also been analyzed and it was observed that PV/T-only, PV/T-PCM and PV/T-PCM with self-cleaning system are 10.46%, 11.08% and 11.91% respectively.

An economic analysis of the proposed system has also been carried out with a view to examine the feasibility of its commercialization. It may be concluded from the analysis that commercialization of PV/T-PCM with self-cleaning system is worthwhile and with mass production, it will become more cost effective. A PV/T-PCM system with novel parallel serpentine pipe thermal collector has been developed that not only incorporates PCM thermal management, but also self-cleaning facility to ensure improved performance. To the best of knowledge, the proposed PV/T-PCM system with self-cleaning approach is first of its kind and deserves commercial application, at least, on household scale. This system can provide both electricity and heat to the households of remote areas that are out of the reach of electricity grid that will contribute to curb power crisis to a good extent. The provision of self-cleaning system makes it excellent choice for applications in coastal regions.

Keywords: photovoltaic thermal, exergy, economic, phase change material, self-cleaning

University of Malaya

TENAGA, EXERGY DAN ANALISIS EKONOMI PERUBAHAN FASA BAHAN BERASASKAN HYBRID FOTOVOLTAIK THERMAL SYSTEMS

ABSTRAK

Pengekstrakan dan penukaran tenaga yang cekap adalah isu hangat di dunia hari ini. Teknologi Photovoltaik (PV) mengalami kelemahan utama disebabkan kecekapan penukaran tenaga yang lemah yang terus memburukkan lagi oleh modul yang terlalu panas. Pengumpul haba photovoltaik hibrid (PV/T) telah membawa perubahan ketara dalam teknologi ini dengan membolehkan pengekstrakan kedua-dua elektrik dan haba dari modul yang sama, sehingga meningkatkan kecekapan keseluruhan. Walau bagaimanapun, terdapat beberapa cabaran teknikal dengan peranti ini yang menghalang penggunaan yang meluas. Kekurangan utama pengumpul PV/T berasaskan air konvensional ialah operasi mereka hanya terhad pada siang hari. Penggunaan bahan-bahan perubahan fasa (PCM) dalam pengumpul PV/T sebagai media penyimpanan haba pertengahan menawarkan perjanjian penyelesaian masalah ini dengan menyimpan sejumlah besar haba. Tujuan kerja penyelidikan ini adalah untuk merekabentuk dan membangunkan sistem PV/T-PCM dengan kemudahan pembersihan diri (PV/T-PCM-SC) dan menilai prestasi melalui tenaga, exergy dan analisis ekonomi. Pengumpul haba PV/T adalah saluran aliran paip serpentian novel yang melepaskan haba maksimum dari modul PV. Asid Lauric PCM yang terkandung dalam paket aluminium foil kebocoran diletakkan di sekitar saluran aliran yang membolehkan tempoh maksima penyimpanan haba terma. Perlindungan kaca PV dilengkapi dengan mekanisme pembersihan diri untuk memastikan pemancar sinaran solar yang baik membolehkan lebih banyak tenaga untuk dipintas. Untuk membuat kajian prestasi komparatif dengan modul PV rujukan, tiga sistem, iaitu, PV / T-sahaja, PV / T-PCM dan PV / T-PCM dengan pembersihan diri telah dibangunkan. Analisis tenaga yang berdasarkan undang-undang termodinamik pertama, memberikan kecekapan terma maksimum PV/T-sahaja, PV/T-PCM dan PV/T-PCM

University of Malaya

dengan sistem pembersihan diri masing-masingsebanyak 74.62%, 87.72% dan 77.60%. Selain itu, analisis dari semua sistem menunjukkan kecekapan eksperimen maksimum PV/T-sahaja, PV/T-PCM dan PV/T-PCM dengan sistem pembersihan diri masing-masingadalah 12.98%, 12.19% dan 12.68%. Prestasi elektrik dari ketiga-tiga sistem ini juga telah dianalisis dan diperhatikan bahawa PV/T-sahaja, PV/T-PCM dan PV/T-PCM dengan sistem pembersihan diri adalah 10.46%, 11.08% dan 11.91%.

Analisis ekonomi sistem yang dicadangkan juga telah dijalankan dengan tujuan untuk mengkaji kemungkinan pengkomersialannya. Ia boleh disimpulkan dari analisis bahawa pengkomersialan PV/T-PCM dengan sistem pembersihan diri adalah berbaloi dan dengan pengeluaran besar-besaran akan menjadi lebih efektif. Sistem PV/T-PCM dengan pemungut haba paip serpentine novel yang telah dibangunkan yang bukan sahaja menggabungkan pengurusan haba PCM, tetapi juga sebagai kemudahan pembersihan diri untuk memastikan prestasi yang lebih baik. Untuk pengetahuan yang terbaik, sistem PV/T-PCM yang dicadangkan dengan pendekatan pembersihan diri adalah yang pertama dan layak untuk aplikasi komersil, sekurang-kurangnya pada skala isi rumah. Sistem ini boleh memberi bekalan elektrik dan haba kepada isi rumah kawasan terpencil yang tidak dapat dicapai dari grid elektrik yang akan menyumbang untuk membendung krisis kuasa sehingga tahap yang baik. Penyediaan sistem pembersihan diri menjadikannya pilihan yang sangat baik untuk aplikasi di kawasan pantai.

Kata kunci: fotovoltaik thermal, exergy, ekonomi, bahan perubahan fasa, pembersihan diri

University of Malaya

ACKNOWLEDGEMENTS

First, I would like to express my utmost gratitude to the almighty Allah, who has created and erudite me and helped me all the way to finish this work smoothly.

I am extremely grateful for the opportunity to work under the supervision of Professor Dr. Nasrudin Bin Abd Rahim, Associate Professor Dr. Jeyraj A/L Selvaraj and Dr. Adarsh Kumar Pandey. Under their tutelage, I have grown as a student, researcher, and above all as a person. They always blessed me with motivation and moral support without which it was very difficult to complete this study. They have been supportive in both my research and personal life. I truly appreciate the support that I have received from them in every walk of my life.

I would like to thank all of my colleagues at the UM Power Dedicated Advances Centre (UMPEDAC) for providing a great environment to learn and render research. Especial thanks to Mohammed Moinul Islam for giving a great inspiration to complete my thesis successfully. I acknowledge the support of all UMPEDAC staffs and technicians. Without their help, I could not complete my experiments. I would like to acknowledge gratefully the financial support by University of Malaya, the Ministry of Higher Education of Malaysia (MOHE) (UM.C/HIR/MOHE/ENG/32), Institute of Graduate Studies (IGS) and UM Power Energy Dedicated Advanced Centre (UMPEDAC) for supporting this research project. I gratefully acknowledge the privileges and opportunities offered by the University of Malaya.

I would like to thank my father, my mother, my brother and sister for their unwavering support and encouragement. They provided the love and strength that have made me who I am today. Finally, I would like to thank my beloved wife. She supported me in numerous ways, not to mention the love and support she has given me all the way. I will always be indebted to her.

University of Malaya

TABLE OF CONTENTS

Abstract iii

Abstrak v

Acknowledgements vii

Table of Contents viii

List of Figures xiii

List of Tables xix

List of Symbols and Abbreviations xxi

List of Appendices xxv

CHAPTER 1: INTRODUCTION 1

1.1 Background 1

1.2 Problem Statement 6

1.3 Research Objectives 6

1.4 Scope of the Study 7

1.5 Significance of the Study 7

1.6 Organization of the Thesis 8

CHAPTER 2: LITERATURE REVIEW 10

2.1 Introduction 10

2.2 Photovoltaic Thermal Collector 11

2.2.1 Active System 13

2.2.2 Direct System 14

2.2.3 Indirect System 14

2.2.4 Pressurized System 14

2.3 Energy, Exergy and Economic Analysis 15

2.3.1 Energy Analysis 15

2.3.2 Exergy Analysis 20

University of Malaya

2.3.3 Economic Analysis 24
2.4 Phase Change Material 27
2.4.1 Classification of PCMs 29
2.4.2 PCM Selection 30
2.4.3 PCM Application in PV Panel 32
2.4.3.1 PV-PCM system 36
2.4.3.2 Solar water heater 41
2.4.3.3 Thermal management system 42
2.5 Application of PCMs in Solar Thermal Energy 44
2.5.1 Solar thermal power plants 44
2.5.2 Parabolic trough collector 47
2.5.3 Parabolic dish 49
2.5.4 Power tower 50
2.6 Application of PCMs in Heating and Cooling of Buildings 51
2.6.1 Heating application 51
2.6.2 Cooling applications 55
2.7 Overview of Solar PV Module Dust and Cleaning System 56
2.7.1 Dust Accumulation 57
2.7.2 Cleaning Systems 58
2.7.3 Methods used to clean PV panels 59
2.7.3.1 Heliotex technology 59
2.7.3.2 Robotic cleaning system 60
2.7.3.3 Electrostatics cleaning system 60
2.7.3.4 ProCurve cleaning system 60
2.8 Summary of Literature Review and Research Gap 60

University of Malaya

CHAPTER 3: MATERIALS AND METHODOLOGY 62

3.1 Introduction 62

3.2 Fundamentals of the System 62

3.2.1 PV/T System 63

3.2.2 PCM Thermal Control 65

3.2.3 Self-cleaning Method 66

3.3 Designing the Sub-systems 67

3.3.1 Design of PV/T 67

3.3.2 Design of PCM Blocks 69

3.3.3 Design of Self-cleaning System 70

3.4 Fabrication 72

3.4.1 Fabrication of PV/T-PCM System 72

3.4.2 Fabrication of Self-cleaning System 76

3.4.3 Installation and Instrumentation of the Experimental Set-up 79

3.5 Data Collection and Analysis 83

3.5.1 Energy Analysis 83

3.5.2 Exergy Analysis 86

3.5.3 Dust Cleaning Performance Analysis 91

3.6 Economic Analysis 92

3.6.1 Annual-worth Method (Equivalent Uniform Annual Cost) 92

3.6.2 Cash Flow Analysis 93

3.6.3 Market Survey 93

CHAPTER 4: RESULTS AND DISCUSSION 95

4.1 Introduction 95

4.2 Photovoltaic Thermal (PV/T) and Photovoltaic Thermal-Phase change material (PV/T-PCM) systems 96

University of Malaya

4.2.1 Hourly Variation of Different Parameters of PV and PV/T 96
4.2.2 Hourly Variation of Different Parameters of PV and PV/T-PCM 102
4.3 Energy Analyses of PV/T and PV/T-PCM Systems 107
4.3.1 Effect of Irradiation on Electrical Performance 107
4.3.2 Effect of Cell Temperature on Electrical Performance 117
4.3.3 Effect of Water Flow rate on Thermal Performance 126
4.4 Exergy Analysis of PV/T and PV/T-PCM Systems 128
4.5 Photovoltaic Thermal-Phase change material with dust and self-cleaning (PV/T-PCM-Dust and PV/T-PCM-SC) systems 130
4.5.1 Hourly Variation of Different Parameters of PV and PV/T-PCM with dust 130
4.5.2 Hourly Variation of Different Parameters of PV and PV/T-PCM with self-cleaning 135
4.6 The Effect of Dust Cleaning on the Performance of the PV/T-PCM System 141
4.6.1 Effect of Irradiation on Electrical Performance 142
4.6.2 Effect of Cell Temperature on Electrical Performance 149
4.6.3 Effect on Energy Performance 157
4.7 Effect on Exergy Performance 159
4.8 Comparative Performance Evaluation 160
4.8.1 Comparative performance assessment with previous studies 166
4.9 Economic Analysis 167
CHAPTER 5: CONCLUSIONS AND RECOMMENDATIONS 174
5.1 Introduction 174
5.1.1 PV vs PV/T Performance 174
5.1.2 PV vs PV/T-PCM Performance 175
5.1.3 Performance of PV/T-PCM with Self-cleaning System 176

University of Malaya

5.1.4 Economic Analysis 177
5.2 Contribution of the Present Research 178
5.3 Recommendations for Future Work 179
List of Publications 181
References 183
Appendix 204

University of Malaya

LIST OF FIGURES

Figure 1.1: Source of energy 2

Figure 1.2: Solar energy utilization 3

Figure 2.1: A typical liquid flat-plate solar PV/T collector 12

Figure 2.2: Energy stockpiling materials and their groupings 28

Figure 2.3: Characterization of PCMs 29

Figure 2.4: DSC curve of paraffin wax for heating and cooling 31

Figure 2.5: Energy difference between clean and the polluted pair panel 59

Figure 3.1: Working principle of a PV and solar thermal system 63

Figure 3.2: Working principle of a (a) PV/T, (b) PV/T and (c) PV/T-PCM with self-cleaning hybrid systems 64

Figure 3.3: Basic design of a flat plate collector 68

Figure 3.4: PV module and layout of PV/T thermal collector 69

Figure 3.5: Arrangement of PCM packets 70

Figure 3.6: 3D view of flow channel and PCM packets 70

Figure 3.7: Working principle of a self-cleaning system 71

Figure 3.8: 3D design of self-cleaning mechanism in PV panel 72

Figure 3.9: Double serpentine flow channel attached to PV rear side 73

Figure 3.10: Aluminum packets containing PCM 74

Figure 3.11: Aluminum foil cover on the thermal collector 74

Figure 3.12: Ceramic fiber insulation cover on PV/T rear side 75

Figure 3.13: PCM packets covering the thermal collector 75

Figure 3.14: Self-cleaning system fabrication materials 76

Figure 3.15: Sweeper driving DC motor 76

Figure 3.16: Sweeper driving accesories 77

Figure 3.17: Sweeping microfiber and water flow pipeline 77

University of Malaya

Figure 3.18: Complete self-cleaning system 78
Figure 3.19: Complete PV/T-PCM with self-cleaning system along with reference PV 78
Figure 3.20: Microcontroller based motor control system for water pump and sweeper, block diagram of control circuit with microcontroller pin layout 79
Figure 3.21: (a) Experiment setup and cutway view of the solar PV/T (b) PV/T-PCM and (c) PV/T-PCM with self-cleaning system 80
Figure 3.22: Measuring and data acquisition instruments (a) Data logger, (b) Pyranometer, (c) Flow meter, (d) I-V tracer 82
Figure 3.23: Exergy in/out of a PV module at steady state condition 86
Figure 4.1: Hourly variation of different PV and PV/T parameters (0.5 LPM) 97
Figure 4.2: Hourly variation of different PV and PV/T parameters (1 LPM) 98
Figure 4.3: Hourly variation of different PV and PV/T parameters (2 LPM) 99
Figure 4.4: Hourly variation of different PV and PV/T parameters (3 LPM) 100
Figure 4.5: Hourly variation of different PV and PV/T parameters (4 LPM) 101
Figure 4.6: Hourly variation of different PV and PV/T-PCM parameters (0.5 LPM) .. 102
Figure 4.7: Hourly variation of different PV and PV/T-PCM parameters (1 LPM) 103
Figure 4.8: Hourly variation of different PV and PV/T-PCM parameters (2 LPM) 104
Figure 4.9: Hourly variation of different PV and PV/T-PCM parameters (3 LPM) 105
Figure 4.10: Hourly variation of different PV and PV/T-PCM parameters (4 LPM) ... 106
Figure 4.11: Effect of irradiation on electrical performance of (a) PV/T and (b) PV/T-PCM against the reference PV (0.5 LPM) 108
Figure 4.12: Effect of irradiation on electrical performance of (a) PV/T and (b) PV/T-PCM against the reference PV (1 LPM) 109
Figure 4.13: Effect of irradiation on electrical performance of (a) PV/T and (b) PV/T-PCM against the reference PV (2 LPM) 111

University of Malaya

Figure 4.14: Effect of irradiation on electrical performance of (a) PV/T and (b) PV/T-PCM against the reference PV (3 LPM)..... 112
Figure 4.15: Effect of irradiation on electrical performance of (a) PV/T and (b) PV/T-PCM against the reference PV (4 LPM)..... 116
Figure 4.16: Effect of cell temperature on electrical performance of (a) PV/T and (b) PV/T-PCM against reference PV (0.5 LPM)..... 118
Figure 4.17: Effect of cell temperature on electrical performance of (a) PV/T and (b) PV/T-PCM against reference PV (1 LPM)..... 119
Figure 4.18: Effect of cell temperature on electrical performance of (a) PV/T and (b) PV/T-PCM against reference PV (2 LPM)..... 121
Figure 4.19: Effect of cell temperature on electrical performance of (a) PV/T and (b) PV/T-PCM against reference PV (3 LPM)..... 122
Figure 4.20: Effect of cell temperature on electrical performance of (a) PV/T and (b) PV/T-PCM against reference PV (4 LPM)..... 125
Figure 4.21: Effect of water flow rate on thermal performance of PV/T and PV/T-PCM collector 127
Figure 4.22: Effect of water flow rate on exergy performance (a) PV/T and (b) PV/T-PCM system..... 129
Figure 4.23: Hourly variation of different PV and PV/T-PCM dust parameters (0.5 LPM) 131
Figure 4.24: Hourly variation of different PV and PV/T-PCM dust parameters (1 LPM) 132
Figure 4.25: Hourly variation of different PV and PV/T-PCM dust parameters (2 LPM) 133
Figure 4.26: Hourly variation of different PV and PV/T-PCM dust parameters (3 LPM) 134

University of Malaya

Figure 4.27: Hourly variation of different PV and PV/T-PCM dust parameters (4 LPM) 135
Figure 4.28: Hourly variation of different PV and PV/T-PCM-SC parameters (0.5 LPM) 136
Figure 4.29: Hourly variation of different PV and PV/T-PCM-SC parameters (1 LPM) 137
Figure 4.30: Hourly variation of different PV and PV/T-PCM-SC parameters (2 LPM) 138
Figure 4.31: Hourly variation of different PV and PV/T-PCM-SC parameters (3 LPM) 139
Figure 4.32: Hourly variation of different PV and PV/T-PCM-SC parameters (4 LPM) 141
Figure 4.33: Effect of irradiation on electrical performance of (a) PV/T-PCM-Dust and (b) PV/T-PCM-SC against PV (0.5 LPM)..... 143
Figure 4.34: Effect of irradiation on electrical performance of (a) PV/T-PCM-Dust and (b) PV/T-PCM-SC against PV (1 LPM)..... 144
Figure 4.35: Effect of irradiation on electrical performance of (a) PV/T-PCM-Dust and (b) PV/T-PCM-SC against PV (2 LPM)..... 145
Figure 4.36: Effect of irradiation on electrical performance of (a) PV/T-PCM-Dust and (b) PV/T-PCM-SC against PV (3 LPM)..... 147
Figure 4.37: Effect of irradiation on electrical performance of (a) PV/T-PCM-Dust and (b) PV/T-PCM-SC against PV (4 LPM)..... 149
Figure 4.38: Effect of cell temperature on electrical performance of (a) PV/T-PCM dust and (b) PV/T-PCM self-cleaning against reference PV (0.5 LPM) 150
Figure 4.39: Effect of cell temperature on electrical performance of (a) PV/T-PCM dust and (b) PV/T-PCM self-cleaning against reference PV (1 LPM) 152

University of Malaya

Figure 4.40: Effect of cell temperature on electrical performance of (a) PV/T-PCM dust and (b) PV/T-PCM self-cleaning against reference PV (2 LPM) 153
Figure 4.41: Effect of cell temperature on electrical performance of (a) PV/T-PCM dust and (b) PV/T-PCM self-cleaning against reference PV (3 LPM) 155
Figure 4.42: Effect of cell temperature on electrical performance of (a) PV/T-PCM dust and (b) PV/T-PCM self-cleaning against reference PV (4 LPM) 157
Figure 4.43: Effect of water flow on thermal performance of PV/T-PCM-Dust and PV/T-PCM-SC collector..... 158
Figure 4.44: Effect of water flow on exergy performance of PV/T-PCM-Dust and PV/T-PCM-SC system 160
Figure 4.45: Energy and exergy efficiency comparesum performance of PV and PV/T for different mass flow rates..... 161
Figure 4.46: Energy and exergy efficiency comparesum performance of PV and PV/T-PCM for different mass flow rates 162
Figure 4.47: Energy and exergy efficiency comparesum performance of PV and PV/T-PCM-Dust for different mass flow rates..... 163
Figure 4.48: Energy and exergy efficiency comparesum performance of PV and PV/T-PCM-SC for different mass flow rates 164
Figure 4.49: Improvement in electrical efficiency of PV/T-PCM system by using self cleaning mechanism as a function of the water flow rate..... 165
Figure 4.50: Solar PV panel cash flow diagram 167
Figure 4.51: Solar PV/T water heating cash flow diagram..... 169
Figure 4.52: Solar PV/T having PCM cash flow diagram 170
Figure 4.53: Solar PV/T having PCM and self-cleaning cash flow diagram..... 172
Figure A.1: Circuit diagram of a self-cleaning controller..... 204
Figure A.2: Hardware implementation of control circuit..... 204

University of Malaya

Figure A.3: Universal programmable flash device 205

Figure A.4: Mini instant electric hot tank less water heater system 206

Figure A.5: MP-20RXM Magnetic circulation water pump 206

Figure C.1: Electric water heart cash flow diagram 209

Figure D.1: Lauric acid DSC test curve 210

Figure D.2: Paraffin DSC test curve 210

Figure D.3: I-tetradecanol DSC test curve 211

Figure D.4: Decanoic acid natural DSC test curve 211

Figure D.5: Decanoic acid for synthesis DSC test curve 212

University of Malaya

LIST OF TABLES

Table 2.1: Different types of flat plate collector pipe absorbers and their thermal efficiencies 12

Table 2.2: Thermophysical properties of paraffin wax 31

Table 2.3: Points of interest and inconveniences of distinctive thermal management procedure 34

Table 2.4: Description of the fins used in the three experimental systems 38

Table 2.5: Thermophysical properties of RT25, GR40 39

Table 2.6: Storage properties of PCM 46

Table 2.7: Power generation cycle properties 46

Table 2.8: Thermo-physical properties of the used Iraqi paraffin wax 50

Table 3.1: Properties of PCM materials 66

Table 3.2: Specification of PV module 72

Table 3.3: Specifications thermal conductive paste 73

Table 3.4: Ceramic fiber paper for Solar PV rear insulation 75

Table 3.5: Properties of the monitoring equipment 82

Table 3.6: PV, PV/T and PV/T-PCM system characteristics 90

Table 4.1: The measured parameters at mass flow rate of 4 LPM 101

Table 4.2: The measured parameters at mass flow rate of 4 LPM 106

Table 4.3: The measured parameters at mass flow rate of 2 LPM 133

Table 4.4: The measured parameters at mass flow rate of 4 LPM 141

Table 4.5: Performance of electrical, thermal and exergy efficiency on PV and PV/T collector 162

Table 4.6: Performance of electrical, thermal and exergy efficiency on PV and PV/T-PCM collector 163

University of Malaya

Table 4.7: Performance of electrical, thermal and exergy efficiency on PV and PV/T-PCM-Dust 164

Table 4.8: Performance of electrical, thermal and exergy efficiency on PV and PV/T-PCM-SC collector 165

Table 4.9: Optimum performance attained with PV/T, PV/T-PCM and PV/T-PCM with self-cleaning systems 166

Table 4.10: Comparative performance assessment of present research with previous studies 166

Table A.1: Microcontroller programs and pin configuration 205

Table B.1: The breakdown cost of electrical water heater 207

Table B.2: The breakdown cost of solar PV module 207

Table B.3: The breakdown cost of thermal collector 207

Table B.4: The breakdown cost of PCM 208

Table B.5: The breakdown cost of self-cleaning system 208

Table C.1: Cost of running an electric water heater 209

University of Malaya

LIST OF SYMBOLS AND ABBREVIATIONS

A/F	:	sinking fund factor
A/P	:	capital recovery factor
A_W	:	annual worth
A_{rc}	:	annual running cost
A_o, A	:	collector area (m^2)
A_o	:	ideal factor
A_c	:	PV module surface (m^2)
C	:	heat capacity
CF	:	capacity factor
C_{afic}	:	change of aluminium foil insulation cover
$C_{p,s}$, $C_{p,l}$	:	specific heats of PCM in solid and liquid phase (J/kg.K)
$C_{p,w}$	:	specific heat capacity of water (J/kg.K)
$C_{p,PCM}$	:	specific heats of PCM (J/kg.K)
Ex_{in}	:	exergy in (W)
Ex_{out}	:	exergy out (W)
Ex_{loss}	:	exergy loss (W)
E_{xd}	:	energy destruction (W)
$E_{XPV/T}$	:	photovoltaic thermal exergy (W)
E	:	energy yield (W)
F	:	amount of money accumulate
FF	:	fill factor
G	:	Solar radiation (W/m^2)
h_{conv}	:	convective heat transfer coefficient (W/m^2 K)
$h_{rad\text{-}1\ \&\ 2}$	:	radiation losses

University of Malaya

I_c : initial cost

I_{lc} : installation cost

i : interest rate

I : current (A)

k : global losses factor (W/m^2 °C)

n_1 : day of year

N : life time

N_1, N_c : number of glass covers

$\dot{m}$: flow rate of water (LPM)

m_{PCM} : mass of PCM

ΔM : total mass of dust accumulated (kg)

L, L_F : latent heat (kJ/kg)

P : amount of money

P_l : plate thickness (m^2)

P_{max} : maximum PV power output (W)

PV : photovoltaic

PCM : phase change material

P_{sc} : packing factor of the solar module

q : electronic charge (c)

Q_1 : latitude

Q_{ch} : heat charging phase

Q_a : heat derived from the absorption surface (W/m^2)

$\dot{Q}_u$: useful energy gain (W)

R_c : running cost

SC : self-cleaning

STC : standard testing condition

University of Malaya

T : temperature (°C or K)

T_{a1} : average temperature of the environment (°C)

T_b : back panel temperature (°C)

T_m : temperature of the main or absorption surface (°C)

$T_{m,PCM}$: melting point of the PCM (°C)

U : total heat loss coefficient (W/m^2 K)

V_w : wind velocity (m/s).

V : voltage (V)

Greek symbols:

α : absorption factor

β : collector slope (degree)

Δ : gradient or temperature different

δ : inclination angle (degree)

ε_g : emissivity of glass

ε_p : emissivity of collector plate

τ : transmission factor

σ, κ : Stefan-Boltzmann constant (5.669×10^{-8} (W/m^2)/K4)

η : efficiency

η_o : total efficiency

Subscripts:

a : ambient

c : cell

cl : cleaning

el : electrical

ex : exergy

f : final

University of Malaya

i	:	initial
i	:	input
m	:	melting
max	:	maximum
mp	:	maximum power
o	:	output
oc	:	open circuit
p	:	temperature gradient
p	:	peak
pol	:	polluted
s	:	sun
sc	:	short circuit
t	:	time
th	:	thermal
u	:	usable
w	:	water

University of Malaya

LIST OF APPENDICES

Appendix A: Microcontroller circuit design and specifications of electrical heater and water pump 204

Appendix B: Cost breakdown of the sub-systems 207

Appendix C: Cash flow diagram and results of electrical water heater 209

Appendix D: Phase change materials DSC test results 210

University of Malaya

CHAPTER 1: INTRODUCTION

1.1 Background

Energy has the greatest immediate, current and residual impacts on the socio-economic development of a country. Recently there has been a worldwide increase of 44.2% in energy demand due to the increased economic and technological development over the projected period of 2006-2030 (Rahman & Lee, 2006). The global economy has grown at 3.3% per year over the past 30 years and during this period the electrical energy demand has increased by 3.6%. According to the International Energy Outlook 2017, the world energy consumption will increase by 5% between 2016 and 2040 (AEO, 2017). Presently, the major contributors of the energy comes from fossil fuel the burning of which releases the gaseous and toxic pollutants which are responsible for the global warming and greenhouse gas (GHG) effects. This in turn will result in unpredictable global climate changes, foreboding stratospheric ozone depletion, loss of biodiversity, ominous hydrological systems change and the reduction in supplies of freshwater, land degradation and portentous stresses on the life line continuity food chain (Saidur et al., 2010).

Renewable energy is now being continuously explored and prudently introduced in many countries around the world not only for harnessing the energy but also to solve the environmental degradation problems. These are still rampant in the form of uncontrollable devastating floods caused by unmanageable deforestation, hill denudation and unfavorable weather changes made worse by the uncaring humans who blatantly polluted the water courses which are the crucial sources of potable water for human and industrial use (Ibrahim et al., 2014a).

Figure 1.1 categorizes various sources of energy under renewable and non-renewable energy resources, such as, biomass (plant and animal waste converted into fuel), biogas (in sewage treatment plant which produces usable methane), solar ray, wind, water and

University of Malaya

geothermal energies which are grouped under renewable energy sources because they are non-exhaustible and occur in great abundance. Underground high-pressure hot steam from volcanic regions, wave, tidal and ocean thermal gradient sources are also considered as geothermal energy. Fossil fuels, like coal, oil and natural gas are grouped with nuclear fusion and nuclear fission under non-renewable sources because they can be depleted and there are major obstacles encountered in their utilization, management and operation involving very high risk of radioactive exposure (Ong, 1994; Hossain, 2013).

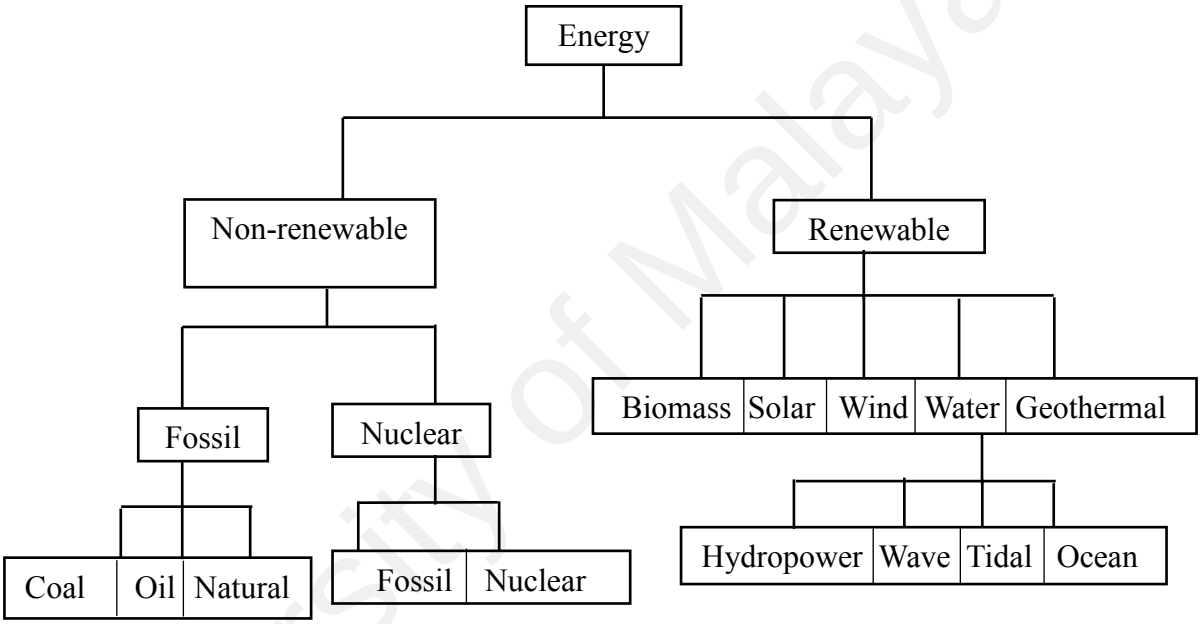

Figure 1.1: Source of energy
(Ong, 1994; Hossain, 2013)

Renewable energies are critical components for achieving sustainable development goal, particularly solar energy is very important in terms of harnessing a clean energy from the environmental solar ray. During the next decades, solar energy is not only the most likely but also most potentially to be one of the most promising sources of clean energy. The major applications of solar energy can be classified into two categories (et al., 2009; Sarhaddi et al., 2010), viz.:

i) Solar thermal collectors (STC), which convert solar energy into thermal energy.

ii) Solar photovoltaic (PV) system, which converts solar energy into electrical energy.

University of Malaya

The various applications of the solar energy are as shown in Figure 1.2.

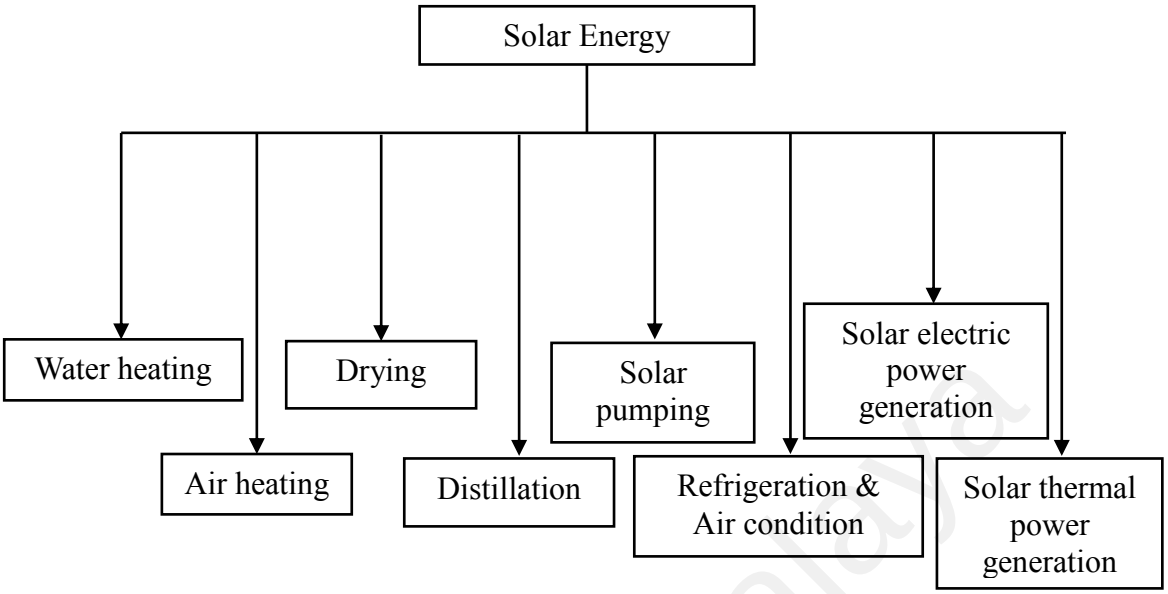

Figure 1.2: Solar energy utilization
(Hossain, 2013)

Hybrid power systems are combinations of two or more energy conversion devices (e.g. electricity generators or storage devices), or two or more fuels for the same device when fully integrated. Their system efficiencies are typically higher than that of the individual technologies used separately, and higher reliability can be achieved with the current energy storage technologies (Jun et al., 2011; Dursun, 2012). PV modules converts only 13% to 16% of the incident solar radiation into electricity, depending on the type of cell materials, location of installation and several other environmental factors; the remaining energy being wasted as heat. Hybrid photovoltaic thermal (PV/T) systems can extract heat from PV modules, which is then employed for heating air or water. A system installed at a higher solar radiation will give a better economic benefit to their lower initial cost (Kalogirou & Tripanagnostopoulos, 2006; Singh & Tiwari, 2017).

Electrical efficiency of the PV system decreases rapidly as the module temperature increases. On the other hand, an external electrical energy is required to circulate the working fluid through the system of the solar thermal collector. Therefore, a higher electrical efficiency of a PV module might be achieved by removing the heat through the

University of Malaya

circulation of cooling water. In order to eliminate an external electrical energy loss the PV module has to be cooled and should be logically combined with the solar air/water heater collector which is called the solar photovoltaic thermal (PV/T) collector system giving the added advantage of being able to produce the thermal and electrical energies simultaneously. Beside the higher overall energy performance, the advantage of the PV/T system lies in the reduction of the demands on physical space and equipment cost through the use of common frames and brackets as compared to the separate PV and solar thermal systems which are placed side-by-side (Mohsen et al., 2009; Sarhaddi et al., 2010).

Normally, the efficiency of an ordinary solar PV module which converts electricity from the incoming solar radiation is around 15%, the rest being dissipated as heat energy. However, more than 50% of this waste heat can be generated from the solar energy (Skoplaki & Palyvos, 2009). The concept of a PV/T is still in the research stage even though the market is quite high as witnessed by the abundant manufacturers of the related equipment. Many theoretical and experimental studies of the PV/T are being carried out with water or air as the heat transfer medium (HTF) (Tyagi et al., 2012c). Researchers and inventors have also focused on the suitable products and systems with the best marketing potential which can develop the technology and advancements that can enhance the environmental ecology (Chow, 2010).

There will be several technologies, which can advantageously be applied to harness and harvest more thermal energy from the PV/T collector, such as, nanomaterials, phase change materials (PCM), etc. One of the methods of latent heat energy storage is by using PCMs wherein the material can store energy at a particular temperature by changing its phase. Enormous amount of work on the PCMs is being carried out around the world to fulfil the demand on usage of solar energy through more efficiently effective methods and systems (Abhat, 1983; Regin et al., 2008). The PCM study was initiated in 1940 by Telkes

University of Malaya

and Raymond and research works on the holistic entity were vigorously pursued further up to a certain turning, most probably due to the acute lack of the associated sophisticated equipment of the period until it was significantly needed due to the critical energy crisis in the late 1970s and early 1980s, and since then researches on the PCMs have gained much interest, especially, in the solar energy applications, such as, solar heating (Telkes & Raymond, 1949; Fuqiao et al., 2002; Lu et al., 2017). During this period many studies had been carried out by the researchers recorded in the form of books and research papers to galvanize further interests (Schmidt, 1981; Beckmann & Gill, 1984; Garg et al., 1985).

The performance investigation of a solar PV/T collector can be carried out through energy or exergy analysis (Yazdanpanahi et al., 2015b). Exergy is the energy that is available to be used. In thermodynamics, the exergy of a system is the maximum useful work possible during a process that brings the system into equilibrium with a heat reservoir. When the surroundings are the reservoir, exergy is the potential of a system to cause a change as it achieves equilibrium with its environment. After the system and surroundings reach an equilibrium, the exergy is zero. Determining exergy was also the first goal of thermodynamics. The exergy analysis can be more detailed on the realistic and practical views of process than the energy analysis itself performed in isolation. The overall exergy efficiency of the solar PV/T collector is the ratio of collected heat exergy and electrical energy from the solar radiation. The exergy is calculated by using the second law of thermodynamics to represent the values of the percentage of the energy converted from the solar radiation (Farkas et al., 2017). In addition, economic analysis can be used to determine the life cycle assessment to develop a hybrid PV/T collector system, which can be combined with a thermal absorber collector system. Most of the thermal collectors need a proper design to collect heat or to cool the system for a better performance, higher efficiency and extending the life-span of the cells. This research

University of Malaya

approach will be on the new absorber designs and a self-cleaning mechanism system specially catered to collect the thermal energy using water or PCM materials.

1.2 Problem Statement

The following specific problems have been identified in the present research work:

- Single renewable energy source that suffer from low energy efficiency are not sufficient for supplying energy sustainably.
- To achieve an efficient yet inexpensive thermal collector design and fabrication have been a major problem in the PV/T technology.
- Most of the thermal collectors need a proper design for collecting heat or cooling purposes for better efficiency performances, especially, the extension to the lifespan of the cells. This research will approach four new absorber designs for collecting thermal energy using the PCM materials.
- Effective integration of the PCM with the basic PV/T system is a challenge.
- Dust accumulation on the PV glass surface is a major hindrance to obtain an optimum energy harvest from the system.

1.3 Research Objectives

The objectives of the present research work are as follows:

1. To develop an innovative hybrid PV/T system with the PCM to increase the efficiency of the PV.
2. To design and develop a self-cleaning mechanism for the proposed PV/T-PCM system.
3. To perform an experimental investigation on the electrical and thermal performance of the newly developed PV/T-PCM with self-cleaning system under Malaysian weather condition.

University of Malaya

4. To carry out a comparative study on energy and exergy performance of the newly developed PV/T-PCM with self-cleaning system with that of the PV, PV/T, PV/T-PCM systems under the same conditions.
5. To evaluate the economic feasibility of the proposed PV/T-PCM with self-cleaning system

1.4 Scope of the Study

The main scopes of this study are as given below:

- To introduce a unique design of PV/T thermal collector and self-cleaning system that ensures enhanced thermal and electrical efficiency.
- To develop a forced thermosiphon based hybrid solar PV/T collectors and to apply both these systems separately to identify the most thermal and cost efficient PV/T system.
- To apply the prepared PCMs to the thermal absorber collector to reduce the PV temperature and possible enhancement in the overall efficiency of the system.
- The present work focuses on the energy, exergy and economic analyses of the application of PCM for thermal management of PV/T and implementation of self-cleaning system to achieve improved performance.

1.5 Significance of the Study

The contribution of this study would be most profoundly appreciated in Malaysia which optimistically stipulates the overall target of becoming an industrialized country by 2020. Similarly, the Ministry of Energy, Communication and Multimedia (MECM) has elaborated on the vision for the energy sector for 2020. According to MECM vision, every member of the Malaysian society should have access to high quality, secure electrical power and other convenient forms of energy supply in a sustainable, efficient and cost-effective manner. However, Malaysia's energy sources primarily comprise oil,

University of Malaya

natural gas, hydropower and coal and recently renewable energy sources, such as, solar power and biomass are being exploited. This study will be providing the necessary steps to utilize the renewable solar energy. In Malaysia, solar energy conversion deserves a serious consideration as the potential for solar energy generation in Malaysia depends mainly on the availability of the solar resource which varies with locations. In view of this anomaly, it is necessary to carry out a general assessment of the solar energy potential nationwide first and can then be followed up by detailed assessments in promising locations. The solar resource is a crucial step in planning a solar energy conversion project and detailed knowledge of the solar resource at a site is needed to estimate the cost effective performance of a solar energy conversion project. The economic analyses will help to identify the most promising future cost and life cycle assessments of those projects. The present study has contributed to the social community with a new type of solar PV thermal absorber, which can be utilized for domestic and industrial purposes as well.

1.6 Organization of the Thesis

This dissertation comprises five chapters with chapter 1 containing the background of the research, research aims and objectives and the significance of the study itself in broadening the body of existing knowledge. The contents of the other chapters are as follows:

CHAPTER 2: This chapter presents the review of the literature which contains five parts, namely, i) the energy analysis, ii) the exergy performance, iii) the economic analysis of the photovoltaic thermal collector, iv) the overview of phase change materials and, v) the meticulous review on the solar PV module dust and cleaning system.

University of Malaya

CHAPTER 3: The research methods of approach and operation in this research are presented in this chapter. The detailed methodology of design and development of the PV absorber, PV/T-PCM and PV/T-PCM module with the self-cleaning (SC) system has also been fully discussed. Basic equations of energy, exergy and economic evaluation have been presented in this chapter as well.

CHAPTER 4: This chapter presents the detailed results and discursive arguments on the design and development of the PV/T, PV/T-PCM and PV/T-PCM-SC systems. A comparative study has also been presented among the designed three different PV/T systems. Every system has its own pros and cons, however, the PV/T-PCM-SC system is found to be the best amongst the three and can be implemented on a large scale for domestic as well as industrial uses.

CHAPTER 5: This chapter consists of the conclusions and suggestions on the subject matter in which the main outcome of the dissertation has been precisely narrated, especially, on the main outcomes of the solar PV power and efficiency performances as compared with the PV/T-PCM-self-cleaning performances. The solar PV/T and PV/T-PCM outlet water thermal performance as compared with the electric water heater has been fully described as well. The challenging suggestions have been proposed for future work.

University of Malaya

CHAPTER 2: LITERATURE REVIEW

2.1 Introduction

In recent years, solar energy applications have grown rapidly to meet strict environmental protection requirements and electricity demands. Renewable energy sources like solar, wind, bioenergy, hydropower and geothermal energies offer highly promising CO_2 free alternatives. Despite the general awareness of the advantages of renewable energy utilization, this source of energy contributed only about 1.6% of the world energy demand in 2012. The trend is estimated to rise up to 2.2% in 2035. The delivered energy is utilized in 4 major industrial sectors, namely construction, agriculture, mining and manufacturing. The highest percentages of energy usage in the industrial sector of a few selected countries around the world, such as, China is 70%, Malaysia is 48%, Turkey is 35% and USA is 33% (IEO, 2016). The literature review of this thesis will give an overview of the present status in the related field and shows the future work in the relevant field.

Since 1970s, many research and development works have been done in photovoltaic thermal systems. Many innovative designs and products have already been forwarded for their quality evaluation by academics and professionals alike (Victoria, 2009). In 1980s, the research work was focused mainly on the flat-plate collectors. Later on, researcher analysis on the light concentration PV/T systems (Raghuraman, 1981; Braunstein & Kornfeld, 1986; Cox & Raghuraman, 1985; Lalovic, 1986). In the late 1980s for about 10 years, Garg and some researchers did detailed analyses on thermal efficiency of hybrid PV/T air and liquid heating system (Bhargava et al., 1991; Agarwal & Garg, 1994; Garg et al., 1994). The thermal efficiency calculation of flat-plate collector with the use of modified Hottel-Whillier-Bliss model was also performed (de Vries, 1998). In the mid-1990s work started in various parts of the world on creating models for various types of

University of Malaya

PV/thermal blend systems (Victoria, 2009). Many theoretical and experimental studies of PV/T were conducted with either water or air as the coolant (Florschuetz, 1975; Florschuetz 1979; Wolf, 1976; Kern & Russell, 1978; Hendrie, 1979). Single PV system can produce about 38% electricity, depending on the locations (Kalogirou & Tripanagnostopoulos, 2006). The early age PV/T system used air, water or evaporative collectors with monocrystalline/polycrystalline/amorphous silicon (c-Si/pc-Si/a-Si) or thin-film solar cells, flat-plate or concentrator types, glazed or unglazed panels, natural or forced fluid flow, stand-alone or building-integrated features, etc., (Chow, 2010; Jaaz et al., 2017). At the point when the PV module was operated under dynamic cooling condition, the temperature dropped appreciably yet the efficiency of the solar cells managed to increase between 12% to 14% (Teo et al., 2012). The total energy saving efficiency of the PV/T collector without and with reflectors are found to be 60.1% and 46.7% respectively. The thermal efficiency approximately was improved by 80% while at the same time cooling of the PV cells was made possible (Tyagi et al., 2012c; Lianos, 2017). Excessive temperature can cause serious degradation of the solar cell material and shorten the lifespan of the module. Among those technologies or designs, the system of utilization of air, liquid, heat pipes, PCM and thermoelectric (TE) devices do not only aid cooling of PV cells but also supply useful heat energy for many applications (Adham et al., 2015).

2.2 Photovoltaic Thermal Collector

Conventional solar thermal collectors are of two types, either non-concentrating or concentrating. Non-concentrating collectors includes mainly Flat Plate Collectors and Evacuated Tube Collectors, while the concentrating type covers Parabolic, Compound Parabolic Collectors and Cylindrical Trough Collector, Parabolic Dish Reflector and Heliostat Field Collector. Figure 2.1 shows a typical liquid flat plate collector while Table 2.1 shows different types of flat plate collectors (Adnan et al., 2009).

University of Malaya

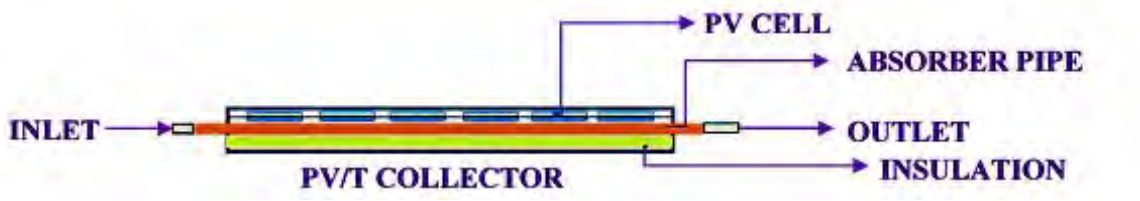

Figure 2.1: A typical liquid flat-plate solar PV/T collector

Flat-plate solar PV/T collectors are the most widely recognized for private water heating and space heating purposes. An ordinary flat-plate PV/T collector comprises an absorber, straightforward cover sheets and a protected box as shown in Figure 2.1. The absorber is normally a sheet of high thermal conductivity metal with tubes or conduits either coordinated or connected. Its surface is painted or covered to amplify radiant energy assimilation and at times to limit radiant emission (Dubey & Tiwari, 2008). The protected box gives the structure and fixing which decreases heat loss from the back or sides of the collector. The cover sheets, called coating, enable the daylight to go through onto the absorber yet protect the space in the absorber to keep cool air from streaming into it. In any case, the glass reflects a little bit of the daylight, which does not reach the absorber (Grigorios, 2009).

Table 2.1: Different types of flat plate collector pipe absorbers and their thermal efficiencies
(Adnan et al., 2009; Chong et al., 2012; Hossain, 2013)

Collectors type	**Thermal efficiency**
Direct flow	48%
Oscillatory flow	60%
Spiral flow	70%
Serpentine flow	48%
Parallel-serpentine flow	70%
Web flow	62%
Modified Serpentine-Parallel	68%
Prototype of V-trough	70%

The PV/T collector design which can achieve temperatures of up to 200°C when no fluid moves through it and along these lines every element of the materials utilized must have the capacity to repulse such heat. The absorber is generally made of metallic

University of Malaya

materials, for example, copper, steel or aluminum. The collector can be made of plastic, metal or wood, and the glass cover must be fixed with the purpose that heat does not escape and the collector itself is shielded from dust and dirt, creepy crawlies or sticky substances (Adnan et al., 2009; Chong et al., 2012).

The collector is highly protected at the back and sides to diminish the heat losses. However, there are still some collector heat losses because of the steep temperature gradient between the glass cover and the absorber with the ambient air as the convection losses are caused by the point of inclination and the dispersal effect between the glass cover and the absorber plate, while the radiation losses are caused by the exchange of heat between the absorber and the environment (Joshi et al., 2009c). The absorber plate which covers the full opening area of the collector must perform three functions: i) to absorb the maximum possible amount of solar radiation, ii) to transfer this heat into the working fluid at a minimum temperature difference, and iii) to lose a base measure of heat back to the encompassing environment (Ong, 1994). Other parts of the collector, such as, storage tanks can be connected to the water inlet and outlet flow part.

2.2.1 Active System

If the solar PV/T collectors are located at a level higher than the water storage tank, the water would not circulate between the collectors and the storage tank by natural convection. In this case, an electric pump would be required to circulate the water wherein the differential temperature controller will manage the operation of the pump (Hossain, 2013). The controller consists of temperature sensors located at the outlet of the last collector in the array and near the bottom of the water storage tank. When the temperature at the collector outlet is higher than that at the bottom of the storage tank by a few degrees, the pump is automatically activated and when the temperature of the storage tank is higher than that in the collector, the pump is then automatically deactivated (Noro et al., 2016).

University of Malaya

2.2.2 Direct System

A direct system is one in which the domestic hot water supply draw-off pipes should be non-toxic for use in contact with the solar PV/T collectors (Tripanagnostopoulos et al., 2002). The materials for construction of the collectors, storage tank and connecting pipes must be appropriately compatible in order to avoid bimetallic corrosion. Another problem common to all direct systems is the possibility of 'furring' or even 'scaling' of the tubes due to hardness of the cold water supply (Hossain, 2013).

2.2.3 Indirect System

In an indirect system, the domestic hot water supply draw-off pipe is isolated from the collector fluid by incorporating a heat exchanger in the storage tank. The heat transfer fluid in the collector may or may not be water-based, and circulation may be by either forced or natural circulation. Such a system is used when a clean, uncontaminated hot water supply is required or where freezing or corrosion is to be avoided in the collector panel (Slimani et al., 2016). An anti-freeze solution is mixed in the heat transfer fluid in the primary or collector circuit to keep the heat transfer fluid in a liquid state. A sealed expansion tank or an automatic air release valve is installed at the highest point of the primary circuit to prevent an air-lock in the collector circuit (Hossain, 2013).

2.2.4 Pressurized System

In the indirect system, the heat transfer fluid in the primary fluid circuit is completely sealed from the atmosphere. The fluid expands on being heated wherein the system becomes pressurized and provision for expansion is usually provided in the form of a diaphragm expansion vessel (Thakare et al., 2016). Low temperature is used if the difference in height between the cold water feed tank and the storage tank is not too large and a high-pressure system is used if the cold water feed is pressurized using a pump. Usually, pressurization is referred to the solar collector or primary circuit (Hossain, 2013).

University of Malaya

2.3 Energy, Exergy and Economic Analysis

This study has been conducted through three different renewable hybrid systems, such as, PV/T, PV/T-PCM and PV/T-PCM modules with a self-cleaning process. All renewable or non-renewable energy systems need a basic analysis, such as, energy, exergy in order to investigate their entire performances. However, economic analyses help to understand the system utilization, future payback cost and lifespan of usage, etc.

2.3.1 Energy Analysis

Solar PV/T collectors resembles conventional flat plate thermal collectors with an extra electrical part (PV) integrated upon it. Different methods have also been developed for modeling and simulating the thermal performance of the solar thermal collector. Many types of conventional flat plate solar thermal collectors with metal absorber plates and glass covers are widely used to transform the solar energy into heat. The performance of evacuated flat plate solar thermal collectors that have a working temperature above 100°C and the performance of evacuated tube integral collector storage solar water heater have both been appropriately measured and modeled (Ammari & Nimir, 2003; Ahmed & Mohammed, 2017; Bianchini et al., 2017).

Most of the solar energy devices work on the greenhouse effect. In order to understand this phenomenon, one needs to refer to the principles of thermal radiation which basically is the radiant energy emitted by a medium by virtue of its temperature. The wavelengths covered by the thermal radiation range approximately between 0.1 to 100μm. Short wave radiation is in the wave length of between 0.1 to 3.0μm. Solar radiation at a source temperature of about 5762 K is in the short wavelength range. Long wave radiation occurs when the wave length is greater than 3.0μm. They originate from sources near ambient temperature (Jaisankar et al., 2009; Hasan et al., 2010; Ho et al., 2010).

University of Malaya

The solar energy which is transmitted through the glass heats up any object on which the solar rays may strike. The amount of energy absorbed and the degree of heating up depends upon the coefficient of absorption. The objects in turn reradiate the energy as a heat loss at a low temperature (around 300 K) which is in the form of a long wave length radiation. Since glass is opaque to long length wave radiation, heat is thus trapped within the glass enclosure. However, a small proportion of the radiated energy from the low temperature source is lost through convection and conduction. This phenomenon is known as the greenhouse effect in which it is observed that the inside of a greenhouse is always much warmer than the outside (Hossain, 2013).

The sun has an effective surface temperature of about 5762 K and emits most of its energy between the short wave lengths of 0.10 and 3.00μm. A blackbody at a temperature of about 300 K emits radiation at a wave length above 3.00μm. Silica glass transmits 92% of the incident radiation in the wave length range between 0.35 and 2.80 μm and it is opaque at longer and shorter wavelength. The wave length band of up to 0.35μm contains 4.52% of the total solar emissive power and the wave length band between 0.35 and 2.80μm contains the rest of the solar emissive power. Therefore, 92.79% of the total radiant energy incident on the glass is in the transparent wave length range between 0.35 and 2.80 mm, hence, 85.37% of this solar radiation is transmitted through the glass (Gupta & Kaushik, 2010). These collectors are normally designed for use without top glazing or bottom insulation because of the low operating temperatures which are generally below 50°C. In Malaysia, the temperature is not so very high where the daily average temperature is approximately between 24°C and 32°C, hence, the category of the heating system is in the low temperature range.

University of Malaya

The conversion efficiency of a solar PV is relative to the daylight that the PV cell changes over into the electrical energy. This is an essential part of a solar panel because efficiency change is fundamental to making the PV energy competitive with more conventional source of energy (e.g., fossil fuels). Normally, in the event that one proficient solar panel can give as much energy as two less-productive panels, at that point the cost of that energy will be reduced. For example, the earliest PV devices was just able to convert around 1% to 2% of the daylight energy into electrical energy. Presently, the PV devices can convert 7% to 17% of the radiant light energy into electrical energy (Frankl, 2010; About, 2012; Kirn & Topic, 2017).

Solar photovoltaic energy conversion is a one-advance conversion process which produces the electrical energy from the light energy (Lianos, 2017). The sun is the source of energy and light consists of bundles of energy which are called photons whose energy depends just on the recurrence or shading. At the point when the photons are adequately thought to energize the electrons, they are then bound into strong materials up to higher energy levels where they are allowed to move. An extraordinary case of this photoelectric impact is the commended analysis which was clarified by Einstein in 1905 (Lianos, 2017).

The photovoltaic impact of the solar cells permits an immediate transformation of the light energy from the sun's beams into power, subsequently, it is the systematic process of transferring the energy inside a semiconductor material of positive and negative shafts of electric charges through the activity of light. This material highlights two regions: one is showing an overabundance of electrons while the other is an electron shortfall separately referred to as n-type doped and p-type doped. At the point when the n-type doped is carried into contact with the p-type doped, abundance of electrons from the n-type material diffuse into the p-type material. The initially n-doped area turns out to be emphatically charged and the p-doped area turns out to be adversely charged. For that specific reason, an electric field is consequently set up between them, which tends to

University of Malaya

constrain the electrons once again into the n-doped area and gaps once more into the p-doped region (Report, 2001).

This p-n region is naturally called the p-n intersection. By putting metallic contacts in the n and p regions, these regions will react as a diode. At the point when the intersection is lit up with photons having energy equivalent to or higher than the width of the adversely charged particles, these photons will then yield their energy to the particles. Every photon makes an electron move from the valence band to the conduction band. The p intersection gaps can move around the material, and along these lines, they will combine with an electron-gap. In the event that an excess of electron-gap occurs at the cell's terminals, the electrons from the n region will move back to the gaps in the p region through an external factor which increases the electrical potential (Markvart, 2002; GCEP, 2006).

The solar cell is a fundamental building piece of the solar phovoltaic mechanism which has been considered as a two-terminal gadget, much the same as a diode of some sort, which produces a photovoltage when charged by the sun's beam. This solar phovoltaic cell is, typically, a thin piece of a semiconductor material of around 100 cm^2 the surface of which is provided with mirror to absorb the radiant energy, however, much of the solar ray can be absorbed and shows up as a dull blue or dark light. At the point when the photovoltaic cells are charged by the sun's radiant energy, the associated unit produces a DC photovoltage of 0.5 to 1 volt and can produce a photocurrent of a few milliamps per cm^2 (Markvart, 2002; GCEP, 2006).

The main objective of the PV solar cell research and development is to reduce the cost of photovoltaic cell and modules to a level that will be competitive with the conventional methods of generating electric power. Basically, there are two methods of increasing the efficiency of a solar cell: (1) an appropriate choice of the semiconductor materials will enable the energy gaps to match the solar spectrum and facilitate the perfection of their

University of Malaya

optical, electrical and structural properties, (2) a properly constructed innovative engineering device will mobilize a more effective electrical charge collection as well as a better utilization of the solar spectrum through the single and multijunction approaches (Shevaleevskiy, 2008; Piebalgs & Potočnik, 2009).

At the moment, there is no proper description of what constitutes a high efficiency device which, essentially, is a component of a given innovation on how it impacts on the general cost structure. In any case, in the present situation, it is conceivable to subjectively arrange a selected group of materials into various efficiency functions: (1) ultrahigh-efficiency (>30%) devices are accomplished by utilizing a multifunction pair cell, as GaAs and GaInP2; (2) high-efficiency (>20%) cells are by and large manufactured by utilizing high quality, single–precious stone silicon materials; (3) high efficiency cells (12%-20%) are of common various polycrystalline and indistinct thin-film semiconductor materials, for example, polycrystalline silicon, shapeless and microcrystalline silicon, copper gallium indium selenide (CIGS), cadmium telluride (CdTe) and direct efficiency cells (<12%) (Deb, 2000).

The first solar power harnessing system in Malaysia was built in 2003 at Kampung Denai in Rompin on the eastern shore of Peninsular Malaysia. In a current development, the Tenaga Nasional Bhd (TNB), which is Malaysia's primary electrical power supplier, launched the development of Malaysia's first solar power plant in Putrajaya. At an approximate cost of RM 60 million (US$ 40 million) per megawatt, the project signifies a major break-through in exploiting the utilization of a sustainable power source in the country. The project would be required to empower the administrator to comprehend the system on a long period of time before setting out on the development of solar power plants on a greater scale (Shaharin et al., 2011).

University of Malaya

2.3.2 Exergy Analysis

An energy analysis is one in which the amount of energy utilized and processed will validate the energy efficiency. Energy analysis is performed based on the first principle of thermodynamics, though the exergy analysis in light is based on the second principle of thermodynamics (Sudhakar & Srivastava, 2014). The concept of exergy was developed by Willard Gibbs in 1873 and the terminology of exergy (*ex*) was created by Zoran Rent in 1956 (Rant, 1956; Pathak et al., 2014). It has been known that exergy is the work potential and it is obtained from an evaluated energy.

Exergy analysis has been recognized by many researchers and engineers to be a useful tool for the evaluation of the energy and economic performance of thermodynamic system in general. Exergy analysis gives an optional method for assessing and contrasting the solar PV energy output. Exergy investigation depends on the different evaluation representing usable energies, called exergy or accessibility, and unusable energy, called irreversibility (Dubey et al., 2009; Sudhakar & Srivastava, 2014). The exergy analysis has been progressively connected in the course of the most recent few years to a great extent because of its advantage over energy analysis. To perform energy and exergy investigations of the solar PV, the amounts of input and output of energy and exergy must be evaluated (Pandey, 2013; Kalogirou et al., 2016).

The exergy analysis can be used to evaluate both energy and exergy efficiencies. Gunerhan and Hepbasli (2007) considered the execution analysis of solar water heating system supported the exergy analysis. The analyses has been done under the atmosphere of the state of Izmir region (Turkey). Their fundamental research was basically to investigate the different components of the system, viz., flat plate solar collector, a heat exchanger and a water pump, other than to analyze the various effects of datum water temperature on exergy efficiency of different components and consequently the general

University of Malaya

system. The exergy results of the solar collector have been found to vary from 2.02% to 3.37%, that of the heat exchanger varies from 16% to 51.72% and that of the circulating pump varies from 10% to 16.67%, whereas the overall system exergy efficiency varies from 3.27% to 4.39% respectively. Ceylan (2012) developed a new temperature controlled solar water heater (TCSWH) and studied it based on the energetic and exergetic investigations. The analyses were conducted at 40ºC, 45ºC, 50ºC and 55ºC and the outlined system was additionally contrasted with the thermosiphon system. A definite correlation amongst the TCSWH and thermosiphon systems was performed by calculating the stored energy, storage tank water temperatures, volume/weight of water in the capacity tank and system efficiencies for both of the systems. The most noteworthy weight of water had been observed to be 108 kg by setting the control device at 40ºC. The normal energetic efficiency was observed to be 65% for the TCSWH and 60% for the thermosiphon system separately, and in this method, TCSWH was observed to be superior to that of thermosiphon system for a similar arrangement of working parameters. Sahin et al. (2007) had investigated the thermodynamic characteristics of the solar photovoltaic (PV) cells using the energy and exergy analyses. The authors found that the energy efficiency varied from 7% to 12% and the exergy varied from 2% to 8% respectively.

Joshi et al, (2009a) had described a model of solar PV/T system, where the exergy was analyzed in terms of outdoor weather condition. Joshi et al. (2009b) explored the performance of a PV system alone and a PV/T system utilizing the energy and exergy analyses under the atmosphere of New Delhi (India). He found that because of the PV/T system, the exergy efficiency differed from 11% to 16%. However, analysis on the PV alone, the exergy efficiency was found to be varying from 8% to 14%. Marletta and Evola (2013) had used the second low exergy analysis on water cooling system of the PV/T collector. Joshi et al. (2009b) did the intensive audit on the performance of the PV and PV/T systems to assess the energy and exergy efficiency from which he found that the

University of Malaya

exergy efficiency of the PV/T system was higher than the PV system alone as the former produced a thermal yield plus power. Al-Shamani et al. (2014) did a review of the performance and development of solar collector systems in which they reviewed the research focused on the covered and the uncovered water photovoltaic thermal collector types and their exergy analyses as well as simulation and experimental works. An overview of the PV/T collector system exergy analysis shows that the uncovered PV/T collector produces the highest electrical and thermal exergy (Marletta & Evola, 2013b). Tiwari et al. (2011) did a literature survey on the thermal modeling of a photovoltaic (PV) module and hybrid PV/T systems. The solar PV and PV/T performances on the electrical and thermal outputs were based on the mass flow rates. His survey result showed that the photovoltaic thermal module had a better performing system and further refinement work can tremendously improve its performances.

The exergy analysis can also be applied on the PV/T module with the phase change material (PCM) in the hybrid (PV/T-PCM) system to evaluate both the energy and the exergy performances. Michels and Pitz-Paal (2007) did a research on a cascaded thermal energy storage and a signal stage thermal energy storage system and they found that the energy utilization efficiency was higher than the traditional signal stage thermal energy storage system. Later on Tian and Zhao (2013) investigated and compared those systems and the results showed that the cascaded thermal energy storage not only gave a higher energy efficiency (up to 30%) but also achieved the exergy efficiency (up to 23%) more than the signal stage thermal energy storage system. Robles et al. (2007) utilized water as a PCM where he made a bifacial PV module to accordingly source the solar radiation long wavelength beams to create heat and transmit short wavelength beams to the PV module to deliver power in which he found that the bifacial PV module created around 40% more electrical energy than a conventional PV/T system. Hammou and Lacroix (2006) had proposed a hybrid thermal energy storage system using a PCM for improving

University of Malaya

heat storage of the solar and electrical energies from the PV module in which they stored the solar heat during sunny days and utilized it at night or during cloudy days. On the other experiment, they obtained the smooth electrical energy during off-peak period and utilized it during the peak periods. The results of their study showed that the electricity consumption for space heating is reduced by 32% and more than 90% of the electricity consumed during the off-peak period (Tyagi et al., 2012d). Hellstrom et al. (2003) investigated the impact of optical and thermal performance of a flat-plate solar collector onto which they added a Teflon film as a second glazing front into the PV panel from which the results showed that the overall performance was increased by 5.6% at 50°C. Martinopoulos et al. (2010) utilized polycarbonate honeycombs to improve a heat transfer in solar collectors. Metal foams (2009-2012) reviewed results showed high thermal conductivities and large specific surface area which were confirmed by many researchers to have the abilities to significantly enhance a heat transfer in phase change materials (PCMs). However, as far as the authors are aware of, metal foams have not so far been examined nor experimented for their potential capability to enhance heat transfer in recuperating tubes (Tian & Zhao, 2009; Tian & Zhao 2011; Tian & Zhao 2012; Zhao et al., 2010).

In the solar PV/T hybrid systems, the energy and exergy analyses form very important tools when sustainability and design are considered. Exergy analysis provides a more representative performance evaluation to discover possible configuration of renewable-energy systems. However, an exergy analysis is also useful when considering either the system is working alone or in complement with other system in order to identify sources of irreversibility (Kalogirou et al., 2016).

University of Malaya

2.3.3 Economic Analysis

Malaysia is one of the world's largest exporters of natural rubber, palm oil, tropical hardwoods, and so on. The country is also one of the few fortunate countries in the world where adequate supplies of oil and natural gas are available. The 1960 to 2015 GNP per capita is about US$4909.30-10878.40 and in Malaysia, conventional fuel supplies are readily and cheaply available. Solar energy is therefore considered only as a supplementary fuel source for water heating (Trading, 2017).

Water heaters are still considered luxurious household items in Malaysia. However, with the rising standard of living, now the trend is towards water heater after air conditioners which are being increasingly installed, especially, in the urban areas. It was thought previously that the middle-income group would be the most likely potential users of solar water heaters. However, the higher income group has provided the impetus to the solar water heater market. The demand for solar water heaters would depend upon the public acceptability based on economics, aesthetics, reliability and the availability and cost of conventional fuel.

It is difficult to estimate accurately the amount of hot water required daily by an average household. Different people use different amount of water and at various temperature levels. For a typical house with 3 to 4 occupants, a system with a 136 1iter hot water storage capacity can be installed. For larger houses with more than 4 occupants, a 272 1iter capacity system is recommended (Ong, 1994). Supplementary heating is unnecessary because there are hot sunny days throughout the year. Large storage tanks with electric booster elements are expensive both to install and to operate. Thermosyphon-flow systems are preferred for obvious economic reasons since they do not require circulation pumps and control units.

University of Malaya

The retail installed price of a 272 liter capacity solar hot-water heater system is presently in the region of MYR 4000.00. On one hand, a comparable 90 1iter electric storage-type heater costs around MYR 750.00 installed, while an instantaneous-type gas water heater retails for about MYR 500.00. On the other hand, the 272 1iter solar heater serves all the hot water outlets in a house. Therefore, in order to provide a similar central service, two units of the electric heater and three units of the gas heater would be required. The difference in initial costs between the solar and the conventional electric or gas system is hence around MYR 2500.00. The equivalent annual operating energy cost for an electric heating module is about MYR 755.00 and about MYR 328.00 for gas heating module. Thus, in a 4-year period, the capital cost on the domestic solar hot water system will have paid for itself as against the domestic conventional hot water system.

Furthermore, although gas heaters are the most economical, however they are more hazardous to operate with a devastating effect should any leakage occur in the gas piping system. In actual practice, 5 to 10 years are more realistic if the actual usage of hot water is considered. However, in a solar hot water heater system, the stored energy has no economic value if the hot water collected is not utilized.

Flat plate solar heat collector panels are recommended, as they are more economical to operate than the concentrating-cum-tracking types. Because of the large proportion of diffusion to direct radiation, concentrating units are generally felt to be less efficient than the flat plate units. A typical 272 1iter capacity domestic solar water heater unit would require at least 4.0 m^2 of collector area. Placed side by side, the collector panels would cover only a very small area of the building roof. In order to keep the plumbing short, the storage tank would have to be sited fairly close to the panels, leading to the close-coupled system. Aesthetically speaking, the storage tank should be hidden from view (Chen et al., 2009).

University of Malaya

Once the collector panels are set up on top of a roof, blending with the roof design or kept out of sight, it should operate reliably with a minimum of maintenance for a number of years. But, because of dirt and dust deposition in a dusty environment, the glass covers would have to be periodically cleaned to ensure high solar radiation collection efficiency. This periodic cleaning operation could be done by a group of service cleaners for a modest fee. If designed for a longer life, say, 20 years, it would be more attractive for potential users to invest in the system (Ammar et al., 2009).

For commercial and industrial utilization, forced-circulation solar water heating would have to be adopted in most cases. This is because of the large volume of water storage required. It would be better to locate the storage tanks on the roof if space is available, as this would lead to savings in piping cost and better operating efficiency. If a circulation pump is employed, a temperature differential controller would have to be incorporated into the system to activate the pump when sufficient solar radiation is incident upon the collector and to stop it when radiation is low. A typical unit for a large hotel use would be a 15 m^3 storage capacity system with about 400 m^2 of collector area (Ammari & Nimir, 2003). One of the economic considerations in installing solar water heater unit is to allocate an available area for an optimum sun radiation that it can get.

Despite the fact that Malaysia has reasonable climatic conditions for the development of solar energy and solar water heaters, there is still not much interest shown in the market because of the absence of a clear cut understanding on the working and potential advantages of solar water heaters, especially, on the high initial cost of solar water heater systems as against the simple and moderately sensible cost to buy the electric water heaters as the majority of the Malaysian families are still utilizing electric water heaters to heat their boiling water needs (Ali et al., 2009).

University of Malaya

2.4 Phase Change Material

Phase change material (PCM) are specifically applied as a Thermal energy storage (TES) medium which has been explored mostly in the recent 20 years, whilst at the same time the data is quantitatively colossal and yet hard to discover for convenient dissemination. The PCMs have three unique states, namely, hardening, liquefying and gaseous states where softening and setting are the fundamental characteristics. During these processes, the materials have the capacity to store and discharge substantial amount of energy. Taking into account of these characteristics, the PCMs are now entirely used for discharging thermal energy as well as expanding the applications (Sharma et al., 2009).

The examination of the TES can be performed by utilizing the PCMs as they manage the energy stockpiling process with effective accessibility to potential solar energy source. For the most part, sunlight based radiation, which is the most accessible source in renewable energy, can play a great role in the PCM's applications. The utilization of PCMs in the solar energy is exceptionally prevalent in the cogeneration hardware, where the power costs can be diminished during the maximum hours of usage. In these days, the PCMs are being utilized as a part of the security of energy supply, for example, PC usage, healing centers, heat assurance and idleness and so forth. Then again, utilizing the PCMs can likewise maintain a lesser use of additional hardware, which is expected to decrease the additional cost but with more additional work advantages, e.g., the range of thermal energy assurance and dormancy, where the PCMs have creditably performed in the business sector (Zalba et al., 2003b).

The usefulness of the TES is described by Abhat in (1983) which is the most related examination with PCMs application are referred by Lane in (1983) and Dincer and Rosan in (2002) respectively. Those tests involved the checking on a brimming which could reveal the types of material utilized with potential characteristics in view of their inherent

University of Malaya

physical properties, arrangement, points of interest and disadvantages. They utilized different tests with different procedures to determine the behavior of those materials during melting and freezing cycles. Figure 2.2 demonstrates an order of energy stockpiling materials (Zalba et al., 2003a).

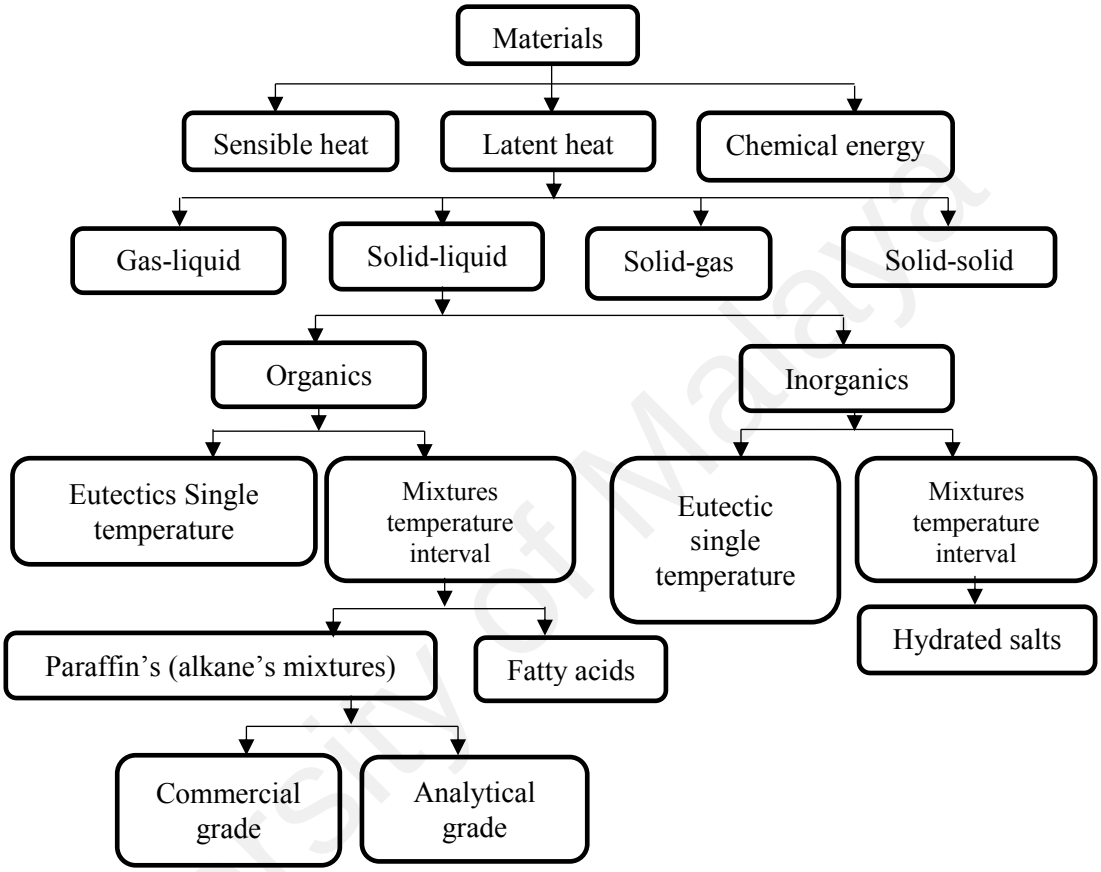

Figure 2.2: Energy stockpiling materials and their groupings (Sarier & Onder, 2012; Zalba et al., 2003a)

University of Malaya

2.4.1 Classification of PCMs

A PCM is a material which can absorb a high heat energy of combination, such as, softening and hardening at a precise temperature, whilst at the same time capable of putting away and discharging huge amounts of energy at almost constant temperature as and when required. PCMs are essentially of three types: natural, inorganic and eutectic, which can be accessible to storage and discharge of extensive amount of energy in a particular temperature range. There are numerous natural and inorganic materials in the PCM which can be distinguished in their inert heat energy of combination and softening temperatures. In view of the need of the above attributes, it is thus quite cogent to recognize the softening stage where a large portion of the PCMs does not fulfill the required stockpiling properties. Figure 2.3 demonstrates an arrangement of the PCM (Sharma et al., 2009).

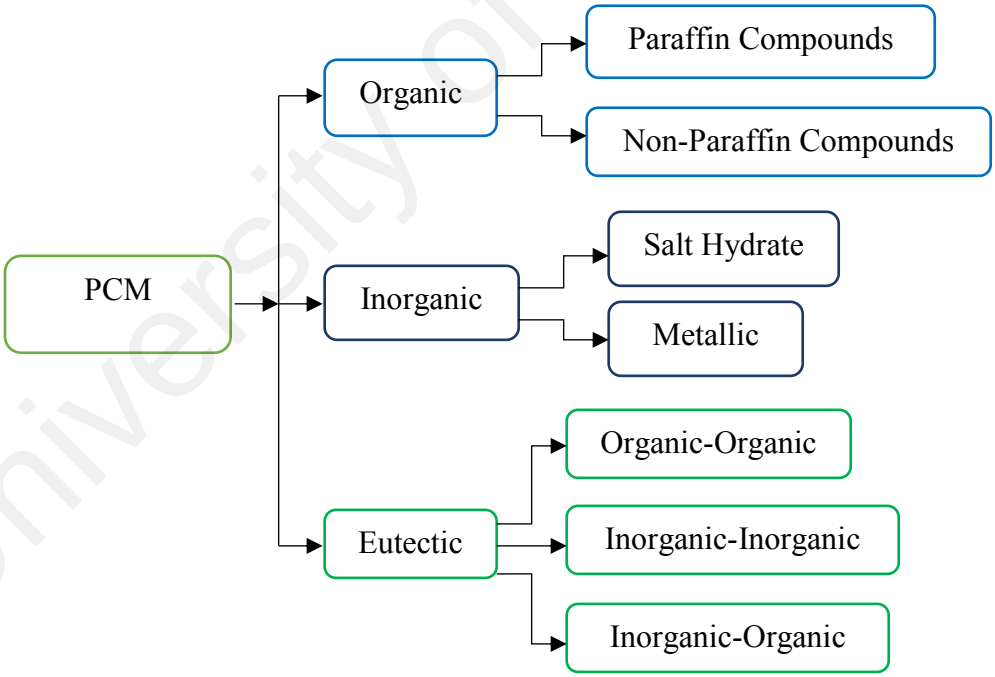

Figure 2.3: Characterization of PCMs
(Sharma et al., 2009; Xu et al., 2015)

No single material can have all the required properties of a perfect thermal stockpiling medium. One needs to utilize the accessible materials and attempts to compensate for the poor physical properties by a satisfactory framework plan.

University of Malaya

2.4.2 PCM Selection

The PCMs with a suitable adjustable temperature was chosen in the application because they have high idle heat energy, high thermal energy conductivity and special heat energy which have been found to be very suitable for a solar water heating (SWH) application (Agyenim et al., 2010). The qualities supplied by the manufacturer may change (Zalba et al., 2003a; Agarwal & Sarviya, 2016). Hence, in the pre-design stage of the PCM, it is suggested to use the right thermophysical properties of the PCMs which are for the most part described by calorimetric examinations, like Differential Scanning Calorimeter (DSC), and Differential Thermal Analysis (DTA) (Al-Hinti et al., 2010; Jamil et al., 2006). Generally, a few relevant items can be connected to the machine to gauge the relevant heat properties (Kuznik et al., 2011). Paraffin wax is the most suitable alternative because of its accessibility, non-destructiveness, good liquefying temperatures, and a minimal operating effort (Ho & Gao, 2009; Al-Hinti et al., 2010), hence the paraffin wax PCM (Sigma-Aldrich item no. 327212 (Sigma-Aldrich, 2013)) was chosen for this test. The liquefying temperature, enthalpy, and specified heat energy were measured by a DSC instrument (Perkin Elmer Pyris calorimeter DSC4000). The DSC was kept running from 30°C to 85°C at 5°C/min heating rate. The DSC curve is as shown in Figure 2.4, illustrating the heating and cooling cycles of the PCM. In the DSC curve, the dissolving temperature of the PCM was measured from the related onset temperature of the heating curve (Joulin et al., 2011). In this exploratory study, the dissolving temperature was found to be 56.06°C. The thermophysical properties of the paraffin wax utilized as a part of the analysis are as shown in Table 2.2.

University of Malaya

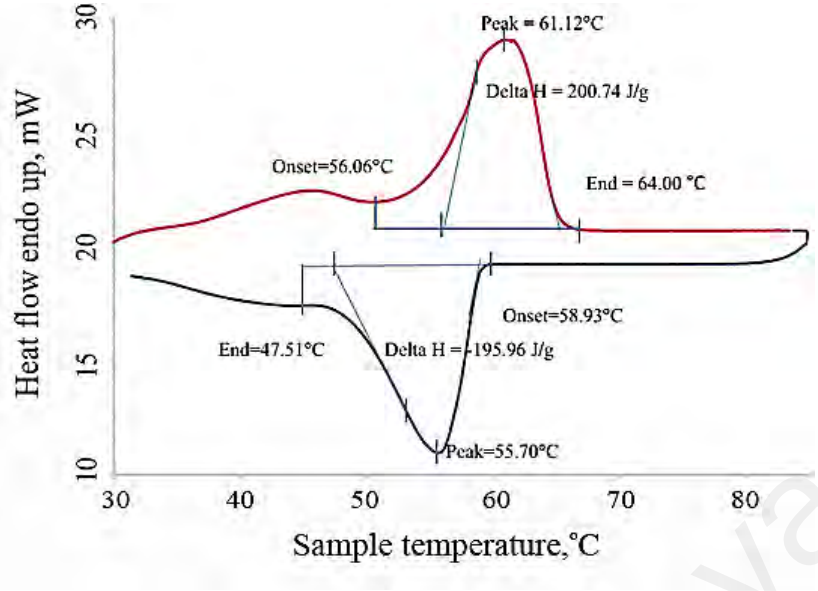

Figure 2.4: DSC curve of paraffin wax for heating and cooling (Mahfuz et al., 2014)

Table 2.2: Thermophysical properties of paraffin wax (Mahfuz et al., 2014)

Property	Values	Density
Melting point	56.06°C	900 kg/m^3
Melting end point	64.99°C	
Freezing start point	58.93°C	
Freezing end point	47.51°C	
Melting peak temperature	61.12°C	
Freezing peak temperature	55.70°C	
Specific heat of solid (b30°C)	2.565 J/g°C	
Specific heat of liquid (N65°C)	2.439 J/g°C	
Melting latent heat	200.74 J/g	
Freezing latent heat	195.97 J/g	

The researcher proposed a numerical investigation of an integrated collector storage solar water heater (ICSSWH). Two numerical models in three-dimensional demonstrations are created. The first model exhibits a sensible heat storage unit (SHSU) and the first numerical model is accepted. Taking into account of the high probability of error to be encountered between the numerical results and the trial information from writing, this sort of solar water heater introduces the characteristic of its high night

thermal losses, thus, the incorporation of a PCM specifically in the energy collector to study its impact on the ICSSWH thermal performance is proposed. As a result of this experiment, a second 3D CFD model is produced and arrangement of numerical repetitive tests are directed on two types of entities (myristic corrosive and RT42-graphite) in three ranges (R= 0.2 m, R= 0.25 m and R= 0.3 m) of this PCM layer. Numerical results demonstrate that during the day-time, the latent heat storage unit (LHSU) performs better than the one where myristic corrosion is utilized as PCM. With respect to the night working of this solar energy gathering system, it is found that the LHSU is more powerful for both PCMs as it permits lower thermal losses and better thermal storage capacity (Chaabane et al., 2014).

After going through the literature, it is found that none of the literature gives the consolidated review on the application of the PCMs in all of the solar energy systems. Therefore, in this chapter an attempt has been made to present the recent developments and advances in the applications of PCMs in the solar energy systems. The innovative configuration of the shapes and arrangement of pipes are very important in a collector, in the sense that the pipe should be properly heated by the sun. Thus, if the design is more effective, then the output temperature will increase. The parallel 2-side serpentine flow absorber collector and a modified pipe arrangement were used throughout the plate collector for the first time.

2.4.3 PCM Application in PV Panel

The working temperature of a PV cell can be as high as 80ºC in the event of availability of higher solar radiation intensities that raises the intrinsic carrier concentration in crystalline silicon photovoltaic (PV) cells to create an immediate higher immersion and to lower the voltage of the cells (Mazer, 1997). The temperature induced increment increase in current is less than the concomitant decrease in voltage yielding a net decrease

University of Malaya

in the power output of the PV. Measuring the power-voltage attributes of the PV panel at different temperatures causes a temperature-ward power loss coefficient (Radziemska & Klugman, 2002). A crystalline silicon PV module working above 25ºC normally demonstrates a temperature-ward power decrease with a coefficient of between 0.4%/K (Weakliem & Redfield, 1979) and 0.65%/K (Radziemska & Klugman, 2002). A general mix of the PV module into structures seemed to increase the PV module working temperature to the point that it accounted for a 9.3% further decreased power output compared with the non-incorporated PV module (Krauter et al., 1999). This necessitates the requirement for a successful temperature regulation of building integrated photovoltaics (BIPV). Different heat removal methods utilized to maintain a PV module at lower temperatures are as illustrated in Table 2.3.

University of Malaya

Table 2.3: Points of interest and inconveniences of distinctive thermal management procedure (Hasan et al., 2010)

	Natural air circulation	**Forced air circulation**	**Hydraulic cooling**	**Heat pipes**	**Thermoelectric (Peltier) cooling**	**PCM thermal management**
Advantages	– low initial cost – no maintenance – easy to integrate – longer life – no noise – no electricity consumption – passive heat exchange	–higher heat transfer rates compared to natural circulation of air –independent of wind direction and speed –higher mass flow rates than natural air circulation achieving high heat transfer rates –higher temperature reduction compared to natural air circulation	–higher heat transfer rate compared to natural and forced circulation of air –higher mass flow rates compared to natural and forced circulation of air –higher thermal conductivity and heat capacity of water compared to air –higher temperature reduction	–passive heat exchange –low cost –easy to integrate	–no moving parts –noise free –small size –easy to integrate –low maintenance costs –solid state heat transfer	–higher heat transfer rates compared to both forced air circulation and forced water circulation –higher heat absorption due to latent heating –isothermal natural of heat removal –no electricity consumption –passive heat exchange –no noise –no maintenance cost –on demand heat delivery

University of Malaya

Table 2.3, continued

Disadvantages	–low heat transfer rates –accumulation of dust in inlet grating further reducing heat transfer –dependent on wind direction and speed –low thermal conductivity and heat capacity of air –low mass flow rates of air –limited temperature reduction	–high initial cost for fans, ducts to handle large mass flow rates –high electrical consumption –maintenance cost –noisy system –difficult to integrate compared to natural air circulation system	-higher initial cost due to pumps – higher maintenance cost compared to forced air circulation – higher electricity consumption compared to forced air circulation, – less life compared to forced air circulation due to corrosion	–low heat transfer rates –dust accumulation on the inlet grating –dependent on the wind speed and direction	-heat transfer depends on ambient conditions –active systems –require electricity –reliability issues costly for PV cooling –no heat storage capacity –requires efficient heat removal from warmer side for effective cooling	–higher PCM cost –some PCMs are toxic –some PCMs have fire safety issues –some PCMs are strongly corrosive –PCMs may have disposal problem after their life cycle is complete

University of Malaya

Solid-liquid PCMs have been utilized as temperature controllers in special applications (Lu, 2000; Tan & Fok, 2007; Wang et al., 2007; Pasupathy et al., 2008). A one dimensional heat transfer model was created to study the cooling effect produced by integrated PCM in electronic packaging and a design optimization was clearly described (Lu, 2000).

2.4.3.1 PV-PCM system

Phase change material with PV to frame a PV/PCM system is an effective way to utilize the PV system with enhanced efficiency. To anticipate the heat and liquid element behavior of a PV/PCM system, a two-dimensional limited volume thermal exchange model was constructed hydrodynamically to highlight the Navier-Stirs energy mathematical statements (Huang, 2002; Huang et al., 2004). Trial information were utilized to accept this two-dimensional limited volume heat exchange mode (Huang et al., 2004). A parametric investigation of an application unit was additionally reported. The tentatively accepted numerical model permitted temperatures, speed fields and vortex development inside the system to be anticipated for an assortment of favourable system arrangements. The improvement in the thermal performance achieved by using metal fins in the PCM container is significant. The fins enable a more uniform temperature distribution within the PV/PCM system to be maintained (Huang, 2002; Huang et al., 2004).

At an insolation of 750 W/m^2 and ambient temperature of 23ºC, the PV cell temperature can rise to more than 45ºC. At the point when the normal ambient temperature is more than 23ºC with the occurrence of the solar radiation above 400 W/m^2, ordinary air-cooling standard plans are inadequate to keep up the high PV performance. Concentrating the PV systems has an extra cooling advantage above these systems. PCMs can absorb/release a lot of energy over a constrained temperature extent during a phase

University of Malaya

change. PCMs are of much use in different applications, such as, the heat storage and the heat transfer of the systems, and additionally for dynamic and inactive dispersive cooling of electronic gadgets. The capacity of a PCM for energy storage and temperature control relies on its heat absorbent/release properties, heat exchange routines and system arrangement (Huang et al., 2006b; Huang et al., 2011).

A good understanding on the heat exchange dynamic process inside a PCM is the key to anticipate precisely the thermal performance of PCM temperature control application system and basic system plan. Customary calorimetry, differential scanning calorimetry (DSC) and differential thermal energy investigation systems are utilized to describe the phase change properties of PCMs. Zhang and Faghri (1996) in his audit detailed the customary routines of PCM's property examination, pointed out that the logical instrumentation was both perplexing and costly and the phase change cannot be externally observed or outwardly studied (Zhang & Faghri, 1996).

Three PV/PCM systems with distinctive inner arrangements assigned as “EA”, “EB” and “EC” (Table 2.4) were built and their performances assessed. The front and back dividers of each PV/PCM system were created from aluminum. The rate of thermal exchange to the PCM was improved by an aluminum straight blade, wire lattice and strip grid balances which were connected to the PCM from the front divider. The inner dimensions of the systems were 0.04 m wide, 0.132 m high and 0.3 m long. The top and bottom parts and the vertical end surfaces of the PCM compartments were made of clear Perspex (0.008 m thick for the system EA and 0.012 m thick for the systems EB and EC) to empower the phase movement to be observed. A 0.050 m thick Polystyrene froth leading group of thermal conductivity of 0.027 Wm^{-1} K^{-1} was utilized to protect the top, base and sides of the system. The front surfaces of the systems were secured by a special

University of Malaya

solar retaining film to give known radiative properties and high solar energy retention (Huang et al., 2006a).

Table 2.4: Description of the fins used in the three experimental systems (Huang et al., 2006a)

System	Maximum fin numbers	Thickness of fins (m)	Length of fins (m)	Width of fins (m)
EA	2	0.005	0.3	0.03
EB	32	0.0005	0.3	0.029, 0.032,
EC	Strip aluminum matrix			0.035, 0.038,
	Uncoated soft-iron wire matrix			0.04

Moderately affordable accessible PCMs have a phase change melting temperature if the PV characterization temperature of 25ºC has been sourced. The RT25 (this particular material is no more accessible, however RT26 and RT27, have comparative properties) and GR40 (Rubitherm, 2000) paraffin waxes chosen for use in these examinations comprise the most straight chain hydrocarbons parts. RT25 is one of a series of paraffin waxes (immersed hydrocarbons) with a general concoction equation of C_nH_{2n+2}. GR40 is a pulverized PCM in which 89.5% of the material is in the 1 to 3 mm size grade. It comprises paraffin wax (C20H42) bound to an inorganic foundation material (SiO2). RT25 and GR40 are non-harmful, synthetically inactive where most materials used do not represent a potential risk to either human or nature. The thermophysical properties of RT25, GR40 and aluminum are as summarized in Table 2.5. The manufacturers' information shows that these PCMs are utilized as a part of the investigations and should display stable thermophysical properties through rehashed phase change cycles.

To scrutinize the changed balance courses of action on the temperature improvement after some time at the front surfaces of every system, the allied descriptions are; systems EA, EB with blades expanding 36 mm into the PCM and EC with the strip aluminum network as shown in Table 2.4. The balances were settled on a level plane in all cases. The insolation level was 750 Wm^{-2} and the surrounding temperature was 23 ± 1ºC. Every one of the systems with inner blades (EA, EB and EC) decreased the temperature rise of

University of Malaya

the PV/PCM system by more than 30ºC as compared with the datum of a single level aluminum plate at 140 min. The PV module temperature decrement was achieved by using systems EB and EC which were bigger than system EA because of the expanded metal surface zone for the heat transfer into PCM in EB and EC (Huang et al., 2006a).

Table 2.5: Thermophysical properties of RT25, GR40
(Rohsenow et al., 1998; Rubitherm, 2000)

Property	**PCM**		**Container**
	RT25 (liquid)	**GR40 (solid)**	
Density (kg m^{-3})			
Solid	785	710	2675
Liquid	749	N/A	Not applicable
Specific heat capacity (J $m^{-3}K^{-1}$)			
Solid	1,413,000	1,065,000	2,415,525
Liquid	1,797.600		Not applicable
Thermal conductivity (W $m^{-1}K^{-1}$)			
Solid	0.19	0.15	211
Liquid	0.18	N/A	Not applicable
Melting temperature (ºC)	26.6	43	Not applicable
Latent heat of fusion (J kg^{-1})	232,000	82,000	Not applicable
Kinematic viscosity ($^{mm2s-1}$) (at 70ºC)	2.4	N/A	Not applicable
Flash point (ºC)	164	187	Not applicable
Volume expansion (K^{-1})	0.001	Almost none	2.34×10^{-5}

Increased temperature in the PV panel is being harnessed by the photovoltaic-thermal (PV/T) systems which have either water or air as the working fluid. Again, the point is that in using a PV/T system also, the energy cannot be obtained in the absence of solar radiation. PCMs can be used in the PV/T systems to maximize and increase the efficiency and improve the reliability of the systems. Integration with the PCMs in PV/T systems is known as photovoltaic thermal/phase change material (PV/T-PCM) system. It is observed that it can accommodate 33% (maximum 50%) more heat storage potential than the traditional PV/T system. Reduction in temperature attained by a PV/T-PCM system is better than that of the regular PV/T system (Islam et al., 2016).

A PV-PCM system can increase the electrical efficiency in the hot climate. The energy-saving performance in the United Arab Emirates (UAE) throughout the year using a PV-PCM system was evaluated. A paraffin-based PCM with a melting range of 38-

University of Malaya

43°C is integrated at the back of the PV panel. As a result, the PV power increased 5.9% due to the cooling effect by using the PCM (Hasan et al., 2017). Thermal and electrical performance of a hybrid PV/PCM system in double skin facades (DSF) was investigated by (Elarga et al., 2016). The numerical model combines different validated codes for the simulation of optical, thermal, and electrical behavior of PCM, PV and DSF. The adoption of a PCM layer in the DSF cavity, in combination with a semitransparent PV layer, leads to a reduction in the monthly cooling energy demand in the range of 20-30%. Another combination of using both ZnO/water nanofluid and phase change material (PCM) in photovoltaic thermal systems was studied by Sardarabadi et al. (2017). In this study, the average electrical output is increased by more than 13% as compared to that of the conventional PV module. Using a nanofluid instead of deionized water further improved the average thermal output by almost 5% for the PV/T system and when the PCM was also incorporated (i.e., for the PV/T-PCM system), the increase in the thermal efficiency was approximately 9% without any extra energy consumption.

The efficiency of PV panels decreases by approximately 0.5%/K, wherein the possibility to stabilize the temperature on the panel's surface was investigated by Machniewicz et al. (2015). To meet the stated goal, dynamic simulations of the thermal and electrical performances of PV/PCM panels were carried out using the ESP-r software. Based on their results, it is concluded that additional PCM layer on the rear side of a PV panel can effectively increase the efficiency of electricity production with PCM transition temperature of about 20°C with increased electrical efficiency 0.25% of the photovoltaic (PV) panel with the use of a PCM. A modification on the PV panel (Canadian Solar CS6P-M) was made with a phase change material RT28HC (Stropnik & Stritih, 2016), in which their experimental results showed that the maximum temperature difference on the surface of the PV panel without the PCM was 35.6°C higher than on a panel with the PCM for a period of one day. Referring to their empirical results, the average increase of

University of Malaya

electrical efficiency was then re-evaluated for the PV-PCM panel with TRNSYS software. Finally, the simulation result showed that the electricity production of the PV-PCM panel for a city of Ljubljana (Slovenia) was higher by 7.3% for a period of one year.

2.4.3.2 Solar water heater

The energy obtained through a heat excess or through an irregular source (solar radiation, waste heat, and so on) includes the use of a heat storage system. In this state, a test investigation on a storage system utilizing paraffin as a PCM was completed. This system takes the form of two rectangular holes joined behind the safeguard plate of a level plate solar inert energy storage system. Estimations were performed during different climatic conditions and a proposal was made that a PCM was to be added in order to increase the performance of the solar collector around evening time. An investigation on the temperature stratification inside the PCM-rounded pits was also performed. A hypothetical solid–liquid PCM model was utilized to assess PCM liquefied volume part, liquid–solid interfaces, PCM temperature and melting/solidifying stream in the PCM-filled hole, utilized as a part of the trial study (Bouadila et al., 2014), in which a test model was designed and built in order to examine the dissolving process of a coordinated solar inert energy storage system with two PCM-filled pits. The model and the method are as illustrated below. The solar inert energy storage system consisted of electrified steel sheets with an area equivalent to 2 m^2. A straightforward glass panel was spread with 0.004 m thick polyurethane protective cover (transmission and emissivity coefficients of 81% and 94% respectively) was set up at a separation of 0.02 m from the safeguard plate. A polyurethane protection of 0.05 m thick with a thermal conductivity equivalent to 0.028 $Wm^{-1}{}^{o}C^{-1}$, was put behind the system to reduce the thermal losses through the back. A copper channel was utilized as a heat exchanger with an external distance of 0.014 m across and 0.002 m thick (Bouadila et al., 2014).

University of Malaya

2.4.3.3 Thermal management system

A direct solar radiation with a high ambient temperature can raise a Photovoltaic (PV) cell working temperature which is ordinarily negative for its life span and power output. Distinctive temperature conditions of a PV performance have been accounted for and it has been found that the productivity of crystalline silicon cells drops at a rate of around 0.45%/ºC. Different cooling strategies have been proposed to lower the PV cell temperature for higher cell efficiencies. High cooling process by a heat spreader or a heat sink can give enough cooling to get a generally low cell temperature even for a Concentrator PV (CPV). However, the heat sink surface temperature can rise considerably if no proper planned (constrained) ventilators are adequately provided. Common ventilated systems can raise the PV temperature range of 50ºC to 70ºC and forced ventilated systems are found to achieve a lower temperature range of 20ºC to 30ºC at the cost of operational electricity consumption. Constrained de-ionized fluid submersion cooling, plane impingement strategies and heat pipe cooling are mainly pertinent to the CPV systems which can perform in a temperature range from 30 to 96ºC. A PCM system constrained by its melting temperature, quantity of material to be utilized, and different system designs can produce a promising thermal management of flat plate PV potential performance and can maintain the PV temperature below its melting point, e.g., 27ºC for a generally long period of operation. A proposal to re-use the heat energy kept aside in PCM is gaining support (Dengfeng et al., 2013).

Solanki et al. (2008) demonstrated that a light fixation setup could be accomplished by utilizing mirrors or reflectors configured as a part of an Angular shape in which the V-trough dividers can be utilized to focus a light on to a 2-Sun fixation setup and also to create a heat dissemination system from the cells. Tonui and Tripanagnostopoulos (2008) introduced an air cooling system into a commercial PV module arranged as a ventilated PV/T plan by a common stream in which the wind stream was arranged to flow in three

University of Malaya

directions of approaches to enhance a convection heat exchange from the conduit dividers to the air stream. Mei et al. (2003) built up a characteristic ventilation methodology for cooling the PV exterior while at the same time using a surplus heat accessible from the ventilated PV module (Mastani Joybari et al., 2015). Yun et al. (2007) explored a ventilated PV veneer system as a characteristic ventilation system in summer.

Hegazy (2000) considered four unique models of constrained air type of PV/T modules. Russell (1981) arranged a stretched tube loaded with non-conductive fluids as an optical concentrator in addition to a cooling system for PV exhibits on which PV cells were mounted inside the tube and submerged in stationary fluid to establish a refractive list suitable for concentrating the daylight solar radiation onto the cells. Comparable gadgets utilizing dielectric fluid submerging PV cells have been performed by Abrahamyan et al. (2002); Tanaka (2007); Ugumori & Ikeya (1981) and Han et al. (2013). Russell (1982) added solar cells to a heat pipe cooling system which used direct Fresnel lenses to concentrate the sun light directly onto a series of the solar cells mounted along the length of a heat pipe of round cross-sectional area. Heat pipes have been used as a means of cooling the concentrating photovoltaic (CPV) cells as reported by Akbarzadeh and Wadowski (1996) and Farahat (2004) and have been found to be successful in a cooling method to expand a PV effectiveness. The CPV, at high temperature, exchanges heat to the evaporator segment at a high thermal flux in the heat pipe, and the heat is exchanged inside the total internal area. At that point, the heat is transferred to the blades, which are cooled by a regular convection current at a much lower thermal flux. Huang et al., (2006a) further explored the positioning and orientation of the blades in PV/PCM system. The blades improve the heat exchange in the PV and the PCM modules and are useful to hold the PV temperature close to the PCM phase change temperature. A research was conducted on the BIPV by (Huang, 2011) on an altered PV/PCM system, namely, (a) PCM heat capacity, (b) the phase transient

University of Malaya

temperature, (c) the location of the PCM, and (d) the mass in the system fins arrangement. The system has a metal divider, which is turned into a triangular shape to separate and to hold the two PCMs which can accommodate the volume expansion issue so that the divider can be a weight discharge pathway for the melted PCM. The metal mass of the cell gives a decent heat exchange to the two PCMs and is useful for a more drawn out temperature control. The PV front surface temperature developments for distinctive mixes of the two PCMs were reproduced and recorded. It can be seen that within the first hour of operation, the temperature on the front surface of the PV/PCM system has a minimal temperature increase in combination with RT27-RT21 because of its lower dissolving temperature, yet at a later phase, the combination with RT27-RT27 has the ability to control the temperature rise in the PV cells (Dengfeng et al., 2013).

2.5 Application of PCMs in Solar Thermal Energy

Solar radiation reaching earth can be harnessed in two different ways, viz., directly using the solar PV module and indirectly using the solar thermal systems. This section will cover the application of PCMs in different solar thermal energy systems for useful applications.

2.5.1 Solar Thermal Power Plants

Inactive solar thermal energy storage in the PCMs is cycled in the middle of a strong fluid which is almost isothermal and this is the right method in the heat energy storage system from steam source in the solar heat energy power plants utilizing the single reheat Rankine cycle and direct steam generation (DSG). Getting heat energy from a steady temperature storage maintained at a strategic distance from the pressure point creates large temperature variations and higher losses can happen from a normal heat energy storage regime. PCM capacity in materials with high heat energy of combination likewise can also offer a higher energy thickness for every unit mass and volume, prompting lower

University of Malaya

capacity vessels and lower cost of the storage system. Broad surveys of PCM storage alternatives for solar energy plants are also available (Liu et al., 2012). A couple of test systems of PCM energy storage at a lower and medium scale, up to several kW, have been illustrated (Bayón et al., 2010; Laing et al., 2012). The fundamental test in PCM energy storage is to assess the poor heat energy conductivity of the used storage materials that can produce large varieties of results during the release in the thermal resistance between the capacity medium and the steam in which the process produces substantial varieties in the heat energy extraction rate or the temperature of the steam delivered from its capacity or both (Laing et al., 2012). These varieties can significantly affect the performance of the heat energy cycle in the energy plant (Pandey et al., 2018).

Table 2.6 demonstrates the capacity properties utilized as a part of this work. The regular PCM sodium nitrate (NaNO3) was chosen as the capacity material described to possess great accessibility with ease in a high heat of fusion. Like other nitrate salts, it has a low thermal conductivity ($k = 0.514\ W(mK)^{-1}$) and is usually utilized with some thermal conductivity upgrades, for example, graphite/PCM composites or conductive balances. It is said to have the expansion of conductivity upgrade components by providing a higher thermal conductivity estimate, while all other PCM properties are viewed as unaffected by the thermal conductivity improvement. The quality of the outside thermal resistance was computed on a 1.5 mm thick stainless steel divider with a convection coefficient of 1600 $Wm^{-2}\ K^{-1}$ on the steam side (Yogev & Kribus, 2013).

University of Malaya

Table 2.6: Storage properties of PCM
(Yogev & Kribus, 2013)

Property	Value
PCM density	1900 kg m^{-3}
PCM heat of fusion	176 kJ kg^{-1}
PCM melting temperature	306ºC
PCM thermal conductivity	0.514 and 5 W $(mK)^{-1}$
External thermal resistance	7×10-4 m2 KW-1
Nominal discharge time	2 h
Nominal discharge flux	1000Wm^{-2} (planar) 2000Wm^{-2} (radial)
PCM slab thickness	4.3 cm
PCM cylinder inner radius	1 cm
PCM cylinder outer radius	3.1 cm

Table 2.7 displays the parameters of the Rankine cycle model with respect to the cycle parameters that accounted for the illustrative trough DSG plant in Almeria, Spain (Zarza et al., 2006). The probable energy exchange of productivity of the thermal cycle under these conditions was 36.7%. The evaporator weight and immersion temperature were adjusted accordingly to coordinate the behavior of the thermal storage system. This likewise required a change of the LP turbine gulf weight with the purpose to prevent it from entering the immersion zone during the development stage in the HP turbine. Different parameters of the cycle remained consistently all throughout the examination.

Table 2.7: Power generation cycle properties
(Zarza et al., 2006)

Property	Value
Nominal evaporator temperature	305ºC
Nominal evaporator pressure	92 bar
Nominal LP turbine inlet pressure	19 bar
Condenser temperature	46ºC
Condenser pressure	0.1 bar
Turbine inlet temperature	420ºC
Turbine isentropic efficiency	0.92

University of Malaya

In these days for all intent and purposes, every nation of the world bases their prospective models in the misuse of fossil energies in which this mode of energy consumption cannot be kept up indefinitely because of the environmental threat to both the earth and mankind. As a matter of fact, the International Energy Agency (IEA) (IEA, 2015) is currently centered around the moderation, maintainability and unwavering quality of the worldwide energy systems. Henceforth, it is important to create energy choices, for example, thermal energy storage (TES). Among the conceivable TES alternatives, numerous PCMs setup have been experimented by a few scientists as multiphase arrangements of the TES system are being outlined where various types of PCMs with distinctive melting temperatures and enthalpies are integrated or coordinated in arrangement with the purpose to upgrade the general heat transfer performance of the system. This setup is being planned to build low thermal energy storage limits in the single PCM because of the poor PCM thermal conductivities. The most suitable plan of a different PCM system is obtained by setting PCMs in a decreasing melting temperatures but in an increasing ability of melting enthalpies in the heat transfer fluid (HTF) stream during the charging process, and the other path around during the discharging process (Domanski & Fellah, 1996). Hence, to accomplish the best performance of energy change, specialists need to examine the properties of the potential materials without selecting them subjectively but rather selecting the suitable blend with the best possible dimensions for the desired application (Peiró et al., 2015).

2.5.2 Parabolic Trough Collector

Concentrating systems are utilized for power generation applications, however, later applications incorporate mechanical procedural heating and domestic cooking. Kumaresan et al. (2012) had directed an exploratory study to examine the performance of a solar parabolic trough collector (PTC) incorporated with an energy storage unit. The system comprises of a PTC, a TES tank containing 230 L of Therminol 55, which is

University of Malaya

additionally utilized as the heat transfer fluid (HTF) and a positive dislodging pump. A rise in the temperature of the Therminol 55 in the energy storage tank occurs in the test trial conducted for a day, and the operating parameters, similar to the collector's heat gain and thermal efficiencies of the individual/general segments of the system are assessed and reported alongside the operational experience picked up.

The accompanying proposals are recommended to lessen the heat loss during the dissemination of the HTF in the stream circuit (Kumaresan et al., 2012):

(i) Lay the piping inside through the dividers of the lodging element with well-related materials, establishment of choices and associated procedures.

(ii) The idea of utilizing a versatile storage unit for high energy rise in the PCM unit amid the daylight hours, and the utilization of this storage tank similar to the use of a LPG barrel, are prescribed to minimize the heat loss during the charging and energy exchange procedures.

Galione et al. (2015) explored a 50 MWe power plant by utilizing a multi-layered strong PCM thermocline-like thermal storage concept for CSP. The multi-layered solid-PCM (MLSPCM) idea is utilized for outlining a TES system for a CSP plant with the measurements and working states of an illustrative trough plant of 50 MWe, like Andasol 1 (Granada, Spain). The performance assessment of each of the proposed models is, for all intent and purposes, tested by a method using a numerical technique which considers the heat transfer and liquid flow phenomena present in these gadgets. Two arrangements of cases are viewed as one with the target of testing the TES systems separately by characterizing particular working conditions and taking the systems to an intermittent relentless state, while the other is expected to assess their performance following a few days of operation in a CSP plant, in which the climate variability and the thermal behavior of the tank dividers and related parameters are reproduced. Thermal performance parameters, for example, the aggregate energy, the stored/discharged energy and the

University of Malaya

productivity in the utilization of the energy storage capacity, are ascertained and contrasted with those acquired by other thermocline-like setups (single-strong and single-PCM), and with a reference to 2-tank liquid salt system.

2.5.3 Parabolic Dish

This paper researches the utilization of a heat storage extracted from a concentrating solar heater for hot water supply. Paraffin wax was chosen as a suitable phase change energy material and it was utilized for discharging the heat as a part of two diverse protected energy suppliers. The paraffin wax received the boiling water from the concentrating solar dish. This solar energy discharged into the PCM unit which acted as an ideal heat storage medium. The huge amount of solar energy was discharged during the day time while some heat was recovered for a later utilization. The water temperature was measured in a regular interval of time. The four cases were concentrated on utilizing water as a capacity material with and without the solar tracker. Additionally, a PCM unit was used as a heat storage material with and without a solar tracker. The system working time was extended to around 5 hours with a solar tracker by a concentrating dish with an added PCM to the system. The utilized apparatus comprises the accompanying three fundamental parts (Chaichan & Kazem, 2015), namely,

(a) Concentrator,

(b) Heat exchanger,

(c) Conical distiller.

Table 2.8 shows the means of recording the thermo-physical properties of the utilized paraffin wax as a part of the study. Every one of these properties was tested and measured at the Compound Eng. Dept. Research centers, UOT, Baghdad.

University of Malaya

Table 2.8: Thermophysical properties of the used Iraqi paraffin wax (Chaichan & Kazem, 2015)

Material property	Range
Melting temperature (°C)	45
Latent heat of fusion (kJ/kg)	190
Solid liquid density (kg/m^2)	930/830
Thermal conductivity (W/m°C)	0.21
Solid/liquid specific heat (kJ/kg°C)	2.1

2.5.4 Power Tower

Concentrated solar power (CSP) with heat storage capabilities is the need of the occasion to fill the demand and supply gap. As per the current trends, solar power towers will be the least expensive CSP harnessing innovation in 2020 (Sargent and Lundy LLC Consulting Group, 2003). The heat storage entity settles for the time being the confusion between the solar oriented energy supply and the power demand. The best class of heat storage in the solar power tower plants consists of two-tank direct available energy storage utilizing liquid salt made of 60% by weight of $NaNO_3$ and 40% by weight of KNO_3 (Kuravi et al., 2013) which was a solar power tower plant with a two-tank liquid salt energy storage as mentioned by (Carlqvist, 2009). In the charging process, frosty liquid salt is pumped from a cool energy storage tank (290ºC) to the focal receiver where it is heated up to 565ºC after which it is discharged into a hot energy tank. At the point when the discharged energy is required, the hot liquid salt is pumped to a steam creating system that delivers superheated steam at the probable states of 540ºC and 125 bar for a two-phase Rankine-cycle turbine. At that point, the cold liquid salt is returned from the steam generator at 290ºC and discharged to be exposed to the harsh element tank again. It is to be noted that for a period of 6 hours of operation of a 50-MW power plant, roughly, 7300 tonnes (3900 m^3) of $NaNO_3/KNO_3$ equivalent volume of liquid salt are required.

University of Malaya

The properties of $NaNO_3/KNO_3$ liquid salt are obtainable from the Solar Counsel Model (NREL, 2009).

In contrast to the cutting edge of a normal energy storage unit, the phase change energy materials (PCMs) have the capacity of possibly discharging more energy per unit volume, operating at a lower cost for each unit of discharged energy (Gil et al., 2010). The phase change heat capacity has been used in various low temperature applications and is a well thought innovation for a high temperature heat capacity in the concentrated solar power applications. When the solar radiation is available, the heat acquired from the solar collector by the HTF can be discharged into the PCM by changing the physical state of the PCM from a solid state to a fluid state, which is known as the charging process. When the occasion arises for a higher power demand or during shady periods, the discharged heat can be recouped and utilized for a steam energy operation. During the discharging process, the PCM process can be stopped by exchanging the discharged energy with the HTF (Liu et al., 2014).

2.6 Application of PCMs in Heating and Cooling of Buildings

Phase change materials (PCMs) offer potential as a latent heat energy storage technique to provide energy efficient systems in new and existing residential buildings. Due to their unique characteristic of high storage densities and latent heat properties, PCMs deliver opportunities for greater energy storage in many applications for residential buildings. This section will cover the application of PCMs in different heating and cooling systems for building applications.

2.6.1 Heating Application

In the past few years, the use of energy for heating as well as for cooling applications in buildings are daily increasing relentlessly. In most of the developed and developing countries, there are industrial researches conducted to discover the new and more efficient

University of Malaya

technologies to minimize the energy consumption and increase the energy efficiency of new and existing buildings. Presently, the building sector is consuming more than 40 % of the total energy consumption globally. It is also expected that by 2035 this sector will be the fourth largest contributor to CO_2 emissions. Heating is the major global requirement in Europe and other continents. However, cooling is consuming more energy in Asian buildings and structures. To minimize the energy consumption in buildings it is essential to improve the research on solar energy based heating and cooling technologies, as well as in the development of new energy storage materials for building components. PCMs have been proven to possess the potential to store large amount of heat and cold energy during the phase change process. PCMs can provide a solution of high potentialities since they can store and release more energy in the latent form with construction materials in existing or future buildings. In the past decades, PCMs and various building materials were used to increase their thermal mass. PCM is also providing very attractive energy storage capacity for several heating applications in buildings, like walls, wallboards, under floor heating and other parts of the structures. Vicente and Silva (Vicente & Silva, 2014) did experimental work on brick masonry walls with PCM microcapsules. The results showed that the PCMs had a good potential as a thermal energy regulator of the internal space conditions with insulation layers. They also found that PCMs can also contribute significantly to achieve a high energy performance, thus, it can also reduce the use of air-conditioning systems. They used three model wall specimens, i.e., (i) reference masonry wall (without PCM) (M1), (ii) masonry wall with PCM (M2), (iii) masonry wall with PCM and insulation materials (M3). They used 10mm thick insulation of wall (M3) on the outer layers. All wall specimens were with the same external dimensions. The steel microcapsules were filled into a plastic tube and the paraffin PCM in a liquid state. After the wall preparation, each wall was inserted with a ring unit to be tested.

University of Malaya

A piece of PCM was laid under the floor as a heating element in combination with PCM wallboards for space heating by Barzin et al. (2015) and conducted a series of experiments in two identical test huts. They developed a PCM under a floor heating system which showed a successful peak load shifting. A PCM based wallboard system was installed in the interior walls of the room to provide the energy storage. The results showed that the application of the under floor heating system in combination with the PCM wallboards enabled a very efficient energy usage that achieved a total energy saving and electrical cost saving of 18.8% and 28.7%, respectively.

An experimental evaluation of the PCM-based TES units for building applications was done by (Soares et al., 2016) who carried out the heat energy transfer analysis on the PCM based energy storage system filled with different PCMs. They also worked on the PCM arrangement for specific building applications for regulating thermal energy during charging. During discharging of the PCM, five parameters were evaluated, i.e., time for solidifying the PCM in the mid-plane; time for starting crystallization; sub-cooling period; phase-change temperature after sub-cooling; difference between the solidifying temperature and the cooled temperature. The results showed that a physical convection in the free-form PCM must be considered in any simulation to fully describe the energy charging process. However, during discharging, the sub-cooling process must also be considered. Experimental work on the investigation of PCM based TES system for solar air heating applications was also done by Esakkimuthu et al. (2013) who tested the feasibility of PCMs based energy storage unit with a solar air heater and found that at high mass flow rates, the collector efficiency was higher and the value of the heat energy transfer coefficient was higher at the higher mass flow rate. The mass flow rate of 200 kg/h was able to provide the uniform heat energy exchange rate with a minimum additional energy consumption during charging and discharging processes. They also achieved the lower mass flow rate of air during the discharging process to utilize the

University of Malaya

maximum energy capacity of the energy storage system with a uniform supply of heat energy for a longer period after the sunshine hours.

A low cost PCM viz. fatty acids/glycerides based high density polyethylene (HDPE) pellets for energy storage application in building envelopes has been tested by Biswas & Abhari (2014). The cellulose insulation based PCM/HDPE pellets were applied on to an exterior wall of a test building in a hot and humid climate and experiment was carried out for a several months. They also tested the numerical model for the actual performance of the PCM–HDPE pellets on the wall and found its heating and cooling loads reduction with lesser electricity consumption. Agarwal and Sarviya (2016) examined the shell and tube based latent heat energy storage system where paraffin wax was used as the heat energy storage material and air as the heat energy transfer fluid (HTF). The thermal energy performance of the system was evaluated in terms of charging and discharging performances of the stored energy and the results showed that the latent heat energy storage based system was suitable to supply the hot air for drying of food product during non-sunshine hours or when the intensity of solar energy is very low. A new and promising PCM based technology in a concrete core slab as a TES medium was tested for building envelopes by Navarro et al. (2015) who used the idea of an internal slab as a TES system to cover the partial energy demand during heating and cooling periods of the country in which the first idea was to melt the PCM to store the heat energy and the second idea was based on night free cooling. When the external temperature is below the phase change temperature (21°C), the outside air is injected inside the slab to solidify the PCM. In this work, they used prefabricated concrete slabs incorporated with macro-encapsulated PCM in small tubes inserted in its cavities. They also tested this prototype system with a two-storey house with similar ambient air conditions. After the experimental and theoretical examinations, the concept had proven the results to be worthy of demonstration.

University of Malaya

2.6.2 Cooling Applications

After carrying through literature survey on solar energy demand, it was found that the demand of air conditioning in residential and commercial buildings is increasing rapidly especially, in developing and under developed countries. This is due to three main reasons viz.

1) Increase in per capita income due to the development of GDP and economic developments of the country,

2) The rise of the internal heat energy gains of buildings and the urgent demand of comfort by the occupants, and

3) The development of new and viable technologies in the affordable cost for cooling living environment (Ioan & Calin, 2013; Tyagi et al., 2012a).

Due to the huge demand of air conditioning in buildings and industrial sectors, researches on different cooling technologies based on renewable energy have been given much attentive priority (Akeiber et al., 2016; Artmann et al., 2007). The recent meeting held in Paris (France) on the global climate change (COP21) summit was focused to promote renewable energy based technologies to overcome the problems related to climate change. Due to the rapidly growing demand on of building air conditioning, it has thus pushed up the huge production of cooling energy to meet the country's rising energy demand, hence, the energy storage system also be a viable solution (Tyagi et al., 2012b; Yu et al., 2015). Cold energy storage systems by the use of PCMs can also be another effective way to improve the building thermal energy performance. To reduce energy consumption of air conditioning in different sectors, the cold energy can be stored in the PCMs based energy storage for later use. The PCM based system can also be used to avoid the temperature increase in buildings above a certain level (Hasanuzzaman et al., 2016; Sharma et al., 2015). To meet the cooling requirements in commercial and residential sector, PCM can be installed in passive or active systems. Passive systems do

University of Malaya

not use active mechanical system and no additional energy is required. In other words, the hot or cold energy will be stored or released in accordance with the temperature fluctuations in the building when the air temperature rises or falls beyond the thermal comfort. Passive systems are those systems that can be integrated with in the building envelope (roofs, walls, and floors) in the form of false ceiling, wallboard or insulation. They do not need mechanical cooling system to achieve the PCM thermal energy charging or discharging. This PCM can also be used in energy storage units with air-conditioning systems while the cold energy can be stored through the free energy cooling unit or solar energy based absorption cooling system (Osterman et al., 2012). Night ventilation systems have a high potential of energy saving with typical reductions of energy consumption 30% to 50% in respect of cooling load of the building (Tyagi & Buddhi, 2007). If night ventilation system is well designed, peak operating temperatures can be reduced on the following day with typical reductions of 2°C to 5°C. Several studies have been carried out to investigate the potential of PCMs based free cooling system and solar energy based absorption cooling system (Tyagi et al., 2013; Wang et al., 2013; Mastani Joybari et al., 2015). Normally, the effectiveness of these systems are highly dependent on climatic conditions, solar heat gains, overall heat energy transfer coefficient of roof and walls and building thermal mass.

2.7 Overview of Solar PV Module Dust and Cleaning System

There are different types of solar PV cells which make up the solar PV modules, such as, silicon crystalline, multi-crystalline, monocrystalline, and silicon amorphous, etc. In photovoltaic technology, the solar PV cell can be described as a device that produces a direct current and power fluctuating with the flux of sunlight (Ahmed et al., 2013b). Solar PV system can be either grid connected or off-grid application. The output power and efficiency of solar PV is rated by the manufacturer under Standard Test Conditions (STC), solar irradiance of 1000 W/m^2; and panel temperature of 25°C (Carrillo et al., 2017).

University of Malaya

These conditions are easily recreated in a factory but the situation is different for outdoor environment. It is essential to know what are the active elements that can effect and reduce the efficiency of solar PV. The solar PV model efficiency can be affected by the variable meteorological parameters, such as, solar radiation, ambient air temperature fluctuation, humidity, dust, wind speed, tilt angle, shadows, snow, pollen, sea salt, dirt, bird droppings, and so on. The dust may contain ash, limestone or red soil, etc., which can usually stick to the PV array by Van der Waals adhesive forces of particulate matter and it is just as difficult to clean. There are four methods of cleaning the dust from the solar panel, such as, natural (dust drained off by rain drops), mechanical (wiping with soft cloth), electrostatic and electromechanical (Ahmed et al., 2013a).

2.7.1 Dust Accumulation

PV technology is well-known to produce electricity and its worldwide demand is increasing by the day. At the same time because of the worldwide environmental pollution, the PV power production capacity seriously drops. A report says, because of the accumulation of dust and particulate matter on the PV plate, the energy yield of solar power is drastically reduced from 17% to 25% annually in India. In Colorado USA, it was found that 4.1% less light transmission was missing because of dust accumulation on the PV plate (Chandrashekhar, 2017). Hassan et al. (2005) studied the effect of airborne dust accumulation on PV performance and observed a decrease in efficiency from 33.5% to 65.8% for an exposure of 1 to 6 months, respectively, which can be considered as a colossal amount of energy loss in the long run. A recent performance analysis conducted by Kymakis et al. (2009) on a grid connected PV park in Crete Greece, attributes the power loss due to soiling (dust deposition) to the type of dust, the length of time since the last rainfall and the cleaning schedule. The analysis, however is based on a much older study (Townsend & Hutchinson, 2000) and indicates an annual soiling (dust deposition) loss of 5.86%, with the winter losses being 4-5% and 6-7% in summer. In Malaysia, Pande

University of Malaya

(1992) mentioned that PV glass cover dust accumulation reduced the peak power around 18% efficiency and power loss difference between mud and talcum deposition (Pande, 1992). Ju and Fu (2011) of China say that PV glass of 1 year reduction during rainy season and dry season is 0.98 & 0.95 respectively. In order to investigate the dust effect on overall efficiencies of PV energy yield, a research was divided into 3 phases with the first one being on planning, the second one being on development and the last one was on operation. In Saudi Arabia, Alhamdan et al. (2009) used polyethylene sheet to cover 13 square meters of surface light receptors and irradiation was reduced around 9% and one month later after a rain downpour to wash the surface, the irradiation was reduced by 5% loss because of accumulation of dust, soil, sand and the prevailing dry condition. Mekhilef et al (2012) covered PV glass and cells and investigated the effect of dust on the PV performance as function of tilt. The study shows that an average deduction in power output in different countries, for example, a power output reduction in Saudi Arabia by 40%, in Kuwait round 65%, in Egypt 33–65% and in USA 1-4.7% through accumulation of particulate matter, such as, pollens, fungi, bacteria, vehicular & volcanic atmospheric airborne residue (Maghami et al., 2016).

2.7.2 Cleaning Systems

Mani and Pillai (2010) had done some work on PV glass, and thorough investigation on literature survey after 1960, and upon identifying cleaning as well as environmental factors like the causative elements, suggested the best way for cleaning. In high latitude climate, the temperature ranges between -2 to 16°C, where the average annual precipitation is about 31 cm. Those areas should receive an adequate weekly natural cleaning cycle. On the other hand, in the Mediterranean climate, the temperature ranges between 10-40°C, where the annual precipitation is about 42 cm where cleaning is recommended once in a week or 2 weeks depending upon the rate of dust accumulation on the surface. Kaldellis and Fragos (2011) carried out investigation to look into the

University of Malaya

energy production of two PV-panels: the first being clean and the second being artificially polluted with ash and they detected a 30% energy reduction per hour along with 1.5% efficiency loss for ash accumulation reaching up to 0.4 mg/cm^2. The impact of different amount of mass deposition of ash on a PV energy performance was investigated by Ahmed et al. (2013). As shown in Figure 2.5, a drop in energy between the clean and polluted panels is found to vary between 2.3% and 27% as recorded within a period of 1 hour.

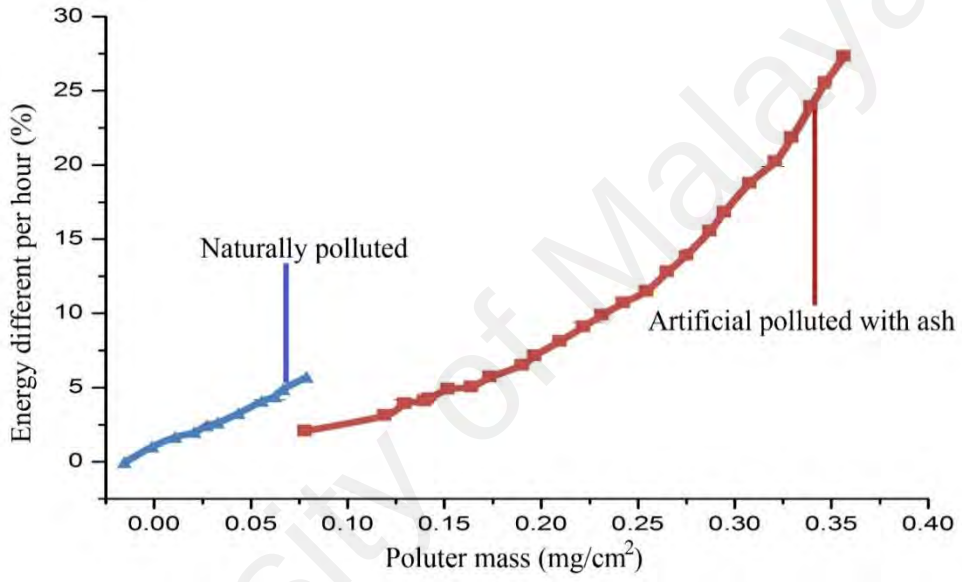

Figure 2.5: Energy difference between clean and the polluted pair panel (Ahmed et al., 2013b)

2.7.3 Methods used to clean PV panels

For solar power to be efficient, some methods need to be used to clean the PV panels. Some cleaning methods or technologies describe bellow:

2.7.3.1 Heliotex technology

Heliotex is an automatic cleaning system which washes the solar panel surface with artificial rinses. The cleaning process can be controlled by microcontroller programming whenever it is necessary and depending on the environment situational conditions (Renewable Energy centre, 2017).

University of Malaya

2.7.3.2 Robotic cleaning system

Robotic cleaning system is designed for cleaning the surface of the PV panels automatically to maximize the output of energy. It is composed of a cleaning head and a drive system. The cleaning head has two cylindrical brushes traveling upward and downward along the PV panel surface edges by a pair of motorized trolleys to generate a clean PC array (Renewable Energy centre, 2017).

2.7.3.3 Electrostatics cleaning system

Electrostatics cleaning technology is called "Harvesting electricity". Electrostatic charge material is used on a transparent plastic sheet or glass which covers the solar panels. There are some sensors to monitor the dust levels and activate the system into a cleaning mode. The dust will be shaken off the solar panels when an electrically charged wave breaks over the surface material (Renewable Energy centre, 2017).

2.7.3.4 ProCurve cleaning system

ProCurve is a manually cleaning system of a solar panel surface. The system contain is provided with microfiber wash sleeve, sleeve bar, a handle and a squeegee channel with rubber. This system is very easy to be in domestic solar PV panels but cannot be used for big PV power plants. (Crossley, 2015).

2.8 Summary of Literature Review and Research Gap

The main objective of the present research is to improve performance of a solar photovoltaic system. From the literature review, it is found that the efficiency can be improved by a combined system, such as solar photovoltaic and thermal collector. In this regard, the hybrid PV/T system with a new absorber collector design may provide better efficiency by reducing the temperature. It will also increase the life cycle of the PV panel due to reduction in temperature. However, it offers many problems during outdoor operations, like low efficiency, temperature increase, absorption of dirt and dust on the

University of Malaya

upper surface due to different environmental conditions. These hybrid collector systems use phase change materials (PCM) for absorbing thermal energy from the PV panel. These materials are used for collecting heat or cooling any system for better performance. The self-cleaning circuit also has already been proposed to solve the dust problem on PV panels. This will not only increase the efficiency but also increase the life cycle of the PV/T system and reduce the payback period also. The experimental data will be evaluated using energy, exergy and economic analyses.

University of Malaya

CHAPTER 3: MATERIALS AND METHODOLOGY

3.1 Introduction

Photovoltaic thermal (PV/T) collectors have been increasingly popularized as different designs are being developed from different perspectives, such as, stand-alone PV/T, building integrated PV/T, etc. While all the designs are still going through researches and development works, it is worthy to focus on how to extend the usability of these devices beyond the sunset. Presently the research work is aimed to develop a sustainable solution for prolonged storage and usage of thermal energy produced by the PV/T as well as to provide a solution to alleviate the dust accumulation problem on the sensitive PV glass surface. To provide a feasible resolution to both problems, a photovoltaic thermal collector using phase change materials as thermal storage and employing an autonomous self-cleaning mechanism, has been proposed. An experimental method of investigation has been adopted to arrive at dependable solutions to the problems as mentioned above. The basic phases involved in this investigation are to design a PV/T-PCM system with a self-cleaning mechanism, to fabricate a prototype of the system, to make experimental runs under various anticipated stringent conditions and finally to analyze the performance of the system based on energy, exergy and economic perspectives. The subsequent sections of this chapter presents the detailed methodology of the present research work including the methods of design, fabrication, experimentation and performance analyses.

3.2 Fundamentals of the System

Before the inception into the design and fabrication of PV/T-PCM with self-cleaning system, it is worthy to discuss on the fundamental working principles of the subsystems, i.e, PV/T system, PCM thermal control and self-cleaning system.

University of Malaya

3.2.1 PV/T System

A photovoltaic thermal (PV/T) system is a combination of technologies that amalgamates photovoltaic (PV) module and solar thermal collector (STC) in a single unit and facilitates the production of heat and electricity simultaneously. The working principles of a PV, a STC and a hybrid PV/T, PV/T-PCM and PV/T-PCM with self-cleaning systems are as shown in Figure 3.1 and Figure 3.2. It can be seen that the solar thermal system is based upon the rules of the open loop system. PV/T technology allows a large portion of the solar energy incident on the collector to be turned into useful thermal and electrical energy. A primary feature of this system is that the efficiency of a PV panel decreases as the cell temperature increases. Water or air flowing through the thermal collector removes the heat from the PV cells, allowing for more efficient operation. In addition, water or air heating and electricity can be produced within the same module, resulting in a more efficient use of valuable restricted space.

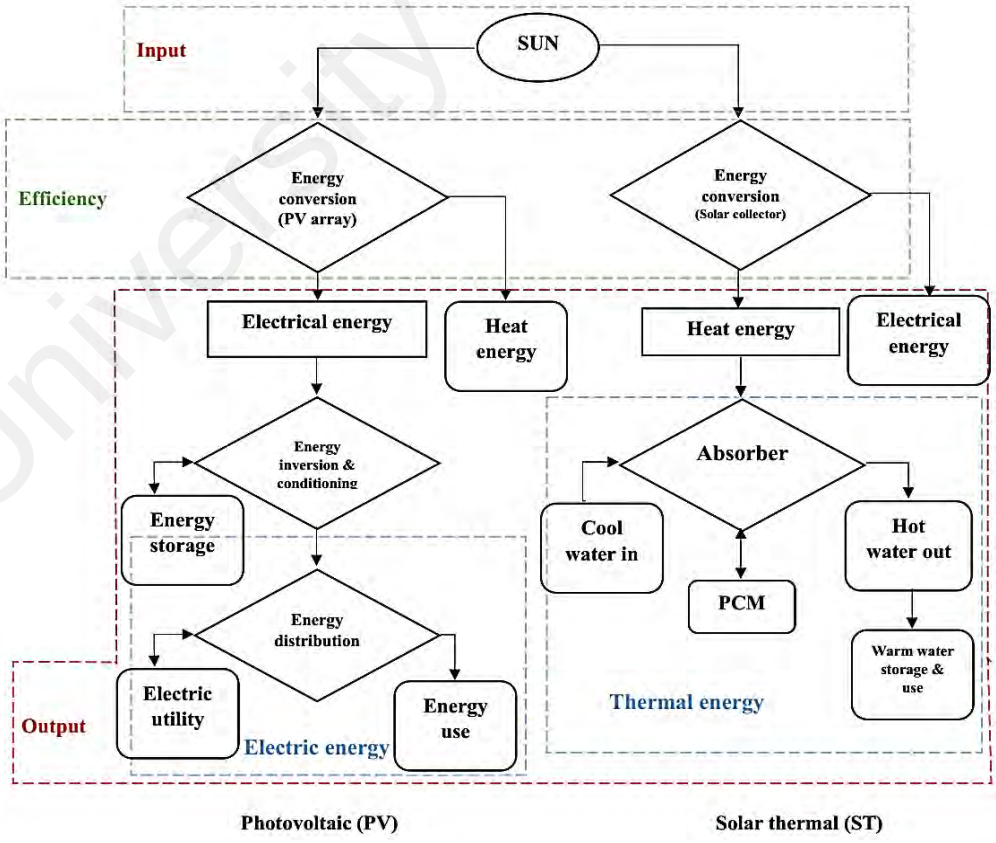

Figure 3.1: Working principle of a PV and solar thermal system (Kumar et al., 2015)

University of Malaya

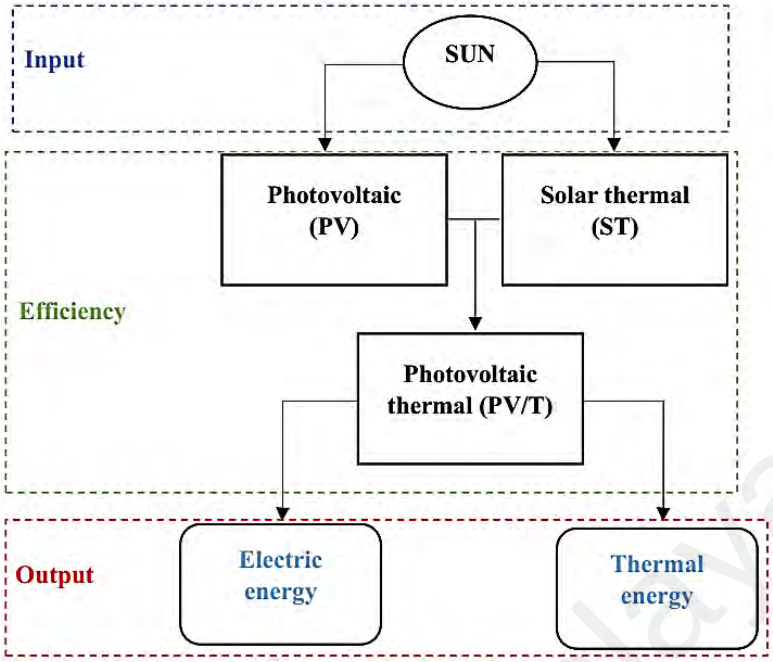

(a)

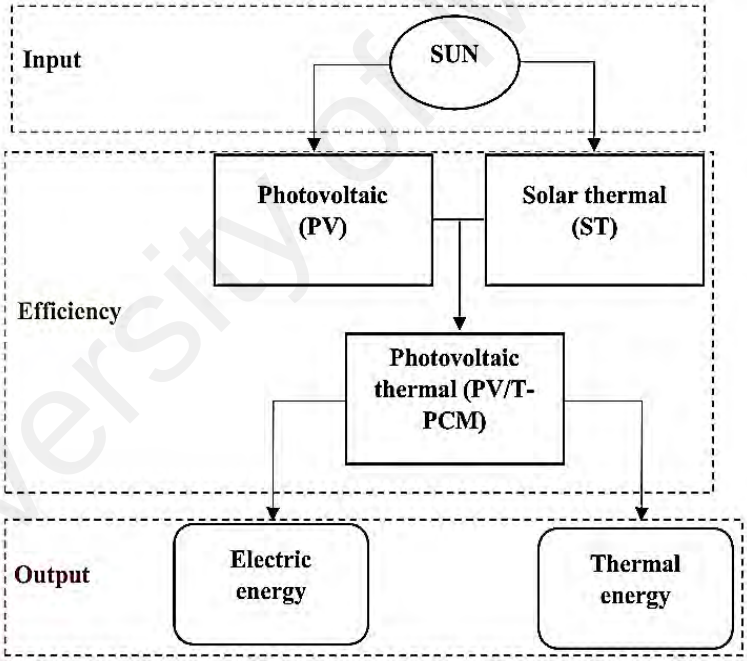

(b)

Figure 3.2: Working principle of a (a) PV/T, (b) PV/T and (c) PV/T-PCM with self-cleaning hybrid systems

University of Malaya

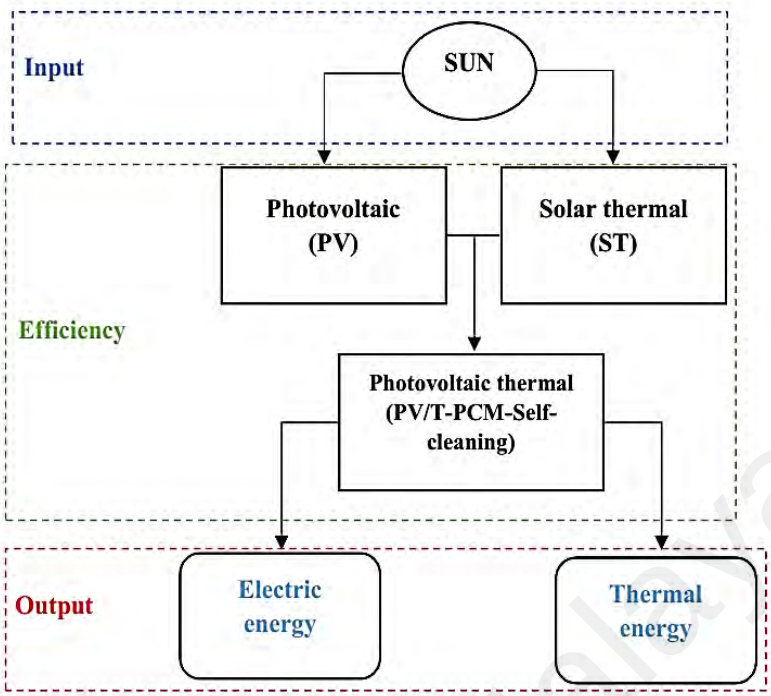

(c)

Figure 3.2, continued

3.2.2 PCM Thermal Control

Thermal storage and management is an important issue in the solar energy conversion sector. Phase change material (PCM) technology is a promising option in thermal management and control since it not only offers a huge amount of heat storage, but also delivers heat at target-oriented temperatures along with a long-term reliability and a processing efficiency.

During a physical phase change of state of a PCM, a large amount of latent heat can be stored or released at an almost constant temperature. Thus, energy can be stored or released at a small temperature difference. The phase change could be solid/liquid or liquid/gas, however, liquid/gas transformations are not practicable due to the large volume changes or high pressures required to store the materials in the gas phase.The energy density could be increased by using a PCM which has a phase change within the temperature range of the storage capacity.

University of Malaya

Any materials to be used for the PCM in the TES systems must have a high latent heat and a high thermal conductivity, in other words, they should have a melting/freezing temperature lying in the practical range of operation, i.e., melt/freeze congruently within a minimum subcooling temperature and be chemically stable, low in cost, nontoxic and non-corrosive. In the present research, five different PCM materials are tested with DSC, from which lauric acid is selected based on experimental requirement. Table 3.1 shows the melting temperature range of the five PCMs.

Table 3.1: Properties of PCM materials (Sigma-Aldrich, 2013)

Name of PCM	Melting temperature range (°C)
Paraffin	52-54
1-tetradecanol	36-40
Lauric acid	44-46
Decanoic acid synthesis	27-32
Decanoic acid natural	29-33

3.2.3 Self-cleaning Method

The solar PV modules are generally employed in dusty environments which are not covered as in the case of most tropical countries. The dust incessantly accumulates on the top surface of the module and ultimately hampers the pure incident light from the Sun, thereby reducing the power generation capacity of the module. The power output can thus be reduced by as high as 50% if the module is not cleaned for a month, tantamount to a great loss of available solar energy (Halbhavi et al., 2015). The accumulated dust sticks on the PV module panel by means of Van der Waals adhesive force, which is mainly dependent on the particle size and moisture content on the surface, where in most cases, it becomes quite difficult to remove the dust which drastically reduces the clearness index of the glass cover and obstruct the intrinsic incident solar radiation to reach the PV cells. Therefore, a self-cleaning system is very highly needed to keep the performance of the module as specified by the manufacturers of the STC.

University of Malaya

There are basically four processes of dust cleaning, e.g., natural (washed by rain drops), mechanical, electromechanical and electrostatic process and if this cleaning process is not done, it can readily lead to a reduction of energy output. However, these cleaning processes cannot be simply performed as they involve touching sensitive panels of the module. The cleaning/maintenance process is to ensure the panels are protected from dirt, dust, pollution and grime, bat/bird droppings and shading issues and this maintenance procedure is normally carried out every twelve months involving a cost of about USD 795 (Country Solar NT., 2016).

3.3 Designing the Sub-systems

The proposed PV/T-PCM with self-cleaning system consists of three distinct sub-systems, viz., the photovoltaic thermal system (PV/T), the PCM thermal control system and the self-cleaning system. Design and development of each of the sub-systems has been mentioned in detail in this section.

3.3.1 Design of PV/T

The design of a PV/T collector requires careful technical and economic analyses to minimize the cost and optimize the performance. A PV/T collector is designed to collect and deliver heat and electricity simultaneously from the same device. Thus, it comprises of two parts: a conventional photovoltaic (PV) module that produces electricity and a thermal collector which is a heat exchanger extracting heat from the module.

A polycrystalline silicon PV module is selected as the electrical component of the PV/T system whereas the heat exchanger part of the PV/T is very much similar to that of a solar thermal collector (STC). However, the design and dimension of the thermal collector is governed by the size and dimensions of the PV module. The two most important design aspects of the PV/T thermal collector are: 1) very close contact with the PV module rear side, and 2) maximum coverage of the heated surface.

University of Malaya

Researchers have proposed several designs of thermal collector that may be arranged in four groups, such as, 1) sheet-and-tube thermal collectors, 2) channel thermal collectors, 3) free-flow thermal collectors, and 4) two-absorber plate thermal collectors (Zondag et al., 2003). The double-serpentine thermal collector proposed in the present research belongs to sheet-and-tube group (the basic layout is shown in Figure 3.3). The tube material is copper and the sheet material is aluminum.

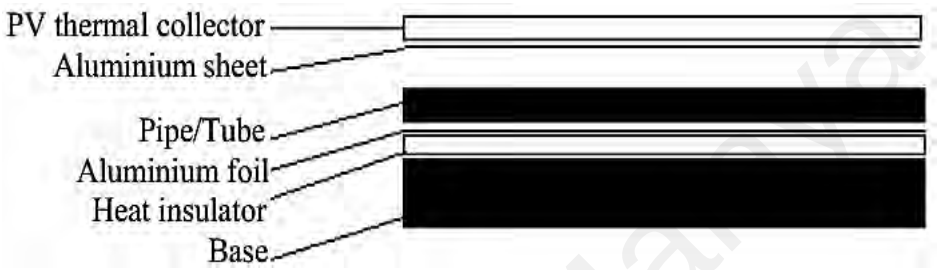

Figure 3.3: Basic design of a flat plate collector
(Zondag et al., 2003)

Type, material and shape of the thermal collector have direct impact on the operating temperature and thermal energy storage effect of the solar PV/T thermal collector. The double-serpentine thermal absorber design is based on sheet-and-tube configuration where the tubes are attached to a flat plate and is made of copper. The detailed design of a thermal collector is as shown in Figure 3.4. A 7.62 cm to 10.16 cm air gap has been kept between each pipe and a 17.78 cm gap between the parallel two sides of the absorber. The inner side air gap is important as when the sunlight strikes the PV module glass plate, the internal air is heated like the inside of a greenhouse. Nevertheless, water flowing inside the copper pipe takes time due to frictional pressure drop to reach the outlet and during this time, water flowing inside the absorber tubes is heated because of the hot water from the collector outlet. One of the advantageous feature of the present collector design is the ease of repairing and replacement of tubes, which is easier than a conventional thermal absorber design.

University of Malaya

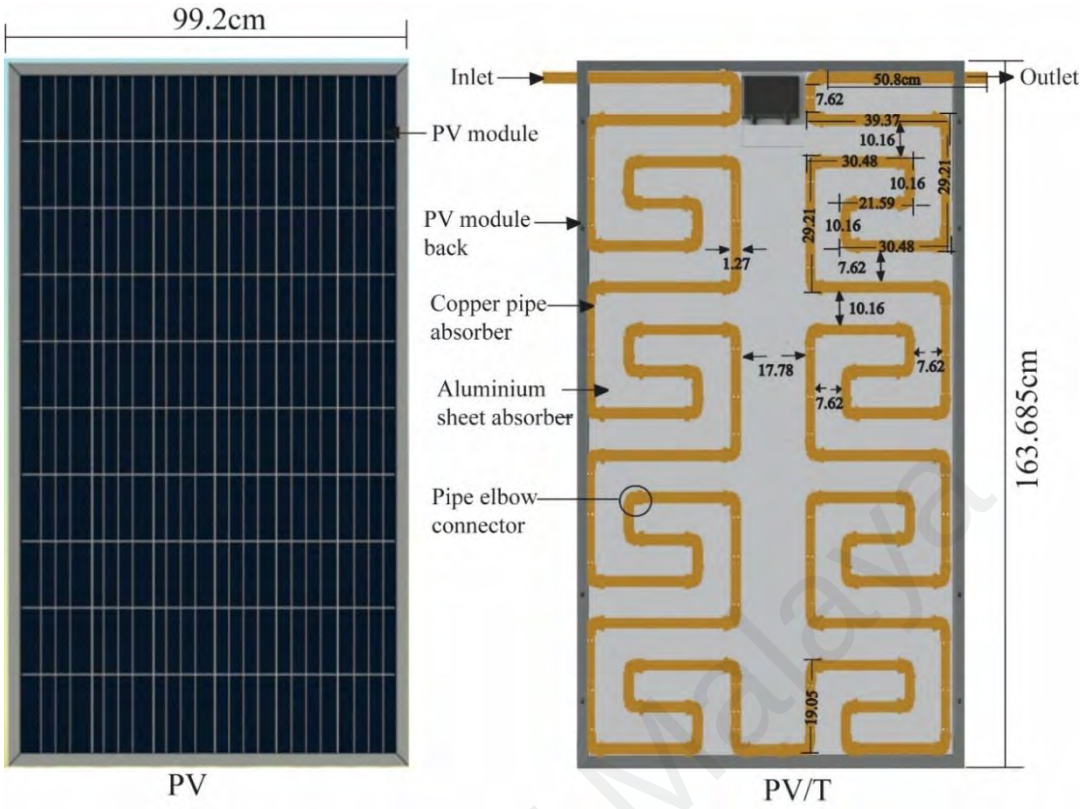

Figure 3.4: PV module and layout of PV/T thermal collector

3.3.2 Design of PCM Blocks

Phase change materials (PCM) include the use of lauric acid which is a powder like compound at room temperature. There are several techniques used to let the PCM to manage its thermal transfer, e.g., in glass container, in pouch, in separate metal box, etc. However, in the present research, aluminum foil packets have been used in the PCM that is not only light in weight, but it also performs efficient heat transfer. Each packet was 38.5 inches in length and 8 inches in breadth; hence, eight such packets were required to cover the 39 in. × 65.5 in. PV module rear surface. The PCM containing aluminum packets are placed in close thermal contact with the copper flow channel and secured to the PV frame by means of another aluminum sheet. Figure 3.5 and Figure 3.6 show the detailed arrangement of the PCM packets on the PV panel rear side.

University of Malaya

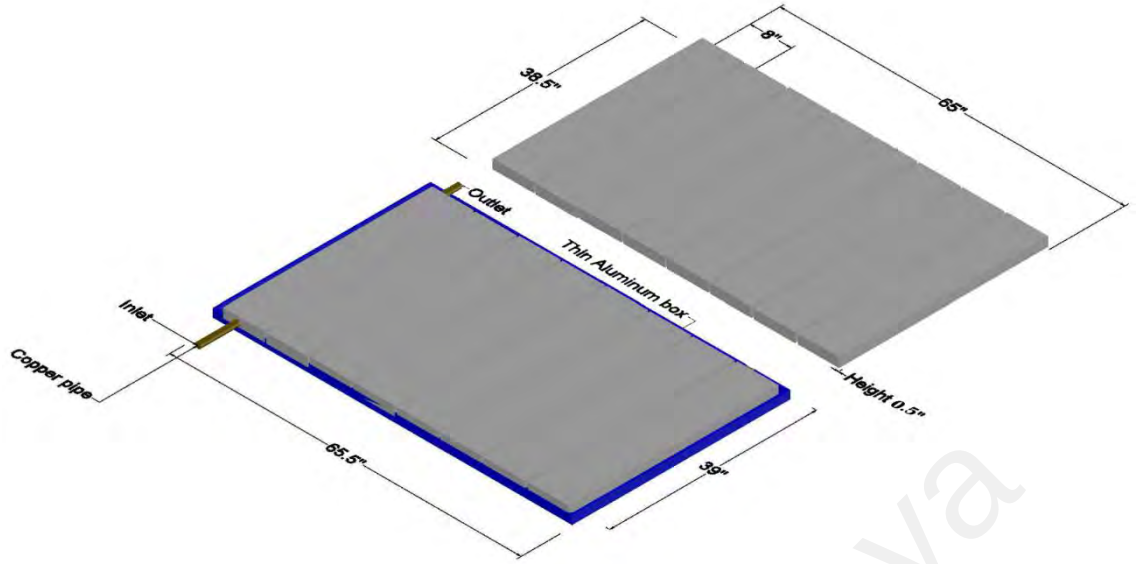

Figure 3.5: Arrangement of PCM packets

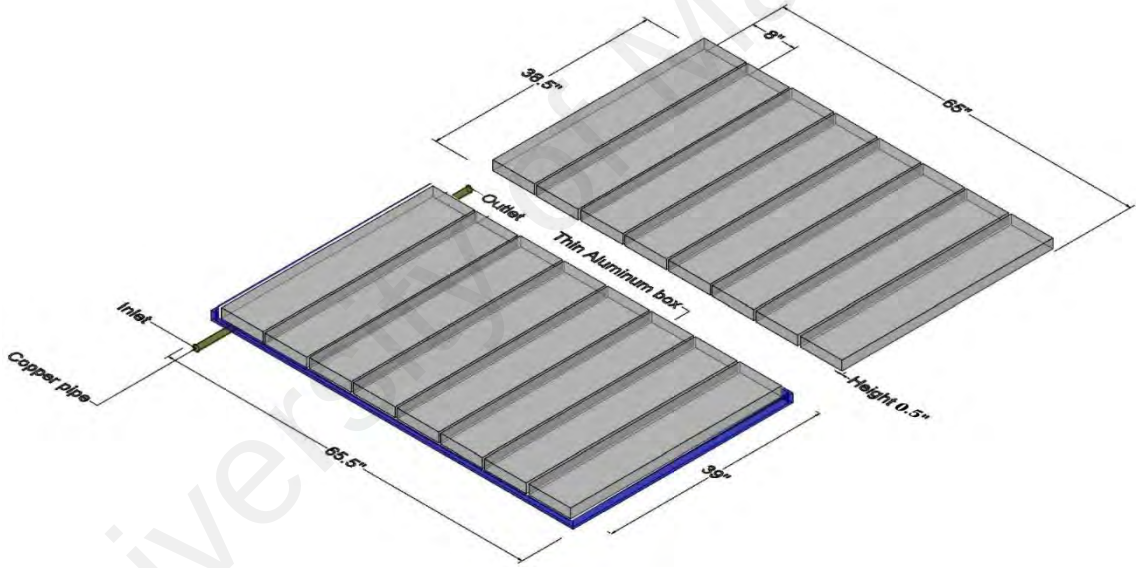

Figure 3.6: 3D view of flow channel and PCM packets

3.3.3 Design of Self-cleaning System

A self-cleaning system has been designed in the present research in order to ensure a regular and automatic cleaning of the PV glass surface. The working principle of a self-cleaning system is as shows in Figure 3.7. The main part of this system is the microcontroller programmable integrated circuit (IC). It is a time-delay and logic based circuit which is controlling a DC motor that rotates in a forward or reverse position. Figure 3.7 shows two DC motors, where DC motor 1 is for small water pump and DC

University of Malaya

motor 2 is for moving the cleaner on the PV panel surface. IC 1 is the main time-delay circuit, which is controlling the relay 1 and 2. Relays are working as a switch on-off mechanism. When IC 1 is activated, relay 1 is switched on too, after which it will switch off and releases the DC power to DC motor 1. A few seconds later, IC 1 will activate relay 2. When relay 2 is activated, it will switch on and will then release the DC power to IC 2. When the DC power is activated, IC 2 will then switch on relay 3 and relay 4 which will then switch off to release the DC power to DC motor 2. Here, relay 3 and relay 4 are connected to the same DC motor 2. These two relays (3 and 4) will switch on and off as forward and reverse position on motor 2. Hence, IC 2 will experience a time delay while waiting for motor 2 to complete its forward and reverse cycle. After each cycle is completed, it will then be repeated until the power is switched on again. Figure 3.8 shows the 3D arrangement of a self-cleaning mechanism.

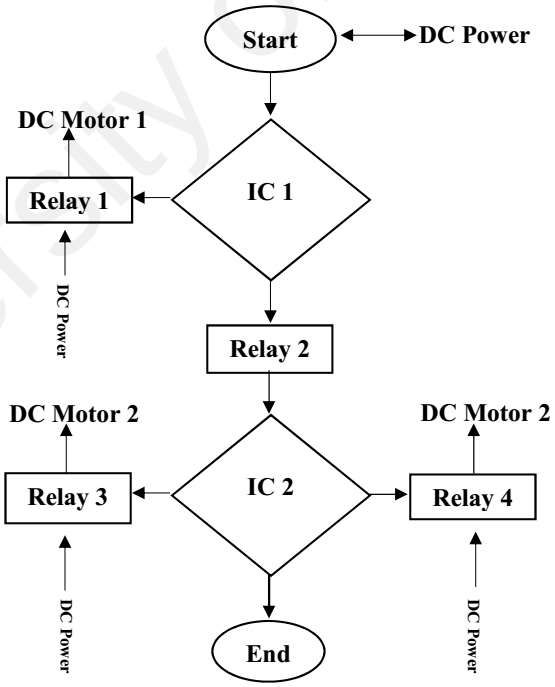

Figure 3.7: Working principle of a self-cleaning system

University of Malaya

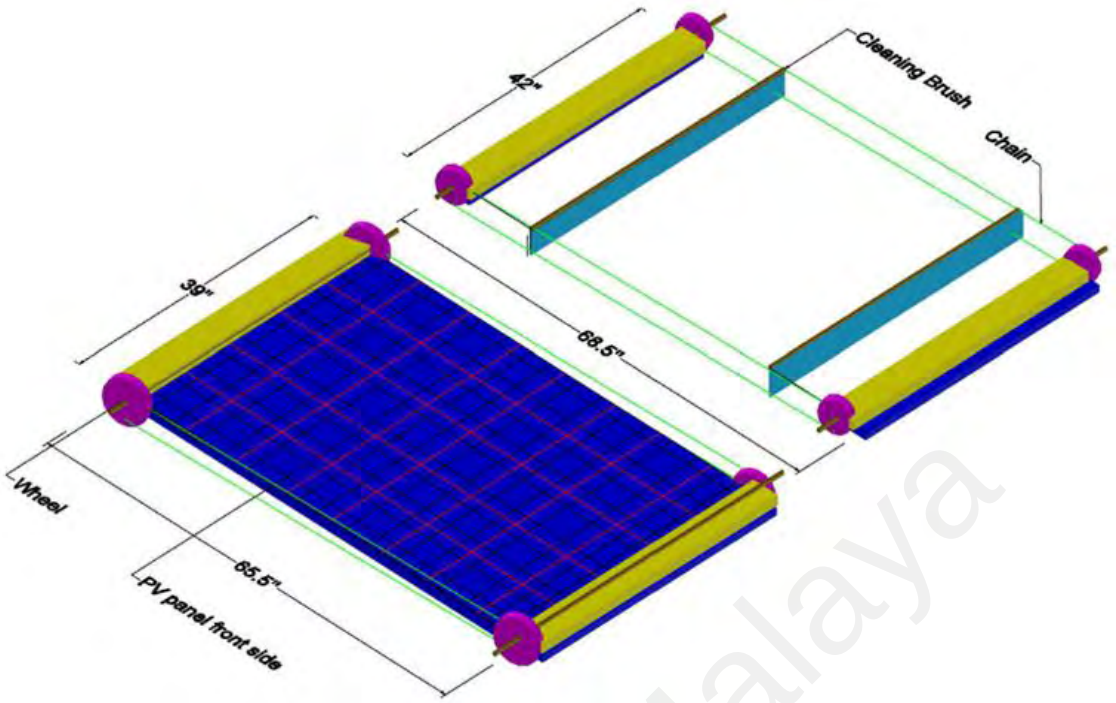

Figure 3.8: 3D design of self-cleaning mechanism in PV panel

3.4 Fabrication

In the present study, two autonomous systems have been designed and fabricated, viz., a PV/T-PCM system and a self-cleaning system. The detailed fabrication steps are discussed in the following sections.

3.4.1 Fabrication of PV/T-PCM System

The PV/T collector comprises of two basic components, viz., a PV as an electrical component and a heat exchanger as the thermal collector. The PV module selected for the fabrication of the PV/T unit is a 250-W 60-cell p-Si module. The detailed specification of the module is given in Table 3.2.

Table 3.2: Specification of PV module

EPV (ENDSUPV industries)	
Model	EC61215 (2nd edition)
Short Circuit Current (I_{sc}) [A]	8.926
Open Circuit Voltage (V_{oc}) [V]	38.194
Maximum Power (P_{max}) [W]	257.597
Current at P_{max} [A]	8.416
Voltage at P_{max} [V]	30.606
*The electrical characteristics are within 0-3% of the indicated values under Standard Test Conditions. (1000W/m^2, 25°C. AM 1.5)	

University of Malaya

Figure 3.9 shows a solar PV panel back with aluminium sheet and copper pipe connected with elbows. This thin aluminium plate covers the back of the PV panel and the aluminium plate cover has a dimension of 157.48 cm high, 83.82 cm width and 0.5 mm thick.

Figure 3.9: Double serpentine flow channel attached to PV rear side

Copper pipes are used because of their high thermal conductivity. The dimensions of the pipes are 1.27 cm in diameter, 1 mm thick and 1475.74 cm long. The copper pipe is attached to an aluminum absorber sheet by means of a thermal conductive paste. The specifications of the conductive paste are as shown in Table 3.3.

Table 3.3: Specifications thermal conductive paste (Lazada.com.my, 2017)

Thermal Conductivity	0.925W/m-k
Thermal Resistance	0.262ºC-in^2/W
Specific Gravity	2.0g/cm^3 at 77ºF (25ºC)
Operating temperature	-30ºC ~ 300ºC
Composition: Silicone Compound Carbon Compound Zinc Oxide Compound	 50% 20% 30%

Figure 3.10 shows the PCM packet which is made of aluminium sheet of 0.5 mm thick. The PCM packet is coated with a high thermal conductivity non-sticky paper. Hence, each dimension of the packet is 1.27 cm in thickness, 21.59 cm width, and 83.82 cm long. The eight packets are then filled up with phase change materials but due to the lack of

University of Malaya

back space, only seven packets are used as shown in Figure 3.13. This is a unique idea to use PCM at the rear side of the PV panel.

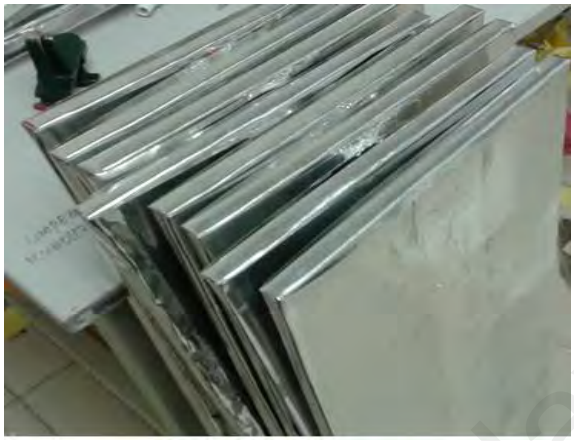

Figure 3.10: Aluminum packets containing PCM

The copper flow channel which has been attached with an aluminum absorber sheet is then covered with an aluminum foil shown in Figure 3.11 and a ceramic fiber sheet is laid over the foil as an insulation shown in Figure 3.12. The composition of the ceramic fiber is given in Table 3.4.

Figure 3.11: Aluminum foil cover on the thermal collector

University of Malaya

Figure 3.12: Ceramic fiber insulation cover on PV/T rear side

Table 3.4: Ceramic fiber paper for Solar PV rear insulation (Alibaba.com, 2018)

Grade	Standard	
Max Temperature (℃)	1260	
Working Temperature (℃)	≤11550	
Colour	Pure white	
Density (kg/m^3)	170-220	
Thermal conductivity (W/m.K)	0.07(400℃)	
Compression Strength (MPa)	0.65	
Chemical composition (%)	Al_2O_3	42-43
	SIO_2	53
	ZrO_2	---
	Fe_2O_3+Ti_2O_3	≤1.2
	Na_2O+K_2O	≤0.5
	CaO+MgO	≤0.3

The complete assembly of the PV/T-PCM system is as shown in Figure 3.13.

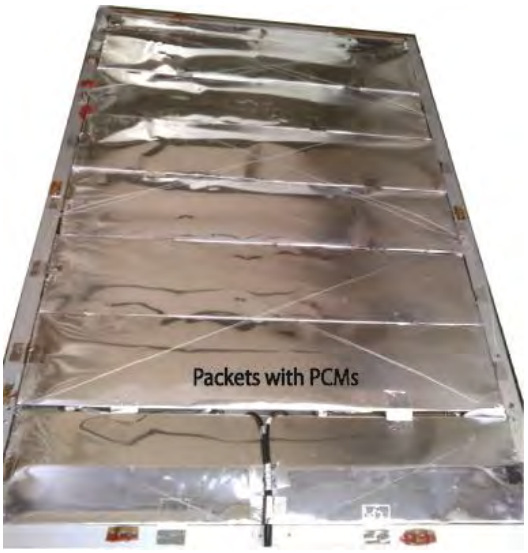

Figure 3.13: PCM packets covering the thermal collector

University of Malaya

3.4.2 Fabrication of Self-cleaning System

The structural frame of the self-cleaning system is made from a hollow aluminum rectangular tube of 25.4mm × 50.8mm × 1727.2mm curtain track of 20mm × 20mm × 1727.2mm, angle bar of 12.7mm × 12.7mm and a square hollow iron tube of 12.7mm × 12.7mm as shown in Figure 3.14. A circular aluminum pipe of 9.52mm diameter is utilized for the motor driving shaft.

Figure 3.14: Self-cleaning system fabrication materials

A high adjustable reversible torque of 24V-2A DC motor is used to drive the dust cleaner's sweeper. The motor can run at variable speeds ranging from 3000 to 6000 rpm from 12 volts to 24 volts. Figure 3.15 shows the DC motor outer configuration where the shaft diameter is 8 mm and 43 mm long.

Figure 3.15: Sweeper driving DC motor

University of Malaya

The motor accessories, such as, bush & bearing, gear belt, gear wheel, and shaft are as shown in Figure 3.16. The inner diameter of the bearing and that of the gear wheel and the outer diameter of the shaft are all of 8 mm. The gear belt and the gear wheel teeth width are also all of 6 mm, which is very convenient and easy to adjust.

Figure 3.16: Sweeper driving accessories

The main part of the self-cleaning system is the sweeper that comprises a microfiber cloth and a water flow line with a 12-V, 9-mA DC water pump (Figure 3.17). The motor is generally operated at around 3000 rpm at 6 V.

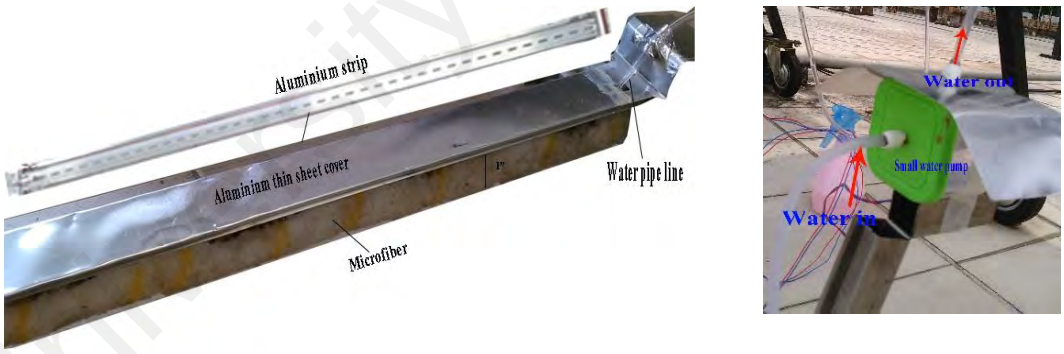

Figure 3.17: Sweeping microfiber and water flow pipeline

The flow diagram for assembling the components of the self-cleaning system is shown in Figure 3.18 and the complete structure of the self-cleaning system attached to the PV/T-PCM module is shown in Figure 3.19.

University of Malaya

Figure 3.18: Complete self-cleaning system

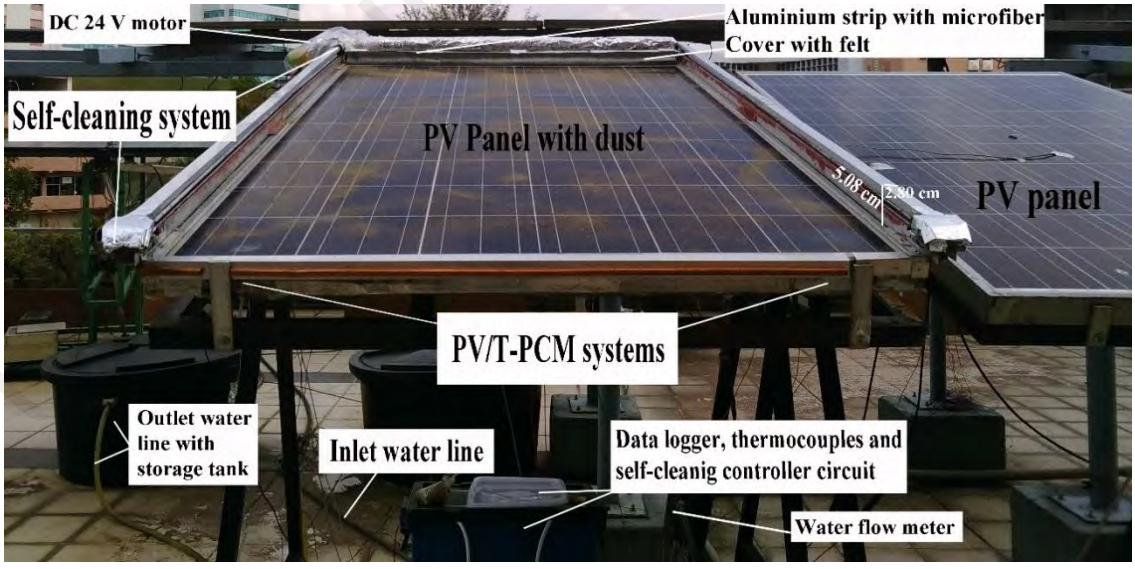

Figure 3.19: Complete PV/T-PCM with self-cleaning system along with reference PV

The automatic control of the motors used for the water pump and the sweeper as well is achieved through a microcontroller (AVR-AT mega 8) based system. Figure 3.20 shows the complete circuit layout for the microcontroller and sensors that consist of a

transistor BC547, resistance (1K), capacitor 100pf, Diode (1N4001), indicator LED, 6 V relay, etc.

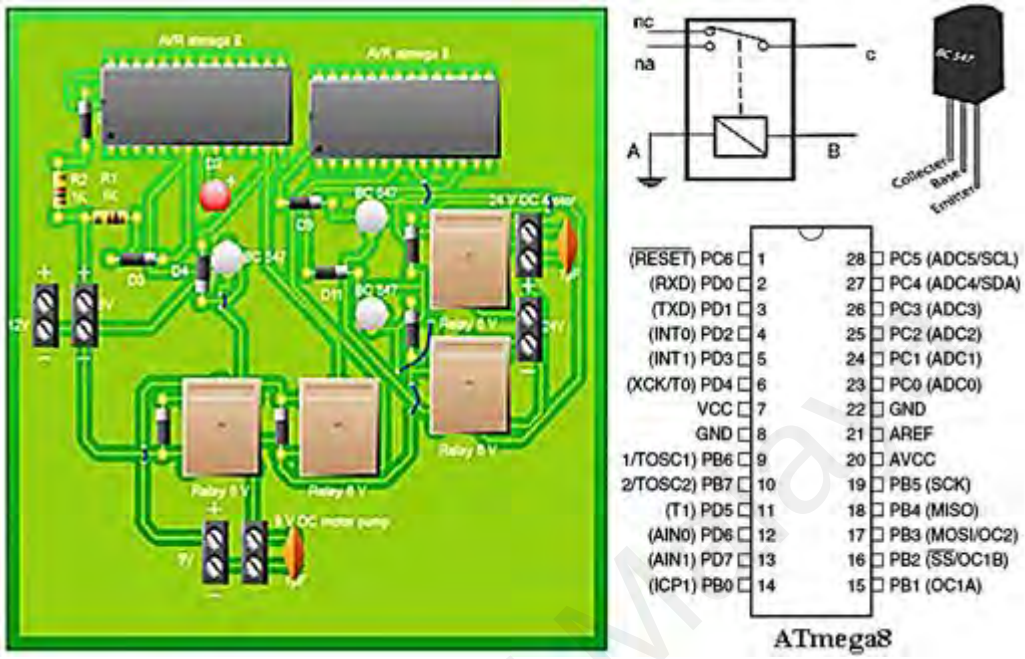

Figure 3.20: Microcontroller based motor control system for water pump and sweeper, block diagram of control circuit with microcontroller pin layout

3.4.3 Installation and Instrumentation of the Experimental Set-up

After the design and fabrication stages have been completed, the sub-systems, i.e., PV/T-PCM and self-cleaning systems are assembled together to form the complete PV/T-PCM module with the self-cleaning system and installed in the UMPEDAC Solar Garden at Level–3, Wisma R&D, University of Malaya, Kuala Lumpur. The experimental set-up has been fabricated and installed in five different steps. First, locate the geographical location of the installation place. The location of the Solar Garden is latitude 3.11° North and longitude 101.66° East (SunEarthTools, 2016). Second, to calculate the slope of the photovoltaic collector by using Cooper's equation (Hossain, 2013; Struckmann, 2008). The slope of the collector is calculated from the equation:

$$\delta = 23.45 \sin[0.9863 \quad (284 + n_1)] \tag{3.1}$$

$$\beta = (Q_1 - \delta) \tag{3.2}$$

University of Malaya

where β is determined the photovoltaic panel slop and δ is the angle of inclination and n_1 is the numerical day of the year. Positive values of β means that the orientation of the surface is towards the equator, while the negative values indicates the direction is towards the (north) pole (Saiful, 2001). Following the above relationship, the slope of the test modules in the present study were kept at 15°. This angle is the constant parameter for the PV and hybrid PV/T collectors. In this way, the collectors are designed to concentrate the sunlight onto the absorber in order to effectively convert the solar energy into the electrical energy. Third, set-up the PV and PV/T collector together with same degree of angle. The fourth step is, set-up the PCM packets under the PV/T thermal absorber copper tube shows in Figure 3.21 (b). This absorber has inlet and outlet water flow tube. So here at inlet side set-up a variable water flow meter shows in Figure 3.21. This is a variable parameter and the range is 0.5 LPM up to 4 LPM. Final step is set-up the self-cleaning mechanism in PV/T-PCM collector shows in Figure 3.21 (c).

The 3D schematic diagram of the experimental setup of a solar PV/T, PV/T-PCM and PV/T-PCM with self-cleaning system is show in Figure 3.21.

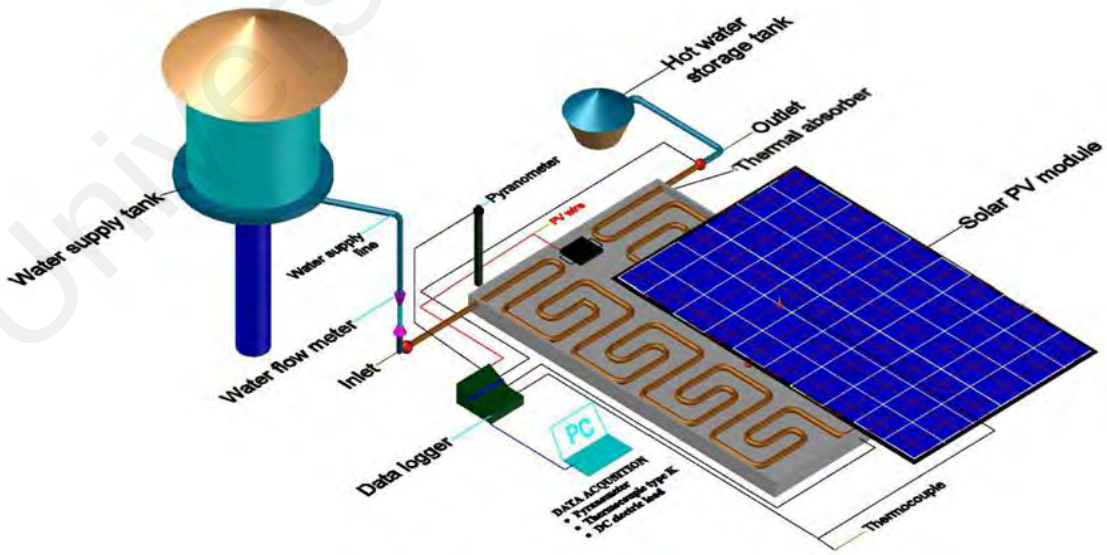

(a)

Figure 3.21: (a) Experiment setup and cutway view of the solar PV/T (b) PV/T-PCM and (c) PV/T-PCM with self-cleaning system

University of Malaya

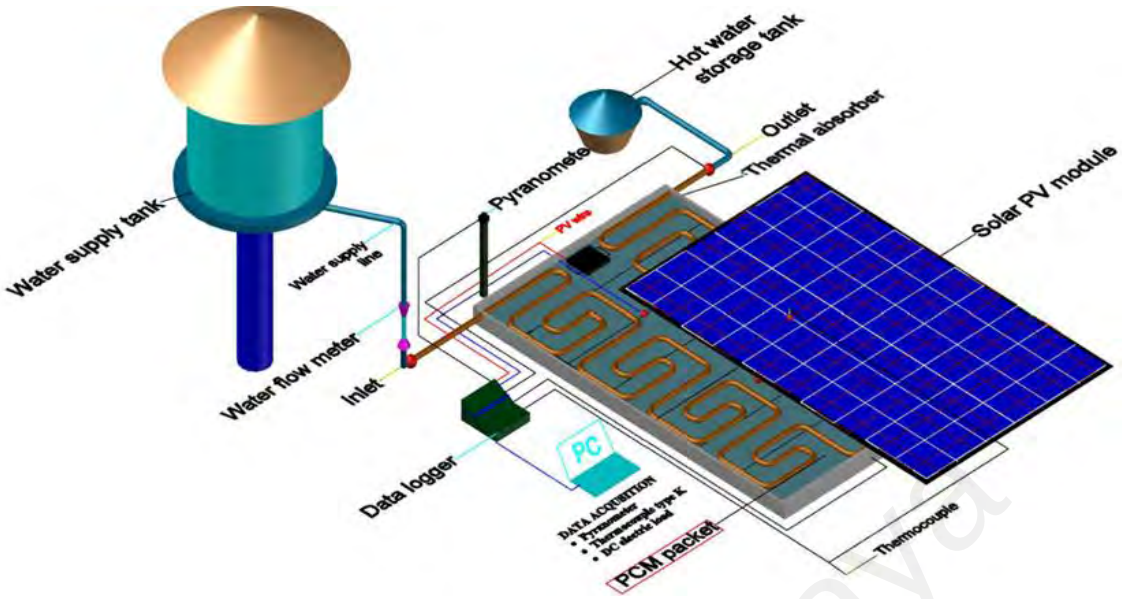

(b)

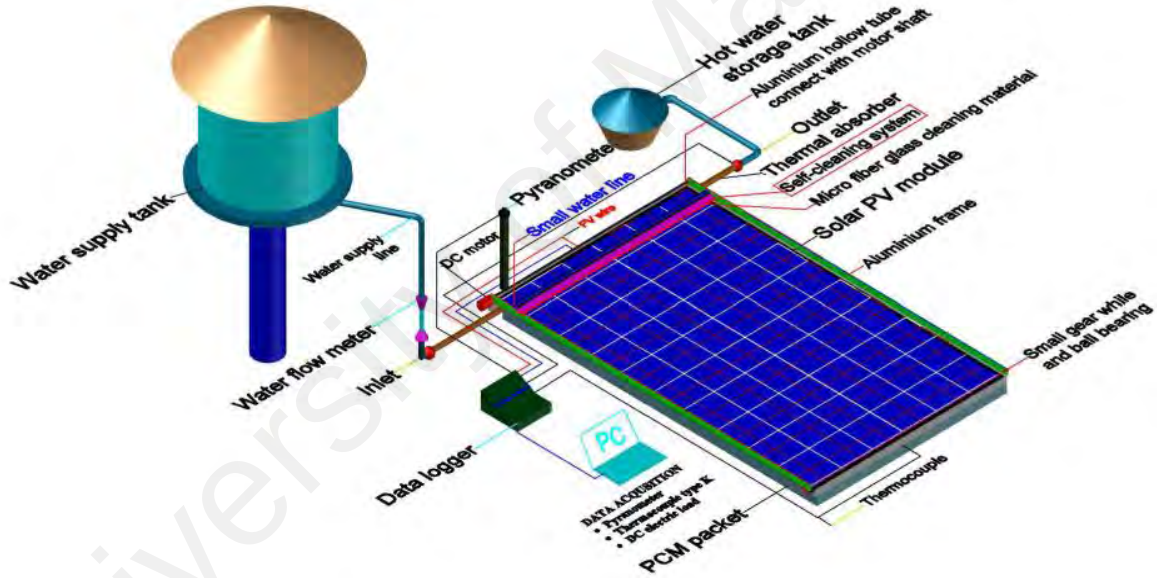

(c)

Figure 3.21, continued

In the present study, data for different parameters, such as, inlet and outlet water temperatures, PV panel top and rear temperature, ambient temperature, wind speed, water flow rate and solar radiation have been measured. For this purpose, instrumentations that were used for measuring different parameters and collection of experimental data are as shown in Figure 3.22. These include thermocouples (K-type) with the heat sensor, Pyranometer, I-V tracer, data logger (series 3), wind speed meter and a computer for data

University of Malaya

acquisition. Table 3.5 shows, the range of capacities and the accuracy of the experimental observing equipment.

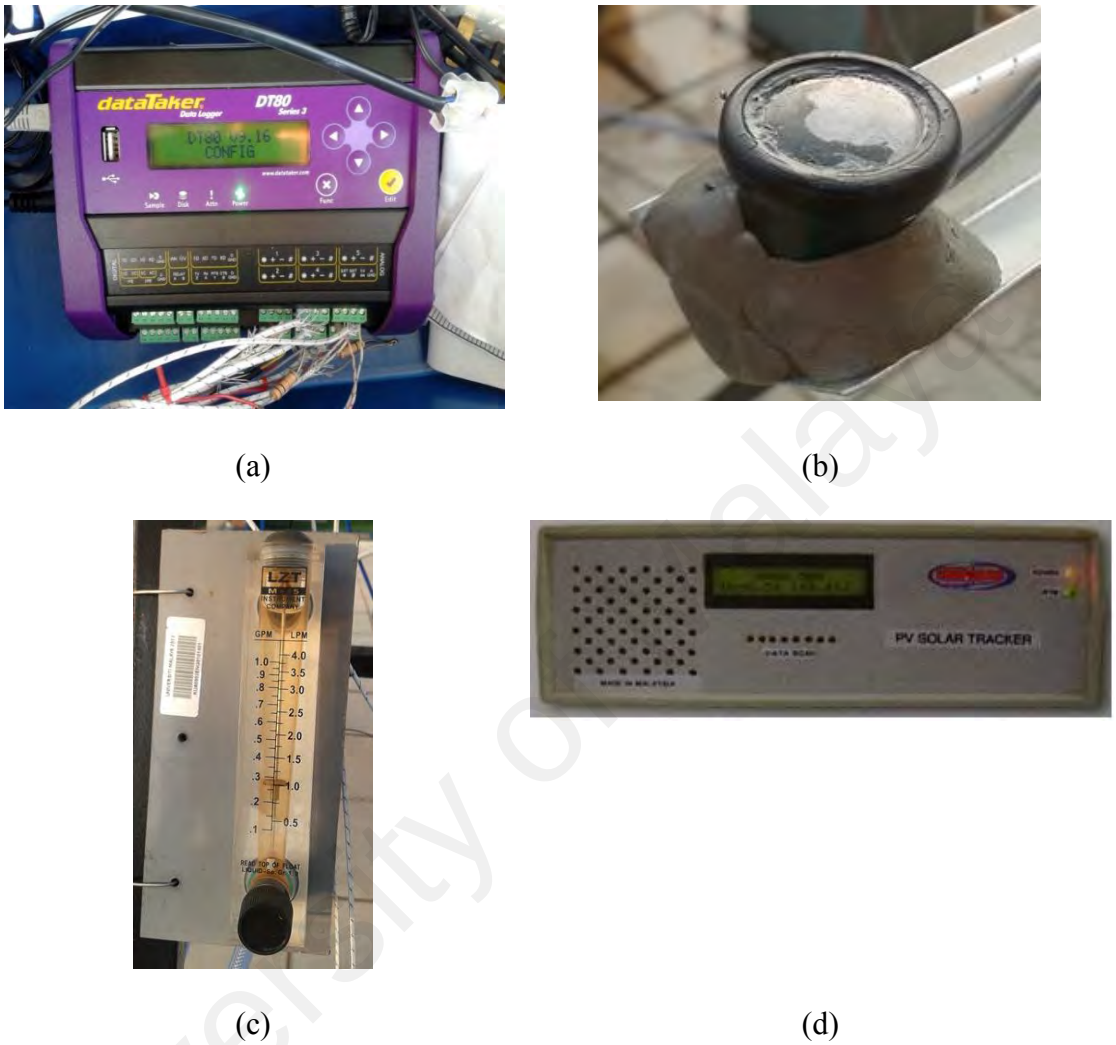

(a) (b)

(c) (d)

Figure 3.22: Measuring and data acquisition instruments (a) Data logger, (b) Pyranometer, (c) Flow meter, (d) I-V tracer

Table 3.5: Properties of the monitoring equipment

Equipment	Range	Accuracy
Data logger (series 3)	-270 to 1372°C	±2%
Pyranometer (silicon)	0-2000 W/m^{-2}	±5%
Anemometer (TM816)	0.3 to 30 m/s	±5%
Flow meter	0.5-4 LPM	±0.5
I-V tracer	0 to 50V & 0 to 16A	±5%
Thermocouple (type K)	-200 to 1000°C	±0.5
Multimeter (DC)	400mV to 1000 V	±0.4
Multimeter (AC)	400µA to 10 A	±0.8
Water thermal sensor	-200 to 1000°C	±0.5

University of Malaya

3.5 Data Collection and Analysis

In this work, experimental data have been collected based on the requirements for calculating the thermal, electrical energy and exergy performances. The data parameters, such as, irradiation, temperatures, maximum power, water flow, wind speed etc., have been taken into account. The solar radiation data had been collected with a help of Pyranometer sensor. The inlet and outlet water, PV front and back panel temperature data had been collected with using the thermocouples. All data had been recorded with the help of Data logger. The wind speed data had been recorded in manually. The PV maximum power data had been collected and recorded using an I-V tracer. The experimental data have been gathered in three different methods. Firstly, a reference solar PV module (60 cell-Polycrystalline, 250W) and PV/T only system was arranged and studied simultaneously under the same outdoor condition (Figure 3.19). Similarly, a PV/T-PCM and a PV/T-PCM modules with a self-cleaning unit was studied separately against the reference PV module. The data had been collected with different dates and different water flow rates ranging from 0.5, 1, 2, 3 and 4 LPM (litres/min). The flow meter has been fixed flow rates during record the data. The self-cleaning system and its separate component parts are as illustrated in Figure 3.18. The data logger, thermocouples, water flow meter and tanks are as shown in the Figure 3.22.

3.5.1 Energy Analysis

The performance of PV/T collectors can be depicted by the combination of efficiency expression (Adnan et al., 2009) which comprises of the thermal efficiency η_{th}, and the electrical efficiency η_{el}, which usually includes the ratio of the useful thermal gain and electrical gain of the system to the incident solar irradiation on the collector's gap within a specific time or period. The total efficiency η_o is used to evaluate the overall performance of the system:

University of Malaya

$$\eta_o = \eta_{th} + \eta_{el} \tag{3.3}$$

The thermal performance η_{th} of the PV/T unit is evaluated for its thermal and photovoltaic performance with the derivation of the efficiency parameters being based on the Hottel-Whillier equations (Hossain et al., 2015). The thermal efficiency (η_{th}) of the conventional flat plate solar collector is calculated using the following formulae as shown below (Ibrahim et al., 2014b; Park et al., 2014):

$$\eta_{th} = \frac{\dot{Q}_u}{A \times G} \tag{3.4}$$

where

Q_u is heat loss,

A is area of collector and

G is solar radiation.

The useful heat gain (Q_u) by PV/T system is given by (Ibrahim et al., 2014b; Park et al., 2014):

$$\dot{Q}_{u,PV/T} = \dot{m}_w C_{p,w}(T_{Out} - T_{In}) \tag{3.5}$$

On the other hand, In a PV/T-PCM system, the total heat gain is due to heat absorbed by water plus sensible heat absorbed by PCM and latent heat absorbed by PCM while changing its phase. Therefore, total heat gain by PV/T-PCM system is given by:

$$\dot{Q}_{u,PV/T-PCM} = \left\{\dot{m}_w C_{p,w}(T_{Out} - T_{In})\right\} + \left\{m_{PCM} C_{p,PCM}\left(T_{m,PCM} - T_{In}\right)\right\} + \left\{m_{PCM} \times L_{PCM}\right\} \tag{3.6}$$

However, the amount of sensible heat absorbed by PCM is negligible as compared to the latent heat absorbed during phase change. Hence, equation (3.6) can be simplified as follows (Hasan et al., 2016):

University of Malaya

$$\dot{Q}_u = \left\{ \dot{m} C_p (T_{Out} - T_{In}) \right\} + \left\{ m_{PCM} \times L_{PCM} \right\} \quad (3.7)$$

where

$\dot{m}_w$ is mass of water flow rate,

m_{PCM} is the mass of PCM as calculated by equation (3.8)

$C_{p,w}$ and $C_{p,PCM}$ are specific heats of water and PCM respectively,

L_{PCM} is the latent of PCM

$T_{m,PCM}$ is the melting point of the PCM,

T_{Out} is outlet water temperature and

T_{In} is inlet water temperature.

The mass of PCM (m_{PCM}) can be calculated as follows (El Khadraoui et al., 2016; Shukla et al., 2009):

$$m_{PCM} = \frac{Q_{ch}}{L_F + \int_i^m C_{p.s}(T)dT + \int_m^f C_{p.l}(T)dT} \quad (3.8)$$

where

$C_{p,s}$, $C_{p,l}$ are specific heat of solid and liquid phase of the PCM, respectively

L_F is latent heat of PCM,

Q_{ch} is heat charging phase,

i, m and f are initial, melting and final temperature of PCM,

dT is the temperature rise.

A solar cell's energy conversion efficiency is the percentage of power converted and collected equation (3.9).

$$\eta_{el} = \frac{P_{\max}}{A \times G} \quad (3.9)$$

University of Malaya

The electrical power output of a PV is:

$$P_{el} = I \times V \tag{3.10}$$

However, the maximum output power in equation (3.10) can be a derivative of equation (3.11).

$$P_{\max} = I_{sc} \times V_{oc} \times FF = V_{mp} \times I_{mp} \tag{3.11}$$

The solar energy absorbed by the PV modules is converted into electric energy and thermal energy, but the thermal energy is dissipated by convection, condition and radiation.

3.5.2 Exergy Analysis

Exergy analysis includes that of energy quality or capacity, thus, leading to evaluation of the most efficient use of energy potential. For the steady-state process during a finite time interval, the overall exergy balance of the solar PV can be expressed as:

Exergy Input = Exergy Output + Exergy Loss + Irreversibility (3.12)

Figure 3.23 shows a steady state condition where no power is produced.

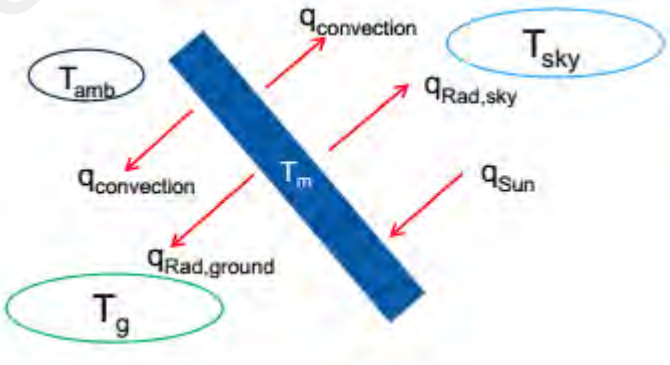

Figure 3.23: Exergy in/out of a PV module at steady state condition (NREL, 2010)

In Figure 3.23, T_m is module, T_{sky} is sky, T_a is ambient and T_g is ground temperature respectively. This is the quality of energy and it is called exergy loss or availability loss.

University of Malaya

The exergy loss is also called irreversibility. The solar radiation emitted by the solar cells is transformed into two types of energy, namely, electrical and thermal energy. The electrical energy is utilized and it is considered as 'electric energy'. However, the thermal energy is dissipated into the ambient environment as a heat loss which becomes exergy destruction.

The most general formulation of the exergy balance of a PV system is as shown in equation (3.13). In the following formulae, $E_{x\,out}$ is the maximum amount of exergy that can be obtained from a system whose supplying energy is $E_{x\,in}$: the energy consumed is equal to the exergy loss $E_{x\,loss}$, as in equation (3.14) (Sudhakar & Srivastava, 2014).

$$E_{x\,in} = E_{x\,out} \tag{3.13}$$

$$E_{x\,in} - E_{x\,out} = E_{x\,loss} \tag{3.14}$$

The exergy efficiency of the PV module can be expressed as the ratio of the total output and total input exergy as shown in equation (3.15) (Sudhakar & Srivastava, 2014).

$$\eta_{ex} = \frac{E_{x_{output}}}{E_{x_{input}}}$$

(3.15)

Equation (3.16) shows the inlet exergy of a PV system which includes the only solar radiation intercity exergy.

$$E_{x_{in}} = A \times G \times \left[1 - \frac{4}{3}\left(\frac{T_a}{T_s}\right) + \frac{1}{3}\left(\frac{T_a}{T_s}\right)^4 \right]$$

(3.16)

The exergy output includes the thermal exergy and the electrical exergy of the PV system.

University of Malaya

$$E_{x_{out}} = E_{x_{thermal}} + E_{x_{electrical}} \tag{3.17}$$

The thermal exergy can be expressed as in equation (3.18):

$$E_{x_{thermal}} = Q\left[1 - \frac{T_a}{T_c}\right] \tag{3.18}$$

where, Q is heat loss,

T_a is ambient temperature and

T_c is the PV cell temperature

The overall heat loss coefficient is U.

$$Q = UA \quad (T_c - T_a) \tag{3.19}$$

where, A is collector area

The overall heat loss coefficient of a PV module includes the convection and the radiation losses

$$U = h_{conv} + h_{rad} \tag{3.20}$$

The convective heat transfer coefficient can be written as follows (Sudhakar & Srivastava, 2014):

$$h_{conv} = 2.8 + 3V_w \tag{3.21}$$

where, V_w is the wind speed.

Radiative heat transfer coefficient between PV array and surroundings can be writing in two equations (3.22) and (3.23) (Ibrahim et al., 2014b):

$$h_{rad-1} = \varepsilon\sigma(T_{sky} + T_c)(T^2{}_{sky} + T^2{}_c) \tag{3.22}$$

$$h_{rad-2} = 1.78 \quad (T_m - T_a) \tag{3.23}$$

Effective temperature of the sky

University of Malaya

$$T_{sky} = T_a - 6 \tag{3.24}$$

The solar cell temperature can be calculated using equations (3.9), (3.21) and (3.23) (Nahar et al., 2017; Rahman et al., 2017):

$$T_c = \frac{P_{sg} G(\tau_g \alpha - \eta_{el}) + (h_{conv} T_a + h_{rad-2} T_b)}{h_{conv} + h_{rad-2}} \tag{3.25}$$

where, P_{sg} is packing factor of the solar module and T_b is the rear panel temperature.

Finally, electrical exergy is equal to the output electrical power of the PV module by using equation (3.26).

$$E_{x_{electrical}} = P_{\max}$$

(3.26)

The exergy analysis (based on the second law analysis) is the most suitable method to get a clear picture on the PV/T solar collector efficiencies and on the degradation of energy during the thermal and the electrical conversion processes. The exergy inflow coming from the solar radiation falling on the collector surface is given by equation (3.27) (Hazami et al., 2016; Ibrahim et al., 2014b):

$$\sum E_{x\,in} - \sum E_{x\,out} = \sum E_{x_d} \tag{3.27}$$

$$\sum E_{in} - \sum (E_{x_{th}} + E_{x_{pv}}) = \sum E_{x_d} \tag{3.28}$$

$$E_{x_{th}} = Q_u \left(1 - \frac{T_a + 273}{T_o + 273} \right) \tag{3.29}$$

$$E_{x_{pv}} = \eta_{pv} \times A \times N_c \times G \times \left[1 - \frac{4}{3} \left(\frac{T_a}{T_s} \right) + \frac{1}{3} \left(\frac{T_a}{T_s} \right)^4 \right] \tag{3.30}$$

$$E_{x_{PV/T}} = E_{x_{th}} + E_{x_{pv}} \tag{3.31}$$

where

E_{xin} is input exergy same as equation (3.16),

University of Malaya

E_{xout} is output exergy,

E_{xth} is thermal exergy,

$E_{XPV/T}$ is photovoltaic thermal exergy,

A is collector area,

N_c is number of collectors,

T_s is sun temperature.

The energy destruction is E_{xd} and

η_{pv} is the PV efficiency.

The exergy efficiency η_{ex} is given by

$$\eta_{ex} = 1 - \frac{E_{x_d}}{E_{x_{in}}} \tag{3.32}$$

The analytical parameters of the solar PV, PV/T and PV/T-PCM systems are as presented in Table 3.6.

Table 3.6: PV, PV/T and PV/T-PCM system characteristics

Description	**Symbol**	**Value**	**Unit**
Collector area	A, A_c	1.64	m^2
Number of glass cover	N_1, N_c	1	
Emittance of glass	ε_g	0.88	
Emittance of plate	ε_p	0.95	
Collector tilt	β	15	o
Specific heat of working fluid	C_p	4185.5	J/kg°C
specific hear	$C_{p,s}$,$C_{p,t}$	2.27, 1.76	kJ/kg.K
Insulation conductivity	k_e	0.07	W/m°C
Initial temperature	i	42.84	°C
Melting temperature	m	43.72	°C
Final temperature	f	45.76	°C
Bottom insulation thickness	L_e	0.006	W/m°C
Latent heat	L_F	228.9	kJ/kg
Plate thickness	PI	0.001	m
Sun temperature	T_s	5777	K
Wind velocity	v	1.1	m/s
Transmittance	τ	0.96	
Absorptance	α	0.90	
Packing factor of the solar module	P_{sg}	0.8	
Total mass of dust	Δm	10-15	g

University of Malaya

3.5.3 Dust Cleaning Performance Analysis

The solar PV module gets its electrical power from the rise in temperature through the solar irradation. A PV module output power is rated by the manufacturers under standard test conditions (STC) with a temperature of 25°C and solar irradiance intensity of 1000 W/m^2. These conditions can be conveniently obtainable in a factory but the situation is different when it is done outdoors where the weather can cause effects on parameters, such as, humidity, temperature, dust, wind speed, tilt angle, etc., as well as on the PV module efficiency itself. PV module efficiency performance can be compared with the dust and cleaning results. This can be done through the use of two identical pairs of PV modules, where one is being cleaned whereas the other is being artificially poluted (Ahmed et al., 2013b). This experiment was also conducted on the same method and the conversion efficiency was carried out using the same equation (3.9) for the PV panel dust analysis. Here the dust deposition (ΔM) can be written as:

$$\Delta M = \frac{\Delta m}{A} \tag{3.33}$$

where,

Δm is the total mass of dust and

A is collector area.

Capacity factor (CF) or Energy yield is defined as the ratio between the actual and the rated output over a period of time Δt and the formula is as illustrated below:

$$CF = \frac{E_{\Delta t}}{P_p . \Delta t} \tag{3.34}$$

where, P_p is a peak power

Capacity factor or Energy yield reduction percentages between the clean CF_0, E_{cl} and the polluted CF, E_{pol} of the PV panel (Ahmed et al., 2013b) is as shown in the following formula:

University of Malaya

$$\Delta(CF) = \frac{CF_0 - CF}{CF_0} \times 100 = \frac{E_{cl} - E_{pol}}{E_{cl}} \times 100 = \Delta E \tag{3.35}$$

Finally, the efficiency difference between the polluted and the clean surface PV panel power is defined as:

$$\Delta\eta = \frac{P_{cl}}{G.A} - \frac{P_{pol}}{G.A} = \frac{E_{cl} - E_{pol}}{G.A.\Delta t} = \frac{(CF_{cl} - CF_{pol})}{G.A} = \frac{CF_{cl} P_{\max}}{G.A} \tag{3.36}$$

3.6 Economic Analysis

The economic analysis will determine the payback period of the system in which the payback period is calculated using one standard method, i.e., the Annual-worth method. A high initial cost and a low operating cost are the usual economic definers where the economic problem is in comparing an initial known investment with an estimated future operating cost.

3.6.1 Annual-worth Method (Equivalent Uniform Annual Cost)

Annual worth (A.W) is the difference between an annual benefit (revenue) and annual cost (Kumar & Tiwari, 2009; Leland T & Anthony J, 1998). It is a gain if it is a net benefit, and a loss if it is a net loss, i.e.

$$AW = B_A - C_A \tag{3.37}$$

where,

B_A is the annual benefit and

C_A is the annual cost.

As a decision-making tool, for acceptance of an option, this expression becomes (Ammar et al., 2009) as follows:

$$B_A - C_A \geq 0 \tag{3.38}$$

where, $C_1 = C_2 = C_3 = C_N = C_A$ are options for selection if B_A-C_A equals to or exceeds zero.

University of Malaya

3.6.2 Cash Flow Analysis

A cash flow formula (3.39) has been utilized for the solar collector systems related economic analysis (Hossain et al., 2015):

$$AW = -(I_c + I_{lc})(A/P, i, N) - A_{rc} - (C_{afic})(A/F, i, N) \tag{3.39}$$

where,

I_c is initial cost,

I_{lc} is installation cost,

A/P is capital recovery factor,

i is interest rate,

N is life span,

A_{rc} is annual running cost and

C_{afic} is change of aluminum foil insulation cover

To use the formula of equations (3.40) & (3.41), any lump-sum payments or benefits must be converted into equivalent uniform periodic time by using of the capital recovery factors *(A/P, i, N)* and *(A/F, i, N)*.

$$A/P = \frac{i(1+i)^N}{(1+i)^N - 1} \tag{3.40}$$

$$A/F = \frac{i}{(1+i)^N - 1} \tag{3.41}$$

3.6.3 Market Survey

A solar energy system is generally defined by a high initial cost and low operational costs as compared with the relatively low initial cost and high operating costs of Electric Water Heater system. Heating water through solar energy also means long-term benefits, such as, free from future fuel shortages and the maintenance of environmental benefits. The cost benefit analysis is performed based on the Annual worth method which deals with two parts, namely, one is the solar water heater cost whereas the other is the electric

University of Malaya

water heater cost and their comparisons. The cost analysis is presented in a cash flow diagram.

The following Appendix B, Table B.2 to Table B.5 is obtained from a survey performed in the Malaysian market. However, Table B.1 shows the cost of electrical water heater, which is only for comparison purpose. This experiment on the flat plate PV, PV/T, PV/T-PCM with the self-cleaning system collectors has derived a total cost as listed in Appendix B. The total cost of constructing a solar PV module at MYR 2000 (US$ 469.21) per unit, solar thermal collector system at MYR 1650.77 (US$ 387.33) per piece, and phase change material at MYR 1753.76 (US$ 411.50) per piece and self-cleaning system at MYR 861 (US$ 202.02) per piece.

University of Malaya

CHAPTER 4: RESULTS AND DISCUSSION

4.1 Introduction

A PV/T water collector with an innovative serpentine flow channel has been designed and fabricated and its performance has been studied as a PV/T-only system, PV/T-PCM system and PV/T-PCM system with self-cleaning mechanism with a view to pick the best alternative among them. This chapter presents the outcomes and the corresponding explanations of the present research work. Upon design, fabrication and installation of the system, data for different parameters, like PV top surface, back surface, inlet water and outlet temperatures were recorded at flow rates ranging from 0.5 to 4 liters per minute (LPM). The results have been categorized in a comparative fashion in three different sections, where Sections 4.3 to 4.7 present the comparative results obtained from a PV, PV/T, PV/T-PCM and dust and self-cleaning system from energy and exergy perspectives and section 4.8 presents an overall comparative study among all the systems. An economic analysis on PV, PV/T-PCM and PV/T-PCM with self-cleaning mechanism has been given in section 4.9, where the economic parameters have been compared with those of an electric water heater to have a comparative view.

As both PV and PV/T hybrid systems work only in daytime, hence, in the performance study of these systems it is a convention to show the variation of the performance parameters over a certain period of daytime when sufficient sunlight is available. The main control parameter in the performance study of PV/T hybrid systems employed in the present investigation is the flow rate of water which has been varied from 0.5 to 4.0 LPM. Thus, all performance parameters have been presented as a function of daytime lapse for each flow rates. However, the representative results for optimum flow rates are 4 LPM from the PV/T and PV/T-PCM modules are presented before the other flow rates such as 0.5 LPM, 1 LPM, 2 LPM and 3 LPM. The results from energy and exergy point

University of Malaya

of view for PV/T-PCM system with self-cleaning and dust has also been presented at water flow rate between 0.5 LPM-4 LPM.

4.2 Photovoltaic Thermal (PV/T) and Photovoltaic Thermal-Phase change material (PV/T-PCM) systems

This section presents the results on PV/T and PV/T-PCM systems with reference to PV system. The hourly variation of different parameters such as temperatures at different state points and solar radiation with respect to time of PV/T and PV/T-PCM systems as compared PV module has been presented in section 4.2.1 and 4.2.2 respectively. Energy and exergy analysis of PV/T and PV/T-PCM systems with reference to PV has been detailed in subsections 4.3 and 4.4 respectively.

4.2.1 Hourly Variation of Different Parameters of PV and PV/T

The hourly variation of solar radiation and different parameters, like ambient temperature (T_a), water temperature difference (T_{out}-T_{in}), cell temperature difference (T_{cell}) and solar radiation (G), etc., have been presented in Figure 4.5 to 4.10. The figures presents the conditions under which the experiments were carried out. Table 4.1 and 4.2 presents the measured PV/T and PV/T-PCM collector parameters, such as inlet (T_{in}), outlet (T_{out}) water temperature, maximum power (P_{max}) at optimum mass flow rate of 4 liter per min (LPM).

The comparative performance study of the reference PV and PV/T-only system has been carried out during the months of May to July in 2016. Significant results were obtained with the mass flow rate were measured 0.5, 1, 2, 3 and 4 LPM, respectively. Figure 4.1 shows the hourly variation of solar radiation and temperatures at different state of points of PV and PV/T for 0.5 LPM water flow rate. The average ambient temperature was found to be 32.70°C. The solar radiation rose to a peak of 996 W/m^2 at 2:15 PM, whereas the cell temperature difference is found 2.17°C. The maximum cell temperature

University of Malaya

difference between PV and PV/T is found 6.16°C when the solar radiation were 796 W/m^2 at 11:30 AM. The highest difference between inlet and outlet water temperature is found 28.23°C at 2:00 PM. Such high temperature rise is basically due to very low mass flow rate of water (0.5 LPM). This shows the importance of flow rate optimization and systems can be used at different flow rates as per the need of needed temperature in real life applications. In Malaysia environmental condition, the radiation intensity at the morning up to 10:00 as low as 200 W/m^2, which is very insignificant for PV and PV/T application. That is why, data acquisition was started up to 16:00 PM.

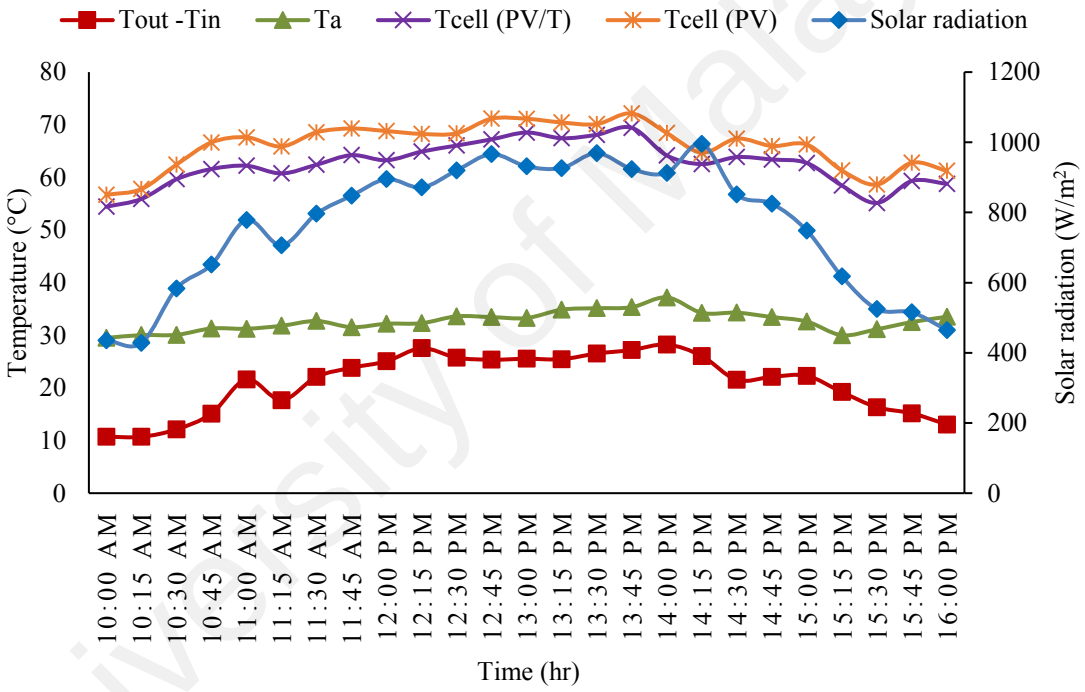

Figure 4.1: Hourly variation of different PV and PV/T parameters (0.5 LPM)

The hourly variation of solar radiation and temperatures at different state of points of PV and PV/T for 1 LPM water flow rate is shown in Figure 4.2. As can be seen from Figure 4.2, the maximum inlet and outlet water temperature difference was found to be 16.99°C at 2:00 PM. However, the average ambient temperature was 32.10°C. The peak solar radiation was 983 W/m^2 at 2:00 PM, whereas the cell temperature difference is found 3.73°C. The maximum cell temperature difference between PV and PV/T found 6.64°C at 3:15 PM when the solar radiation were 627 W/m^2. The maximum temperature

University of Malaya

difference between inlet and outlet temperature at 1 LPM is less than that of 0.5 LPM which is an obvious case, as water flow at 1 LPM is higher as compared to 0.5 LPM and water remains in the thermal absorber for lesser time. While, at 1 LPM the maximum cell temperature difference between PV and PV/T is found to be higher than that at 0.5 LPM which shows that the cooling is more effective at 1 LPM than that of 0.5 LPM.

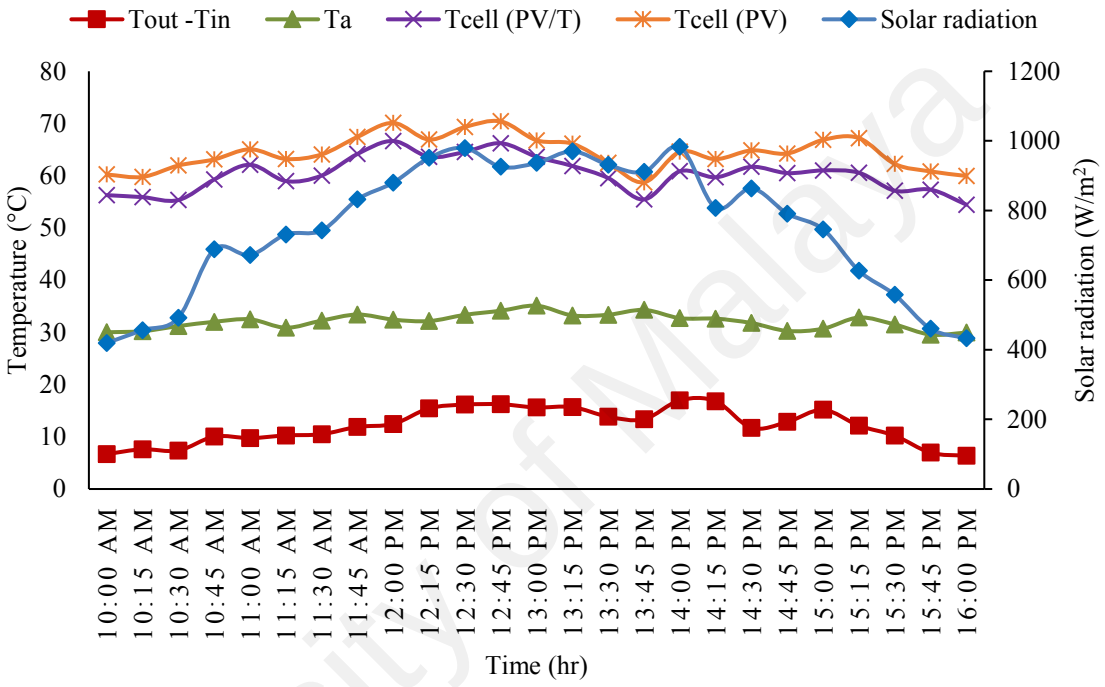

Figure 4.2: Hourly variation of different PV and PV/T parameters (1 LPM)

Figure 4.3 shows the hourly variation of solar radiation and temperatures at different state of points of PV and PV/T for 2 LPM water flow rate. Figure 4.3 shows that the maximum inlet and outlet water temperature difference is found to be 9.54°C at 1:15 PM when the mass flow rate was 2 LPM. However, the average ambient temperature was 32.77°C. The solar radiation reached to its peak of 995 W/m^2 at 1:00 PM, whereas the cell temperature difference is found 8.17°C. The maximum cell temperature difference between PV and PV/T is found 8.95°C at 1:30 PM when the solar radiation were 987 W/m^2. It is found that temperature difference between inlet and outlet at 2 LPM is much lower than that of at 0.5 LPM and 1 LPM this is due to the fact as explained above. Again, the maximum cell temperature difference between PV and PV/T is found to be higher at

University of Malaya

2 LPM than that of 0.5 LPM and 1 LPM therefore, cooling is much more effective at 2 LPM. This is due to the fact that at higher mass flow rate, the water flow is frequent and carries the heat away at frequent manner as compared to lower mass flow rates.

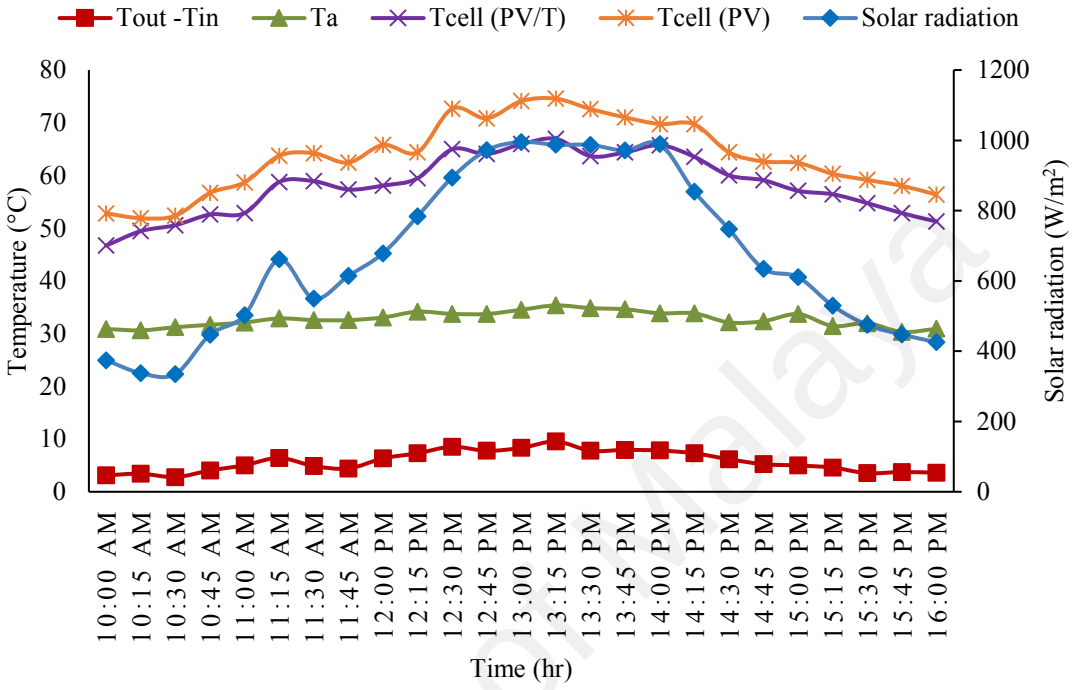

Figure 4.3: Hourly variation of different PV and PV/T parameters (2 LPM)

The hourly variation of solar radiation and temperatures at different state of points of PV and PV/T for 3 LPM water flow rate is shown in Figure 4.4. Maximum inlet and outlet water temperature difference is found to be 6.44°C at 1:15 PM, when the mass flow rate was 3 LPM. However, the average ambient temperature was 32.40°C. The solar radiation reached to its peak of 987 W/m^2 at 1:00 PM, whereas the cell temperature difference is found 5.96°C. The maximum cell temperature difference between PV and PV/T is found 7.48°C at 10:00 AM when the solar radiation were 307 W/m^2. This temperature difference shows that the ambient temperature and solar radiation has significant effect on PV performance. But because of the cooling effect due water flow in PV/T collector this effect is not as much of on the PV/T system. Temperature difference between outlet and inlet has been found to be decreased further as compared to 0.5 LPM, 1 LPM and 2 LPM due to the fact as explained above. The cell temperature difference between PV and PV/T

University of Malaya

module are not that large because in PV/T collector there is only one medium that is, the serpentine circulating water flow. The amount of heat produced inside the collector, only mass flow rates are not enough to absorb and transfer to outlet. This is an important behavior that will be effected on thermal and electrical performance of a PV/T collector.

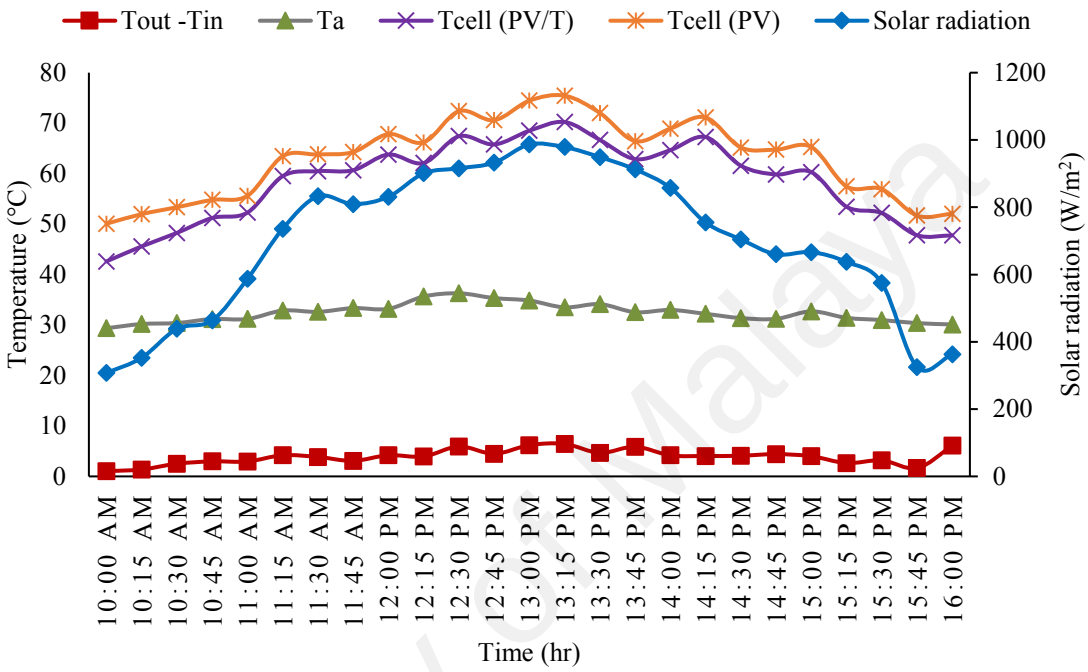

Figure 4.4: Hourly variation of different PV and PV/T parameters (3 LPM)

From Figure 4.5 it may be observed that the solar radiation has been increasing from 304 W/m^2 at 10:00 AM to a peak value of 981 W/m^2 at 1:15 PM, which then decreases to 385 W/m^2 at 4:00 PM. Although, there are several unusual sharp declines in the solar radiation curve it may be concluded that solar radiation is at its peak from 12:00 to 2:00 PM. However, variation in the ambient temperature throughout the day does not follow the same trend, as in the case of irradiation, rather it remains almost constant all along the day with little variation. It is also evident from Figure 4.5 that the temperature rise in water is directly proportional to the hourly variation in solar radiation with the increasing trend in morning, highest increase in the noon and then decreasing trend. The maximum inlet and outlet water temperature difference is found to be 4.30°C at 1:15 PM. It may also be observed from Figure 4.5 that compared to PV cell temperature, the PV/T cell

University of Malaya

temperature remains low throughout the day which is due to the cooling effect of water circulation. The maximum cell temperature difference between PV and PV/T is found 7.13°C when the solar radiation was 805 W/m^2 at 2:00 PM. It is observed that at peak solar radiation the cell temperature difference is 4.71°C.

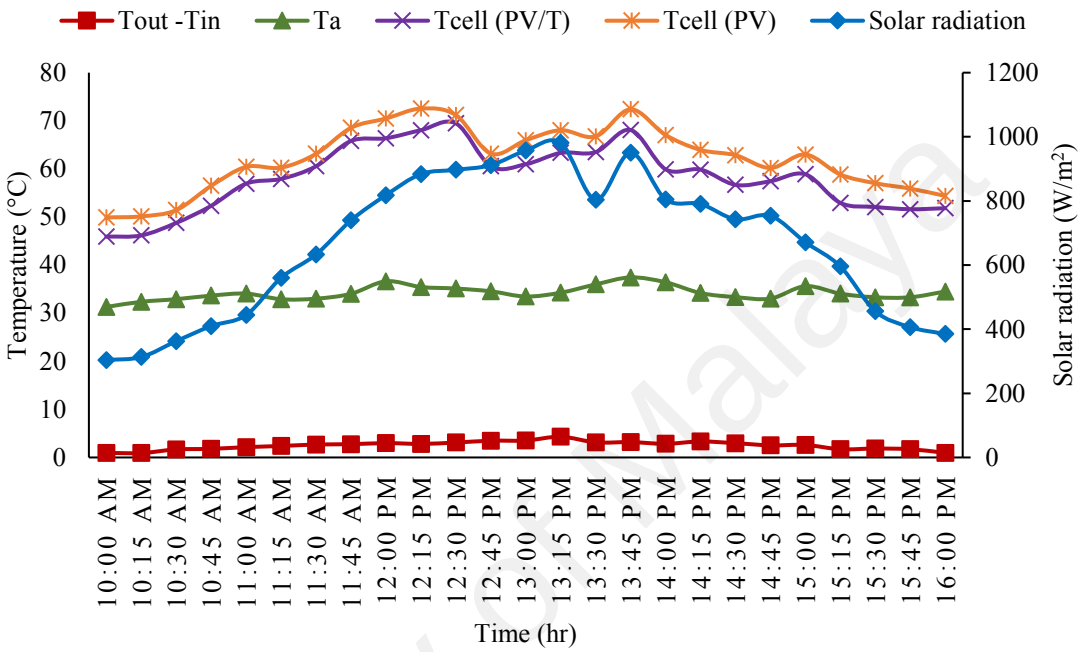

Figure 4.5: Hourly variation of different PV and PV/T parameters (4 LPM)

Table 4.1: The measured parameters at mass flow rate of 4 LPM

Time	T_a (°C)	T_{in} (°C)	T_o (°C)	P_{max} (W)	G (W/m^2)
10:00	31.29	26.01	26.95	66.68	304
10:30	32.91	26.84	28.50	67.80	363
11:00	34.06	27.08	29.23	96.47	444
11:30	33.02	28.84	31.53	117.39	633
12:00	36.63	28.07	31.05	121.43	818
12:30	35.12	29.35	32.45	122.69	897
13:00	33.46	27.47	30.99	144.53	957
13:30	35.98	24.39	27.53	123.64	804
14:00	36.42	25.12	27.97	122.40	805
14:30	33.34	27.02	29.98	117.53	743
15:00	35.61	27.14	29.73	121.15	671
15:30	33.30	25.53	27.39	74.60	456
16:00	34.50	25.50	26.46	79.61	385

University of Malaya

4.2.2 Hourly Variation of Different Parameters of PV and PV/T-PCM

Comparative performance investigation of the reference PV and PV/T-PCM systems has been carried out during the months of August and September 2016. Significant results were obtained with the mass flow rate were measured 0.5, 1, 2, 3 and 4 LPM respectively. Figure 4.6 shows the hourly variation of solar radiation and temperatures at different state of points of PV and PV/T-PCM for water flow rate of 0.5 LPM. The highest difference between inlet and outlet water temperature is found 26.40°C at 1:00 PM. The average ambient temperature was 34.87°C. The solar radiation reached to its peak of 999 W/m^2 at 2:15 PM. The highest difference between cell temperature of PV and PV/T-PCM is found 10.09°C under the peak solar radiation of 999 W/m^2 at 2:15 PM. It can be seen the outlet water temperature reached at maximum at low mass flow rate but because of PCM the cell temperature drops significantly. However, at this mass flow rate outlet water temperature drops around 2°C as compared to PV/T system, which is a notable performance of using PCM.

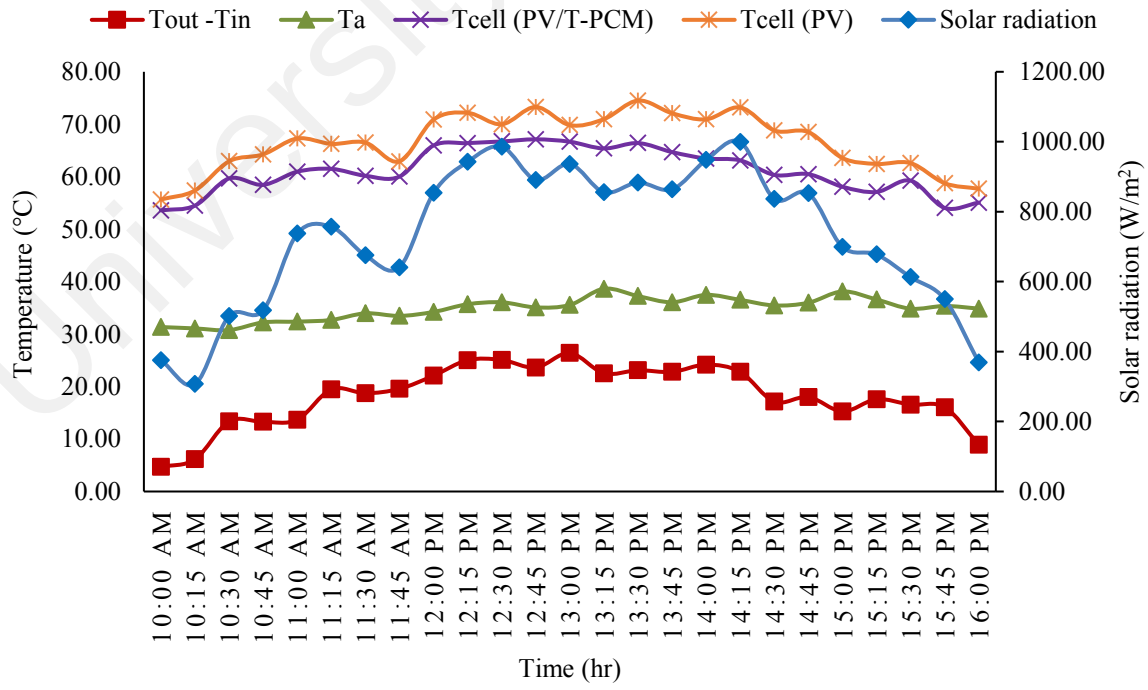

Figure 4.6: Hourly variation of different PV and PV/T-PCM parameters (0.5 LPM)

University of Malaya

Figure 4.7 shows the hourly variation of solar radiation and various temperatures at different state points of PV and PV/T-PCM for a water flow rate of 1 LPM. The highest difference between inlet and outlet water temperature is found 15.73°C at 12:00 PM, whereas the average ambient temperature remained at 32.56°C. At this flow rate the outlet water temperature is decreased but heat transfer rate is increased. The peak solar radiation of 988 W/m^2 was observed at 1:30 PM, whereas the cell temperature difference is found 7.03°C. A maximum drop in cell temperature of 10.26°C with PV/T-PCM system as compared to reference PV is obtained under 947 W/m^2 irradiation at 1:00 PM. It is observed that the cell temperature difference is also increased, as compared to that at mass flow rate of 0.5 LPM. The thermal energy has been stored by a solar panel. That is why, the cell temperature cooling rate is very slow.

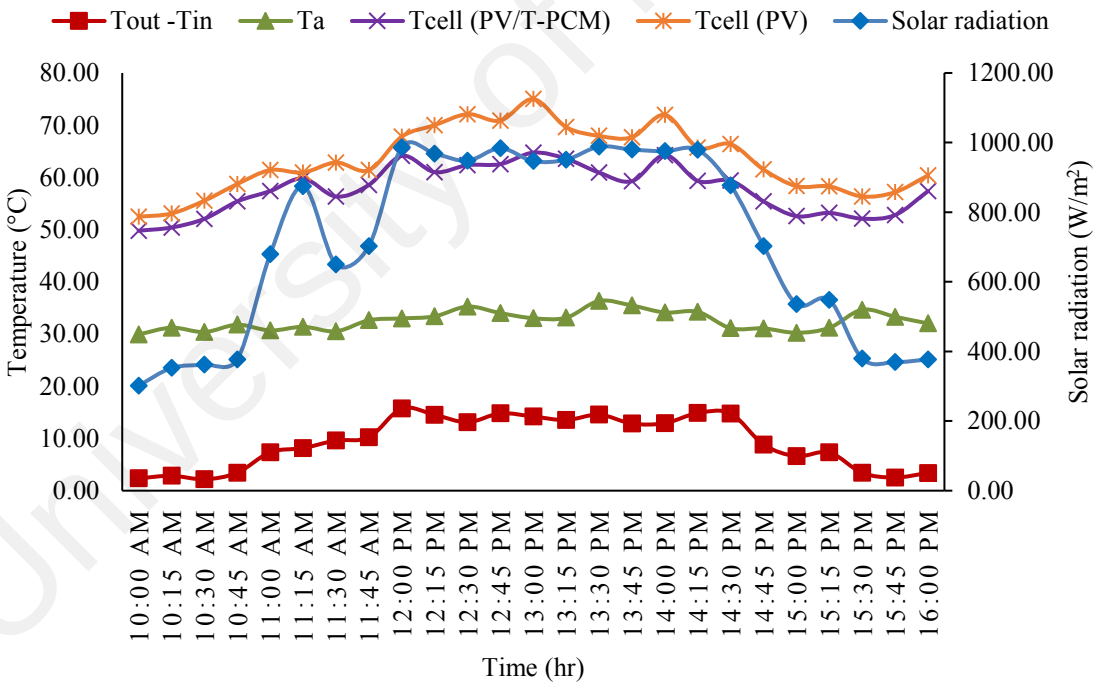

Figure 4.7: Hourly variation of different PV and PV/T-PCM parameters (1 LPM)

Figure 4.8 shows that the hourly variation of solar radiation and various temperatures at different state of points of PV and PV/T-PCM for water flow rate of 2 LPM. Maximum rise in outlet water temperature is found 8.66°C at 1:45 PM. The outlet water temperature is decreased at 2 LPM due to the fact as explained above. The average ambient

University of Malaya

temperature was 34.01°C. The highest solar radiation was recorded 983 W/m^2 at 12:00 PM, whereas the cell temperature difference found is 5.64°C. The maximum cell temperature drop with PV/T-PCM as compared to reference PV is obtained 13.15°C under 363 W/m^2 at 10:00 AM. This temperature difference shows that the ambient temperature and solar radiation has significant effect on the performance of the PV module. However, this effect is not as much of PV/T-PCM system due to the combined cooling effect by water flow and PCM. It can be observed that the cell temperature difference increased as compared to that at the mass flow rate of 1 LPM, because of the improvement in the heat transfer rate.

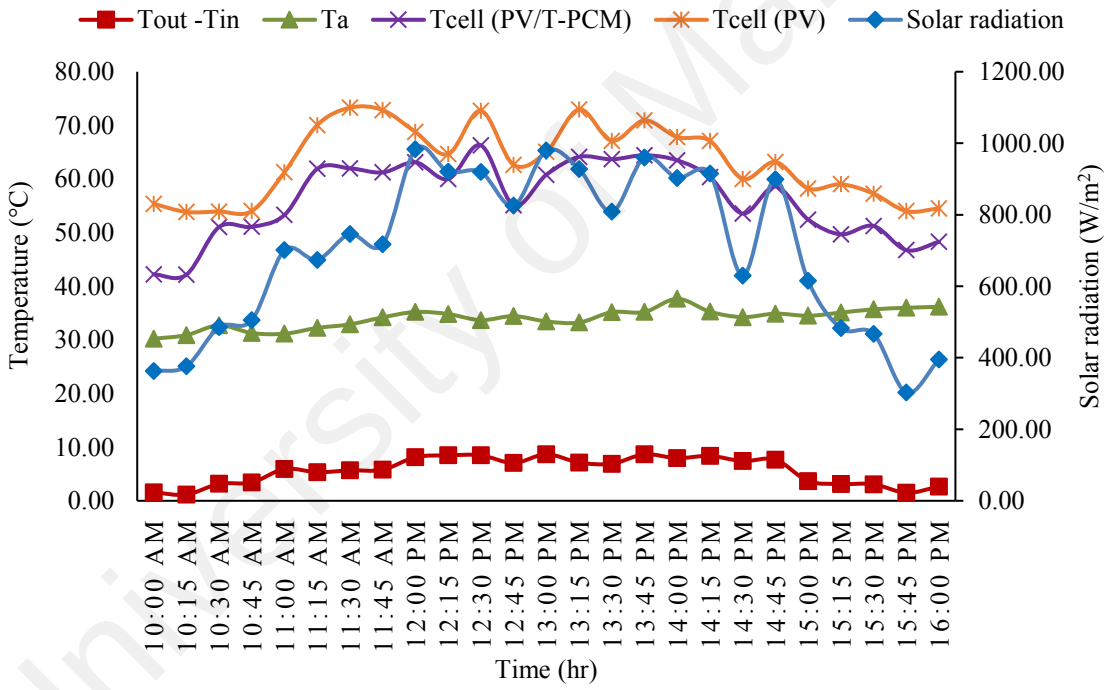

Figure 4.8: Hourly variation of different PV and PV/T-PCM parameters (2 LPM)

Figure 4.9 shows that the hourly variation of solar radiation and temperatures at different state points of PV and PV/T-PCM for a water flow rate of 3 LPM. Maximum rise in outlet water temperature is 5.22°C at 2:15 PM. The average ambient temperature was 33.26°C. The solar radiation reached to its peak of 989 W/m^2 at 1:45 PM, whereas the cell temperature difference found is 6.53°C. The maximum cell temperature difference between PV and PV/T-PCM found 12:45°C under an irradiation level of 449

University of Malaya

W/m^2 at 10:45 AM. Temperature difference between outlet and inlet is found to be decreased further as compared to 0.5 LPM, 1 LPM and 2 LPM due to the fact as explained above. It is clear that for PV/T-PCM system, as flow rate is increased the outlet water and module temperature are decreased, which means the thermal and electrical performance can be depended on mass flow rates.

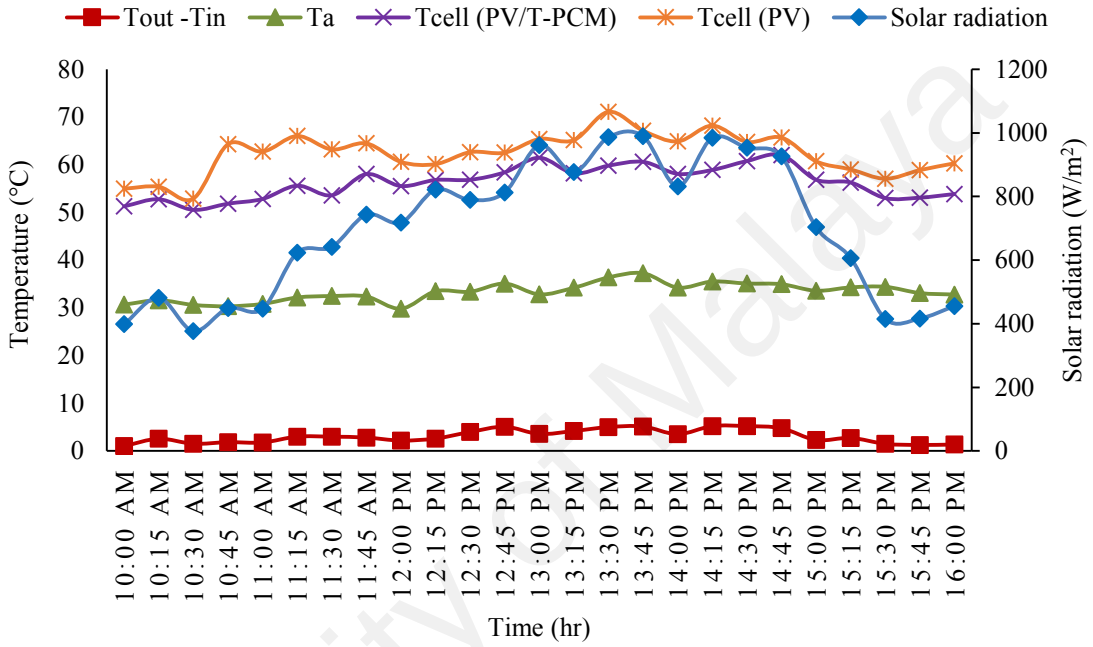

Figure 4.9: Hourly variation of different PV and PV/T-PCM parameters (3 LPM)

From Figure 4.10, it may be observed that the hourly variation of solar radiation increased from 375 W/m^2 at 10:00 AM to a peak of 995 W/m^2 at 1:00 PM, which then decreases to 336 W/m^2 at 4:00 PM. The cell temperature difference between PV and PV/T-PCM at peak solar radiation is 3.33°C. The solar radiation reaches and remains maximum between 12:00 to 1:45 PM. It is also evident from Figure 4.6 that the maximum rise in outlet water temperature is 3.98°C at 1:00 PM. It may be observed from a comparative point of view from Figure 4.10 and Figure 4.5 that compared to PV/T-only system, the PV/T-PCM system offers a greater drop in cell temperature. While the maximum drop in cell temperature with PV/T-only system is around 7.13°C only, the PV/T-PCM system produces a temperature drop of 10.57°C. The PV/T-PCM collector

University of Malaya

has two heat transfer medium: one is thermal collector and another is phase change material. Heat generated from the collector is first transferred to water then PCM, then PCM absorbs huge amount of thermal energy and when it has been melted properly, that thermal energy again transferred to water. These process not only reduce the cell temperature but also increase the thermal and electrical performance of the entire system.

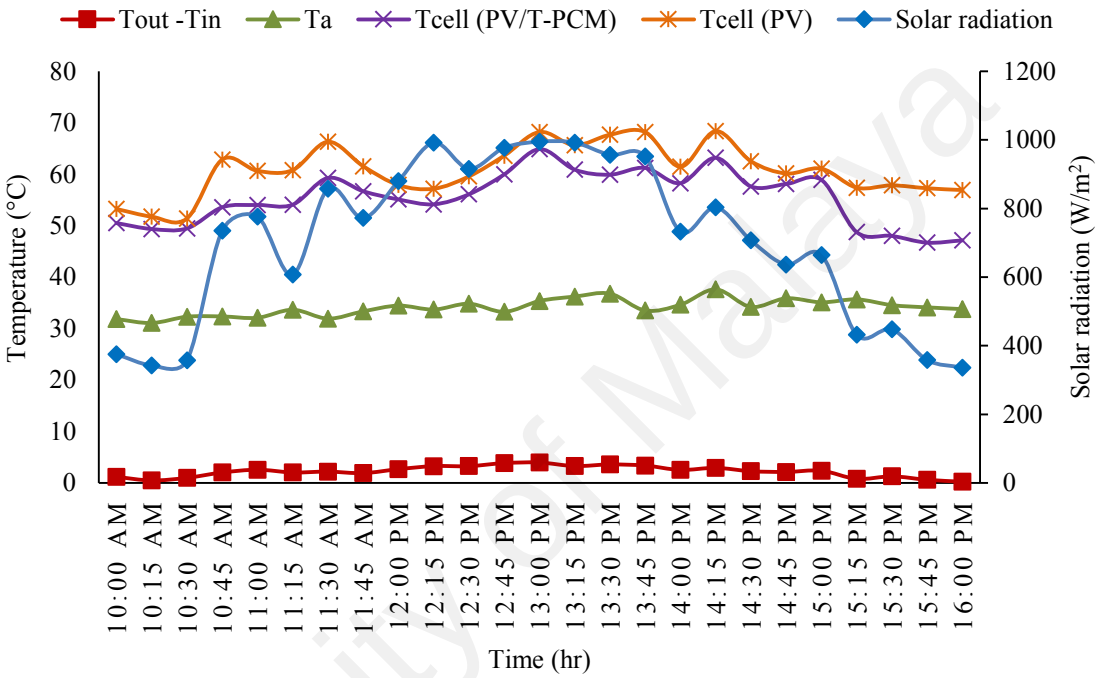

Figure 4.10: Hourly variation of different PV and PV/T-PCM parameters (4 LPM)

Table 4.2: The measured parameters at mass flow rate of 4 LPM

Time	T_a (°C)	T_{in} (°C)	T_o (°C)	P_{max} (W)	G (W/m^2)
10:00	31.85	22.76	23.94	79.67	375
10:30	32.31	21.60	22.61	69.01	358
11:00	32.11	24.11	26.68	146.61	777
11:30	31.94	26.60	28.81	139.16	858
12:00	34.46	28.04	30.73	132.66	880
12:30	34.83	28.65	31.93	140.28	916
13:00	35.36	28.83	32.82	160.29	995
13:30	36.79	29.18	32.78	142.27	957
14:00	34.63	29.85	32.39	142.03	732
14:30	34.21	29.43	31.72	140.47	707
15:00	35.11	29.74	32.13	114.03	665
15:30	34.56	29.89	31.18	102.00	448
16:00	33.79	27.58	27.82	73.54	336

University of Malaya

4.3 Energy Analyses of PV/T and PV/T-PCM Systems

The energy analysis that is based on the first law of thermodynamics presents a rough picture that shows how the input energy has been exploited and which sectors are the prime contributors in the energy consumption. In the present study, the change in different energy parameters, such as, electrical power output, electrical efficiency, thermal efficiency, etc., have been analyzed as a function of the solar irradiation, cell temperature and water flow rate in order to observe which of them has the prominent effect on the energy performance of the PV/T and PV/T-PCM systems. It may be mentioned here that an experimental study on PV/T and PV/T-PCM has been carried out for five different flow rates of cooling water, however, representative results of an optimum flow rate have only been presented in the forthcoming sections.

4.3.1 Effect of Irradiation on Electrical Performance

The effect of increased irradiation level on electrical power and electrical efficiency has been illustrated in Figure 4.11 (a) and (b) shows the effect of increased irradiation level on electrical power and electrical efficiency at the mass flow rate of 0.5 LPM. The peak solar radiation is 999 W/m^2, the electrical power of the PV and PV/T-PCM module is 140.64 W and 151.26 W respectively as shown in Figure 4.11 (b). On the other hand, at 996 W/m^2 power output of PV and PV/T module are 142.13 W and 145.61 W respectively as shown in Figure 4.11 (a). The maximum difference between the output power of PV and PV/T module is 15.62 W at 1:15 PM as shown in Figure 4.11 (a). In contrast, this difference between PV and PV/T-PCM is 18.28 W at 10:45 AM as shown in Figure 4.11 (b). The maximum difference between electrical efficiency of PV and PV/T module is 1.02% at 1:15 PM, whereas that of the PV and PV/T-PCM module is 2.14% at 10:45 AM. The maximum electrical efficiency of the PV/T system is 11.40% at 10:00 AM, whereas that of the PV/T-PCM is 13.92% at 10:15 AM as shown in Figure 4.11 (a) and (b). The experimental investigation has been carried out on-site under real ambient

University of Malaya

conditions, wherein the radiation intensity at any time may go down due to shading from cloud, etc. The data acquisition is a continuous process in which some irregular data may also be saved. These irregular data do not show the trend.

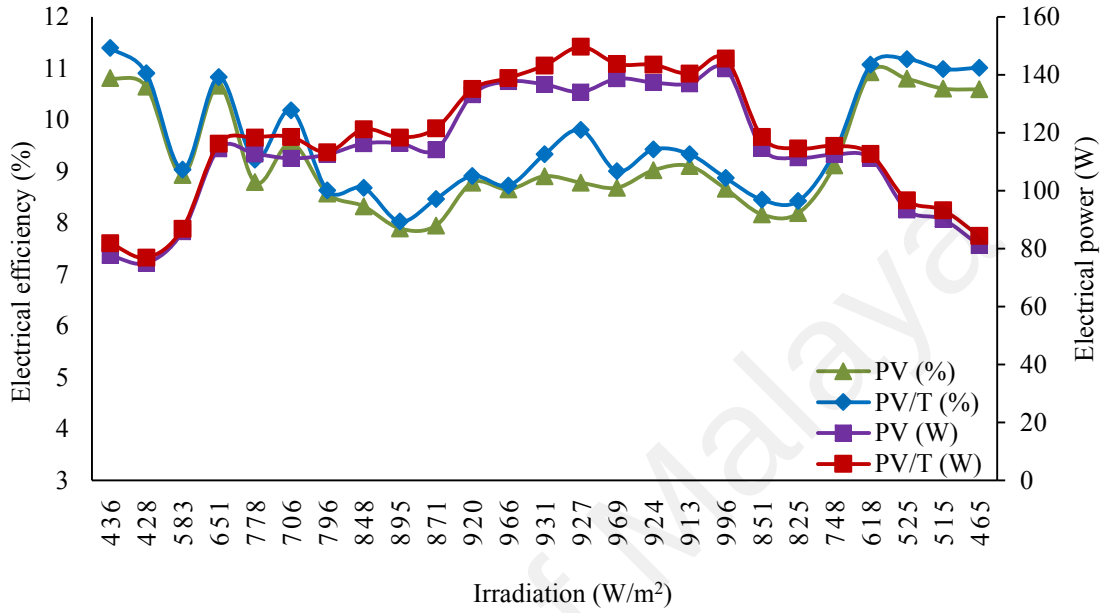

(a) Electrical performance of PV/T against PV

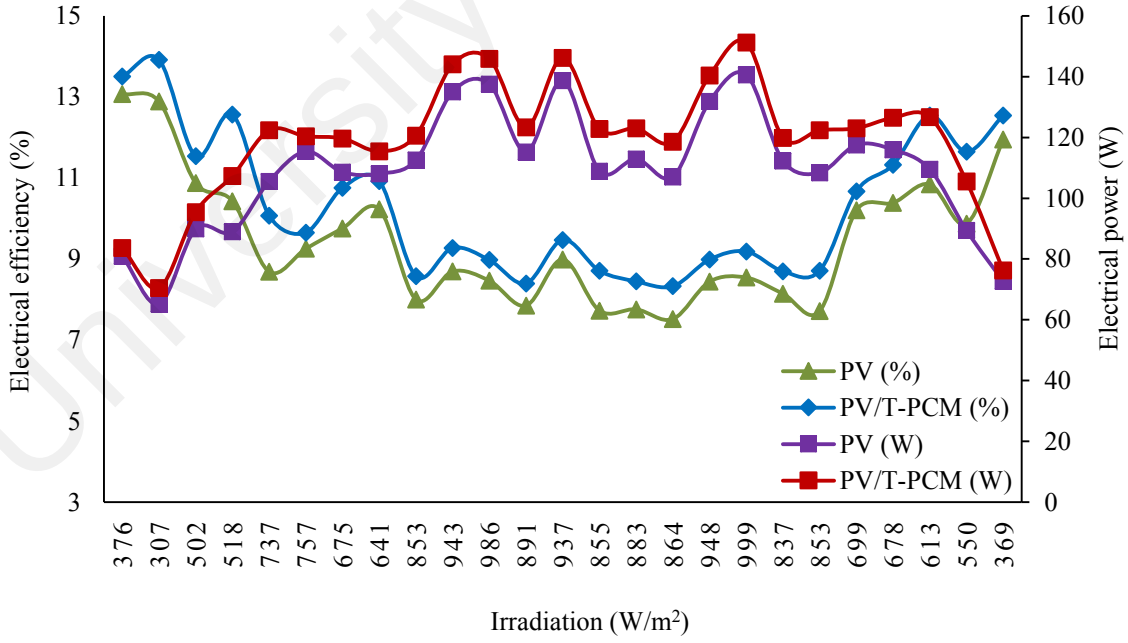

(b) Electrical performance of PV/T-PCM against PV

Figure 4.11: Effect of irradiation on electrical performance of (a) PV/T and (b) PV/T-PCM against the reference PV (0.5 LPM)

University of Malaya

Figure 4.12 (a) and (b) shows the effect of irradiation level on electrical power and electrical efficiency at mass flow rate of 1 LPM. The highest solar radiation attained is 988 W/m^2, at which the electrical power of the PV and PV/T-PCM module is 138.40 W and 145.45 W respectively as shown in Figure 4.12 (b). On the contrary, for PV and PV/T module power output at 983 W/m^2 are 136.13 W and 144.11 W respectively. The maximum difference between the output power of PV and PV/T module is 8.30 W at 2:45 PM as shown in Figure 4.12 (a), while that between PV and PV/T-PCM is 24.97 W at 2:15 PM as shown in Figure 4.12 (b). From Figure 4.12 (a) and (b) it can be observed that the maximum electrical efficiency of the PV/T system is 12.61% at 4:00 PM, whereas that of the PV/T-PCM is 14.25% at 3:45 PM. Also, the maximum electrical efficiency difference between PV and PV/T module is 0.75% at 3:45 PM, whereas that for the PV and PV/T-PCM module is 1.55% at 2:15 AM as shown in Figure 4.12 (a) and (b). The irradiation level increases rapidly at the early part of the day, while during midday the variation becomes minute. That is why, the electrical power and efficiency remain almost same near an average value.

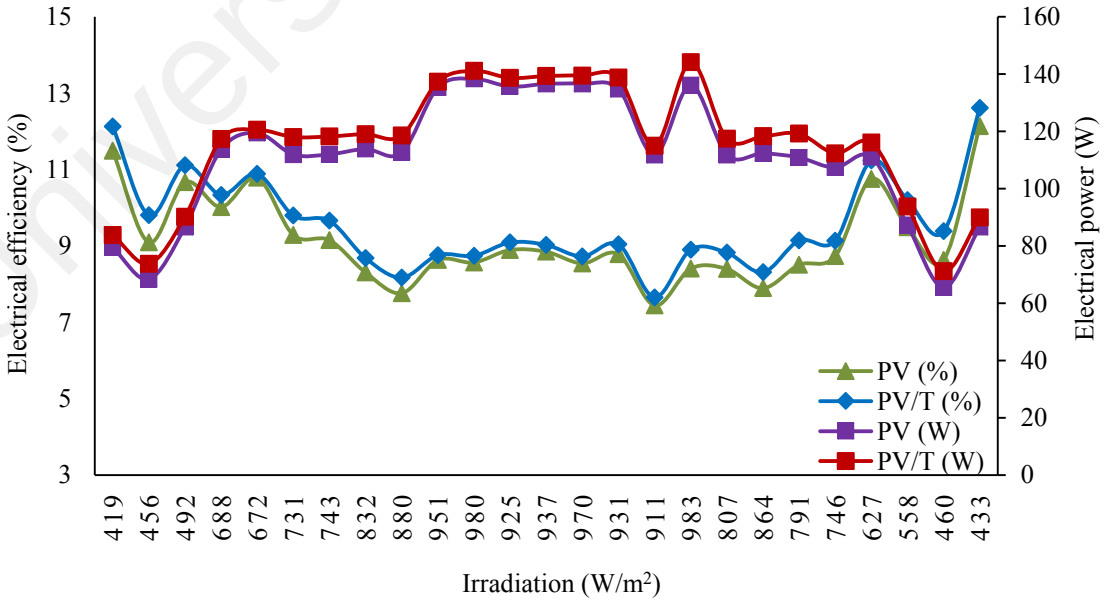

(a) Electrical performance of PV/T against PV

Figure 4.12: Effect of irradiation on electrical performance of (a) PV/T and (b) PV/T-PCM against the reference PV (1 LPM)

University of Malaya

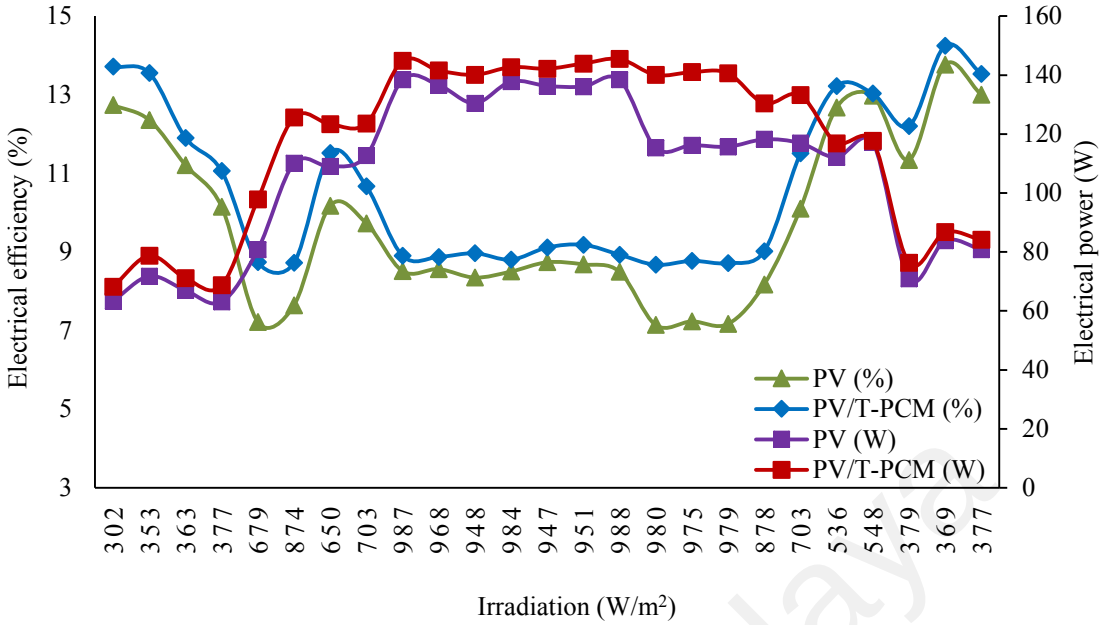

(b) Electrical performance of PV/T-PCM against PV

Figure 4.12, continued

Figure 4.13 (a) and (b) presents the electrical power and electrical efficiency of PV/T and PV/T-PCM systems at a mass flow rate of 2 LPM. The electrical power of the PV and PV/T-PCM module are 133.39 W and 150.06 W respectively under the peak radiation of 983 W/m^2 as shown in Figure 4.13 (b), as compared to that of PV and PV/T module of 132.34 W and 139.73 W respectively at 995 W/m^2 as shown in Figure 4.13 (a). The maximum electrical efficiency of the PV/T system is 12.75% at 10:15 AM, whereas that of the PV/T-PCM is 13.04% at 10:15 AM, respectively as shown in Figure 4.13 (a) and (b). In addition, the maximum electrical efficiency difference between PV and PV/T module is 1.36% at 10:30 AM, whereas that of the PV and PV/T-PCM module is 2.33% at 3:15 PM.

University of Malaya

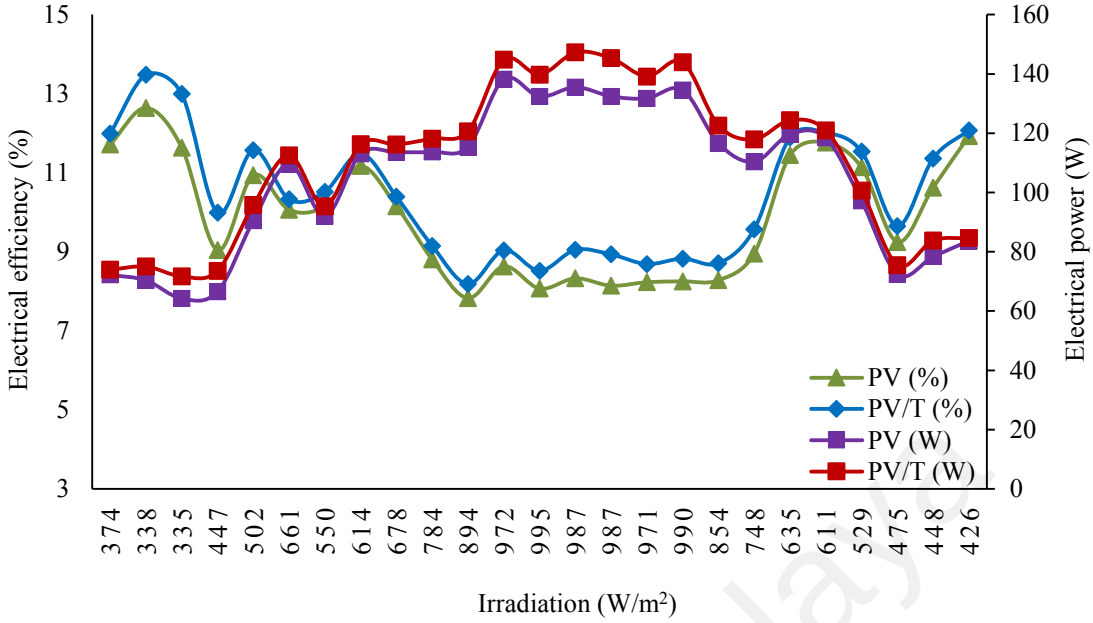

(a) Electrical performance of PV/T against PV

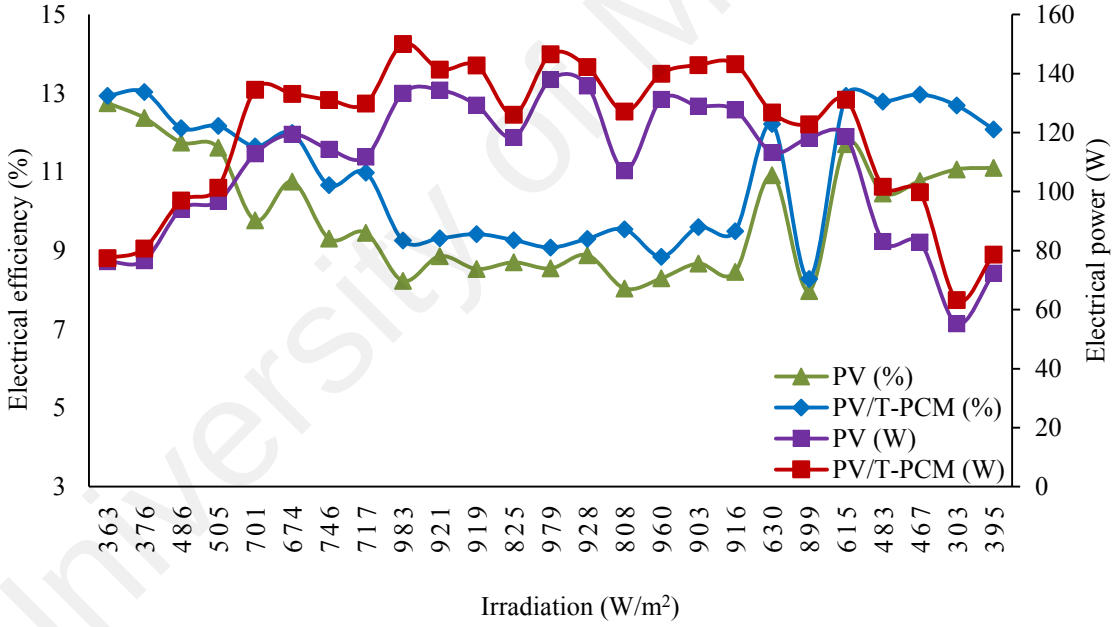

(b) Electrical performance of PV/T-PCM against PV

Figure 4.13: Effect of irradiation on electrical performance of (a) PV/T and (b) PV/T-PCM against the reference PV (2 LPM)

Electrical power and efficiencies at mass flow rate of 3 LPM are shown in Figure 4.14 (a) and (b). At the peak solar radiation of 989 W/m^2, the electrical power of the PV and PV/T-PCM module are 116.62 W and 130.76 W respectively as shown in Figure 4.14 (b), as compared to that for PV and PV/T to be 140.56 W and 148.29 W respectively under

University of Malaya

987 W/m^2 as shown in Figure 4.14 (a). The maximum output power for PV/T module is 148.29 W at 1:00 PM, and the maximum output power for PV/T-PCM module is 140.70 W at 3:00 PM as shown in Figure 4.14 (a) and (b). On the other hand, the maximum electrical efficiency of PV/T system is 14.25% at 4:00 PM and that of PV/T-PCM system is 13.90% at 10:30 AM. Furthermore, from Figure 4.14 (a) and (b) is seen that the maximum electrical efficiency difference between PV and PV/T module is 1.43% at 10:15 AM, whereas that of the PV and PV/T-PCM module is 1.74% at 12:00 PM.

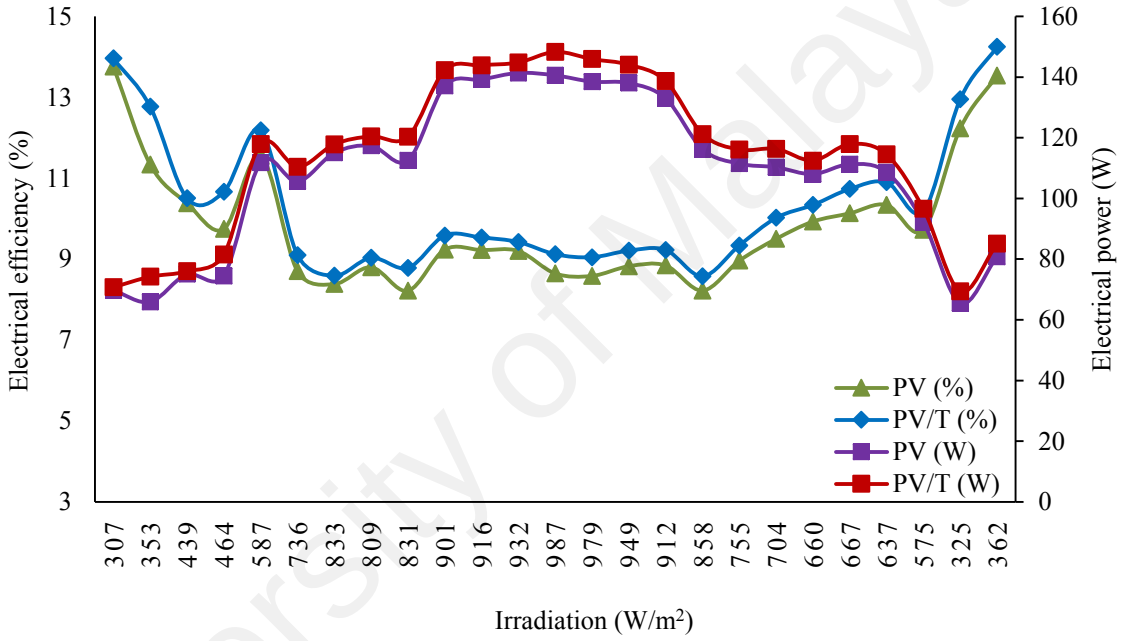

(a) Electrical performance of PV/T against PV

Figure 4.14: Effect of irradiation on electrical performance of (a) PV/T and (b) PV/T-PCM against the reference PV (3 LPM)

University of Malaya

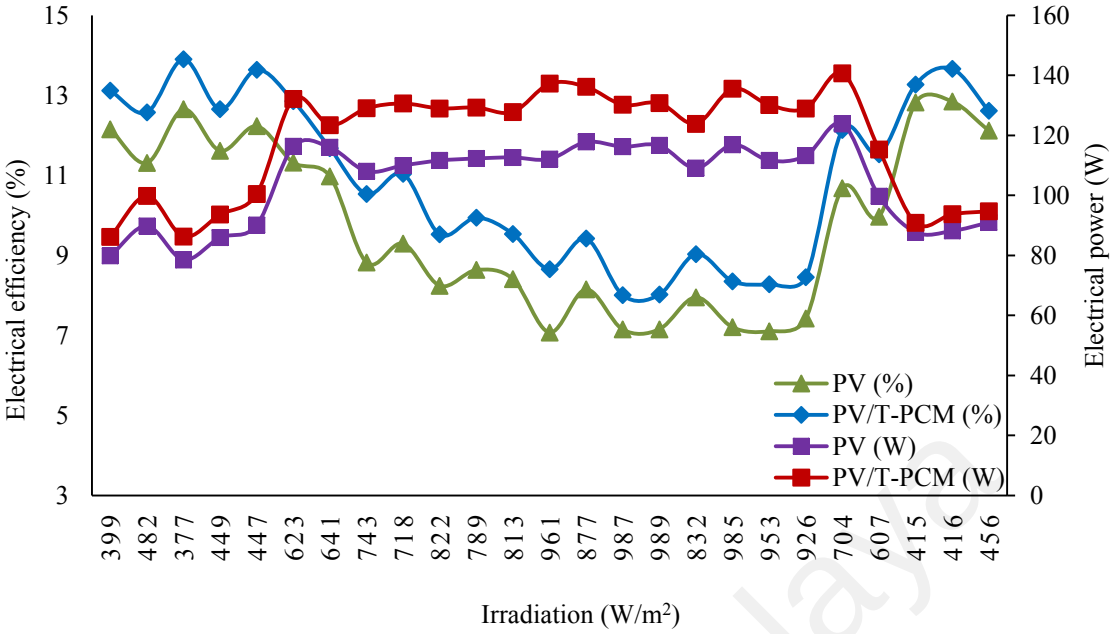

(b) Electrical performance of PV/T-PCM against PV

Figure 4.14, continued

Figure 4.15 at optimum mass flow rate of 4 LPM. It can be seen from Figure 4.15 (a) and (b) that electrical power and efficiency of PV/T as well as PV/T-PCM systems increases with increasing irradiation level. In both cases, it surpasses the power output of the reference PV system over the full range of irradiation. There are some points noticeable from these figures. Firstly, the effect of cooling becomes effective at higher irradiations that is portrayed by the expanding gap between the trend lines of PV and PV/T systems as shown in Figure 4.15 (a) and PV and PV/T-PCM systems as shown in Figure 4.15 (b). The temperature difference between the inlet water and outlet water is very trivial at lower radiation level. As the irradiation level increases, the temperature difference increases to mobilize the rate of heat transfer, which helps to remove more heat from the higher irradiations. This tendency is slightly greater in the case of the PV/T-PCM system, evidently indicating the practical usage of the PCM in temperature control.

University of Malaya

Secondly, the increment rate of power output is steeper in the range of around 300 to 1000 W/m^2. Hence, it may be concluded that the highest output from a PV/T or PV/T-PCM panel in typical Malaysian weather condition can be obtained under irradiation of around 1000 W/m^2. Thirdly, at 995 W/m^2, the electrical power of the PV and PV/T-PCM module is 123.85 W and 160.29 W respectively, as shown in Figure 4.15 (b), as compared to that at 981 W/m^2 of PV and PV/T module of 138.14 W and 148.61 W respectively, as shown in Figure 4.15 (a), thus illustrating a clear enhancement in the power output with the PCM and mass flow rate used for thermal control. Results show that power levels of solar cell vary under different levels of illuminations. The panel current increases in proportional to solar radiation with little increases in panel voltage. Similarly, panel power increases in proportion to solar radiation level. The power variation between PV, PV/T and PV/T-PCM depends on ambient and cell temperature difference, whereas the effect of cell temperature on electrical performance. The difference between maximum output power of PV and PV/T is 10.52 W at 2:15 PM as shown in Figure 4.15 (a), whereas the same value between PV and PV/T-PCM is 36.44 W at 1:00 PM as shown in Figure 4.15 (b). For every 100 W/m^2 increase in irradiation level, output power rose by 11.95 W and 13.12 W for PV/T and PV/T-PCM respectively. Phase change materials possess a good ability of storing large amount of heat, which helps to lower the cell temperature and keeps as near as possible to the STC value, thereby improving the electrical output. Figure 4.15 (a) and (b) show the response of electrical efficiency as a function of the irradiation of PV/T and PV/T-PCM systems respectively both on the performance of the same reference PV module. It is evident from the figures that the efficiency of all types of photovoltaic devices, PV, PV/T, and PV/T-PCM, increases up to an irradiation level of around 300 to 600 W/m^2, which then drops significantly with increased irradiation. Therefore, photovoltaic devices perform best under the above-mentioned range of irradiation in Malaysian condition. While both the PV/T and the PV/T-PCM show better

University of Malaya

electrical efficiency than the reference PV module, the PV/T-PCM system produces a commendably superior performance than the PV/T-only system operating alone. As the irradiation level increases from 303.72 to 981 W/m^2, electrical efficiency drops from 13.32% to 9.19% for PV/T module and 12.98% to 8.55% for PV module as shown in Figure 4.15 (a). On the other hand, as shown Figure 4.15 (b), with irradiation level increasing from 375.26 to 995 W/m^2, electrical efficiency drops from 12.88% to 9.78% for PV/T-PCM module and 12.41% to 7.56% for PV module. Figure 4.15 (a) and (b) shows the maximum difference between PV and PV/T electrical efficiency is 1.05% at 10:45 AM, whereas that between PV and PV/T-PCM system is 2.48% at 11:15 AM. It may be noticed from and that maximum electrical efficiency of the PV/T system is 13.36% at 10:15 AM as shown in Figure 4.15 (a), whereas that of the PV/T-PCM is 14.42% at 3:15 PM as shown in Figure 4.15 (b), which evidently shows distinctive improvement in the electrical performance by employing PCM. For PV/T and PV/T-PCM modules every 100 W/m^2 increase in irradiation level, electrical efficiency drops by 0.80% and 0.55% respectively. This holds good not only for the maximum point, but also for almost the entire range of efficiency, which further establishes the appropriate choice of employing the PCM thermal control in the PV/T systems.

University of Malaya

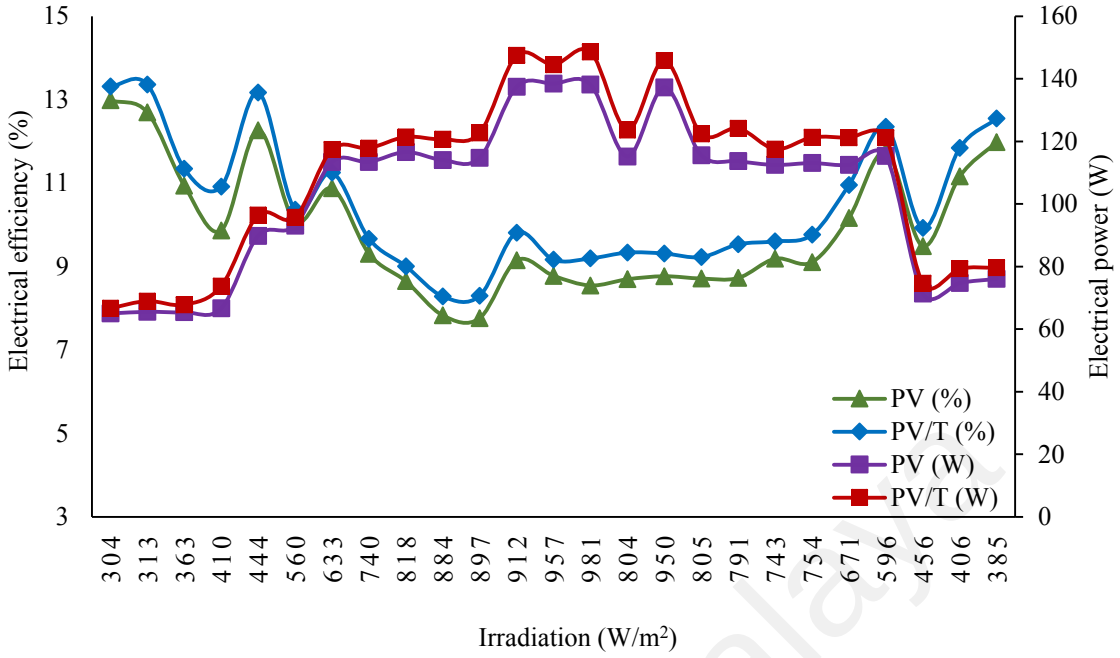

(a) Electrical performance of PV/T against PV

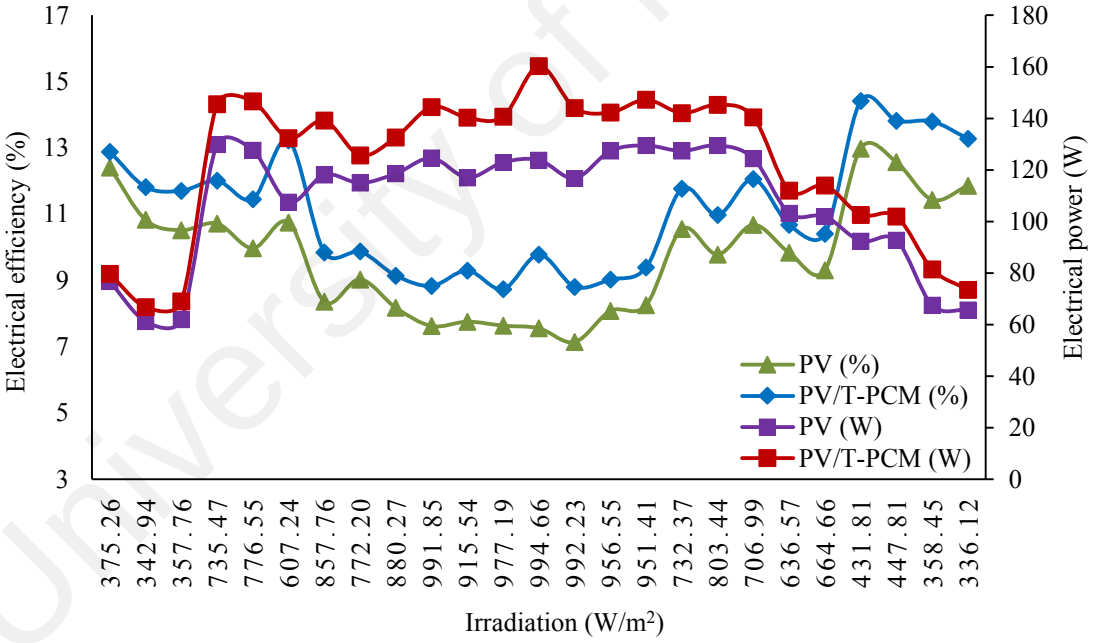

(b) Electrical performance of PV/T-PCM against PV

Figure 4.15: Effect of irradiation on electrical performance of (a) PV/T and (b) PV/T-PCM against the reference PV (4 LPM)

University of Malaya

4.3.2 Effect of Cell Temperature on Electrical Performance

Elevated cell temperature is the major hindrance towards excellent PV performances from which the practice of incorporating the PV cooling system and adoption of subsequent concept of PV/T collectors originate. It has been observed from Figure 4.20 to 4.20 that cell temperature of PV, PV/T and PV/T-PCM rises with increased irradiation level. In the horizontal axis of all the figures two sets of cell temperatures are shown, one is PV references and another one is PV/T and PV/T-PCM cell temperature (highlighted).

Figure 4.16 (a) and (b) shows the effect of cell temperature on electrical power and electrical efficiency at mass flow rate of 0.5 LPM. Figure 4.1 and Figure 4.16 (a) shows the highest solar radiation is 996 W/m^2, the ambient temperature is 34.27°C and the cell temperature difference is 2.17°C. The PV/T output power is observed to increase by 3.49 W at 2:15 PM. Figure 4.6 and Figure 4.16 (b) shows that solar radiation reaches its peak of 999 W/m^2, the ambient temperature to 36.52°C and the maximum cell temperature difference to 4.71°C. PV/T-PCM output power is observed to increase by 10.09 W at 2:15 PM. As can be seen power difference between PV and PV/T is lower than that between PV and PV/T-PCM because of the effect of cell temperature (as explained above). At low mass flow rate (0.5 LPM), cell temperature is dropped very little for PV/T collector, whereas because of PCM this drop is greater for PV/T-PCM system. As a result, PV/T-PCM system produce more power. The variation in the PV and PV/T efficiency is only from 0.06% to 1.02% as shown in Figure 4.16 (a), while that of the PV and PV/T-PCM is from 0.40% to 2.14% as shown in Figure 4.17 (b). On the other hand, cell temperature variation is 6.16°C to 3°C and 4.16°C to 5.81°C for PV & PV/T and PV & PV/T-PCM, respectively.

University of Malaya

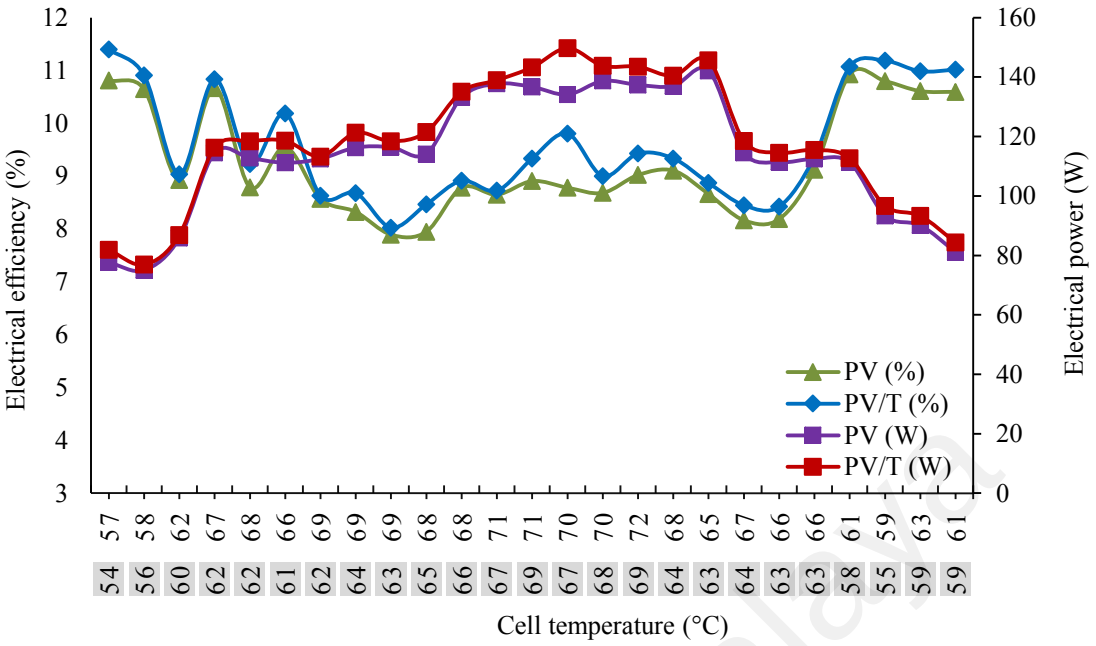

(a) Electrical performance of PV/T against PV

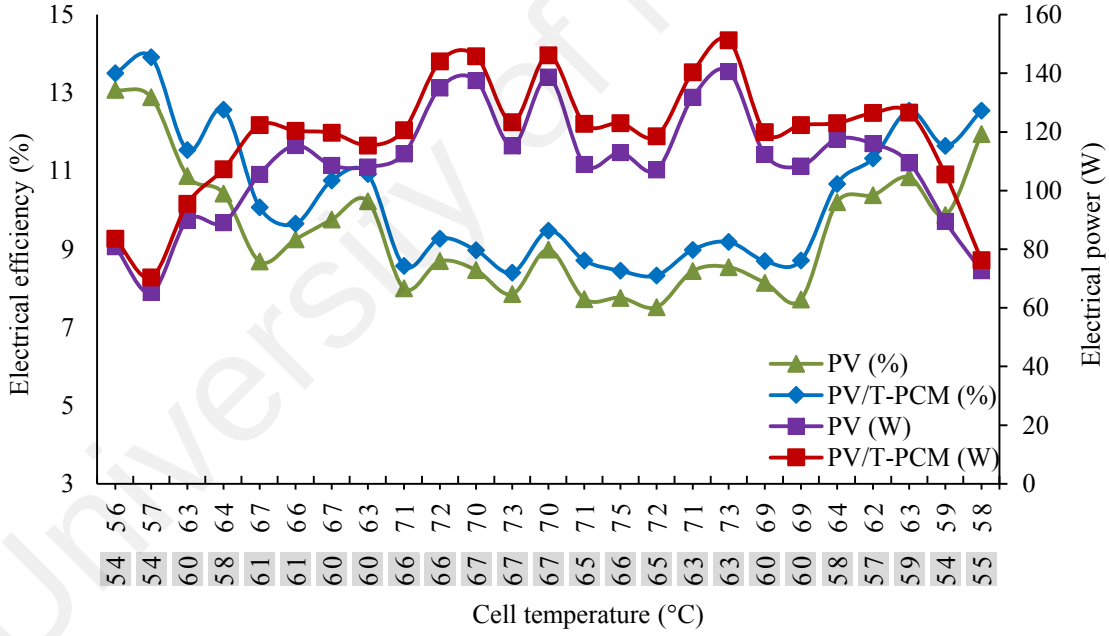

(b) Electrical performance of PV/T-PCM against PV

Figure 4.16: Effect of cell temperature on electrical performance of (a) PV/T and (b) PV/T-PCM against reference PV (0.5 LPM)

Figure 4.17 (a) and (b) shows the effect of cell temperature on electrical power and electrical efficiency at mass flow rate of 1 LPM. Under the peak solar radiation of 983 W/m^2 at 2:00 PM the ambient temperature is 32.72°C and cell temperature difference is

University of Malaya

3.73°C, whereas the increase in PV/T power output is 7.98 W, respectively as shown in Figure 4.2 and Figure 4.17 (a). On the other hand, ambient temperature is 36.34°C and the cell temperature difference found 7.03°C under the peak solar radiation of 988 W/m^2 at 1:30 PM, while the increase in PV/T-PCM output power is 7.05 W at the same time. When the mass flow rate is increased from 0.5 to 1.0 LPM, cell temperature also drops for PV/T collector. On the other hand, for PV/T-PCM system this drop is lower as compared to that at 0.5 LPM. After that the cell temperature is observed to up and down and the power reached at maximum level 24.97 W. It is also observed that around 1:45 to 2:45 PM, the solar radiation was high. Because of PCM, the cell temperature is dropped suddenly and it maintains a little time then again back to its original trend. The variation in the PV and PV/T efficiency is only from 0.10% to 0.75% while that of the PV and PV/T-PCM is from 0.05% to 1.55%, while the cell temperature variation 2.96°C to 3.49°C and 5.08°C to 6.40°C respectively as shown in Figure 4.17 (a) and (b).

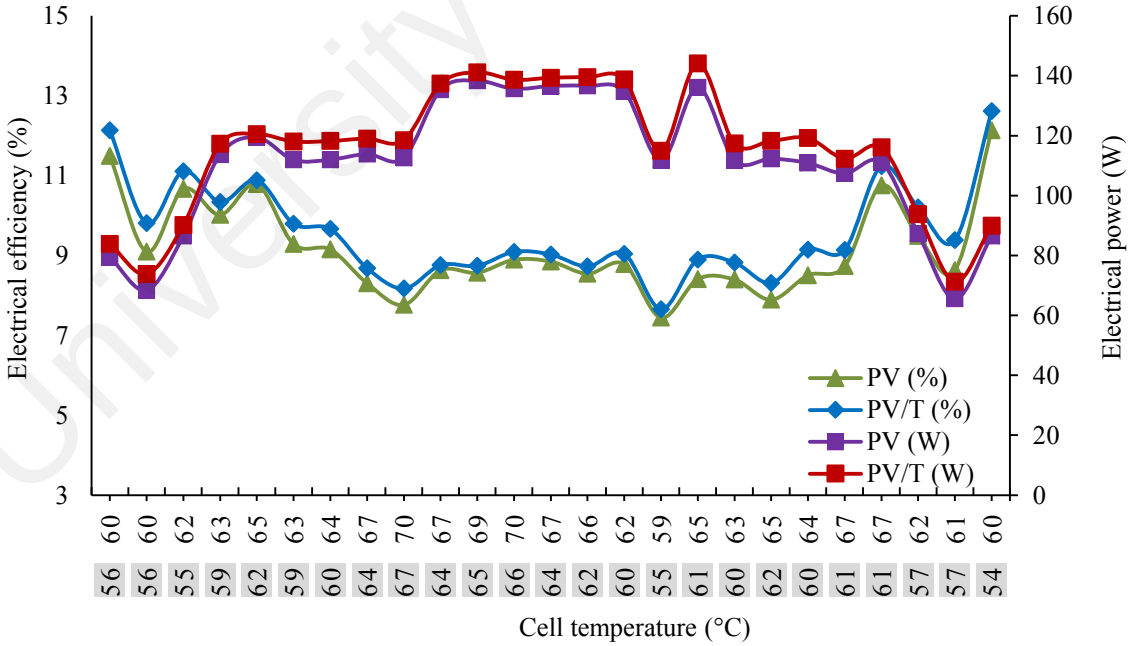

(a) Electrical performance of PV/T against PV

Figure 4.17: Effect of cell temperature on electrical performance of (a) PV/T and (b) PV/T-PCM against reference PV (1 LPM)

University of Malaya

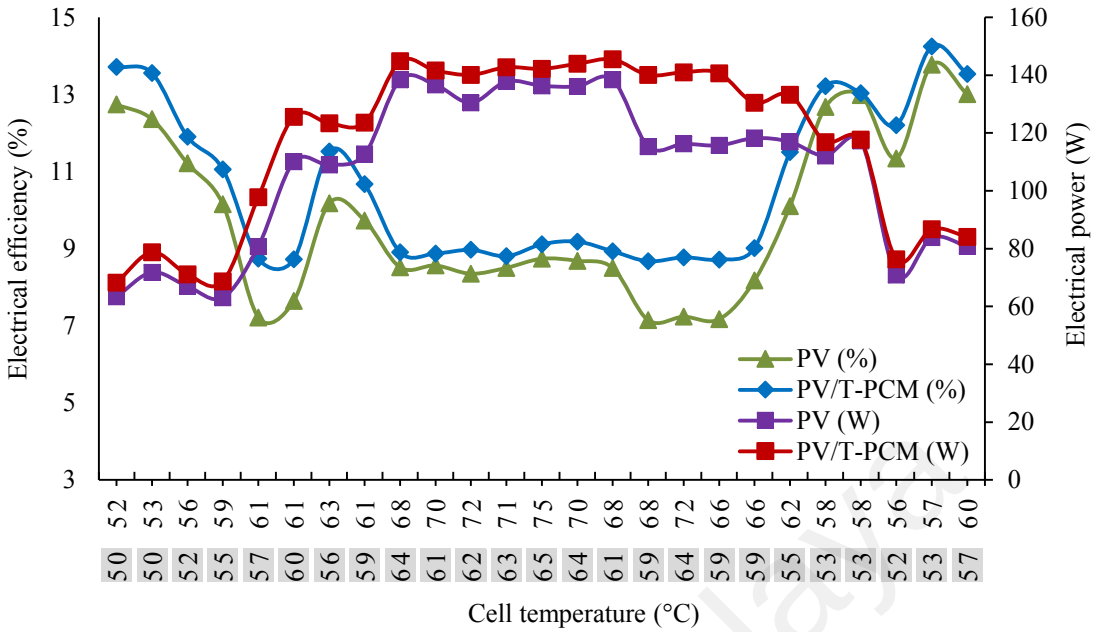

(b) Electrical performance of PV/T-PCM against PV

Figure 4.17, continued

Figure 4.18 (a) and (b) shows the effect of cell temperature on electrical power and electrical efficiency at mass flow rate of 2 LPM. At the peak solar radiation of 995 W/m^2, the ambient temperature was 34.53°C and the cell temperature difference found 8.17°C, with the increase in PV/T output power is 7.39 W at 1:00 PM. On the other hand, ambient temperature is 35.21°C, and cell temperature difference is 5.64°C and the increase in PV/T-PCM is 16.67 W under the peak radiation of 983 W/m^2 at 12:00 noon as shown in Figure 4.8 and Figure 4.18 (b). As the mass flow rate increases from 1 to 2 LPM, the cell temperature of PV/T collector drops, whereas PV/T-PCM that drops are high and output power increases as compared mass flow rate of 0.5 and 1 LPM respectively. Because of increasing mass flow rate with PCM cooling capacity is higher than PV/T system. It is observed, PV/T-PCM maximum power found 21.71 W at cell temperature of 7.98°C. Figure 4.18 (a) and (b) also reveals that the variation in the PV and PV/T efficiency is only from 0.15% to 1.36% while that of the PV and PV/T-PCM is from 0.18% to 2.33%, while the cell temperature variations are 5.10°C to 1.79°C and 13.15°C to 9.33°C respectively.

University of Malaya

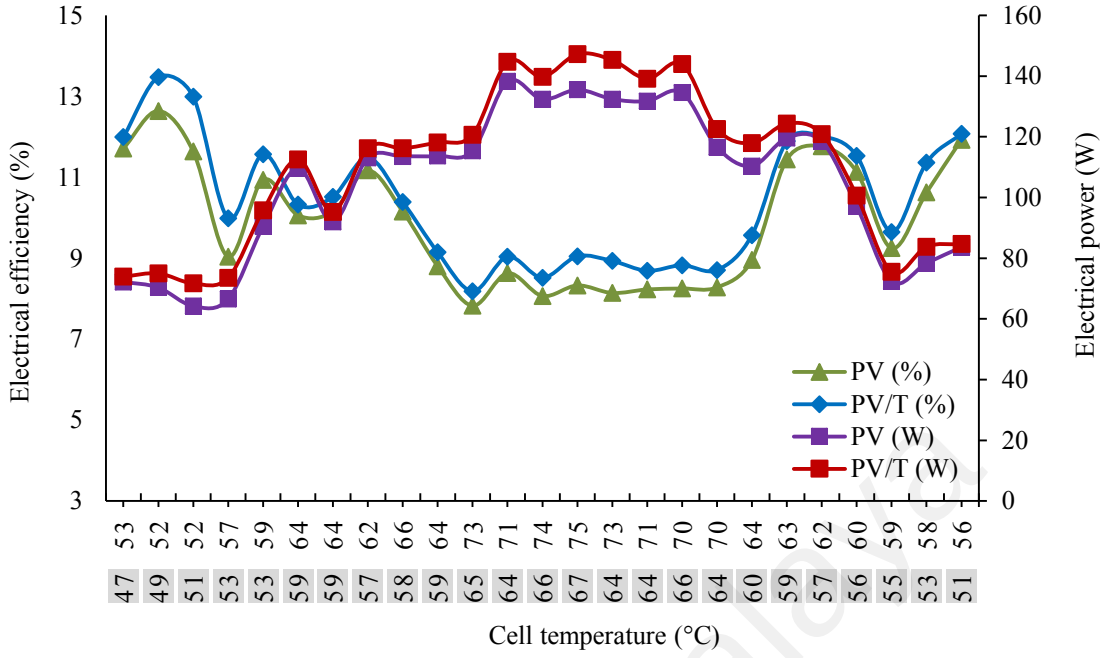

(a) Electrical performance of PV/T against PV

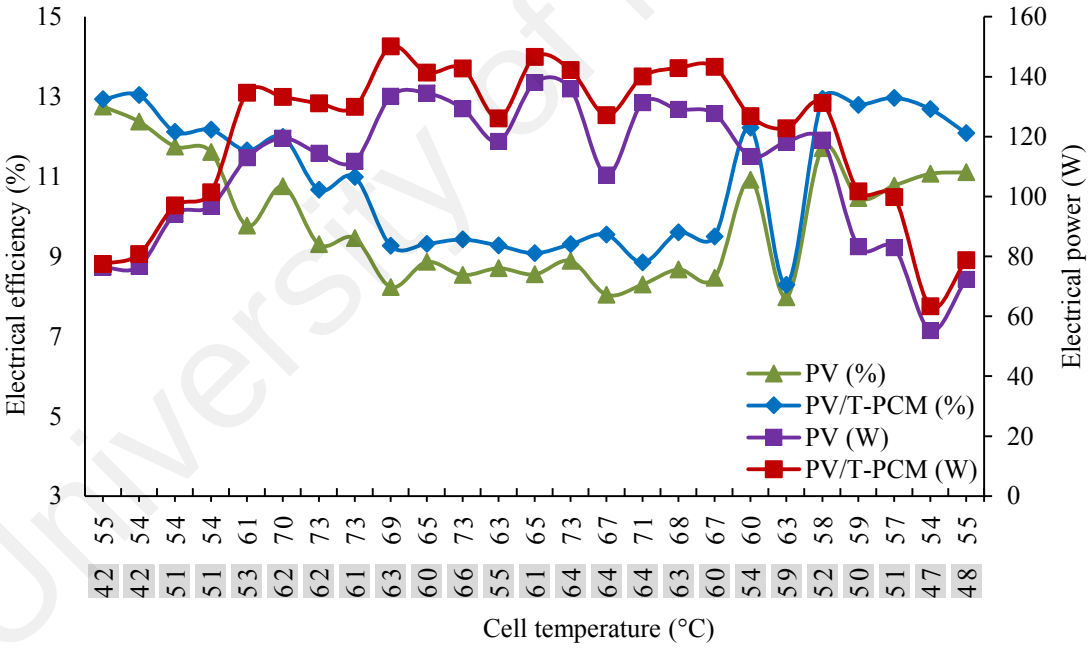

(b) Electrical performance of PV/T-PCM against PV

Figure 4.18: Effect of cell temperature on electrical performance of (a) PV/T and (b) PV/T-PCM against reference PV (2 LPM)

The effect of cell temperature on electrical power and electrical efficiency at mass flow rate of 3 LPM is shown in Figure 4.19 (a) and (b). Under the peak solar radiation of 987 W/m^2, the ambient temperature is 34.85°C and the cell temperature difference is 5.96°C,

University of Malaya

whereas the increase in PV/T output power is 7.73 W at 1:00 PM. For PV/T-PCM system, the ambient temperature is 37.26°C, cell temperature difference is 6.53°C and the increases in output power is 14.13 W at peak radiation of 989 W/m^2 at 1:45 PM as shown in Figure 4.9 and Figure 4.19 (b). As the mass flow rate increases from 2 to 3 LPM, the cell temperature of PV/T collector drops. On the other hand, the cell temperature of PV/T-PCM drop is little as compared that of 2 LPM. The maximum power is found 25.10 W at cell temperature of 3.93°C. Furthermore, the variation in the PV and PV/T efficiency is only from 0.12% to 1.43% while that of the PV and PV/T-PCM is from 0.45% to 1.74%, while the cell temperature variation 5.09°C to 6.39°C and 4.06°C to 5.06°C respectively.

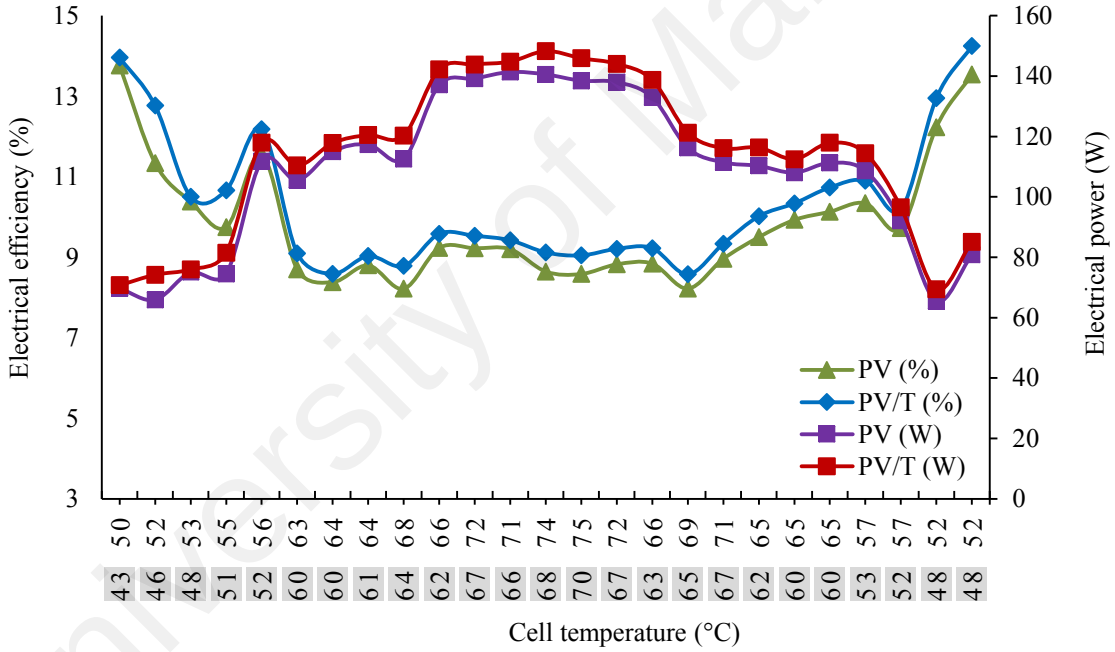

(a) Electrical performance of PV/T against PV

Figure 4.19: Effect of cell temperature on electrical performance of (a) PV/T and (b) PV/T-PCM against reference PV (3 LPM)

University of Malaya

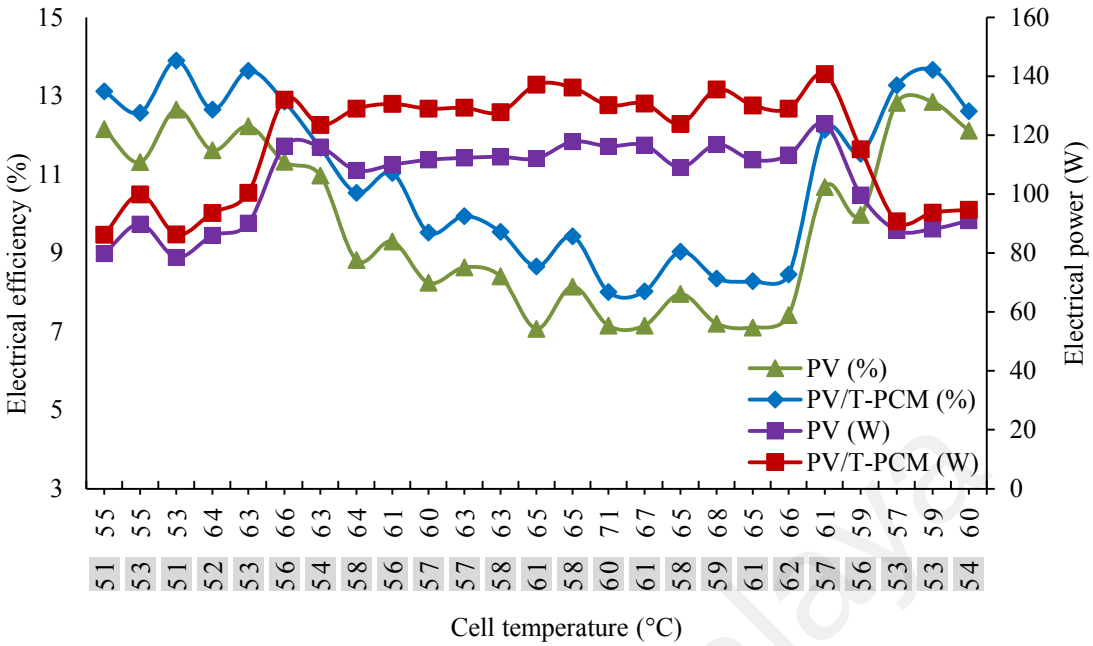

(b) Electrical performance of PV/T-PCM against PV

Figure 4.19, continued

The effect of increased cell temperature on electrical power and efficiency has been notably demonstrated in Figure 4.20 (a) to (b) at optimum mass flow rate of 4 LPM. The adverse effect of increased cell temperature in electrical power output of both the PV/T and the PV/T-PCM systems is apparently conceivable from Figure 4.20 (a) and (b) in which it is readily observed that the corresponding power drop in the PV/T-PCM system is greater than that of the PV/T system for almost the same temperature rise. The reason behind the alternation in power level is that panel temperature leads to a little increase in panel current while it decrease the panel voltage proportionally. Panel power decrease since the voltage decrease rate is more than the increase in current rate. On the other hand, increase in module temperature reduce the band gap of a solar cell, whereby effecting the solar cell output parameters. Open circuit voltage the most affected parameter due to increase in temperature. Figure 4.5 and Figure 4.20 (a) shows that initially the ambient temperature was 31.29°C and the PV, PV/T cell temperature difference were 3.99°C. However, due to low solar radiation the output power difference were 1.68 W. As the solar radiation reaches its peak of 981 W/m^2, the ambient temperature rises to 34.26°C

University of Malaya

and the cell temperature difference becomes 4.71°C. The PV/T power output increases by 10.48 W as compared to reference PV at 1:15 PM, since even at high ambient temperature PV/T cell temperature is decreased by means of water cooling. Figure 4.10 and Figure 4.20 (b) shows the same tendency for PV/T-PCM and PV reference. At 995 W/m^2, the ambient temperature was 35.36°C and the cell temperature difference were 3.33°C and the output power difference was 36.44 W at 1:00 PM. The cell temperature and output power vary because of mass flow rates and PCM cooling capacity. For every 1°C decrease in cell temperature, output power increases by 3.49 W and 8.76 W for PV/T and PV/T-PCM systems respectively.

Drop in the electrical efficiency due to the cell temperature rise is less prominent in photovoltaic thermal systems, especially in the case of a PV/T-PCM system. This is due to the fact that PCMs can exert a better control over the cell temperature rise by its intrinsic ability in absorbing a large amount of heat through alternate melt/freeze cycles at a particular range of temperature. It may be perceived from Figure 4.20 (a) and (b) that the variation in the PV and PV/T efficiency is only from 0.28% to 1.08% while that of the PV and PV/T-PCM is from 0.48% to 2.48% respectively. In addition, electrical efficiency of the PV/T is higher than the PV efficiency demonstrating the favorable effect of cooling. The effect of cooling becomes noticeable at 11:00 AM to 3:15 PM when the PV/T electrical efficiency reaches 12.35% against an 11.75% PV efficiency indicating that cooling is more effective around this time. Electrical efficiency of the PV/T-PCM system is also observed to be higher than that of PV/T-only system. During afternoon, PV/T-PCM system works with efficiencies as high as 13.82% or more. For every 1°C decrease in cell temperature, efficiency increases by 0.23% and 0.37% for PV/T and PV/T-PCM systems respectively. Another notable point from these figures is that for both the power output and the efficiency curves, the gap between the PV and the PV/T-PCM trend lines is wider than that between the PV and the PV/T. This portrays a better relative

University of Malaya

improvement in both the electrical power and the efficiency of the PV/T-PCM system than that of the PV/T system with respect to the PV module. This finding also confirms that the PV/T-PCM system has a superior performance over the PV/T-only system.

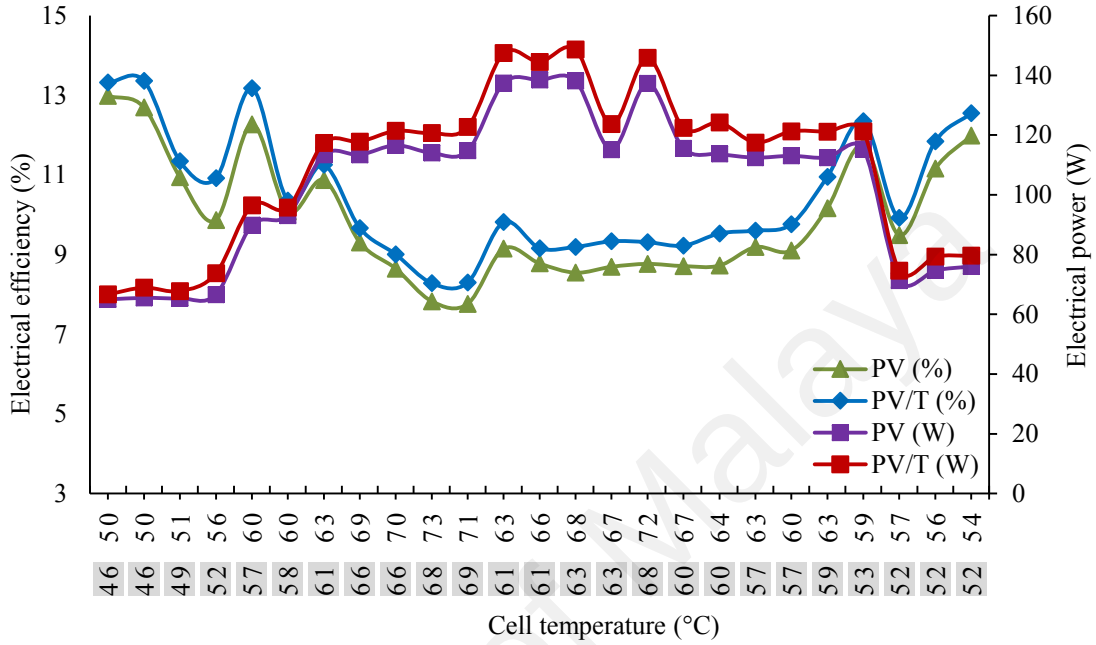

(a) Electrical performance of PV/T against PV

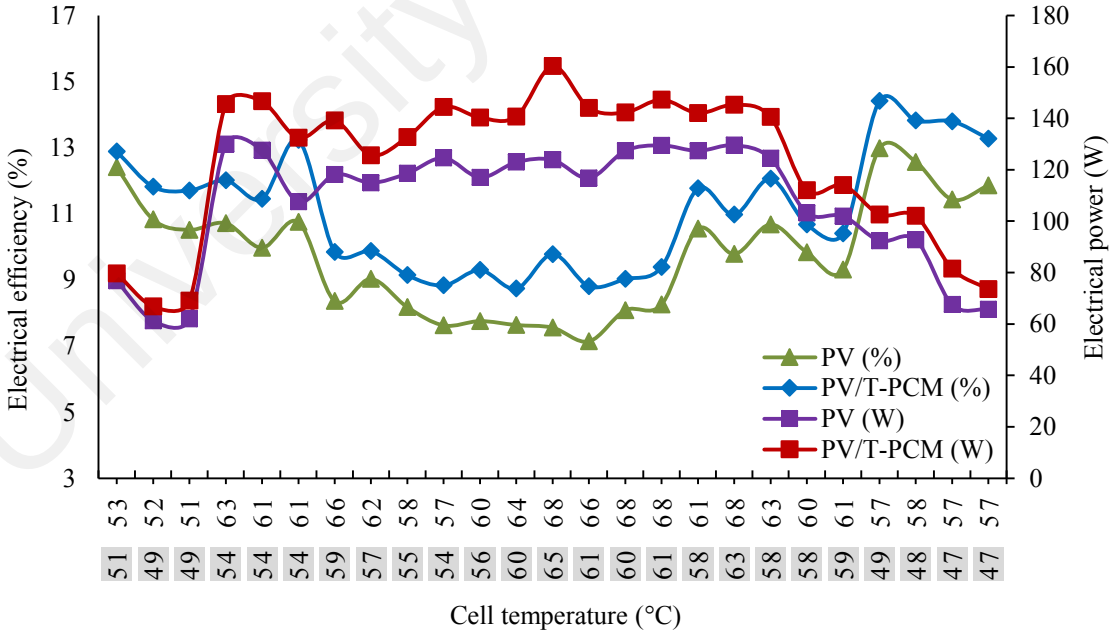

(b) Electrical performance of PV/T-PCM against PV

Figure 4.20: Effect of cell temperature on electrical performance of (a) PV/T and (b) PV/T-PCM against reference PV (4 LPM)

University of Malaya

4.3.3 Effect of Water Flow rate on Thermal Performance

Photovoltaic thermal (PV/T) collectors, as the name implies, are meant for thermal output along with electricity. Moreover, there is a material limit for silicon cells, especially, in terms of life span, after which the electrical performance cannot be improved. On the other hand, there are wide provisions for improvement in the thermal performance by adopting effective thermal energy harvesting techniques. For this particular reason, the thermal performance of PV/T collectors is of great importance which needs to be investigated thoroughly. Thermodynamic performance of any system can be analyzed from two different viewpoints, i.e., one is based on the first law of thermodynamics while the other is its second law. Energy analysis of PV/T and PV/T-PCM systems only based on the first law of thermodynamics has been discussed in this section and second law-based analysis, i.e., exergy analysis which is elaborated in the following section. In both cases, variation in performance parameters have been presented as a function of the mass flow rate of heat transfer fluid (HTF), namely, water.

Thermal performances of PV/T and PV/T-PCM systems have been illustrated in Figure 4.21 (a) and (b), respectively wherein the performance has been portrayed in terms of heat gain, thermal efficiency and outlet water temperature. Although PV/T collectors are meant for both electricity and heat productions, one of the major applications of these devices are in warm water supply. Hence, together with heat gain and thermal efficiency of the device, the level of outlet water temperature has been used here as an index for the thermal performance. Figure 4.21 (a) and (b) present the heat gain as well as the thermal efficiency of PV/T and PV/T-PCM modules, respectively. It can be noticed that both the heat gain and the thermal efficiency follows the trend of a bell-shaped curve although the distribution of the values are not the same nor symmetrical. This trend signifies the fact that there is an optimum flow rate at which the peak performance is obtained. For the PV/T system, the maximum heat gain is 859.92 W at 1 LPM and the highest obtainable

University of Malaya

thermal efficiency is 74.62% at 2 LPM. On the other hand, PV/T-PCM modules provide as high as 1024.01 W with a thermal efficiency of 87.71% at 2 LPM. Hence, the use of PCM can conveniently provide 164.09 W more heat than the conventional PV/T-only system at 13.09% higher efficiency.

Figure 4.21 (c) and (d) show the outlet water temperature along with the inlet water temperature produced by the PV/T and PV/T-PCM systems, respectively. It is obvious that the outlet water temperature decreases gradually with increasing water flow rate which is evident from both figures. Hence, in order to get warm water supply with better thermal efficiency, the flow rate should be maintained between 1 to 2 LPM. Another revealing fact from Figure 4.21 (c) and (d) is that the PV/T-PCM system provides relatively lower outlet water temperature, which is due to the system's huge thermal storage capacity. However, the major benefit of PCM thermal storage is in its extended period of availability of heat which makes the PV/T-PCM modules highly favorable for night time thermal energy supply.

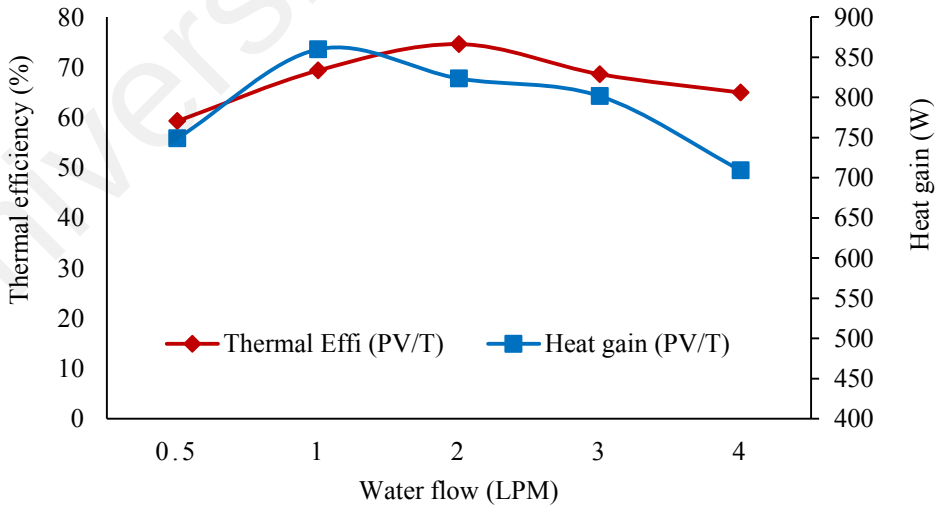

(a) PV/T collector thermal performance

Figure 4.21: Effect of water flow rate on thermal performance of PV/T and PV/T-PCM collector

University of Malaya

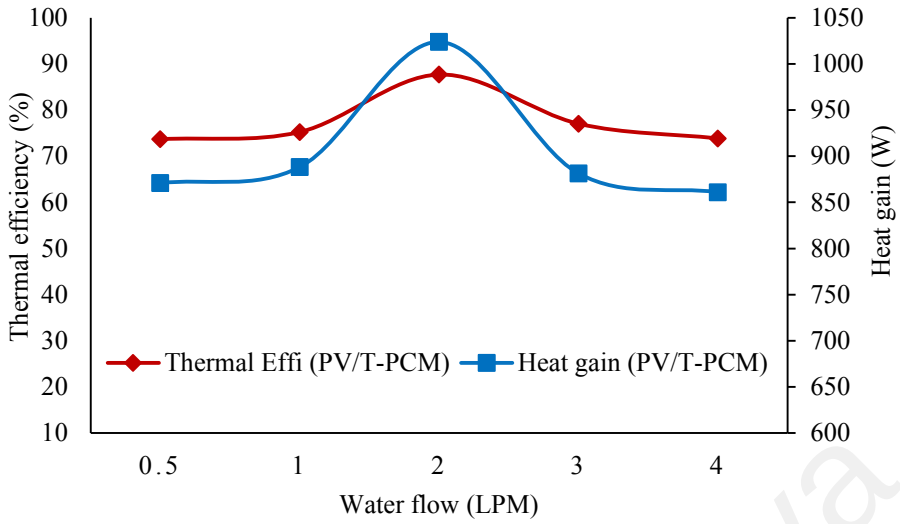

(b) PV/T-PCM collector thermal performance

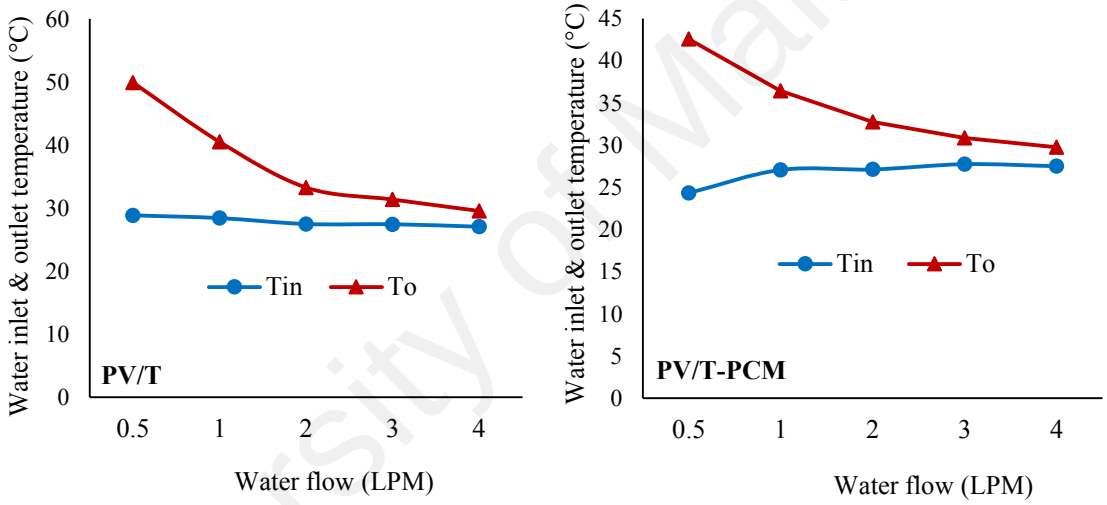

(c) (d)

Figure 4.21, continued

4.4 Exergy Analysis of PV/T and PV/T-PCM Systems

The limitation of the first law of thermodynamics analysis is that it does not account for the energy quality, rather all forms of energies, viz., electric, mechanical, chemical, thermal energy, all of which have values leading to a wrong assessment. The second law of thermodynamics comes to help in this context introducing the concept of exergy which is the thermodynamic property of combined energy quantity and quality to portay the real picture of the energy utilization efficiency. Exergy is the maximum useful work obtainable from a system during a process when the system is brought to an equilibrium

University of Malaya

with a heat reservoir (Perrot, 1998). In other words, exergy is defined as the maximum amount of work that can be produced from a flow of mass or energy as it comes into an equilibrium with a reference environment (Yazdanpanahi et al., 2015a). Therefore, the exergy performance of the PV/T and PV/T-PCM systems have been evaluated in this section to gauge their actual working efficiency. Figure 4.22 (a) to (d) present the exergy performance of the PV/T and the PV/T-PCM systems.

Figure 4.22 (a) and (b) show the exergy output and exergy efficiency of the PV/T and the PV/T-PCM systems, respectively. It may be noticed from the figures that exergy output becomes almost constant after a certain flow rate of 2 LPM for both the PV/T and the PV/T-PCM systems. The highest exergy output obtained with the PV/T is 152.84 W, while that with the PV/T-PCM is 134.10 W respectivly. On the other hand, exergy efficiency keeps on decreasing with increasing water flow rate which is due to the fact that with an increased flow rate of a volume of water the irreversibility increases substantially causing greater exergy destruction. Hence, higher exergy efficiency is attainable at lower flow rates. The highest exergy efficiency obtained with the PV/T is 12.98%, while that with the PV/T-PCM is 12.19% respectivly.

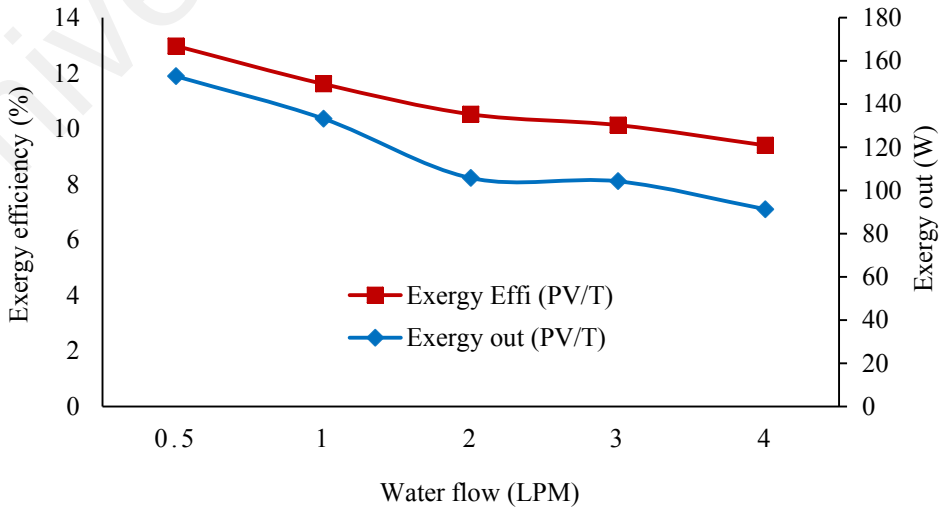

(a) PV/T collector exergy performance

Figure 4.22: Effect of water flow rate on exergy performance (a) PV/T and (b) PV/T-PCM system

University of Malaya

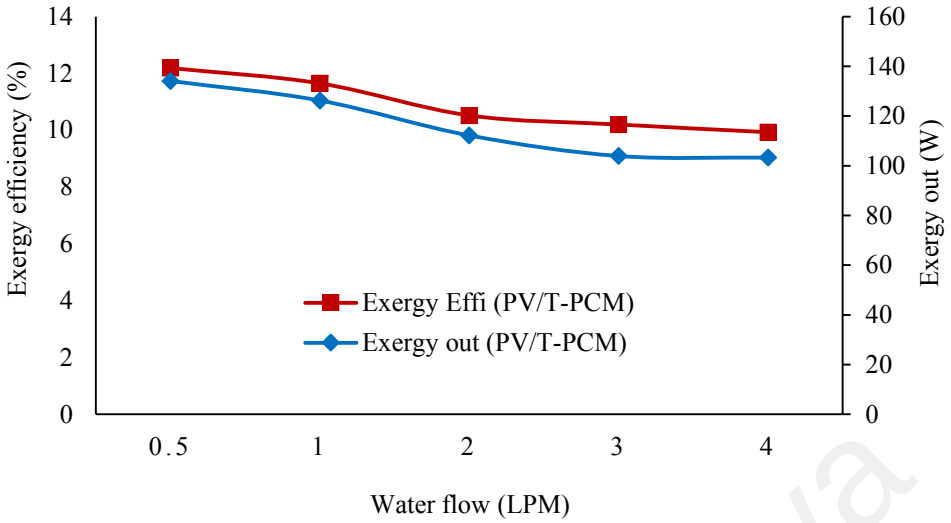

(b) PV/T-PCM collector exergy performance

Figure 4.22, continued

4.5 Photovoltaic Thermal-Phase change material with dust and self-cleaning (PV/T-PCM-Dust and PV/T-PCM-SC) systems

This section presents the results on PV/T-PCM dust and PV/T-PCM self-cleaning systems with reference to PV system. The hourly variation of different parameters such as temperatures at different state of points and solar radiation with respect to time of PV/T-PCM dust and PV/T-PCM with self-cleaning systems as compared PV module has been presented in section 4.5.1 and 4.5.2 respectively. Energy and exergy analysis of PV/T-PCM dust and PV/T-PCM self-cleaning systems with reference to PV has been detailed in subsections 4.6 and 4.7 respectively.

4.5.1 Hourly Variation of Different Parameters of PV and PV/T-PCM with dust

The performance of PV/T-PCM module with dust accumulation on the top glass had been carried out with the mass flow rates 0.5, 1, 2, 3 and 4 LPM respectively. Figure 4.23 shows the hourly variation of solar radiation and temperatures at different state of points of PV and PV/T-PCM with dust for 0.5 LPM water flow rate, when the average ambient temperature was 33.39°C. The maximum rise in outlet water temperature is found 24.55°C at 12:45 PM as shown in Figure 4.23. Solar radiation reached to its peak of 1000

University of Malaya

W/m^2 at 1:30 PM. The maximum cell temperature difference between PV and PV/T-PCM with dust is found 13.46°C, when the solar radiation was 542 W/m^2 at 10:45 AM, whereas at peak irradiation this temperature difference drops only to 3.65°C. At 2:00 PM the cell temperature difference is found 13.29°C and after that it maintained the same trend, because at low mass flow rate (0.5 LPM) the PV/T-PCM with dust thermal collector is not capable of transferring a massive amount of heat.

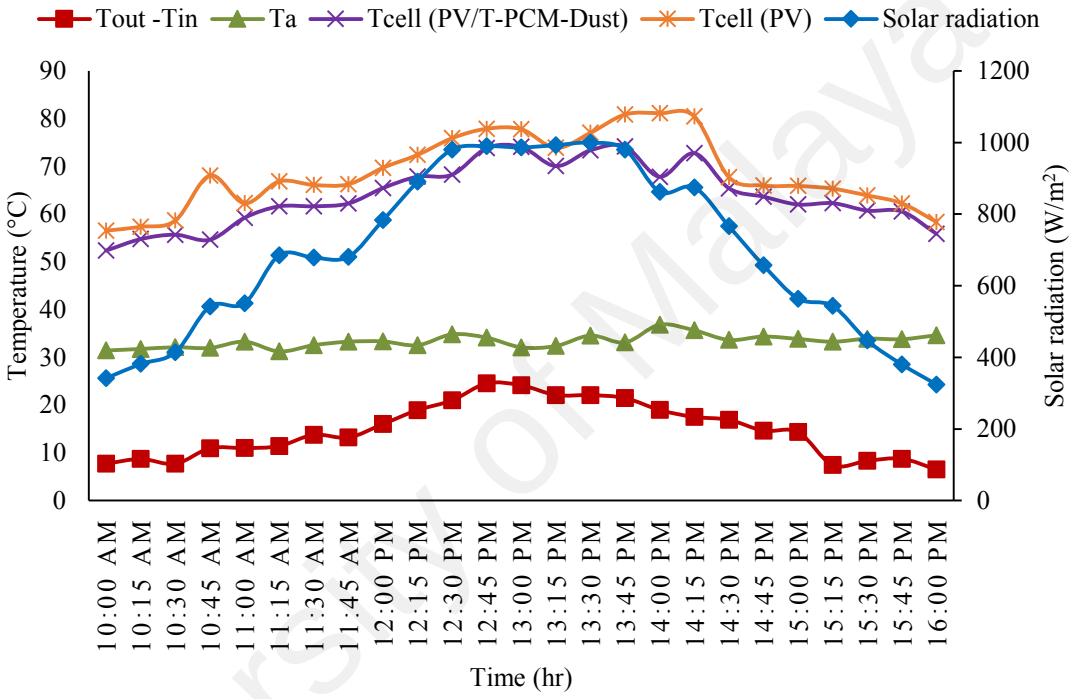

Figure 4.23: Hourly variation of different PV and PV/T-PCM dust parameters (0.5 LPM)

Figure 4.24 shows the hourly variation of solar radiation and temperatures at different state of points of PV and PV/T-PCM with dust for 1 LPM water flow rate, when the average ambient temperature was 33.61°C. The maximum rise in outlet water temperature is found 14.98°C at 1:30 PM shown in Figure 4.24. It may be noticed that at a mass flow rate of 1 LPM the maximum outlet water temperature and thermal performance has been decreased around fifty percent as compared to 0.5 LPM. This variation shows that the thermal collector has been started to transfer the heat from the module. At 12:45 PM under the peak solar radiation of 991 W/m^2 the cell temperature difference found is

University of Malaya

4.60°C. The maximum cell temperature difference between PV and PV/T-PCM with dust is found 9.32°C under 460 W/m^2 at 10:30 AM.

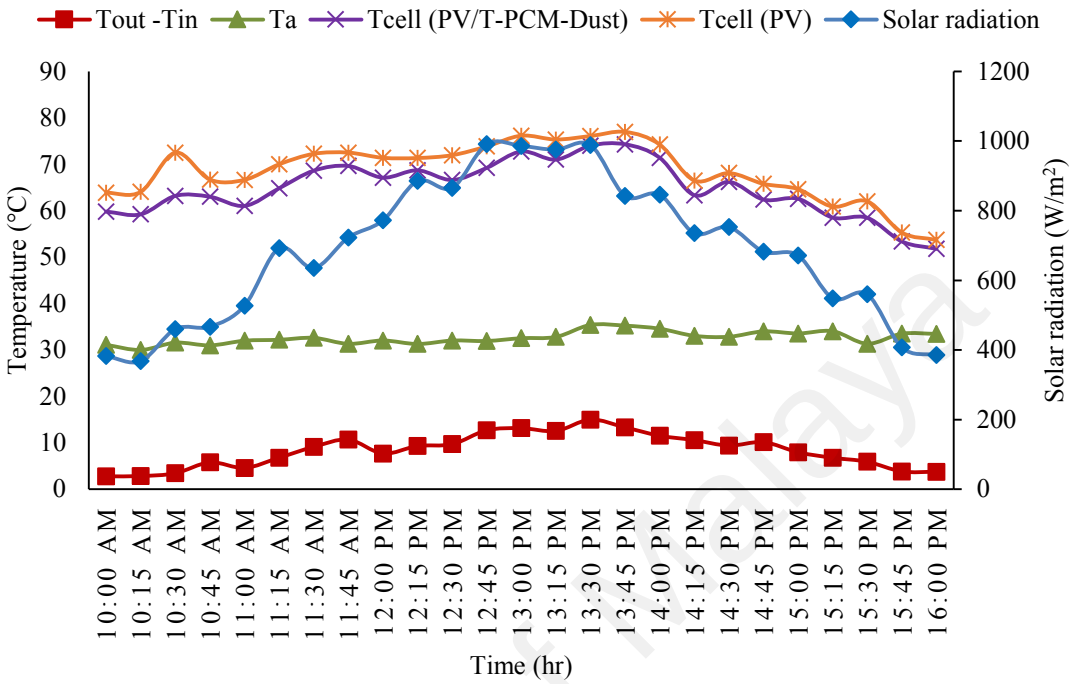

Figure 4.24: Hourly variation of different PV and PV/T-PCM dust parameters (1 LPM)

Figure 4.25 shows the hourly variation of solar radiation and temperatures at different state of points of PV and PV/T-PCM with dust for 2 LPM water flow rate. Figure 4.25, it may be observed that the hourly variation in solar radiation has steadily been increasing from 300 W/m^2 at 10:00 AM to a peak of 989 W/m^2 at 1:15PM, then decreased to 344 W/m^2 at 4:00 PM. Figure 4.25 also shows that the dust covered module produces very little temperature rise in the water. The highest rise in outlet water temperature is 7.69°C with an average value of 4.69°C. Dust is observed to deteriorate the capability of the cooling system to lower the cell temperature, which is evidenced from Figure 4.25 wherein the PV/T cell temperature is seen to surpass the reference PV cell temperature. The maximum difference in cell temperature is found 10.21°C under 600 W/m^2 at 11:15 AM, while at peak irradiation it is 5.35°C only. This is due to the dust particles that has been blocked the expected solar insolation on the PV module. However, in case of PV/T-PCM system, cell temperature is decreasing even the PV/T module is covered with dust.

University of Malaya

Nonetheless, it may be concluded that dust is prime reason for decreasing the PV or PV/T thermal and electrical performance.

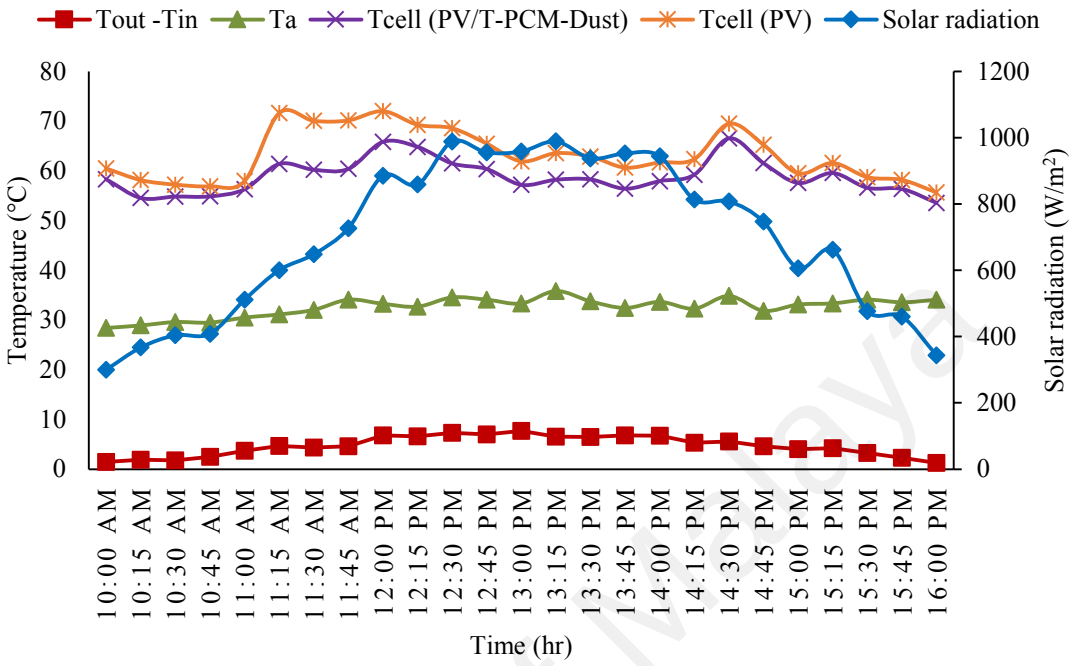

Figure 4.25: Hourly variation of different PV and PV/T-PCM dust parameters (2 LPM)

Table 4.3 presents the PV/T-PCM parameters measured with dust on the collector at optimum the mass flow rate of 2 LPM. The maximum power produced with PV/T-PCM with dust is 146.82 W.

Table 4.3: The measured parameters at mass flow rate of 2 LPM

Time	T_a (°C)	T_{in} (°C)	T_o (°C)	P_{max} (W)	G (W/m²)
10:00	28.40	22.40	23.83	73.34	300
10:30	29.59	23.04	24.81	85.19	404
11:00	30.48	23.13	26.82	96.88	511
11:30	32.03	24.37	28.71	120.20	648
12:00	33.26	25.91	32.68	122.93	885
12:30	34.55	24.97	32.27	146.82	988
13:00	33.33	24.19	31.88	143.62	958
13:30	33.76	24.20	30.69	141.21	938
14:00	33.65	24.22	30.92	147.23	944
14:30	34.85	25.31	30.89	126.58	808
15:00	33.11	25.31	29.33	126.28	606
15:30	34.09	25.15	28.40	84.08	476
16:00	34.08	24.17	25.41	74.00	344

University of Malaya

Figure 4.26 shows the hourly variation of solar radiation and temperatures at different state of points of PV and PV/T-PCM with dust for 3 LPM water flow rate, when the average ambient temperature was 32.34°C. The maximum rise in outlet water temperature is 4.75°C at 1:45 PM. The solar radiation reached to its peak of 996 W/m^2 at 1:00 PM when the cell temperature difference found is 5.06°C, which is much closer to that at optimum flow rate of 2 LPM. The maximum cell temperature difference between PV and PV/T-PCM with dust found 6.42°C when the solar radiation was 882 W/m^2 at 2:00 PM. Temperature difference between PV and PV/T-PCM with dust has been found to be decreased further as compared to 0.5 LPM, 1 LPM and 2 LPM due to the fact as explained above

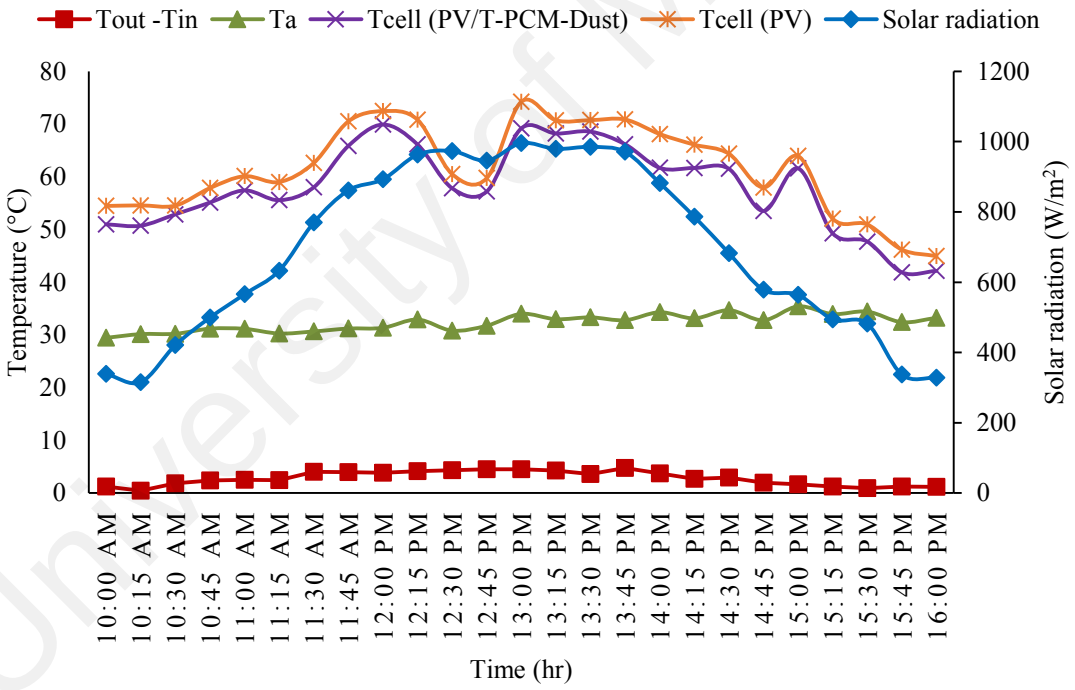

Figure 4.26: Hourly variation of different PV and PV/T-PCM dust parameters (3 LPM)

Figure 4.27 shows the hourly variation of solar radiation and temperatures at different state of points of PV and PV/T-PCM with dust for 4 LPM water flow rate, when the average ambient temperature was 33.88°C. The maximum rise in outlet water temperature is found 3.49°C at 1:00 PM. It is clear that as every 1.0 LPM flow rate is increased, the

University of Malaya

inlet and outlet water temperature decreased by around 50% showing a strong dependence of thermal performance on mass flow rate. The solar radiation reached to its peak of 985 W/m^2 at 1:45 PM when the cell temperature difference is found 7.29°C. The maximum cell temperature difference between PV and PV/T-PCM with dust found 11.10°C under an irradiation of 878 W/m^2 at 12:00 PM. Cell temperature of the PV/T-PCM with dust on module is decreased at maximum solar radiation due to increased flow rate. At this flow rate, it is capable to transfer a massive amount of heat but because of outlet water temperature is low, the thermal performance low as well.

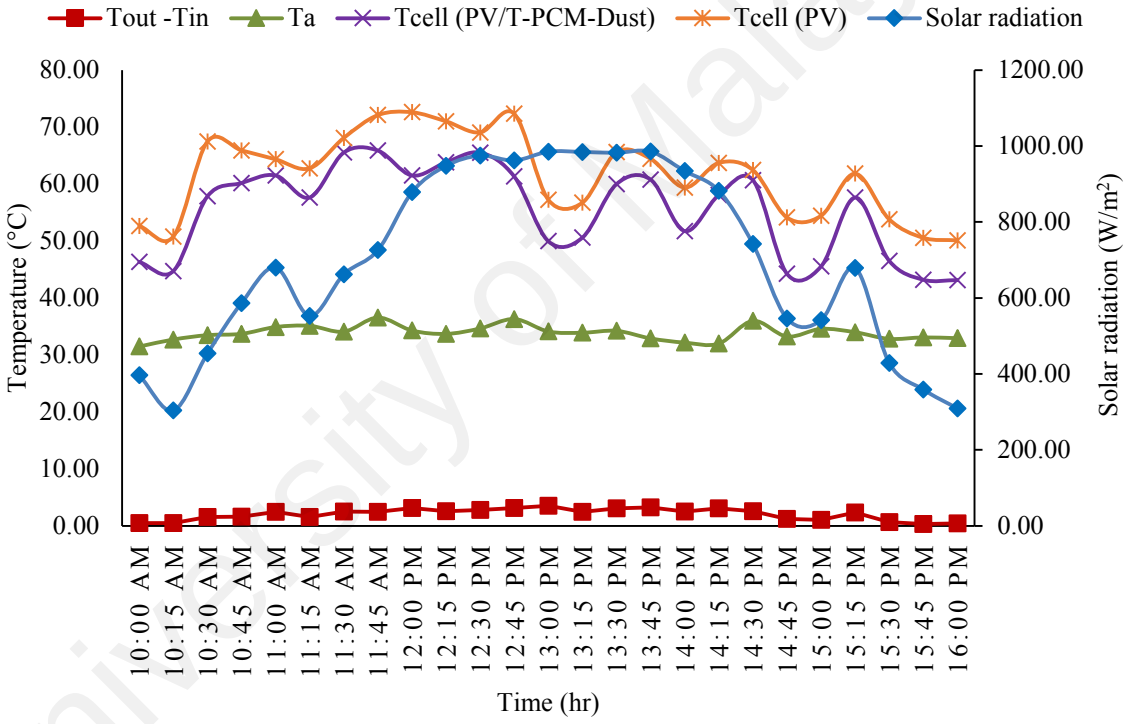

Figure 4.27: Hourly variation of different PV and PV/T-PCM dust parameters (4 LPM)

4.5.2 Hourly Variation of Different Parameters of PV and PV/T-PCM with self-cleaning

The effect of self-cleaning on the PV/T-PCM module had been studied with the mass flow rate of 0.5, 1, 2, 3 and 4 LPM respectively. Figure 4.28 shows the hourly variation of solar radiation and temperatures at different state of points of PV and PV/T-PCM with self-cleaning for 0.5 LPM water flow rate. The maximum difference between inlet and outlet water temperature is found 23.18°C at 12:45 PM when the average ambient

University of Malaya

temperature was 32.16°C. At low mass flow rates, the outlet water temperature can be increased but it will affect thermal and electrical performance, because of the inability to transfer a massive amount of heat. The solar radiation reaches to the peak of 992 W/m^2 at 1:00 PM, when the cell temperature difference between PV and PV/T-PCM with self-cleaning is found 8.97°C. However, the maximum cell temperature difference between PV and PV/T-PCM with self-cleaning is found 12.91°C under 982 W/m^2 at 1:30 PM. It may be noticed that between 11:45 AM to 3:00 PM cell temperature of PV/T-PCM with self-cleaning is getting lowered compared to PV cell temperature, but outlet water temperature is increased. At that time, the thermal absorber and PCM absorb heat from the module, but later on stored heat from PCM is transferred to absorber because of very low mass flow rates.

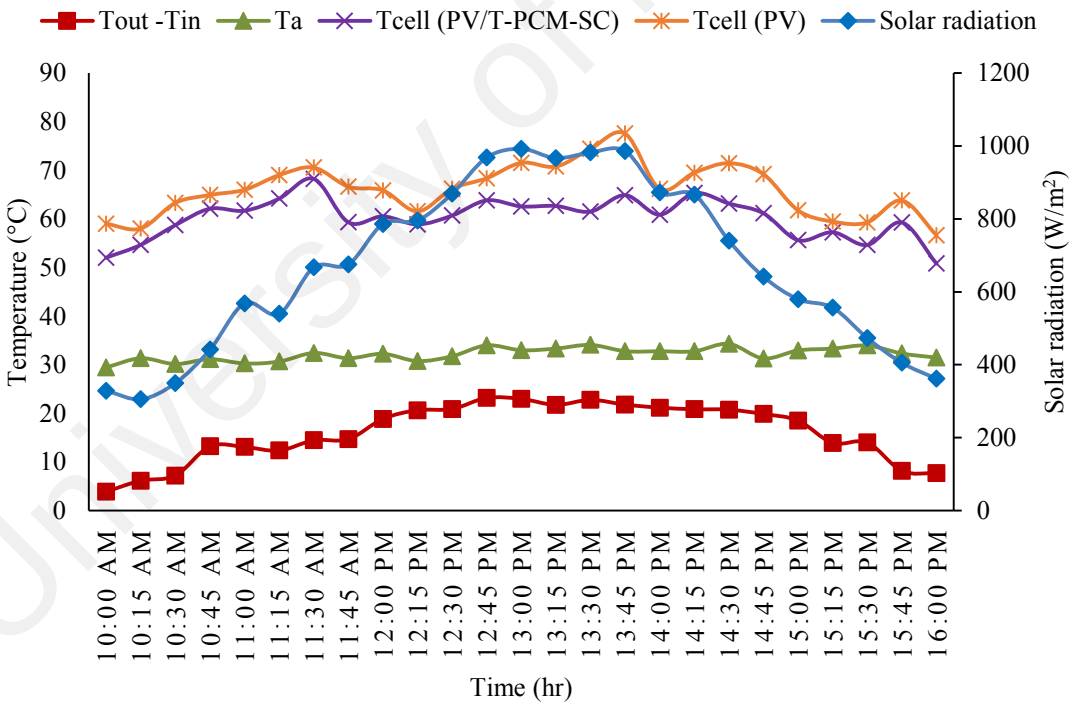

Figure 4.28: Hourly variation of different PV and PV/T-PCM-SC parameters (0.5 LPM)

Figure 4.29 shows the hourly variation of solar radiation and temperatures at different state of points of PV and PV/T-PCM with self-cleaning for 1 LPM water flow rate, when the average ambient temperature was 31.70°C. The maximum difference between inlet

University of Malaya

and outlet water temperature is found 13.20°C at 1:15 PM. At this mass flow rate (1 LPM) the maximum outlet water temperature and thermal performance has been decreased approximately by 50% as compared to that with 0.5 LPM. This variation shows that the thermal collector has been started to transfer the heat from the module. The solar radiation reaches to the peak of 993 W/m^2 at 12:30 PM when the cell temperature difference is found 7.88°C. However, the maximum cell temperature difference between PV and PV/T-PCM with self-cleaning is found 10.20°C under 966 W/m^2 at 1:30 PM. It may be observed that from 10:00 AM to 12:00 PM and 12:15 to 4:00 PM, the PV/T-PCM with self-cleaning cell temperature is getting lowered compared to PV cell temperature, but outlet water temperature is still decreased. Because during that time thermal absorber and PCM absorb heat from the module, but later on stored heat from PCM is transferred to absorber because of very low mass flow rates.

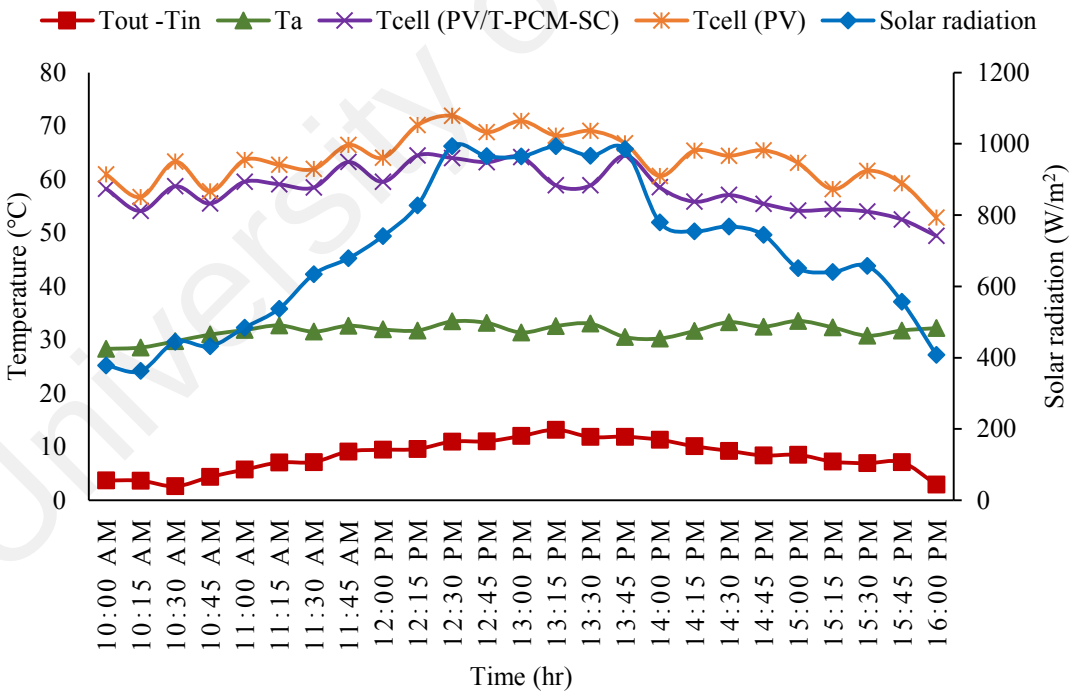

Figure 4.29: Hourly variation of different PV and PV/T-PCM-SC parameters (1 LPM)

Figure 4.30 shows the hourly variation of solar radiation and temperatures at different state of points of PV and PV/T-PCM with self-cleaning for 2 LPM water flow rate, when

University of Malaya

the average ambient temperature was 31.76°C. The highest rise in outlet water temperature is found 7.75°C at 12:45 PM. The highest solar radiation was recorded 981 W/m^2 at 1:00 PM when the cell temperature difference between PV and PV/T-PCM with self-cleaning is found 11.14°C. However, the maximum cell temperature difference between PV and PV/T-PCM with self-cleaning found 14.80°C when the solar radiation were 776 W/m^2 at 2:15 PM. It may be observed that around 11:00 AM to 12:30 PM and 1:00 to 2:15 PM, the PV/T-PCM with self-cleaning cell temperature the same trend as noticed in Figure 4.30. Temperature difference between PV and PV/T-PCM with self-cleaning has been found to be decreased further as compared to 0.5 LPM and 1 LPM due to the fact as explained above.

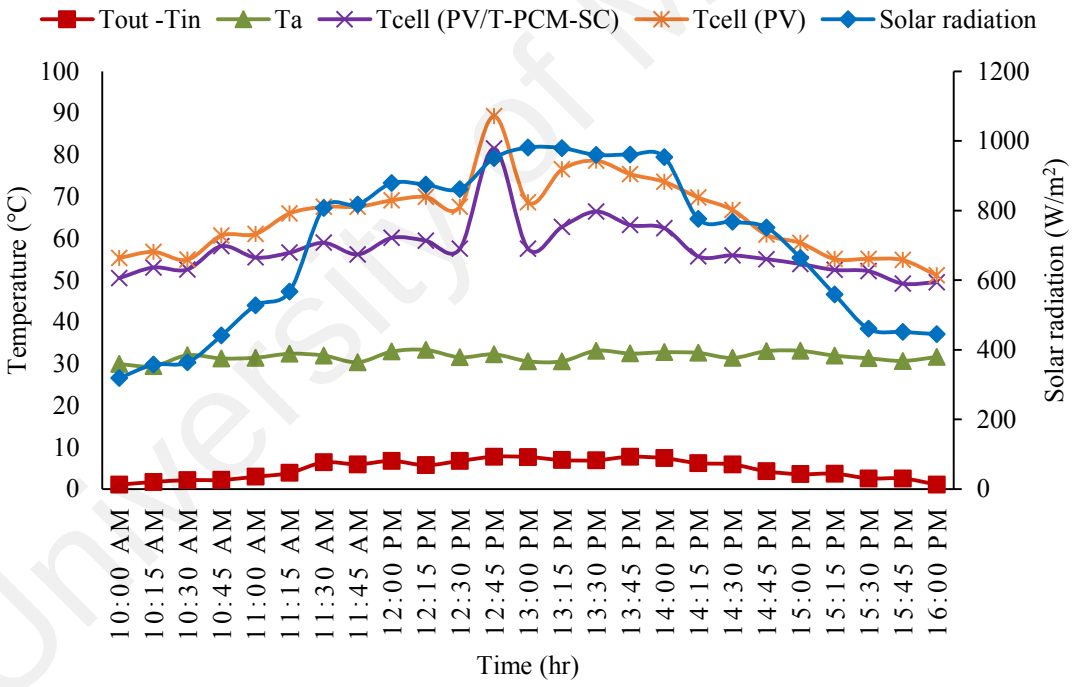

Figure 4.30: Hourly variation of different PV and PV/T-PCM-SC parameters (2 LPM)

Figure 4.31 shows the hourly variation of solar radiation and temperatures at different state of points of PV and PV/T-PCM with self-cleaning for 3 LPM water flow rate, when the average ambient temperature was 32.68°C. The highest rise in outlet water temperature is found 4.99°C at 2:00 PM. The maximum solar radiation was recorded 981

University of Malaya

W/m^2 at 1:00 PM when the cell temperature difference between PV and PV/T-PCM with self-cleaning is found 9.38°C. However, the maximum cell temperature difference between PV and PV/T-PCM with self-cleaning found 12.50°C when the solar radiation were 860 W/m^2 at 12:30 PM. It may be observed that around 11:30 AM to 1:45 PM and 2:15 to 3:00 PM, the PV/T-PCM with self-cleaning cell temperature same trend as depicted in Figure 4.30. It is clear that the PV/T-PCM with self-cleaning system, as flow rate is increased by1 LPM, the inlet and outlet water temperature decreased lower the dust module portraying the strong dependence of thermal and electrical performance on mass flow rate.

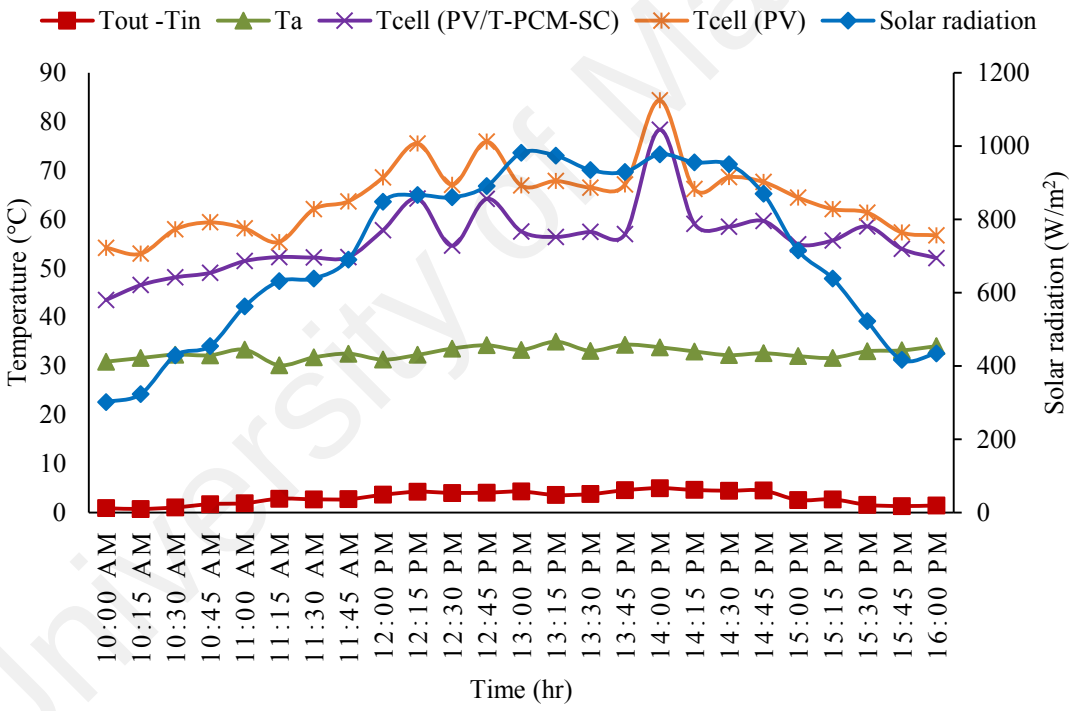

Figure 4.31: Hourly variation of different PV and PV/T-PCM-SC parameters (3 LPM)

Figure 4.32 shows the hourly variation of solar radiation and temperatures at different state of points of PV and PV/T-PCM with self-cleaning for 4 LPM water flow rate. Figure 4.32, it may be observed that the hourly variation of solar radiation is increased from 379 W/m^2 at 10:00 AM to a peak of 989 W/m^2 at 1:00 PM, which then decreases to 437 W/m^2 at 4:00 PM. Self-cleaning effect is observed to lowers the cell temperature as it was

University of Malaya

assisted with water flow. Figure 4.32 shows that the self-cleaning produces very marginal temperature rise in the water with an average value below 3.28°C. Self-cleaning module aided by PCM cooling experience further drop in cell temperature. It may be observed from Figure 4.32 that a self-cleaning module with PCM cooling can lower the cell temperature by 11.51°C. Table 4.4 presents the measured PV/T-PCM with self-cleaning collector parameters at the optimum mass flow rate of 4 LPM. Self-cleaning study shows a reverse effect as compared with dust results. It can be observed from the Figure 4.32, during 10:00 to 11:00 AM, the cell temperature difference is less than 11:15 AM to 2:45 PM; that difference is high. Because the cleaning process was started at 11:00 AM and finished after 11:06 AM. The maximum cell temperature difference can be found after cleaning process, but the difference between inlet and outlet water temperatures is found low. Because during cleaning process the module temperature is cooled down and the heat energy cannot transfer to the water flow and phase change material. After cleaning, the solar intensity and the temperature are rising and the heat moves slowly to the water then PCM. Therefore, the PCM also takes time for melting and storing the thermal energy as well. It is also observing that after 3:00 to 4:00 PM, the cell temperature difference is as usual, and the outlet water temperature is much lower respectively.

University of Malaya

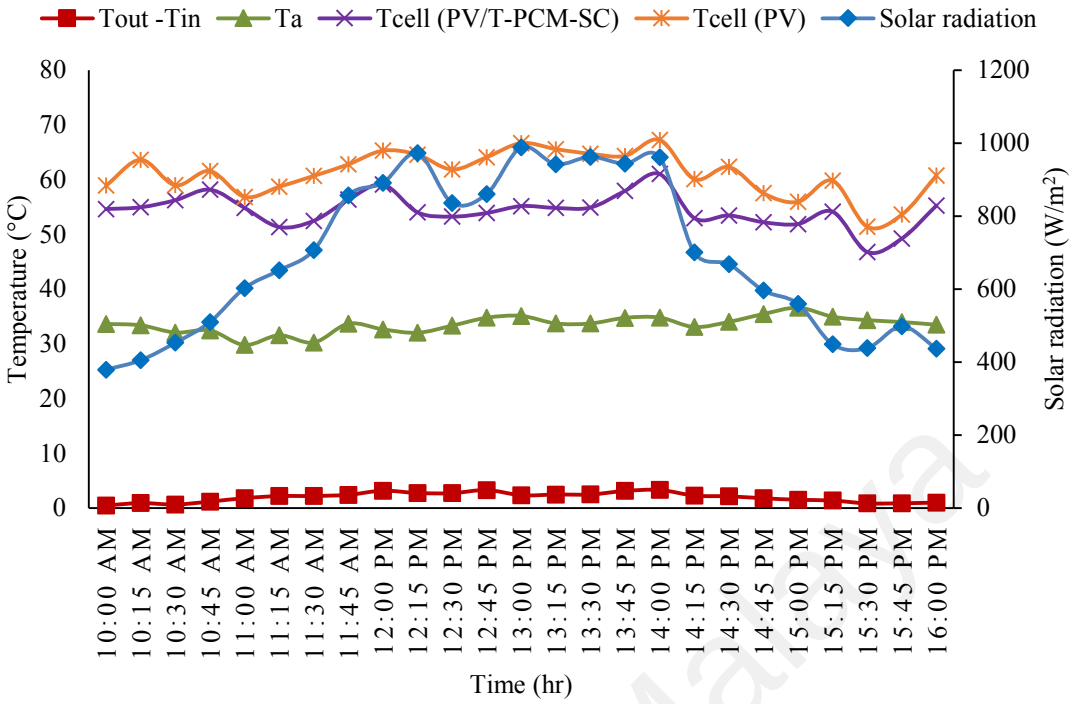

Figure 4.32: Hourly variation of different PV and PV/T-PCM-SC parameters (4 LPM)

Table 4.4: The measured parameters at mass flow rate of 4 LPM

Time	T_a (°C)	T_{in} (°C)	T_o (°C)	P_{max} (W)	G (W/m^2)
10:00	33.63	20.86	21.33	86.08	379
10:30	32.06	24.27	24.90	84.18	453
11:00	29.78	25.45	27.24	125.28	603
11:30	30.23	25.20	27.39	138.53	707
12:00	32.64	24.74	27.90	148.31	891
12:30	33.32	25.18	27.87	150.47	836
13:00	35.10	25.01	27.33	182.74	989
13:30	33.72	25.13	27.59	181.75	963
14:00	34.79	24.24	27.52	172.72	961
14:30	34.01	25.01	27.13	142.10	669
15:00	36.59	25.59	27.08	131.46	559
15:30	34.32	25.32	26.15	84.01	438
16:00	33.48	23.48	24.46	89.29	437

4.6 The Effect of Dust Cleaning on the Performance of the PV/T-PCM System

One of the main hindrances to the photovoltaic performance is the dust accumulation on top of the glass surface. Normally, the electrical performance is enhanced through a clearness index of the glass cover. An innovative self-cleaning mechanism has been

University of Malaya

developed and integrated with the PV/T-PCM module that can conveniently wipe the dusts away by means of a sweeping microfiber assisted by water flow which not only prevents the glass cover from scratches but also weakens the van der Waals adhesive force on dusts from sticking on to the glass surface. The following sections elaborate on the effect of using self-cleaning mechanism on the electrical and thermal performances of the PV/T-PCM system.

4.6.1 Effect of Irradiation on Electrical Performance

The effect of dust on the electrical performance of the PV/T-PCM system shows in Figure 4.33 (a) and (b). Under 1000 W/m^2, the electrical power of the PV and PV/T-PCM with dust module is 138.27 W and 147.86 W respectively, as compared to that of PV and PV/T-PCM with self-cleaning module of 139.02 W and 149.78 W respectively under 992 W/m^2 as shown in Figure 4.33 (a) and (b). It can be observed that at low mass flow rate, the power difference between PV, dust and self-cleaned module are less. Because at low mass flow rate, the panel is unable to transfer the heat from the module. However, the power output of self-cleaned module increases little as compared to dust module because of PCM cooling and water cleaning system. It is also revealed from Figure 4.33 (a) and (b) that the maximum electrical efficiency difference between PV and PV/T-PCM with dust module is 1.19%, whereas that of the PV and PV/T-PCM with self-cleaning module is 1.75%.

University of Malaya

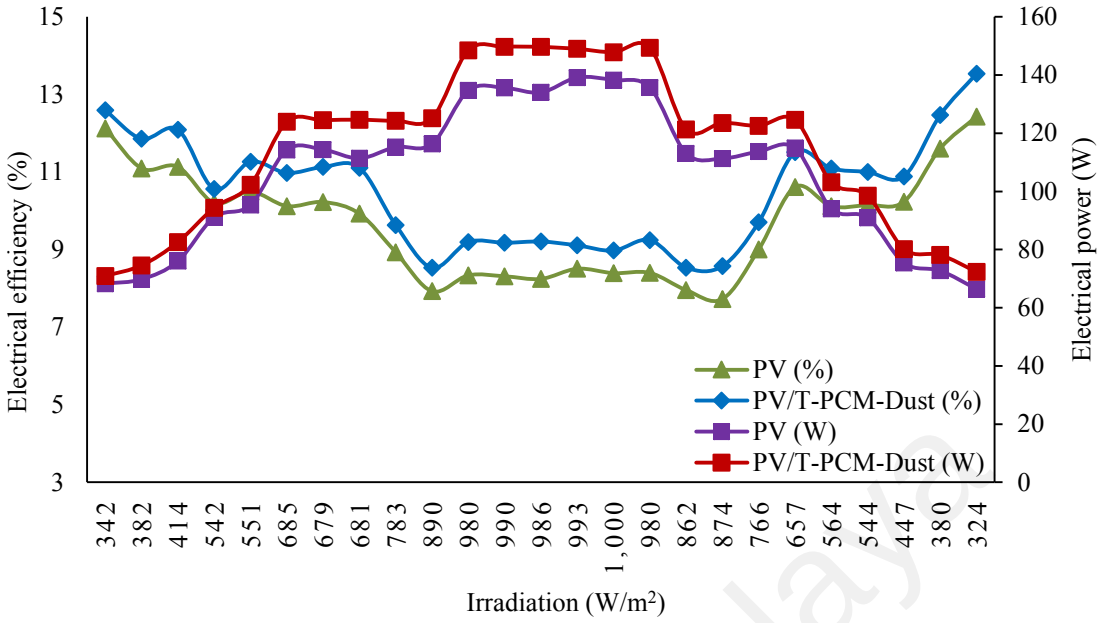

(a) Electrical performance of PV/T-PCM-Dust against PV

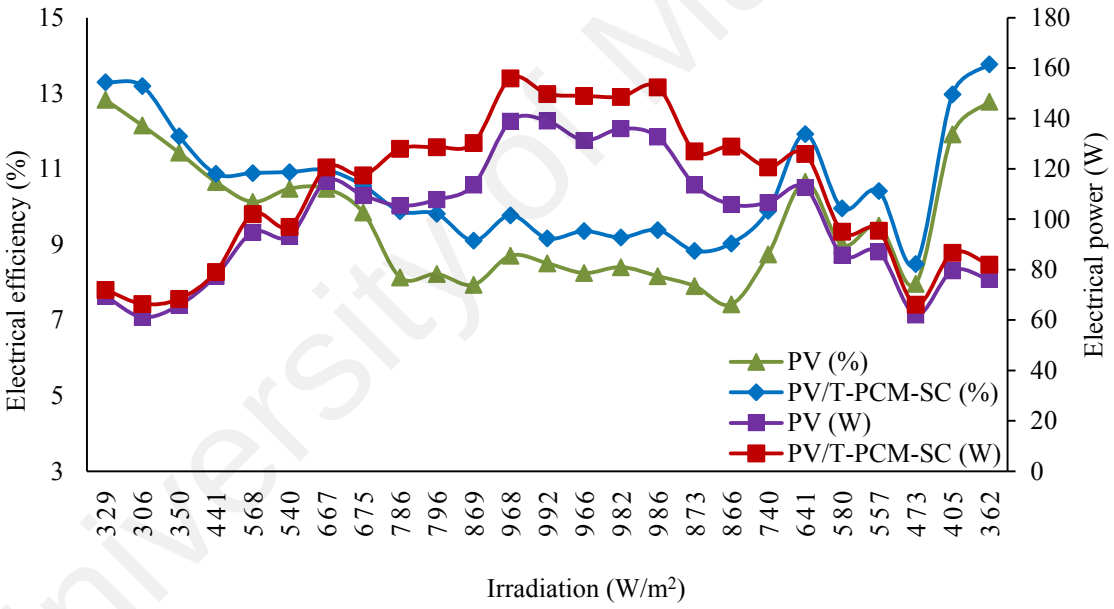

(b) Electrical performance of PV/T-PCM-SC against PV

Figure 4.33: Effect of irradiation on electrical performance of (a) PV/T-PCM-Dust and (b) PV/T-PCM-SC against PV (0.5 LPM)

The electrical performance of PV/T-PCM module with dust and self-cleaning is shown in Figure 4.34 (a) and (b). Figure 4.34 (a) and (b) shows at 991 W/m^2, the electrical power of the PV and PV/T-PCM with dust module is 139.36 W and 147.94 W, as compared to that at 993 W/m^2 of PV and PV/T-PCM with self-cleaning module of 143.59 W and 160.19 W respectively. It can be observed that as the mass flow rate is increased from 0.5

University of Malaya

to 1 LPM the power difference also increases in self-cleaned module as compared to PV and dusty module. At this flow rate, the thermal collector and the PCM heat gain capacity is increased. The maximum difference in electrical efficiencies between PV and PV/T-PCM with dust module is 1.49%, whereas that of the PV and PV/T-PCM with self-cleaning module is 2.28% as shown in Figure 4.35 (a) and (b).

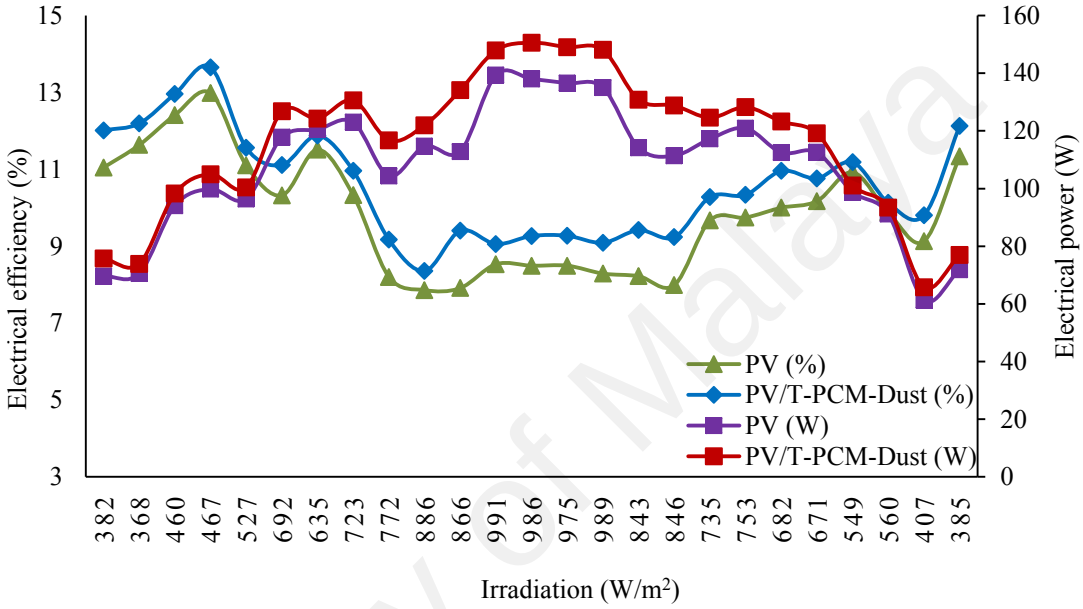

(a) Electrical performance of PV/T-PCM-Dust against PV

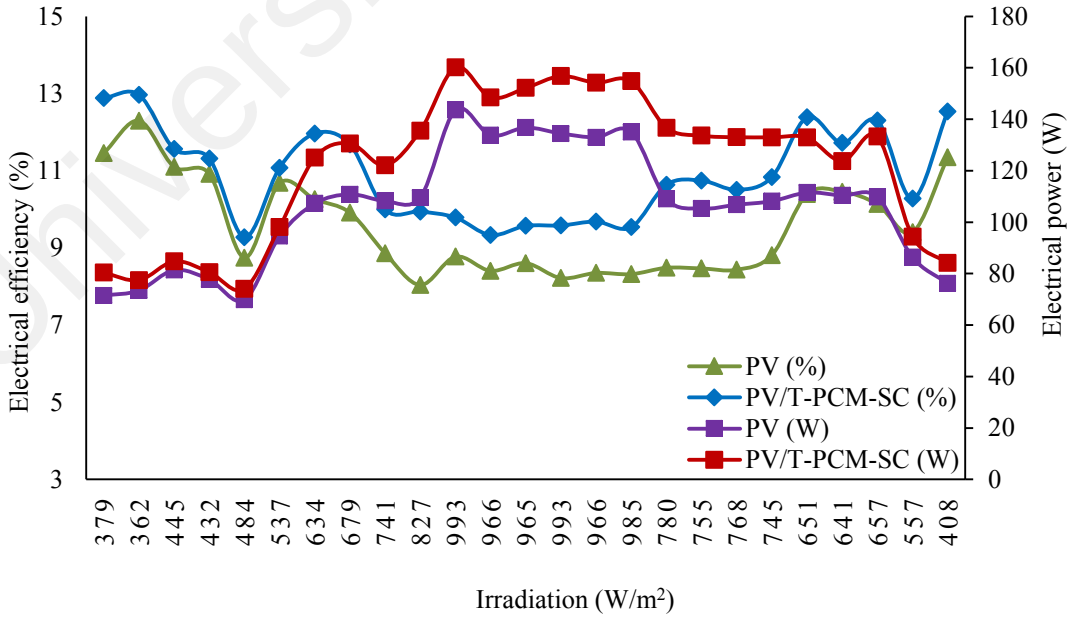

(b) Electrical performance of PV/T-PCM-SC against PV

Figure 4.34: Effect of irradiation on electrical performance of (a) PV/T-PCM-Dust and (b) PV/T-PCM-SC against PV (1 LPM)

University of Malaya

The electrical performance of PV/T-PCM module with dust and self-cleaning is shown in Figure 4.35 (a) and (b). Figure 4.35 (a) and (b) show that at 989 W/m^2, the electrical power of the PV and PV/T-PCM with dust module is 137.47 W and 148.10 W, as compared to that of PV and PV/T-PCM with self-cleaning module of 140.28 W and 165.91 W respectively under 981 W/m^2. It can be observed that as the mass flow rate is increased from 1 to 2 LPM power difference also increases in self-cleaned module as compared to PV and dusty module. At this flow rate, the thermal collector and the PCM heat gain capacity is increased. The maximum difference between electrical efficiencies of PV and PV/T-PCM with dust module is 1.28%, whereas that of the PV and PV/T-PCM with self-cleaning module is 3.12%.

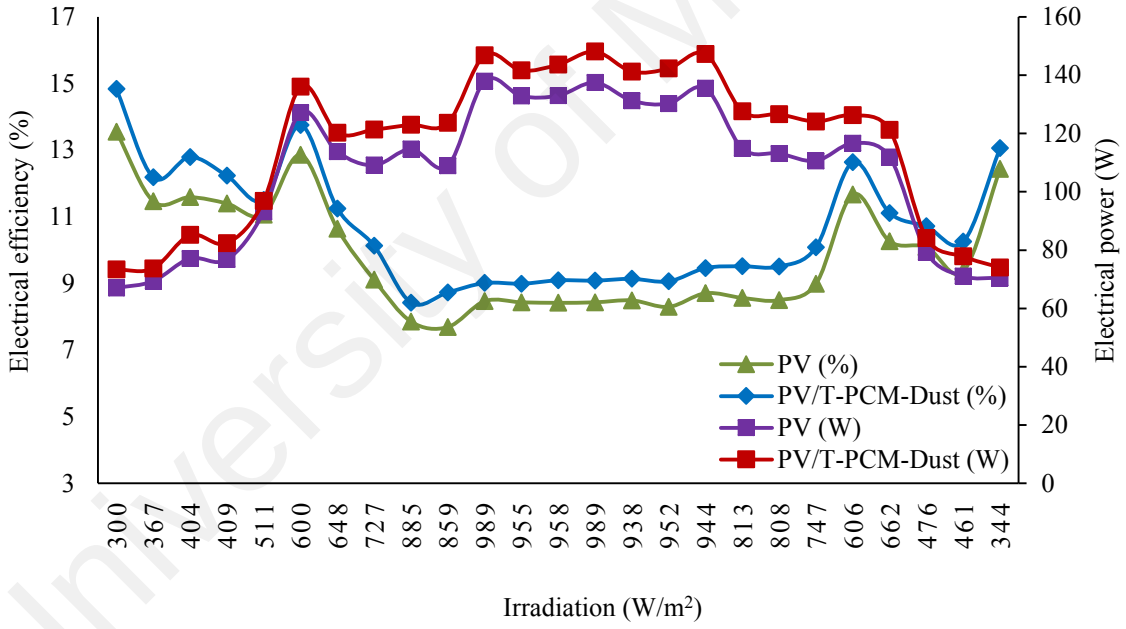

(a) Electrical performance of PV/T-PCM-Dust against PV

Figure 4.35: Effect of irradiation on electrical performance of (a) PV/T-PCM-Dust and (b) PV/T-PCM-SC against PV (2 LPM)

University of Malaya

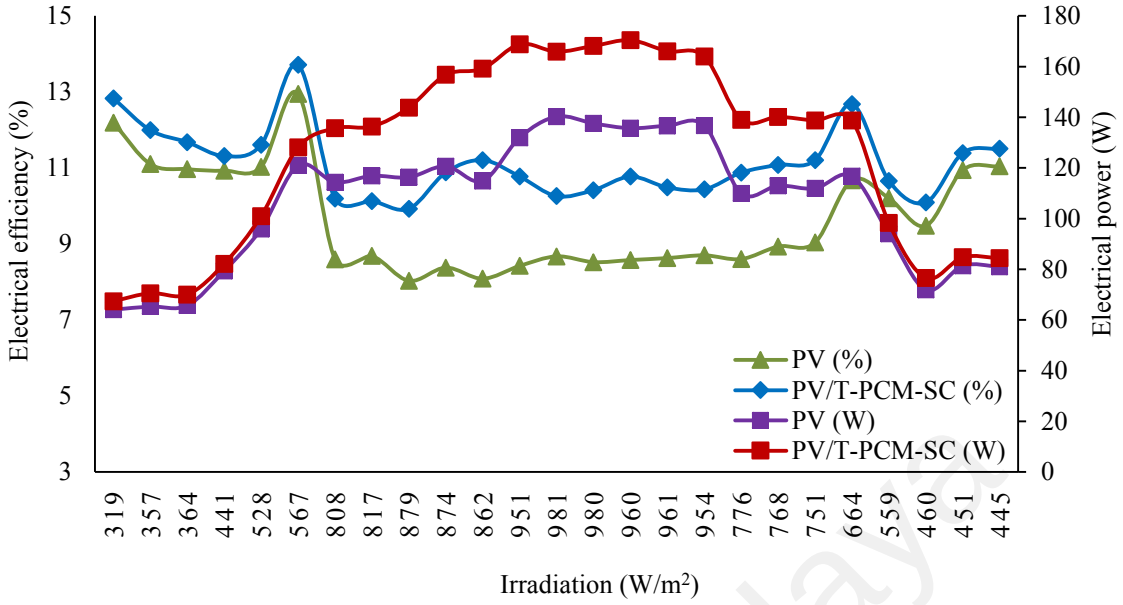

(b) Electrical performance of PV/T-PCM-SC against PV

Figure 4.35, continued

The electrical performance of PV/T-PCM module with dust and self-cleaning is shown in Figure 4.36 (a) and (b). Figure 4.36 (a) and (b) show that at 996 W/m^2, the electrical power of the PV and PV/T-PCM with dust module is 141.51 W and 153.85 W, while that of PV and PV/T-PCM with self-cleaning module of 139.35 W and 165.84 W respectively at 981 W/m^2. It can be observed as mass flow rate increased from 2 to 3 LPM and the power difference also increases in self-cleaned module as compared to PV and dusty module. At this flow rate, the thermal collector and the PCM heat gain capacity is increased for both dust and self-cleaning module. Because of PCM cooling and flow rates increased, the dust module power also proportionally increased. The maximum difference between electrical efficiencies of PV and PV/T-PCM with dust module is 1.84%, whereas that of the PV and PV/T-PCM with self-cleaning module is 3.68% respectively. It is observed that the self-cleaning PV/T-PCM collector gives maximum electrical efficiency at mass flow rate of 3 LPM.

University of Malaya

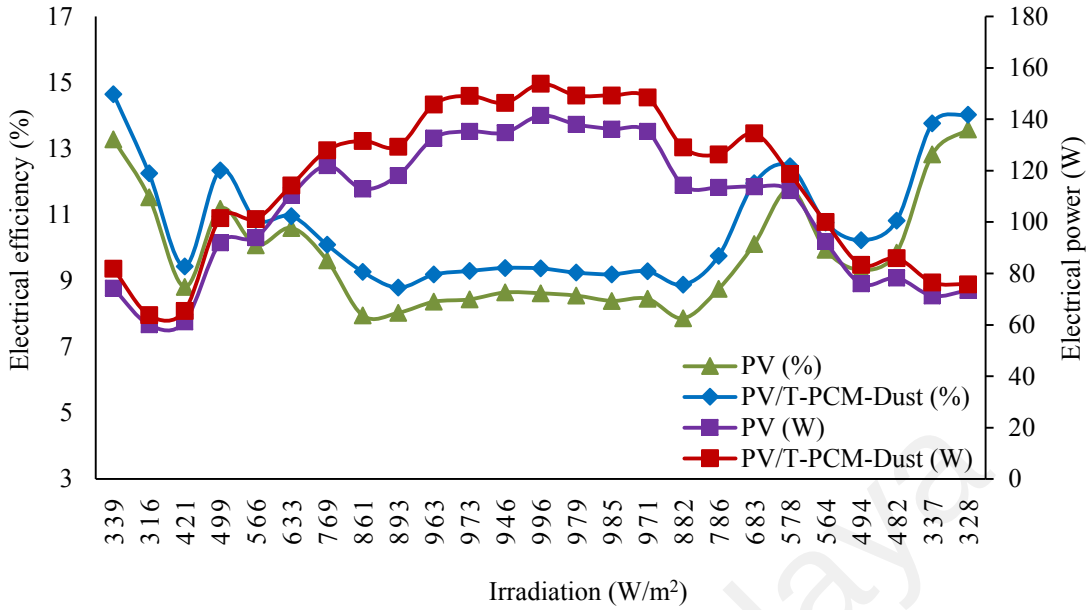

(a) Electrical performance of PV/T-PCM-Dust against PV

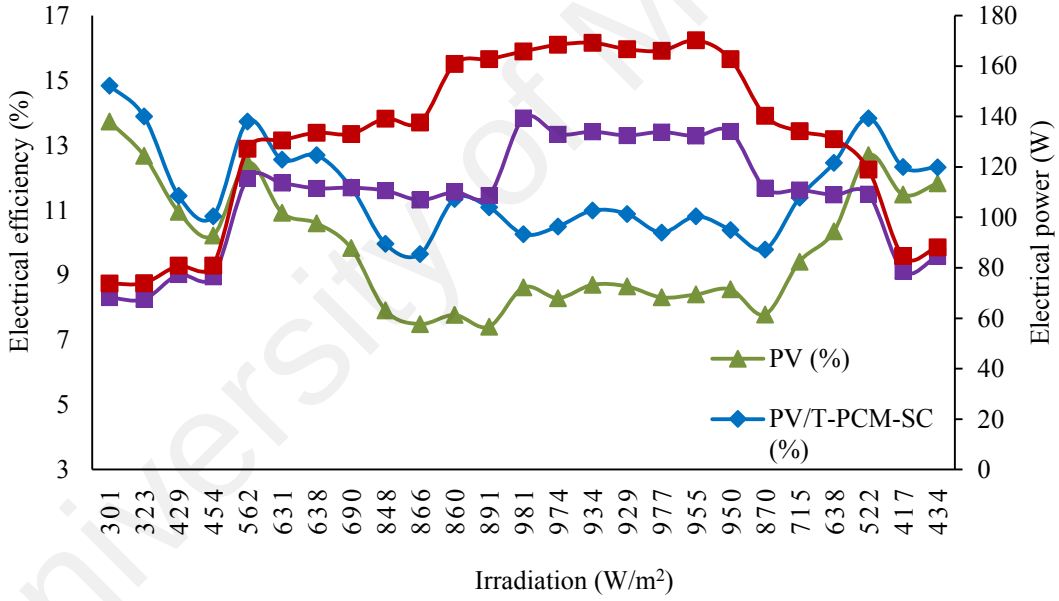

(b) Electrical performance of PV/T-PCM-SC against PV

Figure 4.36: Effect of irradiation on electrical performance of (a) PV/T-PCM-Dust and (b) PV/T-PCM-SC against PV (3 LPM)

The effect of self-cleaning on the electrical performance of the PV/T-PCM system at optimum mass flow rate of 4 LPM has been depicted in Figure 4.37 (a) and (b). It can be seen at 985 W/m^2 that the electrical power of the PV and PV/T-PCM with dusty module is 138.09 W and 143.28 W. On the other hand, electrical output of PV and PV/T-PCM with self-cleaning module are 143.58 W and 182.74 W respectively at 989 W/m^2. The

University of Malaya

panel power increases in proportion with solar intensity level. It can be observed that the PV/T-PCM with dust module power is lower than self-cleaned module because dust has been blocked the potential solar intensity on the panel. However, because of mass flow rates and PCM cooling capacity, the dust module power is increased slightly as compared to the PV panel. On the other hand, self-cleaning system receives more solar intensity with coolant used to clean the module and produce more power. The power variation between PV/T-PCM-Dust and PV/T-PCM self-cleaning also depends on ambient and cell temperature difference. It may be clearly noticed from Figure 4.37 (b) that the electrical power output increases due to the absence of dust. While the highest electrical power with dusty PV/T-PCM module is 148.10 W, the PV/T-PCM with self-cleaning system produces power as high as 182.74 W, a considerable increment in power output. For every 100 W/m^2 increase in irradiation level, output power rises by 11.97 W and 14.90 W PV/T-PCM dust and self-cleaning modules respectively.

The highest variance in electrical efficiency values between PV and PV/T-PCM with dust module is found 1.68% as shown in Figure 4.37 (a) and (b), whereas that of the PV and PV/T-PCM with self-cleaning module is 3.67%. Self-cleaning also increases the electrical efficiency as illustrated in Figure 4.37 (b). It may be observed that electrical efficiency of a self-cleaning PV/T-PCM module is much higher than that of a dusty module with the highest efficiency being near 15.60%. For every 100 W/m^2 increase in irradiation level, the efficiency decreases by 0.55% and 1.18% for PV/T-PCM dust and self-cleaning modules respectively. The reason behind a better electrical performance due to self-cleaning is that the accompanying water flow creates a film of water on the module front which incidentally also allows the system to operate at even lower temperatures than the device itself and by virtue of the fast flowing volume of water, there is a minimal increase in the water temperature as the effect of evaporating water further decreases the temperatures, thus, resulting in increased electrical yields.

University of Malaya

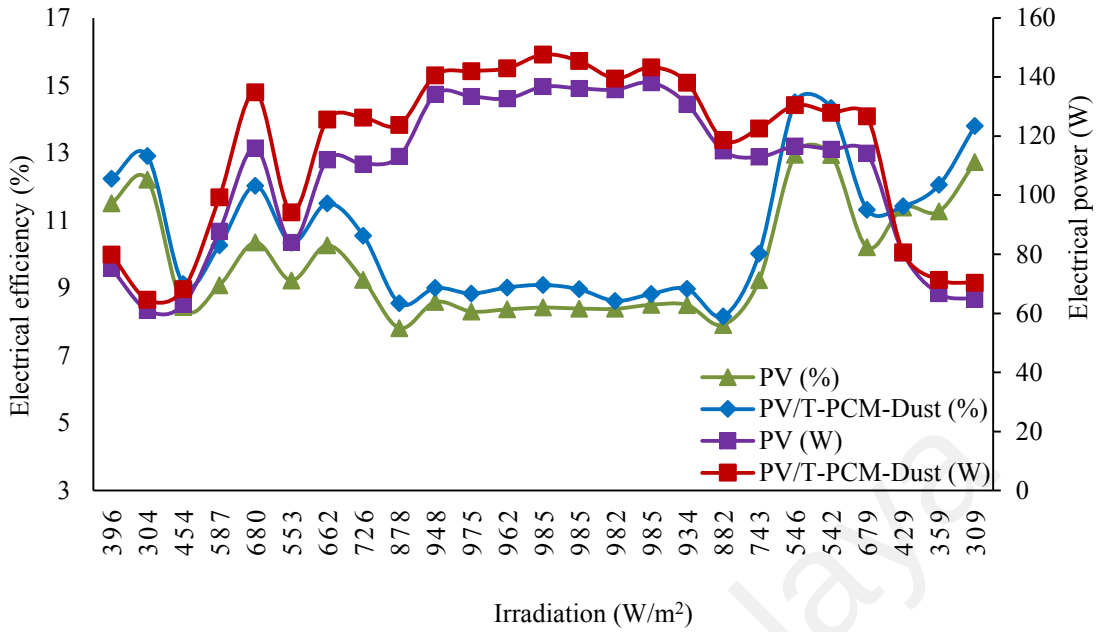

(a) Electrical performance of PV/T-PCM-Dust against PV

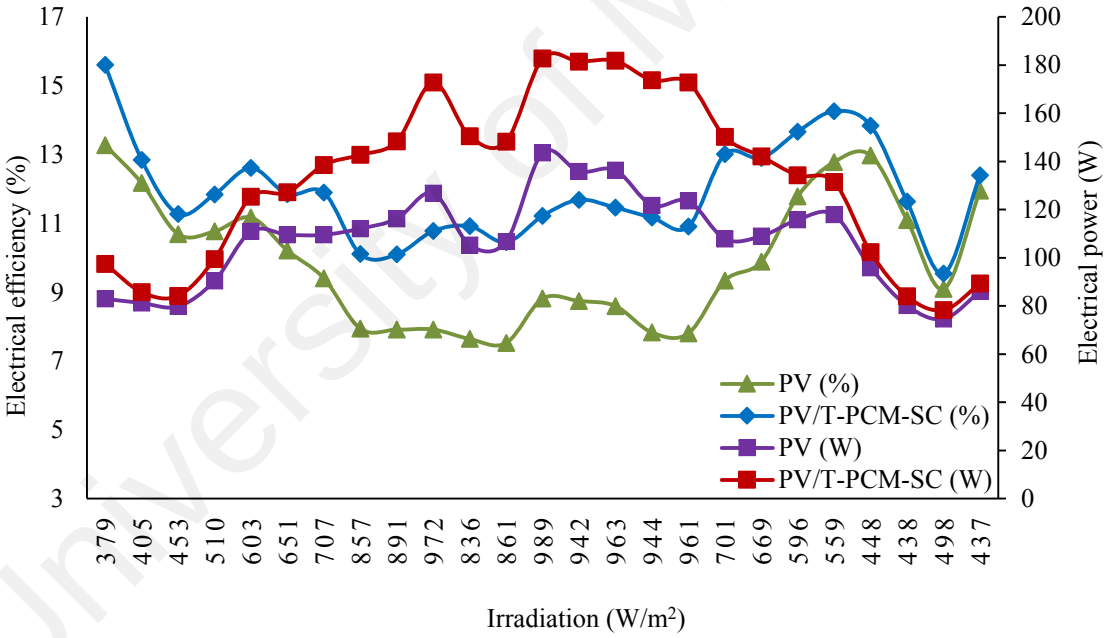

(b) Electrical performance of PV/T-PCM-SC against PV

Figure 4.37: Effect of irradiation on electrical performance of (a) PV/T-PCM-Dust and (b) PV/T-PCM-SC against PV (4 LPM)

4.6.2 Effect of Cell Temperature on Electrical Performance

The effect of cell temperature on the electrical performance of PV/T and PV/T-PCM systems has already been described in the section 4.3.2. In this section will be described the effects of dust and self-cleaning on the PV/T-PCM module electrical performance.

University of Malaya

The horizontal axis in Figure 4.42 (a) and (b) show two cell temperature: one is PV references and another one is PV/T-PCM dust and self-cleaning (highlighted) cell temperature. The effect of cell temperature on electrical performance of PV/T-PCM dust and PV/T-PCM self-cleaning is shown in Figure 4.38 at mass flow rate of 0.5 LPM. Figure 4.38 (a) and (b) shows that the PV and PV/T-PCM dust systems undergoes a power drop of 15.65 W at 3.71°C whereas that of the PV/T-PCM with cleaning system is 23.03 W at 4.20°C. It can be observed that at low mass flow rate, the dusty module output power is lower than self-cleaned module. As self-cleaning system is contained with water, so at the primary level the cell temperature is dropped and cleaned module able to absorb more solar intensity. However, PCM cooling and mass flow rate are important roles to drop the cell temperature for both modules respectively.

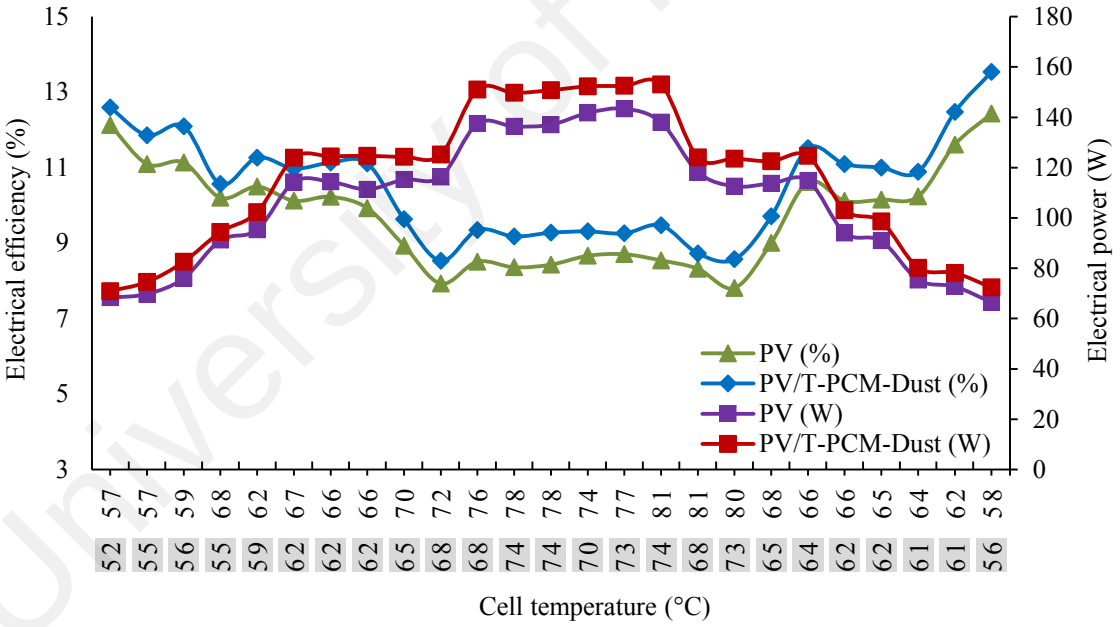

(a) Electrical performance of PV/T-PCM-Dust against PV

Figure 4.38: Effect of cell temperature on electrical performance of (a) PV/T-PCM dust and (b) PV/T-PCM self-cleaning against reference PV (0.5 LPM)

University of Malaya

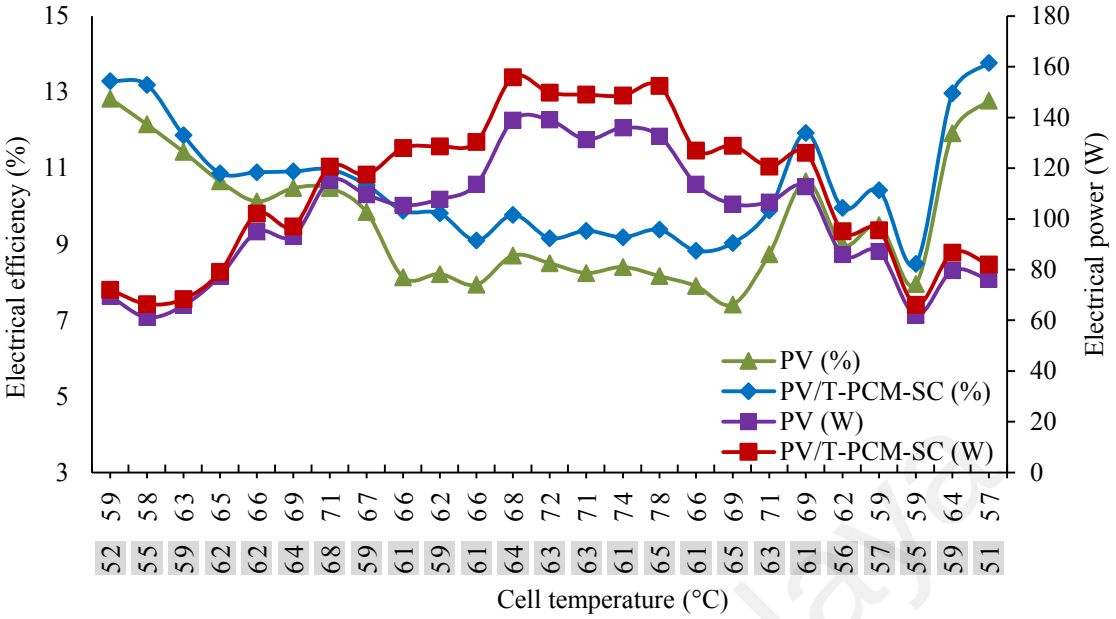

(b) Electrical performance of PV/T-PCM-SC against PV

Figure 4.38, continued

The effect of cell temperature on electrical performance of PV/T-PCM dust and PV/T-PCM self-cleaning is shown in Figure 4.39 (a) and (b) at mass flow rate of 1 LPM. Figure 4.39 (a) and (b) shows that the PV and PV/T-PCM dust systems undergoes a power drop of 21.28 W at 5.34°C whereas that of the PV/T-PCM with cleaning system is 28.32 W at 9.54°C respectively. It can be observed that as mass flow rate is increased from 0.5 to 1 LPM the output power and cell temperature difference are also increases in self-cleaned module as compared to dusty module. However, PCM cooling and mass flow rate are important roles to drop the cell temperature for both modules. It is evident from Figure 4.39 (a) and (b) that the maximum variation in the PV and PV/T-PCM dust collector electrical efficiency is 1.49% at 5.34°C while that of the PV/T-PCM self-cleaning is 2.28% at 9.54°C.

University of Malaya

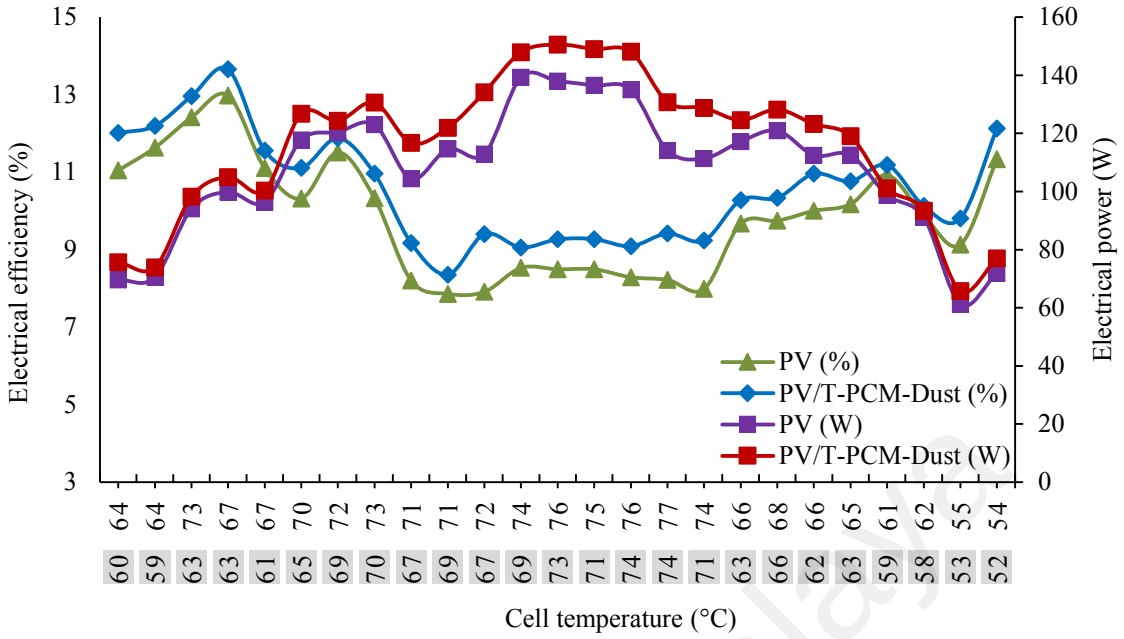

(a) Electrical performance of PV/T-PCM-Dust against PV

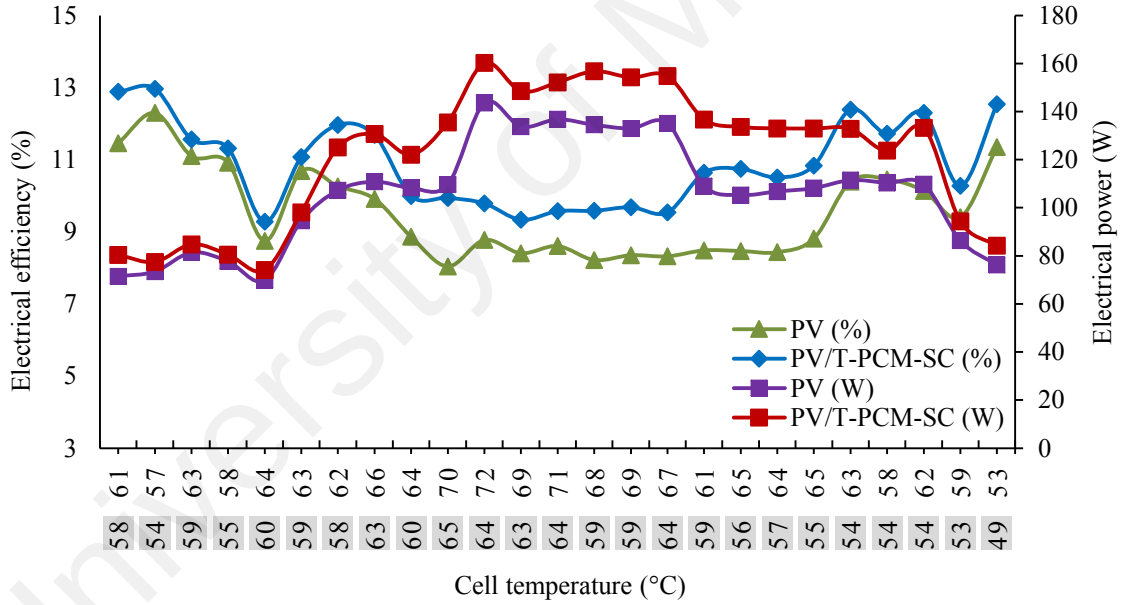

(b) Electrical performance of PV/T-PCM-SC against PV

Figure 4.39: Effect of cell temperature on electrical performance of (a) PV/T-PCM dust and (b) PV/T-PCM self-cleaning against reference PV (1 LPM)

The effect of cell temperature on electrical performance of PV/T-PCM dust and PV/T-PCM self-cleaning is shown in Figure 4.40 (a) and (b) at mass flow rate of 2 LPM. Figure 4.40 (a) and (b) shows that the PV and PV/T-PCM dust systems undergoes a power drop of 14.72 W at 4.44°C, whereas that of the PV/T-PCM with cleaning system is 44.31 W at 10.07°C. It can be observed that as mass flow rate is increased from 1 to 2 LPM the

University of Malaya

output power and cell temperature difference are also increases in self-cleaned module as compared to dusty module. It may be observed from Figure 4.40 (a) and (b) that the maximum variation in the PV and PV/T-PCM dust collector electrical efficiency is 1.28% at 2.17°C while that of the PV/T-PCM self-cleaning is 3.12% at 10.07°C respectively. However, PCM cooling and mass flow rate are important roles to drop the cell temperature for both modules.

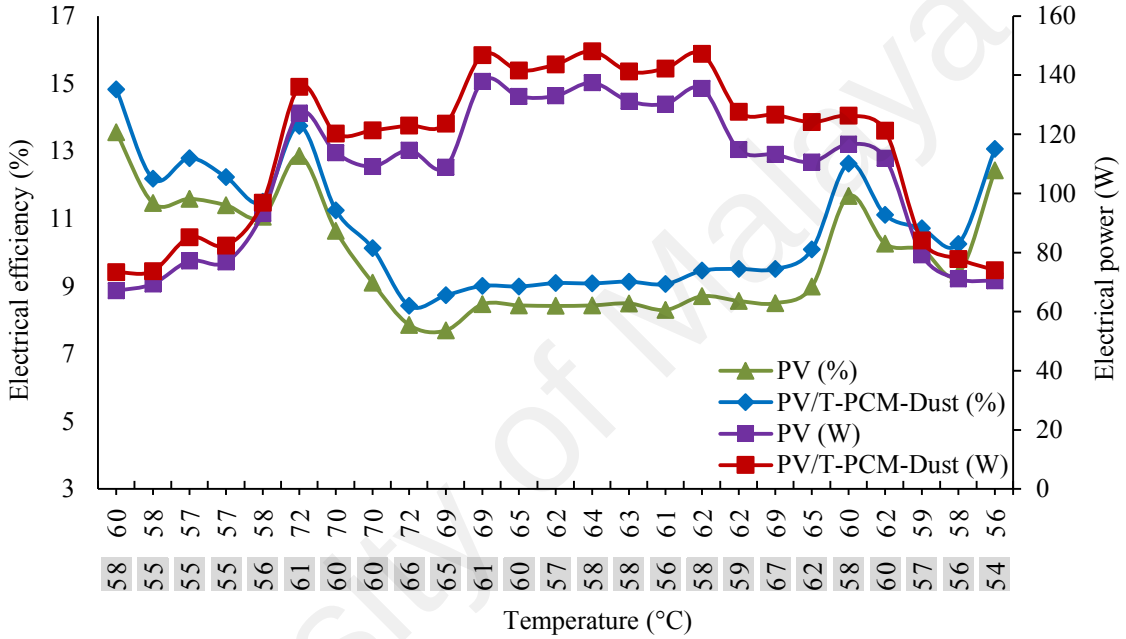

(a) Electrical performance of PV/T-PCM-Dust against PV

Figure 4.40: Effect of cell temperature on electrical performance of (a) PV/T-PCM dust and (b) PV/T-PCM self-cleaning against reference PV (2 LPM)

University of Malaya

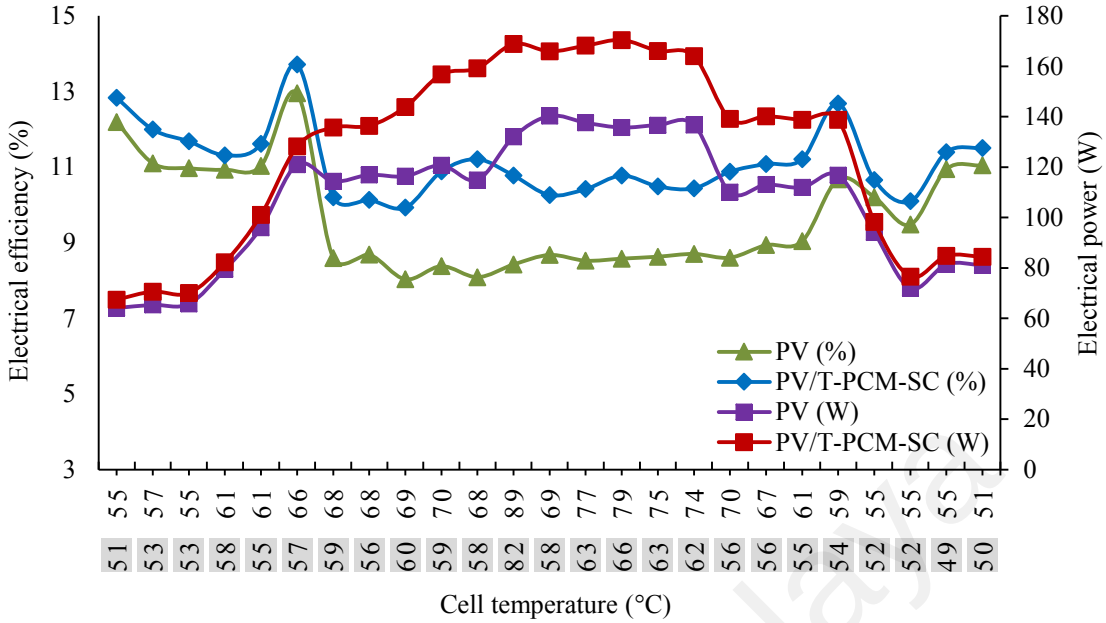

(b) Electrical performance of PV/T-PCM-SC against PV

Figure 4.40, continued

The effect of cell temperature on electrical performance of PV/T-PCM dust and PV/T-PCM self-cleaning is shown in Figure 4.41 (a) and (b) at mass flow rate of 3 LPM. Figure 4.41 (a) and (b) shows that the PV and PV/T-PCM dust systems undergoes a power drop of 20.72 W at 2.86°C whereas that of the PV/T-PCM with cleaning system is 54.07 W at 11.70°C. It can be observed that as mass flow rate is increased from 2 to 3 LPM the output power and cell temperature difference are also increased in self-cleaned module as compared dusty module. It may be seen from Figure 4.41 (a) and (b) that the maximum variation in the PV and PV/T-PCM dust collector electrical efficiency is 1.84% at 2.86°C while that of the PV/T-PCM self-cleaning is 3.68% at 11.70°C. However, PCM cooling and mass flow rate are important roles to drop the cell temperature for both modules.

University of Malaya

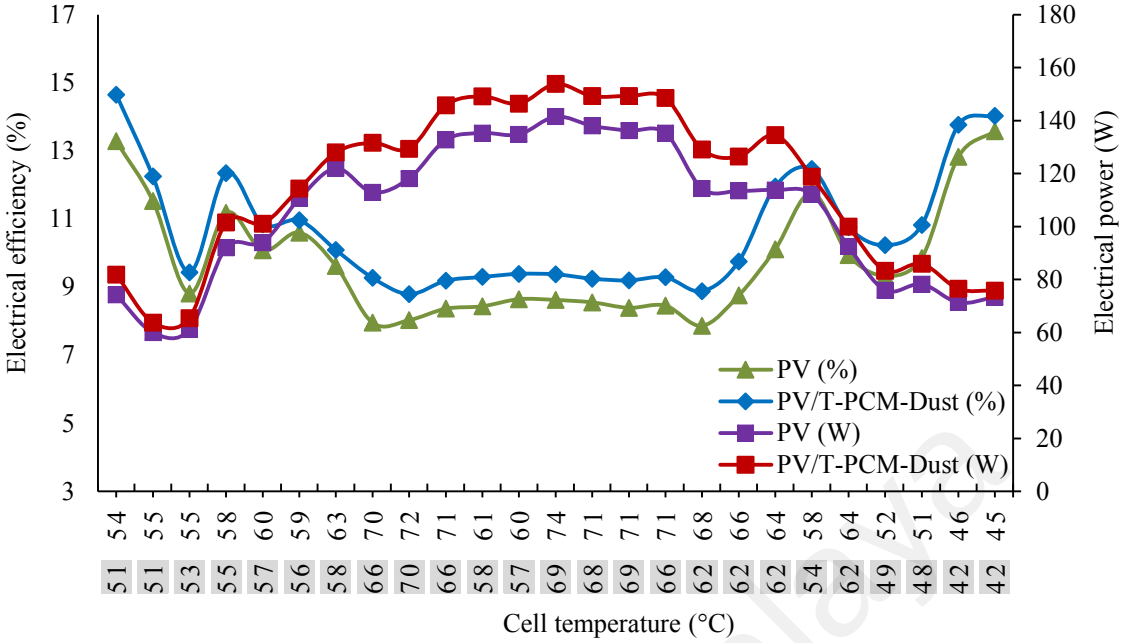

(a) Electrical performance of PV/T-PCM-Dust against PV

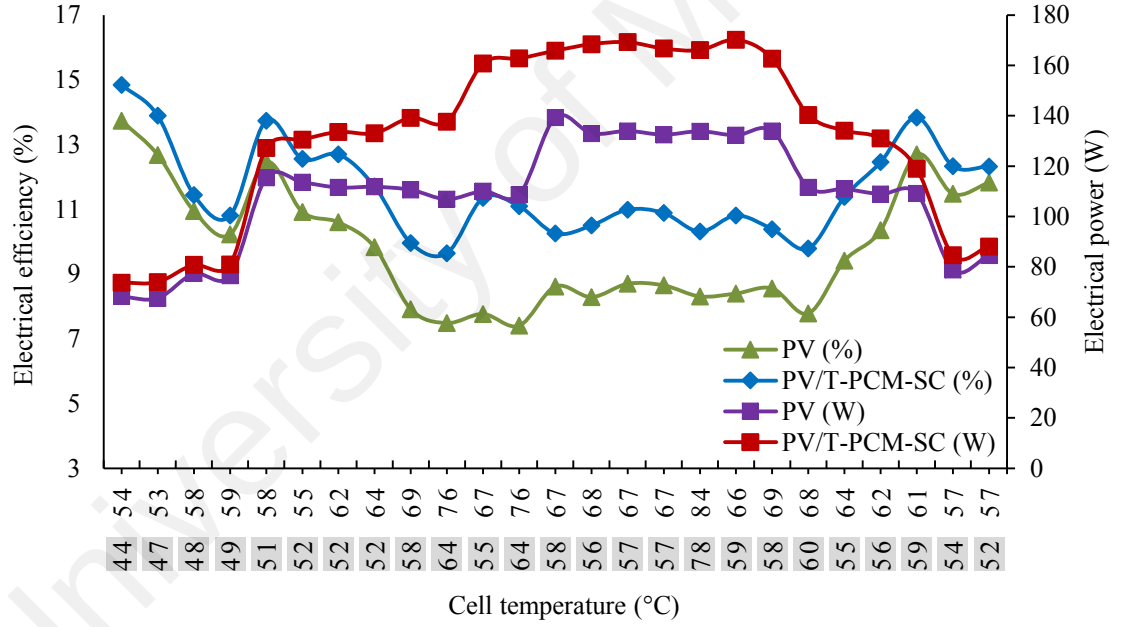

(b) Electrical performance of PV/T-PCM-Dust against PV

Figure 4.41: Effect of cell temperature on electrical performance of (a) PV/T-PCM dust and (b) PV/T-PCM self-cleaning against reference PV (3 LPM)

A notable effect of increased cell temperature on electrical power and efficiency has been observed in Figure 4.42 (a) to (b) at mass flow rate of 4 LPM. The adverse effect of increased cell temperature in electrical power output of both the PV/T-PCM dust and the PV/T-PCM self-cleaning systems is apparently conceivable from Figure 4.42 (a) and (b) in which it is readily observed that the corresponding power drop in the PV/T-PCM self-

University of Malaya

cleaning system is greater than that of the PV/T-PCM dust system at mass flow rate of 4 LPM. The PV and PV/T-PCM dust systems undergoes a power drop of 18.83 W at 2.83°C whereas that of the PV/T-PCM with cleaning system is 51.92 W at 6.39°C, which in turn promotes the potential adoption of the PV/T-PCM with cleaning system to save this amount of power by integrating with the PCM and water cleaning assisted cooling regime. Results show that power level vary because panel current increase a little and voltage decrease proportionally with increased cell temperature. The power variation between PV/T-PCM-Dust and PV/T-PCM self-cleaning are depended on ambient and cell temperature difference.

On the other hand, a drop in the electrical efficiency due to the cell temperature rise is less prominent, especially, in the case of a PV/T-PCM self-cleaning system. However, dust is seen to have significant adverse effects on the electrical efficiency. Electrical efficiency is clearly enhanced by the self-cleaning. As evident from Figure 4.42 (b), electrical efficiency of PV/T-PCM with self-cleaning system exceeds the limit of 15%. It may be perceived from Figure 4.42 (a) and (b) that the maximum variation in the PV and PV/T-PCM dust collector electrical efficiency increases by 1.68% at 2.83°C while that of the PV/T-PCM self-cleaning is 3.67% at 7.13°C. Another notable point from these figures is that for both the power output and the efficiency curves, the gap between the PV and the PV/T-PCM self-cleaning trend lines is wider than that between the PV and the PV/T-PCM dust. This portrays a better relative improvement in both the electrical power and the efficiency of the PV/T-PCM self-cleaning system than that of the PV/T-PCM system with respect to the PV module. This finding also confirms that the PV/T-PCM self-cleaning system has a superior performance over the PV/T-only system.

University of Malaya

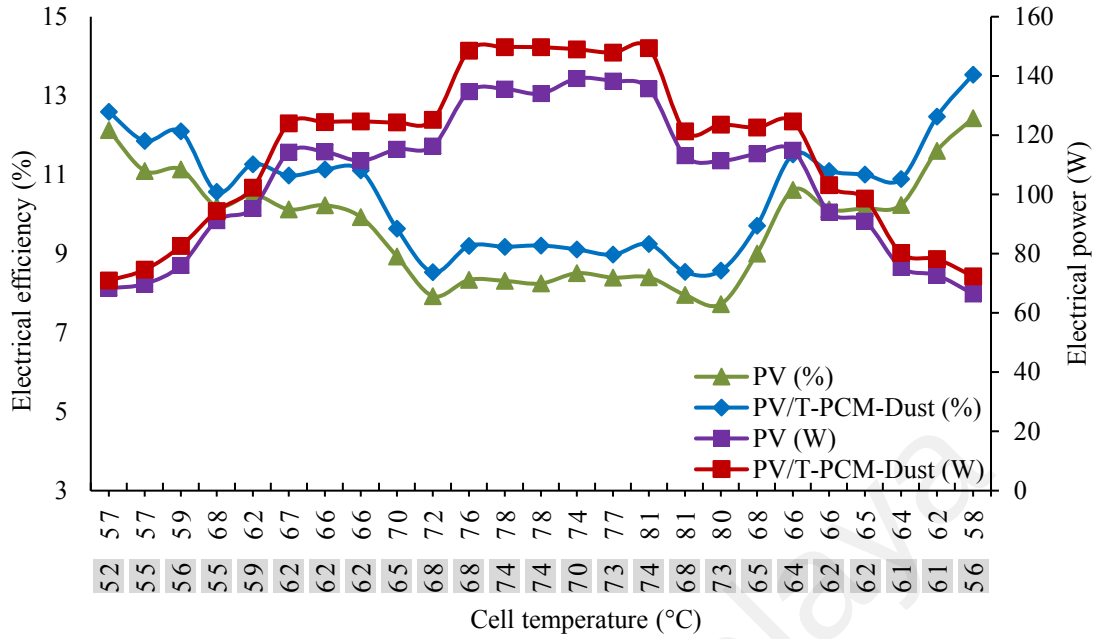

(a) Electrical performance of PV/T-PCM-Dust against PV

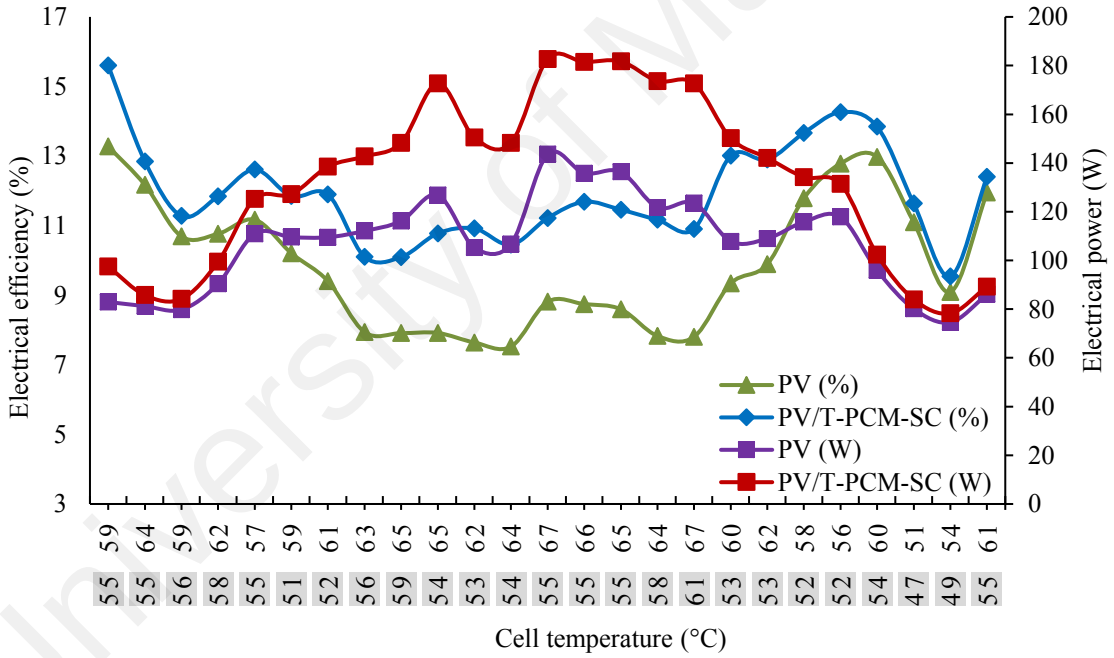

(b) Electrical performance of PV/T-PCM-SC against PV

Figure 4.42: Effect of cell temperature on electrical performance of (a) PV/T-PCM dust and (b) PV/T-PCM self-cleaning against reference PV (4 LPM)

4.6.3 Effect on Energy Performance

The change in the thermal performance of a solar energy module system due to dust cleaning operation has been illustrated in Figure 4.43 (a) to (d). The heat gain and thermal efficiency of the PV/T-PCM system covered with dust and that obtained after dust cleaning process are as shown in Figure 4.43 (a) and (b). It may be noticed that the thermal

University of Malaya

performance in both heat gain and thermal efficiency decrease after the dust cleaning process on the PV glass surface which is mainly due to the instantaneous cooling effect of the water flow with the additional cooling effect as the water film evaporates on the glass which further decreases the glass surface temperature. Hence, a PV/T-PCM module with a self-cleaning system exhibits slightly lower heat gain and thermal efficiency than dust covered module. However, the outlet water temperature obtains better heat gain in the PV/T-PCM with self-cleaning component than that with dust covered panel. While the highest outlet water temperature with a dusty PV/T-PCM module is 40.01°C, the PV/T-PCM with self-cleaning system delivers the outlet water at 43.71°C, hence, the self-cleaning system helps to increase the outlet water temperature by 3.7°C and brings it up to the temperature requirement of household warm water supply. The maximum average thermal efficiency for PV/T-PCM dusty collector has been recorded 78.18%, whereas that of PV/T-PCM self-cleaning is 77.60%.

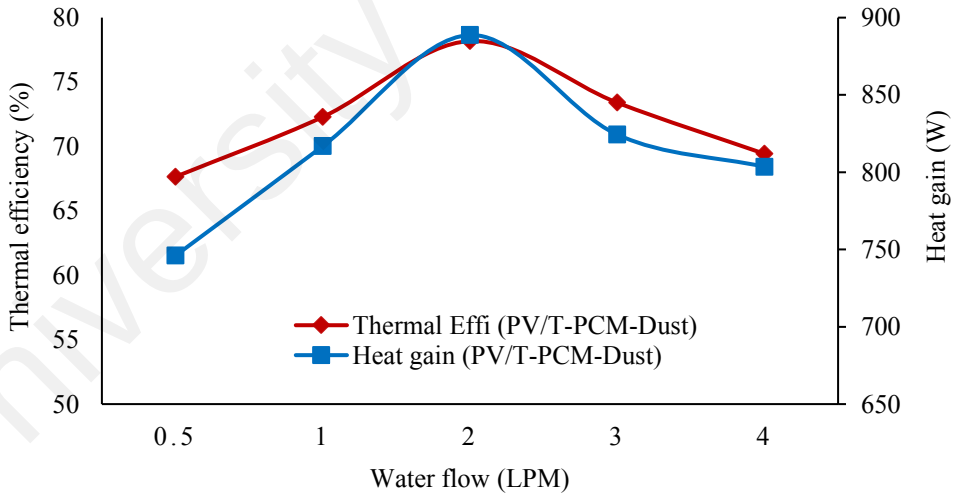

(a) PV/T-PCM-Dust collector thermal performance

Figure 4.43: Effect of water flow on thermal performance of PV/T-PCM-Dust and PV/T-PCM-SC collector

University of Malaya

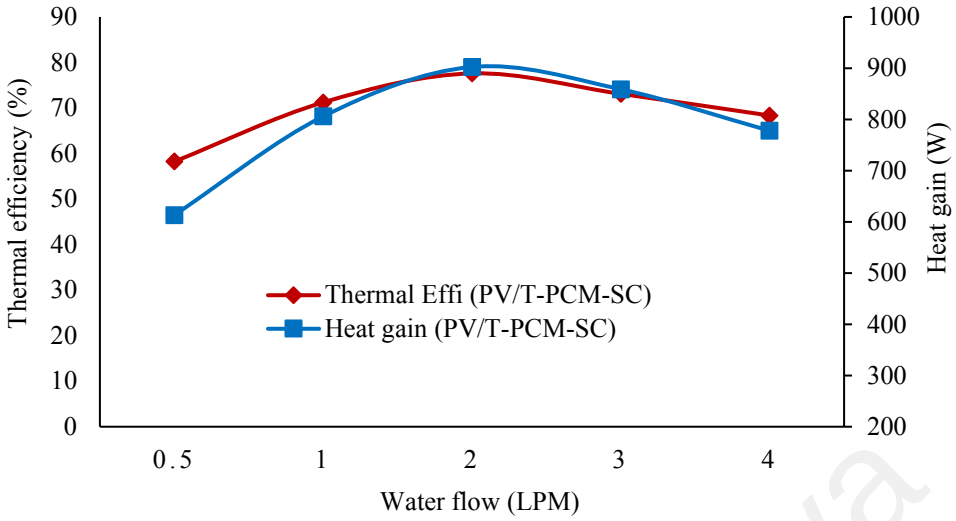

(b) PV/T-PCM-SC collector thermal performance

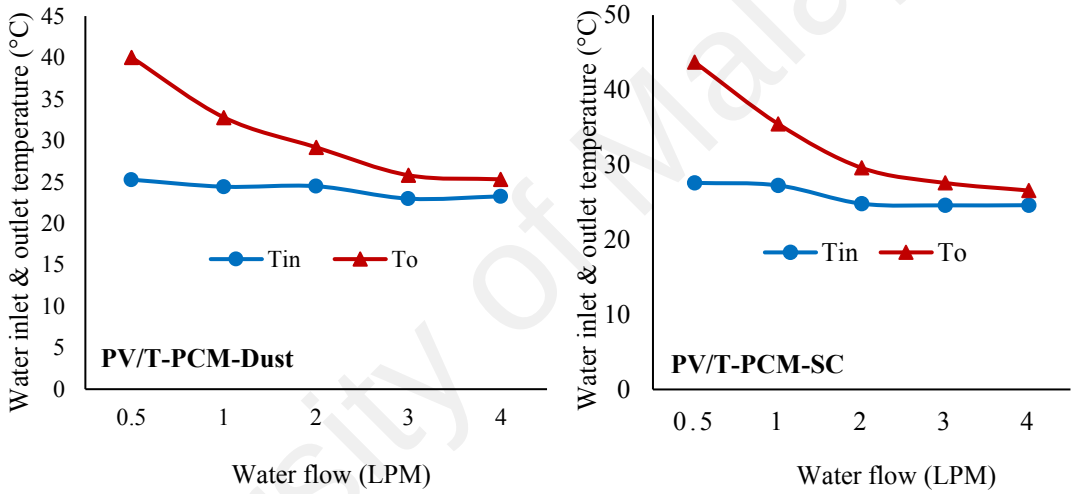

(c) (d)

Figure 4.43, continued

4.7 Effect on Exergy Performance

The effect of dust cleaning on the exergy performance of the PV/T-PCM system has been elaborated in this section as shown in Figure 4.44 (a) to (d). A comparative examination in Figure 4.44 (a) and (b) shows that a self-cleaning system markedly improves the exergy performance. While in the case of a dusty module, the highest exergy output obtained is 125.49 W, whereas a self-cleaning process helps to enhance it as high as 128.76 W, a 3.27% improvement in output. Higher exergy efficiencies have also been achieved by employing self-cleaning mechanism. The highest exergy efficiency obtained

University of Malaya

with dust covered PV/T-PCM module is 11.89%, whereas that with a self-cleaning PV/T-PCM module is 12.68%.

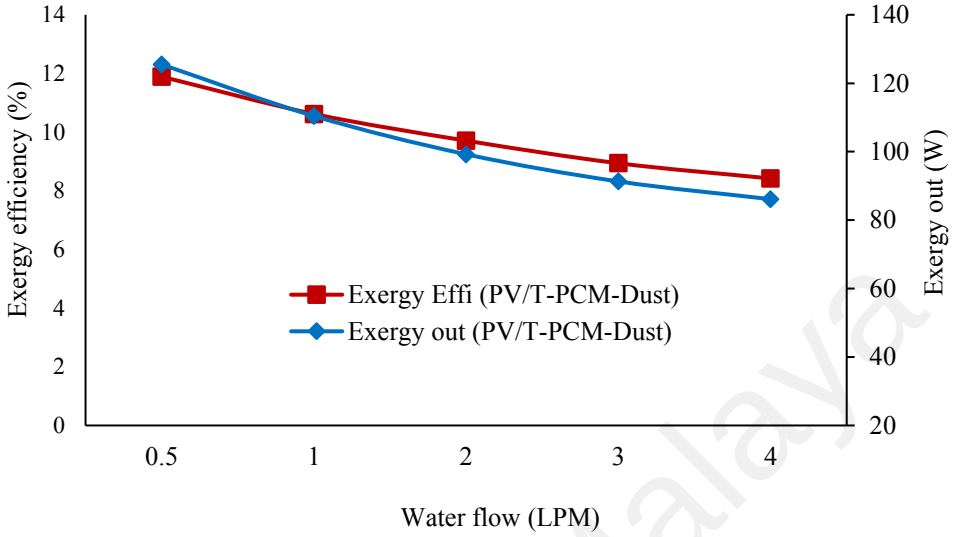

(a) PV/T-PCM-Dust collector exergy performance

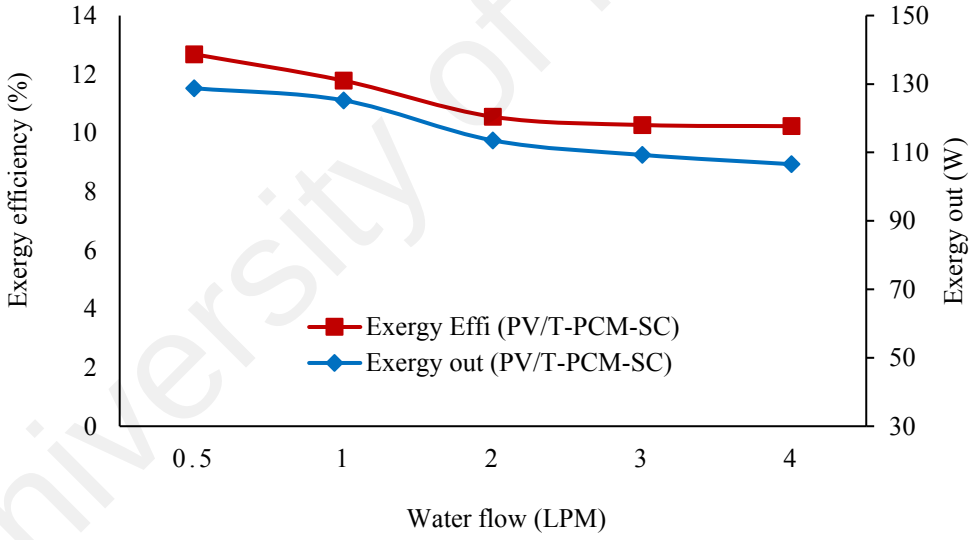

(b) PV/T-PCM-SC collector exergy performance

Figure 4.44: Effect of water flow on exergy performance of PV/T-PCM-Dust and PV/T-PCM-SC system

4.8 Comparative Performance Evaluation

In this section, the performances of a PV/T-only, a PV/T-PCM, and a PV/T-PCM modules with self-cleaning system have been presented in comparison with a reference PV performance so that a relative ranking among the devices is possible.

University of Malaya

Figure 4.45 shows the performance of a PV/T-only system against the reference PV performance. Both electrical and exergy efficiency of the PV/T are observed to be better than those of a PV system. While the maximum PV electrical efficiency obtained is 9.89%, at 4 LPM of water flow rate, the PV/T system offers almost 0.57% increase and delivers electricity with 10.46% efficiency. Exergy efficiency of the PV/T module is enhanced by almost 5.82% as compared to the PV module exergy efficiency. All the efficiency shows in figures 4.45 to 4.48 are instantaneous efficiency reflecting the on-the-spot values of that parameter.

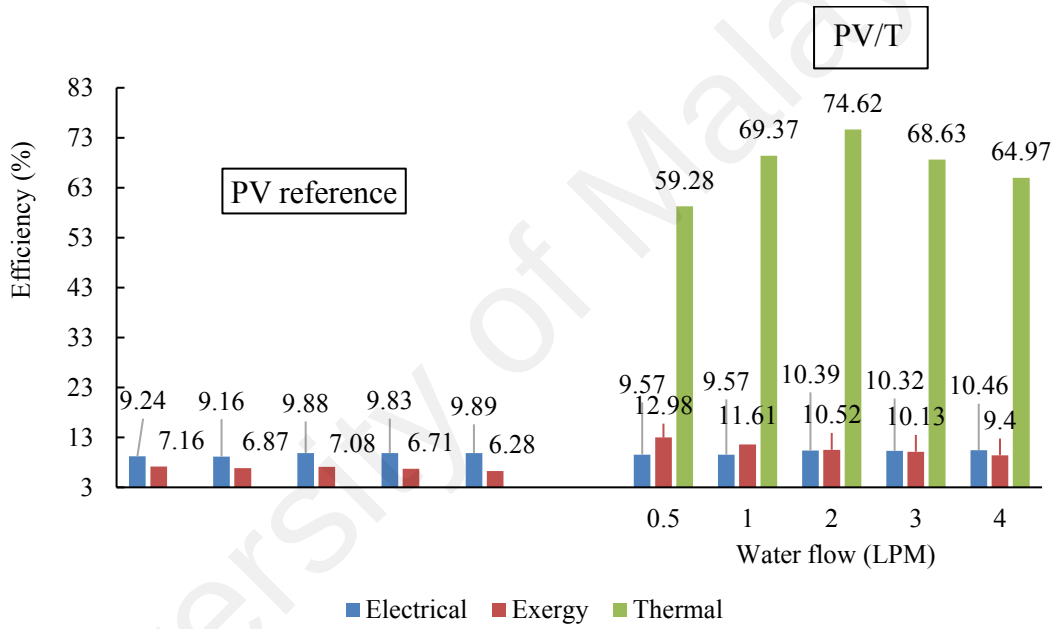

Figure 4.45: Energy and exergy efficiency comparesum performance of PV and PV/T for different mass flow rates

Exergy efficiency is calculated taking into account the exergy destruction from different sources, which is not considered in the calculation of thermal efficiency. That is why the exergy efficiency is very low compare to thermal efficiency. Comparative performance parameters of PV and PV/T systems are also given as in Table 4.5. It can be found from this table that an exergy output of 152.84 W for the PV/T module has improved by 71.66% as compared to 81.18 W from the PV module. The fact is that electrical exergy from a PV module operating alone is lesser than could be extracted from an integrated one because of a major loss of exergy as a result of irreversibility (Sudhakar

University of Malaya

& Srivastava, 2014). Normally, the exergy efficiency of the conventional silicon cell solar module is small as the output exergy is of low quantity. Large exergy losses occur inside the solar module (Sudhakar & Srivastava, 2014).

Table 4.5: Performance of electrical, thermal and exergy efficiency on PV and PV/T collector

Average	PV	PV/T (at optimum mass flow rate)
Electrical efficiency (%)	9.89	10.46
Thermal efficiency (%)	N/A	74.62
Exergy efficiency (%)	7.16	12.98
Exergy out (W)	81.18	152.84

Figure 4.46 shows the performance of the PV/T-PCM system in comparison with the reference PV performance in which 11.08% electrical efficiency of the PV/T-PCM is observed to increase by 1.20% as compared to the 9.88% PV electrical efficiency while the exergy efficiency of the PV/T-PCM is enhanced by more than 5% as compared to the PV exergy efficiency. From Table 4.6, it can be noticed that an exergy output of PV/T-PCM is increased by 58.89% as compared to the reference PV.

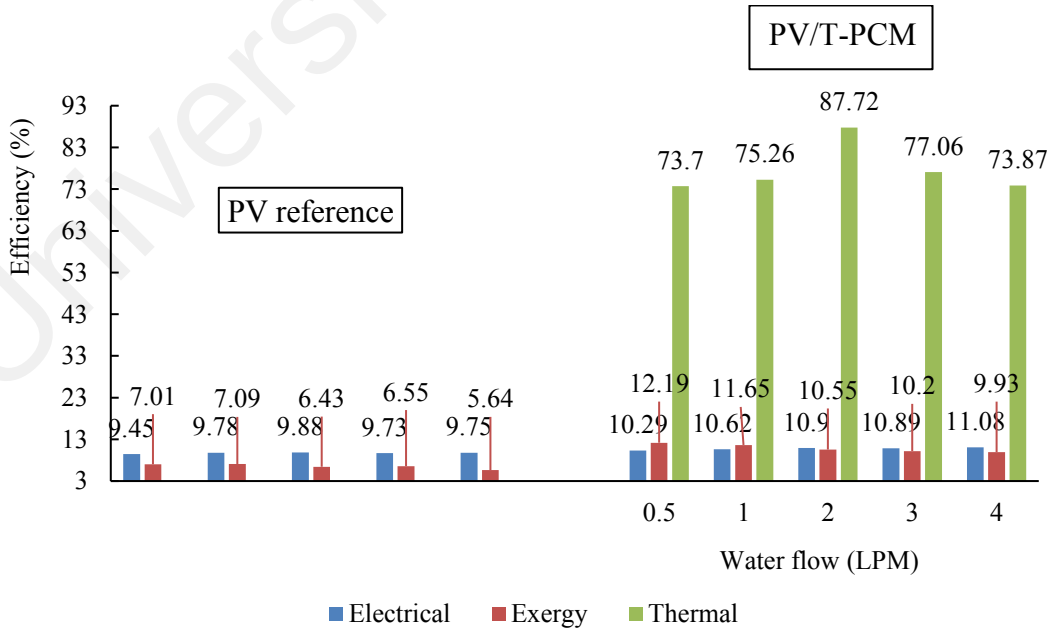

Figure 4.46: Energy and exergy efficiency comparesum performance of PV and PV/T-PCM for different mass flow rates

University of Malaya

Table 4.6: Performance of electrical, thermal and exergy efficiency on PV and PV/T-PCM collector

Average	PV	PV/T-PCM (at optimum mass flow rate)
Electrical efficiency (%)	9.75	11.08
Thermal efficiency (%)	N/A	87.72
Exergy efficiency (%)	7.01	12.19
Exergy out (W)	75.21	134.1

Figure 4.47 shows the performance of a dust covered PV/T-PCM system in comparison with the reference PV performance. The highest electrical efficiency of the dusty PV/T-PCM system is found to be 10.66%, whereas that of the reference PV is 9.85%. Likewise, the highest exergy efficiency of the dusty PV/T-PCM module obtained is 11.89% as compared to 9.11% exergy efficiency of the PV module. From Table 4.7, it can be noticed that the exergy output of the dusty PV/T-PCM module increased negligibly as compared to the reference PV.

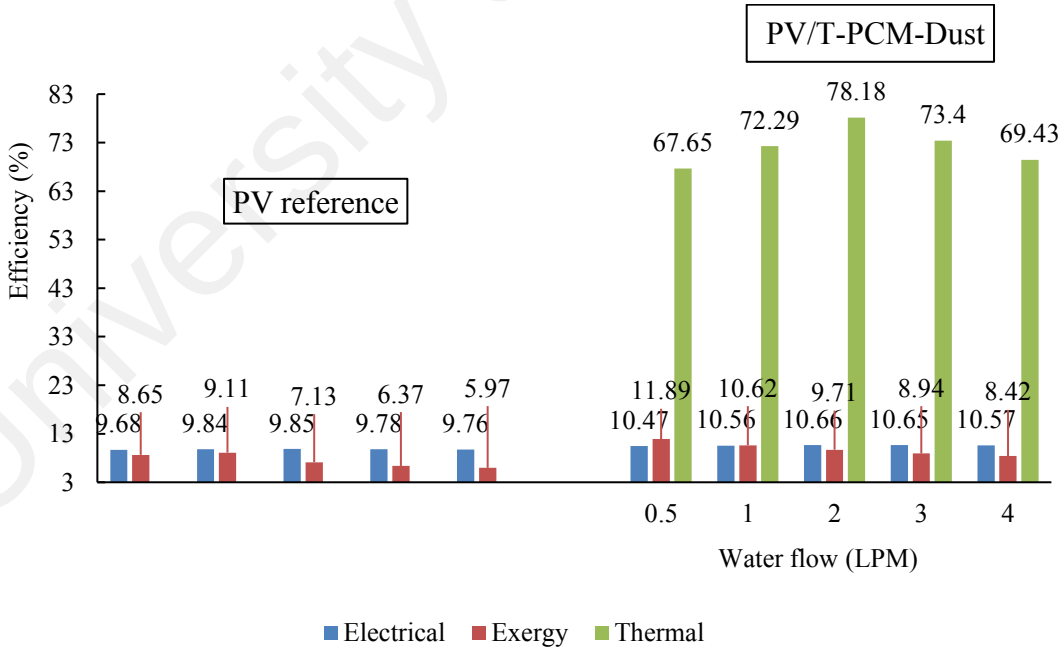

Figure 4.47: Energy and exergy efficiency comparesum performance of PV and PV/T-PCM-Dust for different mass flow rates

University of Malaya

Table 4.7: Performance of electrical, thermal and exergy efficiency on PV and PV/T-PCM-Dust

Average	PV	PV/T-PCM-Dust (at optimum mass flow rate)
Electrical efficiency (%)	9.85	10.66
Thermal efficiency (%)	N/A	78.18
Exergy efficiency (%)	8.65	11.89
Exergy out (W)	90.37	125.49

Figure 4.48 shows the performance of a PV/T-PCM module with a self-cleaning system in comparison with the reference PV performance. The maximum electrical efficiency of the self-cleaning PV/T-PCM module is found to be 11.91%, whereas the highest achievable PV electrical efficiency is 9.89%. Exergy efficiency of a PV/T-PCM with a self-cleaning system is enhanced by 3.99%, it can be noticed from Table 4.8 shows, that an appreciable increase in exergy is found to be 46.57 W.

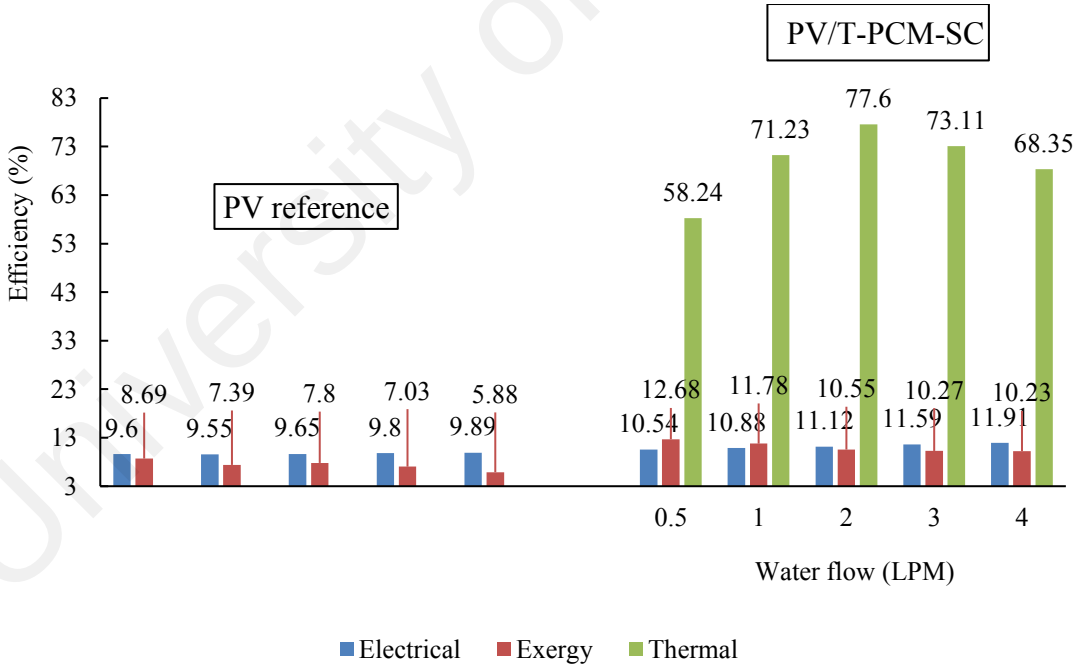

Figure 4.48: Energy and exergy efficiency comparesum performance of PV and PV/T-PCM-SC for different mass flow rates

University of Malaya

Table 4.8: Performance of electrical, thermal and exergy efficiency on PV and PV/T-PCM-SC collector

Average	PV	PV/T-PCM-SC (at optimum mass flow rate)
Electrical efficiency (%)	9.89	11.91
Thermal efficiency (%)	N/A	77.6
Exergy efficiency (%)	8.69	12.68
Exergy out (W)	82.19	128.76

Figure 4.49 shows the electrical efficiency improvement between a self-cleaning and a dusty PV/T-PCM modules at different water flow rates. It is clear that the module equipped with a self-cleaning system attains a higher electrical efficiency at higher water flow rates. The differences between the self-cleaning module and the dust covered module electrical efficiency are 0.07%, 0.32%, 0.46%, 0.94% and 1.34% at mass flow rates of 0.5, 1, 2, 3 and 4 LPM (lit/min), respectively.

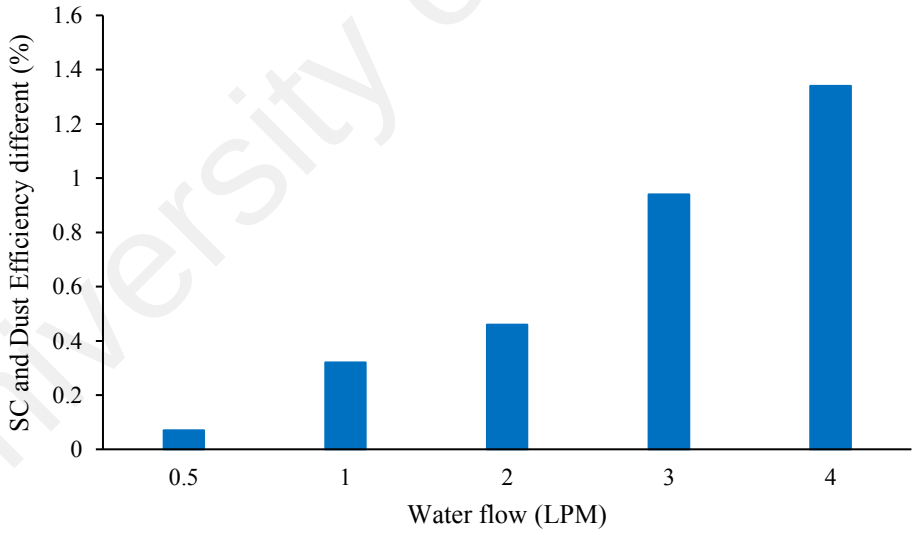

Figure 4.49: Improvement in electrical efficiency of PV/T-PCM system by using self cleaning mechanism as a function of the water flow rate

Table 4.9 gives a comparative picture of the optimum performances between the PV/T, PV/T-PCM, PV/T-PCM-Dust and PV/T-PCM-SC systems. The highest electrical efficiency of 11.91% was obtained by the PV/T-PCM with the self-cleaning system which yields the best thermal efficiency of 87.72%. On the other hand, the PV/T-only system

University of Malaya

delivers the highest exergy of 152.84 W. In order to get a maximum exergy efficiency, the PV module temperature should be controlled by surface cooling on the panel using water (Sudhakar & Srivastava, 2014).

Table 4.9: Optimum performance attained with PV/T, PV/T-PCM and PV/T-PCM with self-cleaning systems

Average	PV/T	PV/T-PCM	PV/T-PCM-Dust	PV/T-PCM-SC
	(At optimum mass flow rate)			
Electrical efficiency (%)	10.46	11.08	10.66	11.91
Thermal efficiency (%)	74.62	87.72	78.18	77.6
Exergy efficiency (%)	12.98	12.19	11.89	12.68
Exergy out (W)	152.84	134.1	125.49	128.76

4.8.1 Comparative Performance Assessment with Previous Studies

Table **4.10** shows comparative results of performance parameters of PV, PV/T, PV/T-PCM and PV/T-PCM-SC system obtained in the present investigation with those obtained in the previous researches. It can be noticed from the table that electrical performances attained with PV (9.89%) and PV/T (10.46%) in the current study agree well with the previous results. However, PV/T thermal performance with proposed system (with thermal efficiency of 74.62%) has improved from the previous studies. On the other hand, electrical efficiency of PV/T-PCM (11.08%) is comparable with those obtained in the previous studies. PV/T-PCM-SC system reached an electrical efficiency of 11.91% which is satisfactory.

Table 4.10: Comparative performance assessment of present research with previous studies

Systems	Electrical efficiency	Thermal efficiency	References
PV/T	6.98%	58.35%	(Yang et al., 2018)
PV/T-PCM	8.16%	70.34%	
PV/T	10.8%	62.37%	(Preet et al., 2017)
PV/T-PCM	13.3%	35.4%	
PV/T-PCM		40% to 50%	(Al Imam et al., 2016)

University of Malaya

Table 4.10, continued

PV	7.1% to		(Al-Waeli et al., 2017)
PV/T	9.92%	72%	
PV/T-PCM	12.32%		
PV	9.89%		**Present study**
PV/T	10.46	74.62%	
PV/T-PCM	11.08%	87.72%	
PV/T-PCM-SC	11.91%	77.6%	

4.9 Economic Analysis

An economic analysis mainly discusses the payback period of the system which can be separated into two parts, i.e., the first is the solar PV panel and the second is the PV/T system. Other results can be seen in Appendix C, which is the electrical water heater cost analysis. These results can project a clear understanding between the renewable and the nonrenewable economic performances. From equations (3.37), (3.39), (3.40) and (3.41), it is possible to forecast the results from the assumed years to draw a cash flow diagram for a solar PV panel system and to calculate the total cost on a period of 25 years lifespan. Data from Appendix B, Table B.2 are required to calculate the module's lifespan at 10% interest rates of the cash flow. This analysis used some assumed values to arrive at some pragmatic amount.

(A) Cash Flow diagram for solar PV panel as flows:

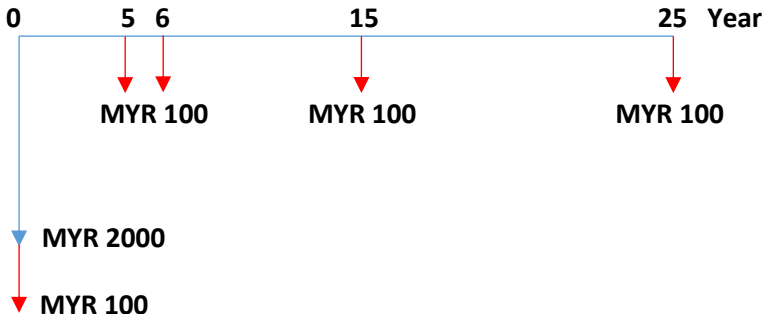

Figure 4.50: Solar PV panel cash flow diagram

University of Malaya

Figure 4.50 illustrates the cash flow diagram of a solar PV module from year 0 to year 25 with values and arrows showing the year and cost per 5-year period of MYR 100 (US$ 23.46). Zero is the initial year, thus, MYR 2000 (US$ 469.25) is the initial cost plus MYR 100 (US$ 23.46) as the installation cost. Whereas the annual running cost is zero. After 15 and 25 years later, MYR 100 (US$ 23.46) extra is added for some additional replacement of component parts.

Cost of using a solar PV panel:

For the first 5 years:

A.W) $_{\text{Solar PV}}$ = MYR -570.35 (US$ 133.82)

For the 6 years of usage:

A.W) $_{\text{Solar PV}}$ = MYR -495.13 (US$ 116.22)

For the 15 years of usage:

A.W) $_{\text{Solar PV}}$ = MYR –279.24 (US$ 65.51)

For the 25 years of usage:

It is assumed that by the 25th year the solar PV panel will again incur a cost of MYR 100 (US$ 23.46) for additional replacement of component parts: MYR –232.36 (US$ 54.51).

For annual benefit calculation, the average PV power output for 6 hours data has been taken form the experiment result. It is calculated, the 6 years cost benefit for PV panel is RM 524.25 (US$ 123.06), where cost of one unit (1 kWh) of electricity in Malaysia is MYR 0.3853 (Chua, 2018). From the equation (3.37), it is calculated, the payback period for PV panel is 6 years.

University of Malaya

(B) Cash Flow diagram for solar PV/T system as flows:

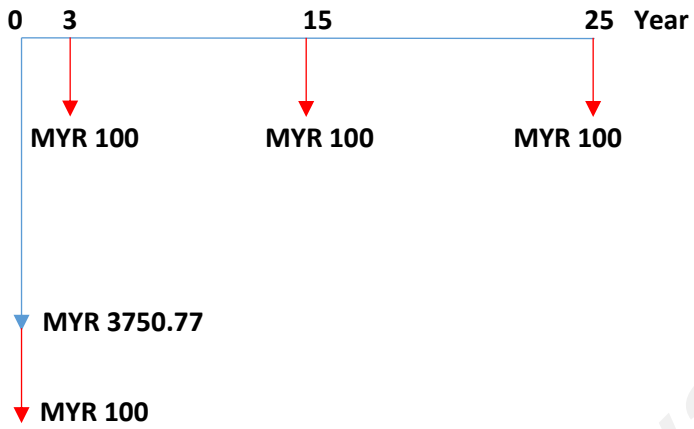

Figure 4.51: Solar PV/T water heating cash flow diagram

The thermal absorber cost is MYR 1750.77 (US$ 410.78). Figure 4.51 illustrates the cash flow diagram of a PV/T from year 0 to year 25 with values and arrows showing the year and cost per 15-year period of MYR 100 (US$ 23.46). From Appendix B, Table B.3, shows zero is the initial year, thus, MYR 3750.77 (US$ 880.09) is the initial cost plus MYR 100 (US$ 23.46) as the installation cost. Whereas the annual running cost is zero. After 25 years of service, a sum of MYR 100 (US$ 23.46) extra is added for some additional replacement of component parts.

Cost of running a solar PV/T system:

For the first 3 years of usage:

A.W) $_{\text{Solar PV/T}}$ = MYR -1578.66 (US$ 370.57)

For the 15 years:

A.W) $_{\text{Solar PV/T}}$ = MYR –509.42 (US$ 119.53)

For the 25th year:

It is assumed that at its 25th year, it will again incur a cost of MYR 100 (US$ 23.46) for additional replacement of component parts: MYR –425.24 (US$ 99.77)

University of Malaya

The negative values in both cases are the cost value for the solar PV and PV/T systems. For annual benefit calculation, the average PV/T power and heat gain for 6 hours data has been taken form the experiment result. The solar PV cost value is the reference value to compare between the solar PV/T system costs. According to the annual worth method, the payback period of the solar PV system will be after 6 years which means that after using the solar PV module for 5 years' service, it will become free of cost. The solar PV/T system cost is high compared to the solar PV but after 3 years later, the cost benefit value is MYR 2072.95 (US$ 486.60). The annual worth for the PV/T module is MYR 494.29. According to the Annual worth method, the payback period of the solar PV/T system will occur only after 3 years. The PV system takes 6 years because the thermal energy has been wasted.

(C) Cash Flow diagram for solar PV/T-PCM system as flows:

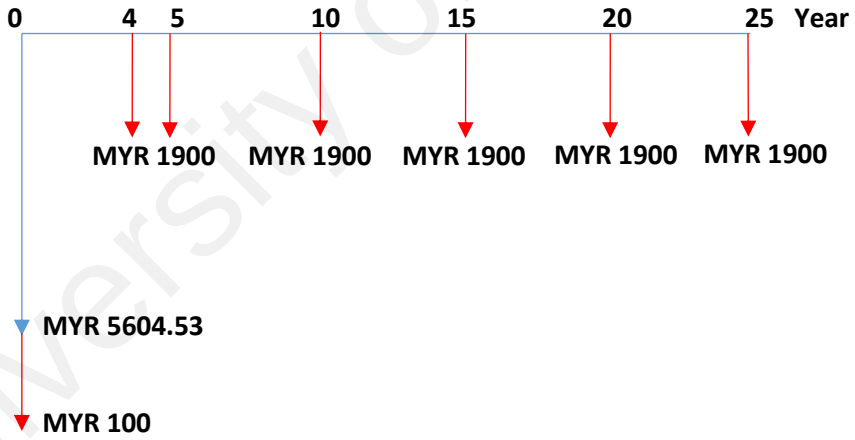

Figure 4.52: Solar PV/T having PCM cash flow diagram

The thermal absorber and PCM materials costs are MYR 1750.77 (US$ 410.22) and MYR 1853.76 (US$ 434.35), respectively. Figure 4.52 illustrates the cash flow diagram of a PCM from year 0 to year 25 with values and arrows showing the year and cost per 5-year period of MYR 1900 (US$ 445.22). From Appendix B, Table B.4, states that zero cost is encountered in the initial year, thus, MYR 5604.53 (US$ 1,313.29) is the initial cost plus MYR 1900 as the installation cost. Whereas the annual running cost is zero

University of Malaya

while the PCM materials 5 years later will need to be replaced costing MYR 1900 (US$ 445.22) extra which is added to the additional replacement of some component parts.

Cost of running a PV/T-PCM system:

For the first 4 years:

A.W) $_{\text{Solar PV/T-PCM}}$ = MYR -2209.00 (US$ 518.54)

For the 5 years:

A.W) $_{\text{Solar PV/T-PCM}}$ = MYR -1816.05 (US$ 434.35)

For the 10, 15, and 20-year period:

A.W) $_{\text{Solar PV/T-PCM}}$ = MYR -1047.60 (US$ 245.51) for 10-year period,

MYR –809.79 (US$ 189.77) for the 15-year period, and

MYR -703.22 (US$ 164.78) for the 20-year period.

For the 25th year period:

It is assumed that at its 25th year period, it will again incur a cost of MYR 1900 (US$ 445.22) for additional replacement of component parts: MYR –647.77 (US$ 151.78).

The negative values in both cases are the cost value for the solar PV and PV/T-PCM systems. For annual benefit calculation, the average PV/T-PCM power and heat gain for 6 hours data has been taken form the experiment result. The solar PV/T-PCM system cost is definitely high as compared to the solar PV system, but after 4 years of usage, the cost benefit value becomes MYR 3320.61 (US$ 779.48). The annual worth for the PV/T-PCM module is MYR 1111.61. That means the PV life cycle can be improved and used for a lower period. The result shows that the solar PV/T-PCM system can be used for a longer lifespan than the solar PV/T system.

University of Malaya

(D) Cash Flow diagram for solar PV/T-PCM-SC system as flows:

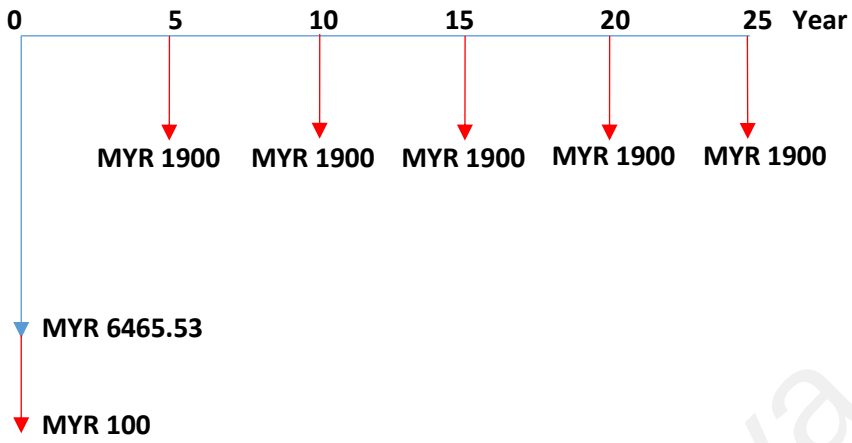

Figure 4.53: Solar PV/T having PCM and self-cleaning cash flow diagram

The thermal absorber, PCM materials and self-cleaning costs are MYR 1750.77 (US$ 410.36), MYR 1853.76 (US$ 434.42) and MYR 861 (US$ 201.77). Figure 4.53 illustrates the cash flow diagram of a PCM from year 0 to year 25 with values and arrows showing the year and cost per 5-year period for MYR 1900 (US$ 445.34). From Appendix B, Table B.4, states that zero running cost is in the initial year, thus, MYR 6465.53 (US$ 1,515.46) is the initial cost plus MYR 1900 (US$ 445.34) as the installation cost. Whereas the annual running cost is zero. Because the PCM materials over the next 5 years need to be replaced, MYR 1900 (US$ 445.34) extra is added for some additional replacements of component parts.

Cost of running a PV/T-PCM-SC system:

For the first 5 years:

A.W) $_{\text{Solar PV/T-PCM-SC}}$ = MYR -2043.18 (US$ 478.90)

For the 10th, 15th, and 20th years:

A.W) $_{\text{Solar PV/T-PCM-SC}}$ = MYR -1187.72 (US$ 278.39) for the 10-year period,

MYR -922.99 (US$ 216.34) for the 15-yer period, and

MYR -804.35 (US$ 188.53) for the 20-year period

University of Malaya

For the 25th year:

It is assumed that in its 25th year of service, the PV/T-PCM-SC system will again incur a cost of MYR 1900 (US$ 445.34) for additional replacements of component parts: MYR -742.63 (US$ 174.06).

The negative values in both cases are the costs of the solar PV and the PV/T-PCM-SC system. The solar PV/T-PCM-SC system cost is definitely high as compared to the solar PV system but after 5 years later, the cost benefit will be MYR 3842.78 (US$ 902.06). With this system, the solar PV panel life cycle can be improved and used for a longer period of useful service. The result shows that the solar PV/T-PCM with the self-cleaning system can be used for a longer useful period than solar the PV and PV/T systems.

The annual worth for the PV/T-PCM module with the self-cleaning system is MYR 1799.60 for a lifespan of 5 years. On the other hand, the annual worth for an electric water supply module is MYR 501.67 for the same period. The difference in the annual worth will be justified by the ecological environmental advantage on less emission carbon dioxide, hence, less carbon tax imposed on the PV/T-PCM with the self-cleaning system. Moreover, PV/T-PCM module with the self-cleaning system will require almost zero maintenance cost up to 4 to 5 years run, while the electric water heater will consume a substantial amount of maintenance cost over that period.

University of Malaya

CHAPTER 5: CONCLUSIONS AND RECOMMENDATIONS

5.1 Introduction

The present research was to investigate the performance of a newly developed PV/T-PCM module with a self-cleaning system and compare with PV and PV/T module under the same operating conditions. Energy, exergy and economic analyses have been carried our based on the total performance of the system. Comparative analyses shows that the overall performance of a PV/T-PCM module with a self-cleaning system is better than that of PV/T, PV/T-PCM and PV. The key findings are enumerated in following sections.

5.1.1 PV vs PV/T Performance

- The highest PV/T electrical power output of 149.72 W is attained with a flow rate of 0.5 LPM which is 5.34% higher than that of reference PV module. On the other hand, the maximum electrical efficiency of 14.25% is obtained with 3 LPM, which is about 3.6% higher that of the reference PV.
- For every 100 W/m^2 increase in irradiation level, PV/T power output escalates by 11.95 W at mass flow rate of 4 LPM, while electrical efficiency drops by 0.80%.
- The average cell temperature of PV/T is found to be 58.23°C at 4 LPM, which is 3.92°C lower than that of reference PV.
- For every 1°C decrease in cell temperature, the PV/T output power increases by 3.49 W and the efficiency increases by 0.23%.
- The maximum PV/T thermal efficiency is 74.62% with a mass flow rate of 2 LPM, while the highest rise in the outlet water temperature is 28.23°C at 0.5 LPM.
- The maximum PV/T exergy output of 152.84 W and the maximum average exergy efficiency of 12.98% is obtained at a mass flow rate of 0.5.

University of Malaya

It can be concluded that electrical performance of PV/T system much better than reference PV. However, PV/T system provides thermal energy, which adds an extra value to the hybrid system.

5.1.2 PV vs PV/T-PCM Performance

- For PV/T-PCM system, both the maximum electrical power output and the maximum efficiency are obtained at 4 LPM.
- The maximum power output is 160.29 W, which is almost 14% higher than that of the reference PV module
- The maximum electrical efficiency is 14.42%, which is 4.72% higher than that of the reference PV.
- For every 100 W/m^2 increase in irradiation level, PV/T-PCM power output increases by 13.12 W at mass flow rate of 4 LPM, while electrical efficiency drops by 0.55%.
- The average cell temperature of PV/T is found to be 55.43°C, which is about 5.34°C at 4 LPM, which is lower than that of reference PV.
- Every 1°C decrease in PV/T-PCM cell temperature is followed by an increases in output power by 8.76 W and electrical efficiency by 0.37%.
- The maximum PV/T-PCM thermal efficiency is 87.72% with a mass flow rate of 2 LPM, while the highest rise obtained is 26.40°C at 0.5 LPM.
- The maximum PV/T-PCM exergy output of 134.10 W is attained at 0.5 LPM and the maximum average exergy efficiency of 12.19% is obtained at a mass flow rate of 1 LPM.
- It can be concluded that the PV/T-PCM thermal efficiency is found better than that of the PV/T-only system. At 2 LPM, the average maximum thermal efficiency

University of Malaya

of PV/T-only system is 74.62%, while that of the PV/T-PCM is 87.72% - a 17.55% enhancement achieved.

It can be concluded that the electrical performance of PV/T-PCM system much better than PV/T and reference PV.

5.1.3 Performance of PV/T-PCM with Self-cleaning System

- At a mass flow rate of 4 LPM, electrical power output of the PV/T-PCM system with dust on the panel is 143.28 W, whereas PV/T-PCM module with a self-cleaning system produces 182.74 W under the same irradiation.
- At 4 LPM, average electrical efficiency of PV/T-PCM module with dust on the panel is 10.66%, whereas that of the PV/T-PCM module with a self-cleaning system is 11.91%.
- The maximum average electrical efficiency improvement due to self-cleaning is 2.02%.
- At 4 LPM, the average cell temperature of PV/T-PCM module is 55.36°C with dust on the panel, whereas that of the PV/T-PCM module with a self-cleaning is 54.36°C. That is, a 1°C drop in cell temperature has been achieved with self-cleaning.
- The highest electrical power obtained with PV/T-PCM module with self-cleaning is 182.74 W, which is almost 19% higher than that with dusty panel.
- The maximum electrical efficiency of PV/T-PCM module with self-cleaning 15.60%, which is about 5.2% higher than that of dust covered module.
- The maximum rise in the outlet water temperature of PV/T-PCM module with self-cleaning is 23.18°C at 0.5 LPM.
- The exergy output of the PV/T-PCM module with the self-cleaning system is 128.76 at 0.5 LPM, which is a 2.6% better than a dusty panel.

University of Malaya

- The exergy efficiency of the PV/T-PCM module with self-cleaning mechanism is 12.68%, which is a 6.64% more than that with dust covered panel.

It can be concluded that overall electrical performance of PV/T-PCM with a self-cleaning system much better than PV/T, PV/T-PCM and reference PV. However, the thermal performance is slightly lower which may be due to the cooling effect from self-cleaning system.

5.1.4 Economic Analysis

The economic viability was determined through a cost analysis for the whole system according to the Malaysian market response as compared to other systems in which the cost of the solar radiation collector was found to be relatively cheap. The initial investment was not so burdensome while its usage for the balance of its useful life would be free of charge as was proven through the cost analysis as fully described in Chapter 4. The total cost of a solar hot water heater was much cheaper when compared with that of an electric water heater, hence, some important salient points worthy of consideration are as summarized below:

- The breakdown cost of a solar PV module is RM 2000 (US$ 469.25) which is expensive but because of its long-term uses, it will be free of maintenance costs as based on the Annual-worth methods from 5 to 6 years later.
- A PV/T system costs approximately MYR 3750.77 (US$ 880.09) which can be free of cost after 3 years later.
- A phase change material costs approximately MYR 5604.53 (US$ 1,313.29) which is considered as a high investment cost but which can be free of maintenance costs after usage of up to 4 years. PCM materials need to change every 5 or 6 years later which means that one time investment can last at least up to 5 years. If the system cost together with the installation cost come around MYR

University of Malaya

1900 (US$ 445.22), and after usage of up to 4 years as based on the Annual-worth methods, then the cost benefit will be MYR 3320.61 (US$ 779.48).

- The results of calculations on the cost analyses show that the solar PV/T and the PV/PCM systems are more economical and become more attractive than the solar PV system operating alone in the long run, thus, it is advantageous for the household family to use the solar water heater which can last up to a period of at least 5 years.
- Subsequently, more household families should be encouraged to install the solar PV/T systems in order to enjoy the long-term economic benefits as well as the clean environment-friendly ecosystem.

5.2 Contribution of the Present Research

In the present research, three systems PV/T, PV/T-PCM and PV/T-PCM-SC overall electrical and thermal performance has been compared each other and with a reference PV panel. A solar PV/T-PCM module with self-cleaning systems has been developed which can advantage to get better electrical performance. This work has a three-fold contribution that are innovative and effective to improve the systems' performances as well. Firstly, the thermal collector is a unique double serpentine pipe flow channel which extracts a maximum heat energy from the PV module. The thermal absorber tube has an orientation band which assistance of water flow redirection. So that the mass flow of water can absorb and remove heat from the panel rear side. Normally, a single PV panel absorbs thermal energy from the solar radiation and that causes the electrical performance is lower than STC condition. Secondly, the use of phase change materials (PCM) in the PV/T collectors, as an intermediate thermal storage media, offers a promising solution to the panel heating problem by storing a larger amount of heat. This technology can help to improve the electrical as well as thermal performance. And thirdly, the innovative contribution is the integration of the PV glass cover with a self-cleaning mechanism

University of Malaya

which can ensure a better transmission of solar irradiation allowing more heat energy to be usefully intercepted.

5.3 Recommendations for Future Work

In the present study the focus was on the realizable scientific means to find the best feasible method for cleaning PV/T module top glass surface along with developing a better thermal storage for extended operation at the cheapest expense. This has been achieved through a self-cleaning mechanism and the application of suitable PCM in PV/T. This newly designed PV/T-PCM with self-cleaning system can be used in isolated rooftop household or commercial installations, which will not only cut down energy usage from the grid but also ensure longer module life. The self-cleaning mechanism can be employed in large scale to clean PV array in big solar power plants. Although the proposed system achieved better performance than PV, conventional PV/T and PV/T-PCM systems self-cleaning system can be improved with new circuitry and control so that the cleaning process will smoothly operate on the PV panel.

Following points should be considered and envisaged in future research:

- The absorber pipe design should be changeable and interchangeable with one another so as to enhance and facilitate future possible challenging work in a new design in such a way that the back panel temperature can be considerably decreased to ease the panel to convert more electrical power.
- In this study, the fluid used is water and the system can still be active without the use of a heat exchanger, hence, nano-particles in the water can be employed that can increase the performance of the heat exchanger.
- The new feature in the solar PV/T exchanger is the automatic activation to run the water pump. It is possible to obtain electricity from the solar PV panel itself but

University of Malaya

the pump controller circuit should be suitably modified, i.e., a change in the system and configuration of the microcontroller IC.

- It is also possible to use a solar tracker to detect the maximum solar radiation and temperature to maximize the resultant effect on the collector.

University of Malaya

LIST OF PUBLICATIONS

Publication in ISI indexed journals:

Pandey, A.K., Hossain, M.S., Tyagi, V.V., Selvaraj, J., Rahim, N.A. (2018) Novel Approaches and Recent Developments on Potential Applications of Phase Change Materials in Solar Energy. Renewable and Sustainable Energy Reviews. 82(1): 81-323

Hossain, M.S., Pandey, A.K., Tunio, M.A., Selvaraj, J., Rahim N.A. (2016). Thermal and economic analysis of low-cost modified flat-plate solar water heater with parallel two-side serpentine flow. Journal of thermal analysis and calorimetry. 123(1): 793-806

Hossain, M.S., Madlool, N.A., Rahim, N.A., Selvaraj, J., Pandey, A.K., Khan, A.F. (2016). Role of smart grid in renewable energy: An overview. Renewable and Sustainable Energy Reviews, 60: 1168–1184.

Proceeding of journal:

Hossain, M.S., Abbas, A.W., Selvaraj, J., Ferdous, Rahim, N.A. (2014). Experiment of a flat plate solar water heater collector with modified design and thermal performance analysis, Applied Mechanics and Materials Vol 624, pp 332-338

Conference papers:

Hossain, M.S., Rahim N.A., Selvaraj, J., Pandey, A.K. (2016) Application of ANOVA Method to Study Solar Energy for Hydrogen Production. Advances in Functional Materials Conference 2016, ICC, Jeju Island, South Korea. Mon, Aug 8 - Thu, Aug 11, 2016.

Selvaraj, J., Hossain, M.S., Rahim, N.A., Pandey, A.K. (2015). Application of ANOVA method to study statistical modeling for hydrogen production using wind energy. International Conference on Power, Energy and Communication Systems, IPECS 2015. Malaysia.

Hossain, M.S., Abbas, A.W., Selvaraj, J., Ferdous, Rahim, N.A. (2014). Experiment of a flat plate solar water heater collector with modified design and thermal performance analysis, International Conference on Mechatronics, Materials and Manufacturing (ICMMM 2014), August 2-4, 2014, Chengdu, China (Best presentation award).

Hossain, M.S., (2014) presenter, 3rd IET International Conference on Clean Energy and Technology (CEAT 2014), 24th to 26th November 2014. CEAT 2014 Sarawak, Malaaysia.

Hossain, M.S., Rahim, N.A., Selvaraj, J., Pandey, A.K. (2017) Energetic evaluation of Photovoltaic and hybrid photovoltaic/thermal (PV/T) systems. Postgraduate research on

University of Malaya

Energy (PRoE) Symposium 2017. 6 & 7 September 2017 (Wednesday & Thursday) Rooftop Garden, (level 5) Hotel Sentral, Kuala Lumpur.

Hossain, M.S., Abdul Malek, A.B.M., Selvaraj, J., Rahim, N.A. (2014) Thermal performance of flat plate solar water heater collector with modified circulating pipe absorber. The 2nd Power and energy conversion symposium (PECS 2014) Melaka, Malaysia. 12 May 2014.

Book chapters:

Hossain, M. S., Pandey, A. K., Tunio, M. A., Selvaraj, J., Rahim, N. A. (2017). The Hybrid Solar Power/Wind System for Energy Production, Observation, Application, and Simulation, Clean Energy for Sustainable Development, 1st Edition, Chapter 10, and Publisher: Elsevier, Editors: Mohammad Rasul. 337-368.

Rahim, N.A., Selvaraj, J., Hossain, M.S, Pandey, A.K. (2016). Emerging Energy Alternatives for Sustainable Development in Malaysia, Emerging Energy Alternatives for Sustainable Environment, Chapter: 4, Publisher: TERI Press, Editors: D P Singh, Richa Kothari and V V Tyagi.75-97.

University of Malaya

REFERENCES

Abhat, A. (1983). Low temperature latent thermal energy storage system: heat storage materials. *Sol Energy, 30*, 313–332.

About, c. (2012). Conversion Efficiency of a PV Cell, http://inventors.about.com/od/pstartinventions/ss/photovoltic_cel_9.htm.

Abrahamyan, Y. A., Serago, V. I., Aroutiounian, V. M., Anisimova, I. D., Stafeev, V. I., Karamian, G. G., . . . Mouradyan, A. A. (2002). The efficiency of solar cells immersed in liquid dielectrics. *Solar Energy Materials and Solar Cells, 73*, 367–375.

Adham, M., Sidding, O., & Hisham, S. (2015). Advancements in hybrid photovoltaic systems for enhances solar cells performance. *Renewable and Sustainable Energy Reviews, 41* 658-684.

Adnan, I., Othman, M. Y., Ruslan, M. H., Alghoul, M. A., Yahya, M., Zaharim, A., & Sopian, K. (2009). Performance of Photovoltaic Thermal Collector (PVT) With Different Absorbers Design. ISSN: 1790-5079. *Wseas Transactions on Environment and Development, 5*(3), 321-330.

AEO. (2017). Annual Energy Outlook 2017, www.eia.gov/aeo. *U.S. Energy Information Administration*.

Agarwal, A., & Sarviya, R. M. (2016). An experimental investigation of shell and tube latent heat storage for solar dryer using paraffin wax as heat storage material. *Engineering Science and Technology, an International Journal, 19* 619–631.

Agarwal, R. K., & Garg, H. P. (1994). Study of a photovoltaic-thermal system—thermosyphonic solar water heater combined with solar cells. *Energy Convers Manage, 35* (7), 605–620.

Agyenim, F., Hewitt, N., Eames, P., & Smyth, M. (2010). A review of materials, heat transfer and phase change problem formulation for latent heat thermal energy storage systems (LHTESS). *Renewable and Sustainable Energy Reviews, 14*(2), 615-628.

Ahmed, D. Z., Hussein, A. K., Sopian, K., Alghoul, M. A., & Chaichan, M. T. (2013a). Impact of Some Environmental Variables with Dust on Solar Photovoltaic (PV) Performance: Review and Research Status. *International Journal pf energy and environment, 7*(4), 152-159.

University of Malaya

Ahmed, O. K., & Mohammed, Z. A. (2017). Influence of porous media on the performance of hybrid PV/Thermal collector. *Renewable Energy, 112*, 378-387.

Ahmed, Z., Hussein, A. K., & Sopiana, K. (2013b). Effect of Dust on Photovoltaic Performance: Review and Research Status. http://www.wseas.us/e-library/conferences/2013/Malaysia/RESEN/RESEN-32.pdf. *Renewable Energy and Environmental Informatics*, 193-199.

Akbarzadeh, A., & Wadowski, T. (1996). Heat pipe-based cooling systems for photovoltaic cells under concentrated solar radiation. *Applied Thermal Engineering, 16*, 81 -87.

Akeiber, H., Nejat, P., Majid, M. Z. A., Wahid, M. A., Jomehzadeh, F., Zeynali Famileh, I., . . . Zaki, S. A. (2016). A review on phase change material (PCM) for sustainable passive cooling in building envelopes. *Renewable and Sustainable Energy Reviews, 60*, 1470-1497.

Al Imam, M. F. I., Beg, R. A., Rahman, M. S., & Khan, M. Z. H. (2016). Performance of PVT solar collector with compound parabolic concentrator and phase change materials. *Energy and Buildings, 113,* 139-144.

Al-Hasan, A. Y., & Ghoneim, A. A. (2005). A new correlation between photovoltaic panel's efficiency and amount of sand dust accumulated on their surface. *Int J Sustain Energy, 24*, 187–197.

Al-Hinti, I., Al-Ghandoor, A., Maaly, A., Abu Naqeera, I., Al-Khateeb, Z., & Al-Sheikh, O. (2010). Experimental investigation on the use of water-phase change material storage in conventional solar water heating systems. *Energy Conversion and Management, 51*(8), 1735-1740.

Al-Shamani, A. N., Yazdi, M. H., Alghoul, M. A., Abed, A. M., Ruslan, M. H., Mat, S., & Sopian, K. (2014). Nanofluids for improved efficiency in cooling solar collectors – A review. *Renewable and Sustainable Energy Reviews, 38*, 348-367.

Al-Waeli, A. H. A., Sopian, K., Chaichan, M. T., Kazem, H. A., Ibrahim, A., Mat, S., & Ruslan, M. H. (2017). Evaluation of the nanofluid and nano-PCM based photovoltaic thermal (PVT) system: An experimental study. *Energy Conversion and Management, 151,* 693-708.

Alhamdan, A. M., & Al-Helal, I. M. (2009). Effect of arid environment on radiative properties of greenhouse polyethylene cover *Sol Energy, 83*, 790–798.

University of Malaya

Ali, B., Sopian, K., Ghoul, M. A., Othman, M. Y., Zaharim, A., & Mahir Razali, A. (2009). Economics of Domestic Solar Hot Water Heating Systems in Malaysia. *European Journal of Scientific Research, 26*(1), 20-28.

Alibaba.com. (2018). Professional 1260 high quality heat resistant isolation ceramic fiber paper, Access data 30/05/2018, https://www.alibaba.com/product-detail/Professional-1260-high-quality-heat-resistant_60795372079.html?spm=a2700.7724838.2017115.31.77177184oEnK6z&s=p. *Website*.

Ammar, A. M. A.-T., Megat, M. H., Kamaruzzaman, S., & Wahab, M. A. (2009). An Economical Analysis for a Stratified Integrated Solar Water Heater with a Triangular Shape. *Journal for the advancement of science & arts, 1*, 17-28.

Ammari, H. D., & Nimir, Y. L. (2003). Experimental and theoretical evaluation of the performance of a tar solar water heater. *Energy Conversion and Management, 44*(19), 3037-3055.

Artmann, N., Manz, H., & Heiselberg, P. (2007). Climatic potential for passive cooling of buildings by night-time ventilation in Europe. *Applied Energy, 84*, 187–201.

Barzin, R., Chen, J. J. J., Young, B. R., & Farid, M. M. (2015). Application of PCM underfloor heating in combination with PCM wallboards for space heating using price based control system. *Applied Energy, 148*, 39–48.

Bayón, R., Rojas, E., Valenzuela, L., Zarza, E., & León, J. (2010). Analysis of the experimental behaviour of a 100 kWth latent heat storage system for direct steam generation in solar thermal power plants. *Applied Thermal Engineering, 30*(17–18), 2643-2651.

Beckmann, G., & Gill, P. V. (1984). Thermal energy storage: basics–design–applications to power generation and heat supply (course in mathematical physics). *Berlin: Springer*.

Bhargava, A. K., Garg, H. P., & Agarwal, R. K. (1991). Study of a hybrid solar system–solar air heater combined with solar cell. *Sol Energy, 31*(5), 471–479.

Bianchini, A., Guzzini, A., Pellegrini, M., & Saccani, C. (2017). Photovoltaic/thermal (PV/T) solar system: Experimental measurements, performance analysis and economic assessment. *Renewable Energy, 111*, 543-555.

Biswas, K., & Abhari, R. (2014). Low-cost phase change material as an energy storage medium in building envelopes: Experimental and numerical analyses. *Energy Conversion and Management, 88*, 1020–1031.

University of Malaya

Bouadila, S., Fteïti, M., Oueslati, M. M., Guizani, A., & Farhat, A. (2014). Enhancement of latent heat storage in a rectangular cavity: Solar water heater case study. *Energy Conversion and Management, 78*, 904-912.

Braunstein, A., & Kornfeld, A. (1986). On the development of the solar photovoltaic and thermal (PVT) collector. *IEEE Trans Energy Convers, EC-1*(4), 31–33.

Carlqvist, A. (2009). Overview of concentrating solar power for electricity production, with emphasis on steam turbine aspects. <http://www.diva-portal.org/smash/record.jsf?pid= diva2:501936>. *Website*.

Carrillo, J. M., Martínez-Moreno, F., Lorenzo, C., & Lorenzo, E. (2017). Uncertainties on the outdoor characterization of PV modules and the calibration of reference modules. *Solar Energy, 155*(Supplement C), 880-892.

Ceylan, I. (2012). Energy and exergy analyses of a temperature controlled solar water heater. *Energy and Buildings, 47*, 630-635.

Chaabane, M., Mhiri, H., & Bournot, P. (2014). Thermal performance of an integrated collector storage solar water heater (ICSSWH) with phase change materials (PCM). *Energy Conversion and Management, 78*, 897-903.

Chaichan, M. T., & Kazem, H. A. (2015). Water solar distiller productivity enhancement using concentrating solar water heater and phase change material (PCM). *Case Studies in Thermal Engineering, 5*, 151-159.

Chandrashekhar, V. (2017). Pollution cuts soalr yiels by 25%. *The times of India (Web news)*.

Chen, B.-R., Chang, Y.-W., Lee, W.-S., & Chen, S.-L. (2009). Long-term thermal performance of a two-phase thermosyphon solar water heater. *Solar Energy, 83*(7), 1048-1055.

Chong, K. K., Chay, K. G., & Chin, K. H. (2012). Study of a solar water heater using stationary V-trough collector. *Renewable Energy, 39*(1), 207-215.

Chow, T. T. (2010). A review on photovoltaic/thermal hybrid solar technology. *Applied Energy, 87*, 365–379.

Chua, J. (2018). Malaysia Has One Of The Lowest Domestic Electricity Prices In The World. http://www.rojakdaily.com/news/article/4384/malaysia-has-one-of-the-lowest-domestic-electricity-prices-in-the-world. *Website*.

University of Malaya

Country Solar NT. (2016). Solar Panel Cleaning, http://www.countrysolarnt.com.au/2016/02/dont-set-and-forget-your-solar-system/. *Website*.

Cox, I. C., & Raghuraman, P. (1985). Design considerations for flat-plate photovoltaic/ thermal collectors. *Sol Energy, 35*, 227-241.

Crossley, R. (2015). 5 Robots that are Revolutionizing How We Clean Solar Panels. https://www.revolvesolar.com/5-robots-that-are-revolutionizing-how-we-clean-solar-panels/. *Website*.

de Vries, D. (1998). Design of a photovoltaic/thermal combi-panel. *Ph.D. Thesis, Eindhoven Technical University, Netherland*.

Deb, S. K. (2000). Recent Developments in High-Efficiency PV Cells. *National Renewable Energy Laboratory*.

Dengfeng, D., Darkwa, J., & Kokogiannakis, G. (2013). Thermal management systems for Photovoltaics (PV) installations: A critical review *Solar Energy, 97* 238–254.

Dincer, I., & Rosen, M. A. (2002). Thermal energy storage, Systems and Applications, John Wiley & Sons *Chichester (England)*.

Domanski, R., & Fellah, G. (1996). Exergy analysis for the evaluation of a thermal storage system employing PCMS with different melting temperatures. *Appl. Therm. Eng, 16*, 907-919.

Dubey, S., Solanki, S. C., & Tiwari, A. (2009). Energy and exergy analysis of PV/T air collectors connected in series. *Energy and Buildings, 41*(8), 863-870.

Dubey, S., & Tiwari, G. N. (2008). Thermal modeling of a combined system of photovoltaic thermal (PV/T) solar water heater. *Solar Energy, 82*(7), 602-612.

Dursun, B. (2012). Determination of the optimum hybrid renewable power generating systems for Kavakli campus of Kirklareli University, Turkey, . *Renewable and Sustainable Energy Reviews, 16*, 6183-6190.

eBlog Entrepreneur. (2010). Calculating Electricity Charges and Usage in Malaysia, http://eblog-entrepreneur.blogspot.my/2010/02/calculating-electricity-charges-and.html. *Website*.

University of Malaya

El Khadraoui, A., Bouadila, S., Kooli, S., Guizani, A., & Farhat, A. (2016). Solar air heater with phase change material: An energy analysis and a comparative study. *Applied Thermal Engineering, 107*, 1057-1064.

Elarga, H., Goia, F., Zarrella, A., Dal Monte, A., & Benini, E. (2016). Thermal and electrical performance of an integrated PV-PCM system in double skin façades: A numerical study. *Solar Energy, 136*, 112-124.

Esakkimuthu, S., Hassabou, A. H., Palaniappan, C., Spinnler, M., Blumenberg, J., & Velraj, R. (2013). Experimental investigation on phase change material based thermal storage system for solar air heating applications. *Solar Energy, 88* 144–153.

Farahat, M. A. (2004). Improvement in the Thermal Electric Performance of a Photovoltaic Cells by Cooling and Concentration Techniques, September 6-8. *proceeding of the 39th International Universities Power Engineering Conference (UPEC 2004), IEEE, New York, New York, ISBN: 1-86043-365-0*, 623-628.

Farkas, I., Kocsany, I., & Seres, I. (2017). Exergy based performance analysis of hybrid solar collectors *Angol*.

Florschuetz, L. (1975). On heat rejection from terrestrial solar cell arrays with sunlight concentration. *In: Proceedings of the 11th IEEE PVSC conference. New York, USA*, 318–326.

Florschuetz, L. (1979). Extension of the Hottel–Whiller model to the analysis of combined photovoltaic/thermal flat plate collectors. *Sol Energy, 22*, 361–366.

Frankl, P. (2010). Technology Roadmap: Solar photovoltaic energy. *International Energy Agency*.

Fuqiao, W., Maidment, G., Missenden, J., & Tozer, R. (2002). A review of research concerning the use of PCMs in air conditioning and refrigeration engineering. *Adv Build Technol, 1*, 1273–1280.

Galione, P. A., Pérez-Segarra, C. D., Rodríguez, I., Torras, S., & Rigola, J. (2015). Multi-layered solid-PCM thermocline thermal storage for CSP. Numerical evaluation of its application in a 50 MWe plant. *Solar Energy, 119*, 134-150.

Garg, H. P., Agarwal, R. K., & Joshi, J. C. (1994). Experimental study on a hybrid photovoltaicthermal solar water heater and its performance predictions. *Energy Convers Manage, 35*(7), 621–633.

University of Malaya

Garg, H. P., Mullick, S. C., & Bhargava, A. K. (1985). Solar thermal energy storage. *Dordrecht, Holland: Reidel Publishing Company*.

GCEP, T. A. R. (2006). An Assessment of Solar Energy Conversion Technologies and Research Opportunities. *Energy Assessment Analysis*.

Gil, A., Medrano, M., Martorell, I., Lázaro, A., Dolado, P., Zalba, B., & Cabeza, L. F. (2010). State of the art on high temperature thermal energy storage for power generation. Part 1—Concepts, materials and modellization. *Renewable and Sustainable Energy Reviews, 14*(1), 31-55.

Grigorios, I. (2009). Flat-Plate Solar Collectors for Water Heating with Improved Heat Transfer for Application in Climatic Conditions of the Mediterranean Region, Durham E-Theses. *School of Engineering and Computing Science, Durham University*.

Gunerhan, H., & Hepbasli, A. (2007). Exergetic modeling and performance evaluation of solar water heating systems for building applications. *Energy and Buildings, 39*(5), 509-516.

Gupta, M. K., & Kaushik, S. C. (2010). Exergy analysis and investigation for various feed water heaters of direct steam generation solar–thermal power plant. *Renewable Energy, 35*(6), 1228-1235.

Halbhavi, S. B., Kulkarni, S. G., & Kulkarni, D. B. (2015). Microcontroller Based Automatic Cleaning of Solar Panel. *International Journal of Latest Trends in Engineering and Technology, 5*(4), 99-103.

Hammou, Z. A., & Lacroix, M. (2006). A new PCM storage system for managing simultaneously solar and electric energy. *Energy and Buildings, 38*, 258–265.

Han, X., Wang, Y., & Zhu, L. (2013). The performance and long-term stability of silicon concentrator solar cells immersed in dielectric liquids *Energy Conversion and Management, 66*, 189–198.

Hasan, A., Alnoman, H., & Shah, A. H. (2016). Energy Efficiency Enhancement of Photovoltaics by Phase Change Materials through Thermal Energy Recovery. *Energies, 9*(10), 782.

Hasan, A., McCormack, S. J., Huang, M. J., & Norton, B. (2010). Evaluation of phase change materials for thermal regulation enhancement of building integrated photovoltaics. *Solar Energy, 84*(9), 1601-1612.

University of Malaya

Hasan, A., Sarwar, J., Alnoman, H., & Abdelbaqi, S. (2017). Yearly energy performance of a photovoltaic-phase change material (PV-PCM) system in hot climate. *Solar Energy, 146*, 417-429.

Hasanuzzaman, M., Malek, A. B. M. A., Islam, M. M., Pandey, A. K., & Rahim, N. A. (2016). Global advancement of cooling technologies for PV systems: A review. *Solar Energy, 137,* 25-45.

Hazami, M., Riahi, A., Mehdaoui, F., Nouicer, O., & Farhat, A. (2016). Energetic and exergetic performances analysis of a PV/T (photovoltaic thermal) solar system tested and simulated under to Tunisian (North Africa) climatic conditions. *Energy, 107*, 78-94.

Hegazy, A. A. (2000). Comparative study of the performances of four photovoltaic/thermal solar air collectors *Energy Conversion and Management, 41* 861–881.

Hellstrom, B., Adsten, M., Nostell, P., Karlsson, B., & Wackelgard, E. (2003). The impact of optical and thermal properties on the performance of flat plate solar collectors. *Renewable Energy, 28*, 331-344.

Hendrie, S. (1979). Evaluation of combined photovoltaic/thermal collectors. *In: Proceedings of the ISES international congress, Atlanta, USA, 3*, 1865–1869.

Ho, C.-D., Chen, T.-C., & Tsai, C.-J. (2010). Experimental and theoretical studies of recyclic flat-plate solar water heaters equipped with rectangle conduits. *Renewable Energy, 35*(10), 2279-2287.

Ho, C. J., & Gao, J. Y. (2009). Preparation and thermophysical properties of nanoparticle-in-paraffin emulsion as phase change material. *International Communications in Heat and Mass Transfer, 36*(5), 467-470.

Hossain, M. S. (2013). Thermal performance and economic analysis of solar photovoltaic water heater under the malaysian climatic condition. *Thesis*.

Hossain, M. S., Pandey, A. K., Selvaraj, J. A. L., Rahim, N. A., & Hoque, K. E. (2015). Thermal and economic analysis of low-cost modified flat-plate solar water heater with parallel two-side serpentine flow *Journal of thermal analysis and calorimetry, 123*(1), 793-806.

Huang, M. (2002). The application of CFD to predict the thermal performance of phase change materials for the control of photovoltaic cell temperature in buildings. . *Ph.D. Thesis, University of Ulster*.

University of Malaya

Huang, M. (2011). The effect of using two PCMs on the thermal regulation performance of BIPV systems. *Solar Energy Materials and Solar Cells, 95*, 957–963.

Huang, M., Eames, P., & Norton, B. (2006a). Phase change materials for limiting temperature rise in building integrated photovoltaics. *Solar Energy, 80*, 1121–1130.

Huang, M., Eames, P. C., & Norton, B. (2004). Thermal regulation of building-integrated photovoltaics using phase change materials. *International Journal of Heat and Mass Transfer, 47*, 2715–2733.

Huang, M. J., Eames, P. C., & Norton, B. (2006b). Experimental performance of phase change materials for limiting temperature rise building integrated photovoltaics. *Journal of Solar Energy, 80* 1121–1130.

Huang, M. J., Eames, P. C., Norton, B., & Hewitt, N. J. (2011). Natural convection in an internally finned phase change material heat sink for the thermal management of photovoltaics. *Solar Energy Materials & Solar Cells, 95* 1598–1603.

Ibrahim, O., Fardoun, F., Younes, R., & Louahlia-Gualous, H. (2014a). Review of water-heating systems: General selection approach based on energy and environmental aspects. *Building and Environment, 72*(0), 259-286.

Ibrahim, A., Fudholi, A., Sopian, K., Othman, M. Y., & Ruslan, M. H. (2014b). Efficiencies and improvement potential of building integrated photovoltaic thermal (BIPVT) system. *Energy Conversion and Management, 77*, 527-534.

IEA. (2015). International Energy Agency, Int Energy Agency n.d. http://www.iea.org, Acc: 29/12/2015. *Website*.

IEO. (2016). International Energy Outlook 2016. *U.S. Energy Information Administration, https://www.eia.gov/outlooks/ieo/pdf/0484(2016).pdf*.

Ioan, S., & Calin, S. (2013). Review of solar refrigeration and cooling systems. *Energy and Buildings, 67*, 286–297.

Islam, M. M., Pandey, A. K., Hasanuzzaman, M., & Rahim, N. A. (2016). Recent progresses and achievements in photovoltaic-phase change material technology: A review with special treatment on photovoltaic thermal-phase change material systems. *Energy Conversion and Management, 126*, 177-204.

Jaaz, A. H., Hasan, H. A., Sopian, K., Kadhum, A. A. H., Gaaz, T. S., & Al-Amiery, A. A. (2017). Outdoor Performance analysis of a photovoltaic thermal (PVT)

University of Malaya

collector with Jet impingement and compound parabolic concentrator (CPC). *Materials, 10*(8), 888.

Jaisankar, S., Radhakrishnan, T. K., & Sheeba, K. N. (2009). Experimental studies on heat transfer and friction factor characteristics of forced circulation solar water heater system fitted with helical twisted tapes. *Solar Energy, 83*(11), 1943-1952.

Jamil, A., Kousksou, T., Zeraouli, Y., Gibout, S., & Dumas, J. P. (2006). Simulation of the thermal transfer during an eutectic melting of a binary solution. *Thermochimica Acta, 441*(1), 30-34.

Joshi, A. S., Dincer, I., & Reddy, B. V. (2009a). Development of Solar Exergy Maps. *International Journal of Energy Research, 33*, 709–718.

Joshi, A. S., Dincer, I., & Reddy, B. V. (2009b). Performance analysis of photovoltaic systems: A review. *Renewable and Sustainable Energy Reviews, 13*(8), 1884-1897.

Joshi, A. S., Tiwari, A., Tiwari, G. N., Dincer, I., & Reddy, B. V. (2009c). Performance evaluation of a hybrid photovoltaic thermal (PV/T) (glass-to-glass) system. *International Journal of Thermal Sciences, 48*(1), 154-164.

Joulin, A., Younsi, Z., Zalewski, L., Lassue, S., Rousse, D. R., & Cavrot, J.-P. (2011). Experimental and numerical investigation of a phase change material: Thermal-energy storage and release. *Applied Energy, 88*(7), 2454-2462.

Jun, Z., Junfeng, L., Jie, W., & Ngan, H. W. (2011). A multi-agent solution to energy management in hybrid renewable energy generation system. *Renewable Energy, 36* 1352-1363.

Kaldellis. J. K., & Fragos, P. (2011). Ash deposition impact on the energy performance of photovoltaic generators *Journal Cleaner Production, 19*(4), 311-317.

Kalogirou, S., & Tripanagnostopoulos, Y. (2006). Hybrid PV/T solar systems for domestic hot water and electricity production. *Energy Conversion and Management, 47*, 3368–3382.

Kalogirou, S. A., Karellas, S., Badescu, V., & Braimakis, K. (2016). Exergy analysis on solar thermal systems: A better understanding of their sustainability. *Renewable Energy, 85*, 1328-1333.

Kern, J., & Russell, M. (1978). Combined photovoltaic and thermal hybrid collector systems. *In: Proceedings of the 13th IEEE photovoltaic specialists. Washington, DC, USA*, 1153–1157.

University of Malaya

Kirn, B., & Topic, M. (2017). Diffuse and direct light solar spectra modeling in PV module performance rating. *Solar Energy, 150*, 310-316.

Krauter, S., Araujo, R. G., Schroer, S., Hanitsch, R., Salih, M. J., Triebel, C., & Lemoine, R. (1999). Combined photovoltaic and solar thermal systems for facade integration and building insulation *Solar Energy, 67*, 239–248.

Kumar, S., & Tiwari, G. N. (2009). Life cycle cost analysis of single slope hybrid (PV/T) active solar still. *Applied Energy, 86*(10), 1995-2004.

Kumar, A., Baredar, P., & Qureshi, U. (2015). Historical and recent development of photovoltaic thermal (PVT) technologies. *Renewable and Sustainable Energy Reviews, 42,* 1428-1436.

Kumaresan, G., Sridhar, R., & Velraj, R. (2012). Performance studies of a solar parabolic trough collector with a thermal energy storage system. *Energy, 47*(1), 395-402.

Kuravi, S., Trahan, J., Goswami, D. Y., Rahman, M. M., & Stefanakos, E. K. (2013). Thermal energy storage technologies and systems for concentrating solar power plants. *Progress in Energy and Combustion Science, 39*(4), 285-319.

Kuznik, F., David, D., Johannes, K., & Roux, J.-J. (2011). A review on phase change materials integrated in building walls. *Renewable and Sustainable Energy Reviews, 15*(1), 379-391.

Kymakis, E., Kalykakis, S., & Papazoglou, T. M. (2009). Performance analysis of a grid connected photovoltaic park on the island of Crete. *Energy Convers Manage, 50*, 433–438.

Laing, D., Eck, M., Hempel, M., Johnson, M., Steinmann, W., MeyerGru¨nefeldt, M., & al., e. (2012). High Temperature PCM Storage for DSG Solar Thermal Power Plants Tested in Various Operating Modes of Water/Steam Flow *SolarPACES 2012. Marrakech*.

Lalovic, B. (1986). A hybrid amorphous silicon photovoltaic and thermal solar collector. *Sol Cells, 19*, 131–138.

Lane, G. A. (1983). Solar heat storage-latent heat materials, Boca Raton, FL. *CRC Press, Inc., 1*.

Lazada.com.my. (2017). MP-20RXM Magnetic circulation water pump, http://www.lazada.com.my/magnetic-circulation-water-pump-mp-20rxm-220v-50hz-46lmin-18mhead-60hz-52lmin-25m-head-ce-certificate-chemical-

University of Malaya

liquidtransport-pump-strong-wear-resistance-and-corrosion-resistance-forwater-and-chemical-liquid-12035232.html?ff=1. *Website*.

Leland T, B., & Anthony J, T. (1998). Engineering Economy. Book. 4th Edition: ISBN: 0-070-115964-9., 46-161.

Lianos, P. (2017). Review of recent trends in photoelectrocatalytic conversion of solar energy to electricity and hydrogen. *Applied Catalysis B: Environmental, 210*, 235-254.

Liu, M., Belusko, M., Steven Tay, N. H., & Bruno, F. (2014). Impact of the heat transfer fluid in a flat plate phase change thermal storage unit for concentrated solar tower plants. *Solar Energy, 101*, 220-231.

Liu, M., Saman, W., & Bruno, F. (2012). Review on storage materials and thermal performance enhancement techniques for high temperature phase change thermal storage systems. *Renewable and Sustainable Energy Reviews, 16*(4), 2118-2132.

Lu, S., Zhao, Y., Fang, K., Li, Y., & Sun, P. (2017). Establishment and experimental verification of TRNSYS model for PCM floor coupled with solar water heating system. *Energy and Buildings, 140*, 245-260.

Lu, T. J. (2000). Thermal management of high power electronics with phase change cooling. *International Journal of Heat and Mass Transfer, 43*, 2245–2256.

Machniewicz, A., Knera, D., & Heim, D. (2015). Effect of Transition Temperature on Efficiency of PV/PCM Panels. *Energy Procedia, 78*, 1684-1689.

Maghami, M. R., Hizam, H., Gomes, C., Radzi, M. A., Rezadad, M. I., & Hajighorbani, S. (2016). Power loss due to soiling on solar panel: A review. *Renewable and Sustainable Energy Reviews, 59*, 1307-1316.

Mahfuz, M. H., Anisur, M. R., Kibria, M. A., Saidur, R., & Metselaar, I. H. S. C. (2014). Performance investigation of thermal energy storage system with Phase Change Material (PCM) for solar water heating application. *International Communications in Heat and Mass Transfer, 57*, 132-139.

Mani, M., & Pillai, R. (2010). Impact of dust on solar photovoltaic (PV) performance: Research status, challenges and recommendations. *Renew Sustain Energy Rev, 14*, 3124–3131.

Markvart, T. (2002). Photovoltaic Solar Energy Conversion. *Energy for Europe Strasbourg*.

University of Malaya

Marletta, L., & Evola, G. (2013a). Thermodynamic analysis of a hybrid photovoltaic/thermal solar collector. *International journal heat technology, 31*(2), 135-142.

Marletta, L., & Evola, G. (2013b). Thermodynamic analysis of a hybrid photovoltaic/thermal solar collector. *Int. J. Heat Technol, 31*(2), 135-142.

Martinopoulos, G., Missirlis, D., Tsilingiridis, G., Yakinthos, K., & Kyriakis, N. (2010). CFD modeling of a polymer solar collector. *Renewable Energy, 35*, 1499–1508.

Mastani Joybari, M., Haghighat, F., Moffat, J., & Sra, P. (2015). Heat and cold storage using phase change materials in domestic refrigeration systems: The state-of-the-art review. *Energy and Buildings, 106*, 111-124.

Mazer, J. A. (1997). Solar Cells: an Introduction To Crystalline Photovoltaic Technology *Kluwer Academic Publications, 108*.

Mei, L., Infield, D., Eicker, U., & Fux, V. (2003). Thermal modelling of a building with an integrated ventilated PV facade *Energy and Buildings, 35*, 605–617.

Mekhilef, S., Saidur, R., & Kamalisarvestani, M. (2012). Effect of dust, humidity and air velocity on efficiency of photovoltaic cells. *Renew Sustain Energy Rev, 16*(2920–5).

Michels, H., & Pitz-Paal, R. (2007). Cascaded latent heat storage for parabolic trough solar power plants. *Solar Energy, 81*(6), 829-837.

Mohsen, M. S., Al-Ghandoor, A., & Al-Hinti, I. (2009). Thermal analysis of compact solar water heater under local climatic conditions *International Communications in Heat and Mass Transfer, 36* (9), 962-968.

Nahar, A., Hasanuzzaman, M., & Rahim, N. A. (2017). Numerical and experimental investigation on the performance of a photovoltaic thermal collector with parallel plate flow channel under different operating conditions in Malaysia. *Solar Energy, 144*(Supplement C), 517-528.

Navarro, L., Gracia, A., Castell, A., Álvarez, S., & Cabeza, L. F. (2015). PCM incorporation in a concrete core slab as a thermal storage and supply system: Proof of concept. *Energy and Buildings, 103* 70–82.

Noro, M., Lazzarin, R., & Bagarella, G. (2016). Advancements in Hybrid Photovoltaic-thermal Systems: Performance Evaluations and Applications. *Energy Procedia, 101,* 496-503.

University of Malaya

NREL. (2009). Solar Advisor Model *National Renewable Energy Laboratory*.

NREL. (2010). Measuring and Modeling Nominal Operating Cell Temperature (NOCT). *National laboratory of the U.S. Department of Energy*.

Ong, K. S. (1994). Solar water heaters Engineering and Applications. ISBN 967-9940-57-8

Osterman, E., Tyagi, V. V., Butala, V., Rahim, N. A., & Stritih, U. (2012). Review of PCM based cooling technologies for buildings. *Energy and Buildings, 49*, 37–49.

Pande, P. (1992). Effect of dust on the performance of PV panels. In: Proceedings of the 6th International Photovoltaic Science and Engineering Conference. *Conference*.

Pandey, A. K. (2013). Exergy analysis and exergoeconomic evaluation of renewable energy conversion systems. Shri Mata Vaishno Devi University. *Thesis*.

Pandey, A. K., Hossain, M. S., Tyagi, V. V., Abd Rahim, N., Selvaraj, J. A. L., & Sari, A. (2018). Novel approaches and recent developments on potential applications of phase change materials in solar energy. *Renewable and Sustainable Energy Reviews, 82,* 281-323.

Park, S. R., Pandey, A. K., Tyagi, V. V., & Tyagi, S. K. (2014). Energy and exergy analysis of typical renewable energy systems. *Renewable and Sustainable Energy Reviews, 30*, 105-123.

Pasupathy, A., Athanasius, L., Velraj, R., & Seeniraj, R. V. (2008). Experimental investigation and numerical simulation analysis on the thermal performance of a building roof incorporating phase change material (PCM) for thermal management *Applied Thermal Engineering, 28*, 556–565.

Pathak, M. J. M., Sanders, P. G., & Pearce, J. M. (2014). Optimizing limited solar roof access by exergy analysis of solar thermal, photovoltaic, and hybrid photovoltaic thermal systems. *Applied Energy, 120*, 115–124.

Peiró, G., Gasia, J., Miró, L., & Cabeza, L. F. (2015). Experimental evaluation at pilot plant scale of multiple PCMs (cascaded) vs. single PCM configuration for thermal energy storage. *Renewable Energy, 83*, 729-736.

Perrot, P. (1998). A to Z of Thermodynamics. Oxford University Press.

Piebalgs, A., & Potočnik, J. (2009). Photovoltaic Solar Energy Development and current research. *European Communities, ISBN 978-92-79-10644-6*(doi: 10.2768/38305).

University of Malaya

Preet, S., Bhushan, B., & Mahajan, T. (2017). Experimental investigation of water based photovoltaic/thermal (PV/T) system with and without phase change material (PCM). *Solar Energy, 155,* 1104-1120.

Radziemska, E., & Klugman, E. (2002). Thermally affected parameters of the current-voltage characteristics of silicon photocell *Energy Conversion and Management, 43*, 1889–1900.

Raghuraman, P. (1981). Analytical prediction of liquid and air photovoltaic/thermal flat plate collector performance. *J Sol Energy Eng, 103*(291–8).

Rahman, M. A., & Lee, K. T. (2006). Energy for sustainable development in Malaysia: Energy policy and alternative energy *Energy Policy, 34* (15), 2388-2397.

Rahman, M. M., Hasanuzzaman, M., & Rahim, N. A. (2017). Effects of operational conditions on the energy efficiency of photovoltaic modules operating in Malaysia. *Journal of Cleaner Production, 143*(Supplement C), 912-924.

Rant, Z. (1956). Exergie, Ein neues Wort für "technische Arbeitsfähigkeit. *Forschung auf dem Gebiete des Ingenieurwesens, 22*, 36–37.

Regin, A. F., Solanki, S. C., & Saini, J. S. (2008). Heat transfer characteristics of thermal energy storage system using PCM capsules: A review. *Renewable and Sustainable Energy Reviews, 12*(9), 2438-2458.

Renewable Energy centre, R. (2017). Solar panel cleaning system. http://energy.asu.edu.jo/index.php/about1. *Website*.

Report, C. (2001). A Guide to photovoltaic (PV) system design and installation. *California Energy Commission*.

Robles-Ocampo, B., Ruíz-Vasquez, E., Canseco-Sánchez, H., Cornejo-Meza, R. C., Trápaga-Martínez, G., García-Rodriguez, F. J., . . . Vorobiev, Y. V. (2007). Photovoltaic/thermal solar hybrid system with bifacial PV module and transparent plane collector. *Solar Energy Materials and Solar Cells, 91*(20), 1966-1971.

Rohsenow, W. M., Hartnett, J. P., & Cho, Y. I. (1998). Handbook of Heat Transfer. *third ed. McGraw-Hill, London*.

Rubitherm, G. (2000). Rubitherm Data Sheet. *Rubitherm GmbH, Hamburg*.

Russell, C. R. (1981). Optical concentrator and cooling system for photovoltaic cells. In: US.

University of Malaya

Russell, R. F. (1982). Uniform temperature heat pipe and method of using the same. in USA.

Sahin, A. D., Dincer, I., & Rosen, M. A. (2007). Thermodynamic analysis of solar photovoltaic cell systems. *Solar Energy Materials and Solar Cells, 91*(2), 153-159.

Saidur, R., Islam, M. R., Rahim, N. A., & Solangi, K. H. (2010). A review on global wind energy policy *Renewable and Sustainable Energy Reviews, 14*(7), 1744-1762.

Saiful, B. (2001). Optimum orientation of domestic solar water heaters for the low latitude countries. *Energy Conversion and Management, 42*(10), 1205-1214.

Sardarabadi, M., Passandideh-Fard, M., Maghrebi, M.-J., & Ghazikhani, M. (2017). Experimental study of using both ZnO/ water nanofluid and phase change material (PCM) in photovoltaic thermal systems. *Solar Energy Materials and Solar Cells, 161*, 62-69.

Sargent and Lundy LLC Consulting Group. (2003). Assessment of parabolic trough and power tower solar technology cost and performance forecasts *Natl. Renew. Energy Lab*.

Sarhaddi, F., Farahat, S., Ajam, H., Behzadmehr, A., & Mahdavi Adeli, M. (2010). An improved thermal and electrical model for a solar photovoltaic thermal (PV/T) air collector *Applied Energy, 87*(7), 2328-2339.

Sarier, N., & Onder, E. (2012). Organic phase change materials and their textile applications: An overview. *Thermochimica Acta, 540*, 7-60.

Schmidt, F. (1981). Thermal energy storage and regeneration (series in thermal and fluids engineering). *New York: McGraw-Hill*.

Shaharin, A. S., Haizatul, H. H., Nik Siti H. Nik Leh., & Mohd S. I. Razali. (2011). Effects of Dust on the Performance of PV Panels. *World Academy of Science, Engineering and Technology, 58*, 588-593.

Sharma, A., Tyagi, V. V., Chen, C. R., & Buddhi, D. (2009). Review on thermal energy storage with phase change materials and applications. *Renewable and Sustainable Energy Reviews, 13*(2), 318-345.

Sharma, R. K., Ganesan, P., Tyagi, V. V., Metselaar, H. S. C., & Sandaran, S. C. (2015). Developments in organic solid–liquid phase change materials and their applications in thermal energy storage. *Energy Conversion and Management, 95*, 193–228.

University of Malaya

Shevaleevskiy, O. (2008). The future of solar photovoltaics: A new challenge for chemical physics. *Pure Appl. Chem., 80*(10), 2079–2089.

Shukla, A., Buddhi, D., & Sawhney, R. L. (2009). Solar water heaters with phase change material thermal energy storage medium: A review. *Renewable and Sustainable Energy Reviews, 13*(8), 2119-2125.

Sigma-Aldrich. (2013). ParaffinWax. http://www.sigmaaldrich.com/catalog/product/aldrich/327212?lang=fi&region=FI.

Singh, D. B., & Tiwari, G. N. (2017). Energy, exergy and cost analyses of N identical evacuated tubular collectors integrated basin type solar stills: A comparative study. *Solar Energy, 155*(Supplement C), 829-846.

Skoplaki, E., & Palyvos, J. A. (2009). Operating temperature of photovoltaic modules: a survey of pertinent correlations. . *Renew Energy, 34*, 23–29.

Slimani, M. E. A., Amirat, M., Bahria, S., Kurucz, I., Aouli, M. h., & Sellami, R. (2016). Study and modeling of energy performance of a hybrid photovoltaic/thermal solar collector: Configuration suitable for an indirect solar dryer. *Energy Conversion and Management, 125,* 209-221.

Soares, N., Gaspar, A. R., Santos, P., & Costa, J. J. (2016). Experimental evaluation of the heat transfer through small PCM-based thermal energy storage units for building applications. *Energy and Buildings, 116*, 18–34.

Solanki, C., Sangani, C., Gunashekar, D., & Antony, G. (2008). Enhanced heat dissipation of V-trough PV modules for better performance. *Solar Energy Materials and Solar Cells, 92*, 1634–1638.

Stropnik, R., & Stritih, U. (2016). Increasing the efficiency of PV panel with the use of PCM. *Renewable Energy, 97*, 671-679.

Struckmann, F. (2008). Analysis of a Flat-plate Solar Collector. http://www.ht.energy.lth.se/fileadmin/ht/Kurser/MVK160/Project_08/Fabio.pdf. . *Heat and Mass Transport, Project Report*.

Sudhakar, K., & Srivastava, T. (2014). Energy and exergy analysis of 36 W solar photovoltaic module. *International Journal of Ambient Energy, 35*(1), 1-7.

SunEarthTools, C. (2016). Tools for consumers and designers of solar. Software. http://www.sunearthtools.com/dp/tools/pos_sun.php.

University of Malaya

Tan, F. L., & Fok, S. C. (2007). Thermal management of mobile phones using phase change materials. *In: IEEE 9th Electronics Packaging Technology Conference*, 836–842.

Tanaka, K. (2007). Solar energy converter using a solar cell in a shallow liquid layer. in US.

Telkes, M., & Raymond, E. (1949). Storing solar heat in chemicals-a report on the Dover house. *Heat Vent, 46*, 80–86.

Teo, H. G., Lee, P. S., & Hawlader, M. N. A. (2012). An active cooling system for photovoltaic modules. *Applied Energy, 90*, 309–315.

Thakare, M. S., Krishna Priya, G. S., Ghosh, P. C., & Bandyopadhyay, S. (2016). Optimization of photovoltaic–thermal (PVT) based cogeneration system through water replenishment profile. *Solar Energy, 133,* 512-523.

Tian, Y., & Zhao, C. Y. (2009). Heat transfer analysis for phase change materials (PCMs). In: Proceedings of the 11th International Conference on Energy Storage (Effstock 2009); Stockholm, Sweden.

Tian, Y., & Zhao, C. Y. (2011). A numerical investigation of heat transfer in phase change materials (PCMs) embedded in porous metals. *Energy, 36*, 5539–5546.

Tian, Y., & Zhao, C. Y. (2012). A Review of Solar Collectors and Thermal Energy Storage in Solar Thermal Applications. *Applied Energy, 104*, 538–553.

Tian, Y., & Zhao, C. Y. (2013). Thermal and exergetic analysis of Metal Foam-enhanced Cascaded Thermal Energy Storage (MF-CTES). *International Journal of Heat and Mass Transfer, 58*(1), 86-96.

Tiwari, G. N., Mishra, R. K., & Solanki, S. C. (2011). Photovoltaic modules and their applications: A review on thermal modelling. *Applied Energy, 88*(7), 2287-2304.

Tonui, J. K., & Tripanagnostopoulos, Y. (2008). Performance improvement of PV/T solar collectors with natural air flow operation. *Solar Energy, 82*, 1–12.

Townsend, T. U., & Hutchinson, P. A. (2000). Soiling analysis at PVUSA. In: Proceedings of the ASES solar conference. *Conference*.

Trading, E. (2017). Malaysia GDP per capita. https://tradingeconomics.com/malaysia/gdp-per-capita. *Website*.

University of Malaya

Tripanagnostopoulos, Y., Nousia, T., Souliotis, M., & Yianoulis, P. (2002). Hybrid photovoltaic/thermal solar systems. *Solar Energy, 72(3),* 217-234.

Tyagi, S. K., Pandey, A. K., Pant, P. C., & Tyagi, V. V. (2012a). Formation, potential and abatement of plume from wet cooling towers: A review. *Renewable and Sustainable Energy Reviews, 16* 3409–3429.

Tyagi, V. V., & Buddhi, D. (2007). PCM thermal storage in buildings: A state of art. *Renewable and Sustainable Energy Reviews, 11*, 1146–1166.

Tyagi, V. V., Buddhi, D., Kothari, R., & Tyagi, S. K. (2012b). Phase change material (PCM) based thermal management system for cool energy storage application in building: An experimental study. *Energy and Buildings, 51*, 248–254.

Tyagi, V. V., Kaushik, S. C., & Tyagi, S. K. (2012c). Advancement in solar photovoltaic/thermal (PV/T) hybrid collector technology. . *Renewable and Sustainable Energy Reviews, 16*(1383– 1398).

Tyagi, V. V., Pandey, A. K., Buddhi, D., & Tyagi, S. K. (2013). Exergy and energy analyses of two different types of PCM based thermal management systems for space air conditioning applications. *Energy Conversion and Management, 69* 1–8.

Tyagi, V. V., Panwar, N. L., Rahim, N. A., & Kothari, R. (2012d). Review on solar air heating system with and without thermal energy storage system. *Renewable and Sustainable Energy Reviews, 16*(4), 2289-2303.

Ugumori, T., & Ikeya, M. (1981). Efficiency increase of solar cells operated in dielectric liquid. *Japanese Journal of Applied Physics, 20*, 77–80.

Vicente, R., & Silva, T. (2014). Brick masonry walls with PCM macrocapsules: An experimental approach. *Applied Thermal Engineering, 67*, 24-34.

Victoria, H. (2009). The Next Solar Frontier: Hybrid PV/Thermal Systems, http://www.renewableenergyworld.com/rea/news/article/2009/12/the-next-solar-frontier-producing-more-energy-with-hybrid-pvthermal-systems. *Conserval Engineering*.

Wang, R. Z., Yu, X., Ge, T. S., & Li, T. X. (2013). The present and future of residential refrigeration, power generation and energy storage. *Applied Thermal Engineering, 53*(2), 256-270.

Wang, X. Q., Mujumdar, A. S., & Yap, C. (2007). Effect of orientation for phase change material (PCM)-based heat sinks for transient thermal management of electric

University of Malaya

components *International Communications in Heat and Mass Transfer, 34* 801–808.

Weakliem, H. A., & Redfield, D. (1979). Temperature dependence of the optical properties of silicon *Journal of Applied Physics, 50* 1491–1493.

Wolf, M. (1976). Performance analysis of combined heating and photovoltaic power systems for residences. *Energy Convers Manage, 16*, 79–90.

Xu, B., Li, P., & Chan, C. (2015). Application of phase change materials for thermal energy storage in concentrated solar thermal power plants: A review to recent developments. *Applied Energy, 160*, 286-307.

Yang, X., Sun, L., Yuan, Y., Zhao, X., & Cao, X. (2018). Experimental investigation on performance comparison of PV/T-PCM system and PV/T system. *Renewable Energy, 119,* 152-159.

Yazdanpanahi, J., Sarhaddi, F., & Adeli, M. M. (2015a). Experimental investigation of exergy efficiency of a solar photovoltaic thermal (PVT) water collector based on exergy losses. *Solar Energy*(118), 197–208.

Yazdanpanahi, J., Sarhaddi, F., & Mahdavi Adeli, M. (2015b). Experimental investigation of exergy efficiency of a solar photovoltaic thermal (PVT) water collector based on exergy losses. *Solar Energy, 118*, 197-208.

Yogev, R., & Kribus, A. (2013). Operation strategies and performance of solar thermal power plants operating from PCM storage. *Solar Energy, 95*, 170-180.

Yu, T., Heiselberg, P., Lei, B., Pomianowski, M., & Zhang, C. (2015). A novel system solution for cooling and ventilation in office buildings: A review of applied technologies and a case study. *Energy and Buildings, 90*, 142–155.

Yun, G. Y., McEvoy, M., & Steemers, K. (2007). Design and overall energy performance of a ventilated photovoltaic facade. *Solar Energy, 81* 383–394.

Zalba, B., Marı´n, J. M., Cabeza, L., & Mehling, H. (2003a). Review on thermal energy storage with phase change: materials, heat transfer analysis and applications *Appl Therm Eng, 23*, 251–283.

Zalba, B., Marín, J. M., Cabeza, L. F., & Mehling, H. (2003b). Review on thermal energy storage with phase change: materials, heat transfer analysis and applications. *Applied Thermal Engineering, 23*(3), 251-283.

University of Malaya

Zarza, E., Rojas, M. E., González, L., Caballero, J. M., & Rueda, F. (2006). INDITEP: The first pre-commercial DSG solar power plant. *Solar Energy, 80*(10), 1270-1276.

Zhang, Y., & Faghri, A. (1996). Semi-analytical solution of thermal energy storage system with conjugate laminar forced convection. *International Journal of Heat and Mass Transfer, 39*(4), 717-724.

Zhao, C., Lu, W., & Tian, Y. (2010). Heat transfer enhancement for thermal energy storage using metal foams embedded within phase change materials (PCMs). *Sol. Energy, 84*, 1402–1412.

Zondag, H. A., Vries, D. W. d., Helden, W. G. J. v., & Zolingen, R. J. C. v. (2003). The yield of different combined PV-thermal collector designs. *Solar Energy, 74*(3), 253-269.

University of Malaya